Polymerisation Efficiency and Shrinkage Effects in Resin Based Dental Restoratives

A thesis submitted to the University of Manchester for the Degree of

Doctor of Philosophy

In

The Faculty of Medicine, Dentistry and Nursing

September 1999

By

Abdusalam M. A. Al-Hindi

B.D.S. - Riyadh, Saudi Arabia

M.Sc. - Manchester, UK

Clinical Academic Group of Restorative Dentistry

Department of Dental Medicine and Surgery

Turner Dental School

Manchester

ProQuest LLC.
789 East Eisenhower Parkway
P.O. Box 1346
Ann Arbor, MI 48106 – 1346

(DXKE1)

Th 21291

TABLE OF CONTENTS

Abstract

The aim of this study was to investigate the polymerisation efficiency and shrinkage effects in resin based dental restorative materials. The study highlights factors affecting the polymerisation efficiency, but the efficiency of the light curing units was first measured. The output light intensity and the temperature rise produced by two units were measured using a radiometer with a flat-response characteristic. The units were the *Elipar Highlight* (Espé Dental AG) and *XL3000* (3M Co). The former unit has a dual-intensity mode of operation: 10 s low plus 30 s high (termed "soft-start") and a full-intensity mode: 40 s high. Its "high" intensity was significantly greater than the *XL3000* Unit, and produced correspondingly greater temperature rises. One of the hypotheses to be tested was whether any useful network-conversion (polymerisation) was attained by application of the 10 s low-intensity phase of the "soft-start" mode. To address this question, the polymerisation efficiency of three representative resin-based restorative materials was studied by measuring depth-of-cure, exotherm, surface hardness and degree of conversion. The *Elipar* Unit was used principally in these studies, with four modes of irradiation: "full" and "soft-start", as above, and either 10 s or 40 s of low intensity light. Most measurements were performed at 23 °C, but some specimen groups were also pre-conditioned at 37 °C.

Depth-of-cure values obtained by "soft-start" were as great as with "full" irradiation. Low-intensity irradiation alone gave significantly reduced, but non-zero cure-depths.

The exotherm of the specimens cured by "soft-start" was lower than those cured by "full" light-intensity. This pattern was also apparent when the lower-intensity (*XL3000*) Unit was deployed.

Surface hardness was measured on upper and lower surfaces of specimens irradiated by different modes. The hardness was greater at upper, relative to lower surfaces with "full" intensity. The lower-surface hardness with low intensity was minimal or nil with some materials. However, quite appreciable hardness was attained for upper surfaces with low intensity, confirming the definite network-creating potential of even low light-levels. This was further clarified on a more molecular basis by investigating the degree of conversion [**DC**] of the materials by FT-IR spectroscopy. Specimens were cured by the, above-mentioned, four-modes of irradiation. "Soft-start" generated equivalent DCs to "full" mode.

Polymerisation shrinkage-strain kinetics were studied by using the 'bonded-disk' technique, in which the axial shrinkage of a thin disc was recorded. Some hitherto

unexplored variables were examined, from which it was concluded that use of a more rigid glass base-plate was desirable. Effects of "soft-start" and "full" intensity curing were investigated. During the first 10 s, the polymerisation shrinkage was minimal, with low-intensity light, compared to the rapid rise in shrinkage with full light-intensity. But the final equilibrium shrinkage-strain was not significantly different. It was concluded that light-programmed "soft-start" polymerisation was beneficial in reducing the rapidity of kinetic-profile of the shrinkage-strain event. When combined with the preceding studies on degree-of-cure, this shows that early network-growth can occur during this period of minimal early shrinkage. Some molecular flow or network re-arrangement must be possible. A novel discovery was that an acrylate-based composite material exhibited an *inherent* "soft-start" regime under full-irradiation conditions. Shrinkage strain increased with temperature because of greater network conversion.

Finally, polymerisation shrinkage-stress kinetics of resin-composites were measured with a newly designed apparatus, based around a cantilever load cell. This apparatus gave reproducible results of the polymerisation shrinkage-stress magnitudes. Materials were again cured with "full" intensity and "soft-start" modes. The "soft-start" mode significantly reduced the final shrinkage-stress of some materials, but not others. This was an important finding showing that, although more difficult to conduct, stress measurements are a valuable adjunct to strain studies of shrinkage phenomena.

Declaration

I declare that no portion of the work referred to in the thesis has been submitted in support of an application for another degree or qualification of this or any other university or other institute of learning.

A. Al-Hindi

September, 1999

Notes on Copyright

Dedication

I owe a great deal to my parents Mohammed Al-Hindi, and Mariam Goase and indeed I feel very proud in dedicating this thesis to them. Dedicated with all my love and respect to my wife Samirah Al-Hindi and my children Arwa and Albara to whom I indebted for all my success. Also I would like to dedicate this thesis to my brothers and sisters.

Acknowledgements

A thesis is never an easy undertaking, nor done in isolation. Accordingly, I am deeply grateful to a number of individuals and government agencies that have supported and guided me.

Firstly, I would like to express my deepest appreciation to my supervisor Dr. David C. Watts for his guidance during the entire thesis, and helpful criticism. His knowledge and interest in the laboratory work were a great motivation. Without Dr. Watts' interest and invaluable feedback, this work would be never have reached its present standard. He is gratefully acknowledged and will be always remembered as a source of direction.

I would like to say thank you to Mr. A.J. Cash for his constructive suggestions and technical help.

Special thanks are due to Mrs D. Knight for her help and co-operation. I would like to acknowledge my postgraduate colleagues in the Biomaterials Science Unit. Special thanks are due to the late Mrs Sarah Blake from the Chemistry department for her help and advice.

I gratefully acknowledge the financial support given to me by the Ministry of Health of Saudi Arabia, and the support and guidance the of Saudi Arabian Cultural Attaché in London.

Chapter 1
General Literature Review

1.1 Introduction

Alternatives to dental amalgam have been available for several decades. These have been tooth-coloured restorations. The demand for tooth-coloured restorations has increased due to the aesthetics, concern about toxic effects of mercury released from amalgam, and less tooth destruction experienced with tooth-coloured restorations. With all the advantages of tooth coloured restorations it may seem surprising that amalgam is still in use at all.

1.2 Tooth-Coloured Restorative Materials

As civilisation has progressed, there has been continued refinement and diversification of the materials available for dental restoration. The need for restorative materials that have the appearance of natural tooth tissues and that can be placed directly into cavity preparations in a plastic condition, with less time required and finally less cost, have captivated scientists for many generations.

Silicate restorative materials were introduced in the late 1800's and were used extensively until about 1970. Unfilled acrylic polymers for direct aesthetic restorations were introduced about 1945 and were improved until they were used considerably in the 1960's. Composite dimethacrylates were introduced about 1960, and have been used increasingly until they now dominate the materials used for direct aesthetic restorations. Glass ionomers were introduced in 1972 and have been used primarily for restoration of cervically eroded areas, fillings for deciduous teeth, and combined with composite as a "sandwich technique" (Craig, *et al.*, 1983). The first light-curable glass-ionomer cement was described in the late 1980s, and this was formed as a result of combining a conventional glass-ionomer cement with a light-cured resin composite (Antonucci *et al.*, 1988).

Three main types of amalgam replacement material have been developed for use as direct

dental restorations:

(1) Resin Composites

(2) Glass Ionomer Cements

(3) Resin-Ionomer Hybrids

1.2.1 Resin-Composites

The term 'composite material' refers to a combination of at least two chemically different materials with a distinct interface separating the compound (McCabe, 1990). A composite dental restorative material is one in which an inorganic filler has been added to a resin matrix in such a way that the properties of the matrix have been upgraded (Baum, *et al.*, 1985).

The initial types of composite contained about 50% by volume (77% by weight) of inorganic fillers, with an average particle size 8 - 15 μm. The surface of the filler was treated with special organo-silane compounds, so that it would bond well to the organic matrix. This class of composite is referred to as 'conventional' composite and was classified according to ADA specification No. 27, as a Type II material.

The large particle size of the fillers of conventional composites made this type difficult to finish, so microfilled composites were developed that used colloidal silica as filler, and an average particle diameter of 0.04 μm. The weight percent of filler for the microfilled composites is substantially lower than for the conventional composite and values range from 33% to 50%, being classified according to ADA specification No. 27 as a Type I material.

Combinations of inorganic fillers that contain particles of approximately 5 μm diameter and colloidal silica, were called 'blended composites', and were classified according to ADA specification No. 27 as a Type III material.

Most of the composites are based on a polymer system called Bis-GMA, which, together with different monomers, constitutes the organic matrix. A few products use urethane dimethacrylates rather than the Bis-GMA system.

1.2.2 Glass-ionomer Cements (GIC)

Polyacrylic acid as a replacement for phosphoric acid in zinc phosphate cements, resulted in the development of polycarboxylate cement (Smith, 1968). The understanding of the fundamental acid-base chemistry of that cement led to the development of glass-ionomer cement (Wilson and Kent, 1972; Wilson and Prosser, 1984). The concept was to combine the strength, rigidity and fluoride release properties of silicate glass powder with the biocompatibility and adhesive qualities of poly (acrylic acid) liquid (Wilson and McLean, 1988).

The original composition of the silicate glass powder used in GIC's was based on the formulation SiO_2 - Al_2O_3 - CaF_2 - $AlPO_4$ -Na_3AlF_6 . GIC glass contains a high percentage of aluminium as different aluminium salts (Crisp, *et al.*, 1976).

Some current GIC's may contain a co-polymer of acrylic acid or maleic acid, with di-carboxylic or tri-carboxylic acid to control the viscosity of the polycarboxylic acid. Some of these acids can also provide greater reactivity. Higher molecular weight co-polymers may also be used to improve the physical properties of some GIC's and the problems associated with high viscosity. The incorporation of powders of poly (acrylic acid) or co-polymers with the glass to produce a blended powder that sets when it is mixed with water or a tartaric acid solution, overcomes the problem of high viscosity. (Prosser, *et al.*, 1986; Wilson, *et al.*, 1977).

1.2.3 Resin-Modified Ionomer Hybrids

These recently developed hybrid materials are now available, which are intermediate in character between classical photo-polymerisable resin-composites and essential components of glass-ionomers (Antonucci and Stansbury, 1989; Watts, 1992).

Benefits of these materials have been enumerated; long working time, command set, adhesion, fluoride release and reduced moisture sensitivity (Sidhu and Watson, 1995; Quian and Huth, 1998). They have shown improved aesthetics, physical and mechanical properties, particularly flexural and compressive strengths compared to the GICs. The fluoride release is comparable to that of GICs and recharging has also been demonstrated

(Craig, 1997). Furthermore, higher bond strength to enamel and dentine has been reported, which appears to be sufficient for use in orthodontic bonding agents (Compoton *et al.*, 1992). Besides, they have been shown to bond to composites via the formation of a catalyst-rich air-inhibited layer which polymerises with the resin, and so offer suitable alternatives to conventional GICs in the sandwich technique (Burgess *et al.*, 1993; Chadwick and Woolford, 1990). Bonding to amalgam has also been demonstrated (Aboush and Elderton, 1990).

Nonetheless, they have some potential limitations, namely; setting exotherm, phase-separation, monomer leaching, decrease in translucency due to differences in refractive index between polyacid matrix and polymerised monomer, polymerisation shrinkage and hygroscopic expansion. Regarding aesthetics, most RMGIC can not be polished as well as composites, predisposing them to abrasion and attraction of food deposits and stain, hence their aesthetics is inferior to composites and compomers (Christensen, 1996; Sidhu *et al.*, 1996).

1.3 Components of Resin Composite Materials

The characteristics of composite resins depend on three important components (Lutz and Phillips, 1983):

1. Matrix monomer (organic) components,
2. The dispersed phase components (the fillers).
3. The interfacial phase (coupling agents).

1.3.1 Matrix Monomer Components

The majority of materials have been based on the viscous aromatic dimethacrylate monomer 2,2-bis[4-(2-hydroxy-3-methacryloyloxypropoxy)- phenyl] propane (Bis-GMA) and a branched Bis-GMA. Because of its large molecular size and chemical structure, it is superior to many monomers of lower molecular mass by virtue of (a) lower volatility; (b) lower polymerisation shrinkage; (c) more rapid hardening, and (d) production of stronger and stiffer resin. In order to achieve a suitable viscosity in which to incorporate fillers, Bis-GMA is thinned with a variety of other monomers such as triethyleneglycol

dimethacrylate (TEGDMA) and dietheylene glycol dimethacrylate (DEGDMA). Some materials contain alternative monomer systems in which all or part of the Bis-GMA is replaced by aliphatic or aromatic urethane dimethacrylates (UDMA) to obtain more effective light curing, lower water absorption and greater toughness. Some products contain UDMA as the only monomer, whereas other products contain this monomer in combination with other monomers, such as Bis-GMA and TEGDMA.

1.3.2 Dispersed Phase Components (the fillers)

The filler or reinforcing ceramic phase in the early materials was a ceramic oxide, such as silica or alumina, or a glass, including some soft, hence polishable, glasses (Glenn,1982).

Recent generations of materials have been formulated with a high proportion of hard strong particles in order to produce composites of high strength, approaching that of tooth substance. A high proportion of ceramic may also reduce polymerisation shrinkage. To reduce the thermal dimensional change of the composite to a value matching that of tooth substance, fillers have been selected from the fused quartz form of silica or special glasses such as lithium aluminium silicate having zero or even negative thermal expansion coefficients. Radiopaque glasses containing elements such as Ba, Sr, and Zn have now been substituted for all or part of the silica used in earlier products (Watts, 1992).

The physical and mechanical properties of the resin composites are improved in relation to the amount of the filler added (Ferracane, 1995). However, abrasive wear and other mechanical characteristics depend on the particle size distribution and the way in which they are packed together, as well as the largest size (Watts, 1992).

1.3.3 The Interface Phase (Coupling Agent)

If optimum properties of the composite are to be achieved and maintained, it is important that the filler particles be bonded to the resin matrix. This allows the more plastic polymer matrix to transfer stresses to the stiffer filler particles. A properly applied coupling agent can impart improved physical and mechanical properties and provide hydrolytic stability by preventing water from penetrating along the filler-resin interface. The coupling agent most commonly used is organosilane 3-methoxy-propyl-trimethoxy-silane (Phillips, 1991).

This is a difunctional molecule which at one end has the characteristics of a methacrylate monomer whilst at the other it has a silane group capable of interacting and bonding with glass or quartz surfaces. Hence, it is able to set up a bond between the resin and filler components in a composite system (McCabe, 1990).

1.3.4 Viscosity Controllers

The Bis-GMA oligomer is a highly viscous liquid, so to improve the handling qualities during mixing and insertion, low viscosity liquid such as methyl methacrylate (MMA), ethylene-glycol dimethacrylate (EGDMA), or triethyleneglycol dimethacrylate (TEGDMA), (Craig 1981) is used. As mentioned above, some materials incorporate an alternative monomer system to control the viscosity, by which all or part of the Bis-GMA is replaced by aliphatic or aromatic urethane dimethacrylates.

By using an alternative monomer system lower viscosity, lower water sorption, greater toughness, but more particularly, greater susceptibility to ultraviolet (UV) or VL curing are obtained (Ruyter and Sjovik, 1981; Glenn, 1982).

1.3.5 Inhibitors and Stabilisers

Polymerisation inhibitors are used in resin composites to ensure adequate shelf life and ambient light stability by preventing premature polymerisation. They are incorporated at levels that do not inhibit the initiating system during curing. Compounds that inhibit polymerisation of the diacrylates are 4-methoxyphenol (PMP) and 2,4, b-tritertiary butyl phenol (BHT). These compounds are used in amounts of 0.1 percent or less. Both inhibitors help to provide the necessary working time during mixing, and before polymerisation is initiated (Craig, 1981).

1.3.6 Initiators

In self-cure systems, the most commonly used initiator is benzoyl peroxide (BP); 1 - 2% on the monomer. Heat, light, and some chemicals, can cause the decomposition of BP, resulting in a free radical that initiates polymerisation, so it is recommended that composites be stored in a cool, dark, clean environment.

For systems using visible light, other types of free radical initiators are employed, such as ∝1-2-diketones, e.g. benzil or camphorquinone (CQ) and an amine reducing agent: dimethyl-aminoethyl methacrylate [DMAEMA] or [DMPTI] (Taira *et al*, 1988).

1.3.7 Accelerators

Self-cure systems must be formulated in two parts such as two pastes with the initiator in one part and the accelerator in the other part.

Tertiary aromatic amines such as N, N-dimethyl-P-toluidine [DMPTI] and N,N,-dihydroxyethyl-P-toluidine [DHEPTI], are used to interact with benzoyl peroxide at room temperature to produce free radicals needed to initiate the matrix polymerisation reaction (Craig, 1981).

The DHEPTI leads to better colour stability than the traditional DMPTI (Asmussen, 1980). Yellowing of the set composite from the amine and its by-products can be minimised by the incorporation of an UV absorber; (Glenn, 1982; Smith, 1985). Dimethyl amino-ethyl methacrylate [DMAEMA] is now widely used, (Watts, 1992).

1.4 Classifications of Resin Composites

The first classification system was one introduced by Lutz and Phillips (1983) and was based on the average size of the filler particles, manufacturing techniques, and the chemical composition of the filler particles. Since then, other systems have been suggested by Marshall, *et al.,* (1988), Hosoda *et al.* (1990) and more recently Lang *et al.*, (1992).

1.4.1 Conventional composites

Conventional resin composites (Bowen, 1962; Leinfelder, 1989) are also referred to as traditional resin composites (Lutz and Phillips, 1983; Roulet and Øysaed, 1987; Hosoda *et al.*, 1990). Macrofiller particles are mechanically ground or crushed from larger pieces of purely inorganic materials such as quartz, glass, borosilicate, or a ceramic, and the size of the filler particles ranges from 1 - 100 μm (Lutz and Phillips, 1983; Hosoda *et al.*, 1990). In recent years even smaller, softer and more rounded macrofiller particles (1 - 5

μm) have been incorporated into the traditional composites (Lutz and Phillips, 1983). The particle size for this group of resin composites has also been reported as 30 - 59 μm (Leinfelder, 1991).

1.4.2 Microfilled Composites

The particles of pyrolytic silica are used exclusively in the so-called microfilled composites. These very fine particles act as thickening agents and create technical problems in mixing large amounts into liquid monomers. A few percent of these fillers are incorporated in composites based on larger particle size fillers to minimize setting out problems. Many micro-filled materials are produced by incorporation of pyrolytic silica into monomer, which is then polymerised and ground. This ground polymer, containing the dispersed filler, is then used to make a paste with further monomer. The presence of this organic filler is also an aid in reducing polymerisation contraction.

The filler loading is generally within the range 30 - 60 weight percent or 50 - 65% (Leinfelder, 1989). The average size of these filler particles is 0.04 μm (Bowen, 1962; Hosoda, 1990; McCabe 1990; Ferracane, 1995) or 0.04 – 0.2 μm (Lutz and Phillips, 1983), and 0.04 - 0.06 μm (Leinfelder, 1991).

The microfilled composites were divided into subclasses according to the type of the pre-polymerised resin fillers incorporated. These included splintered, spherical and agglomerated microfilled composites.

1.4.3 Hybrid or Blended Composites

Attempts to combine the advantages of macro and microfine fillers have led to composites containing amounts of microfine material and a major amount of silica or glass fillers with a particle size in the range of 0.5 - 5 μm. A multiplicity of combinations of sizes, shapes and particle size distributions has become available in these so-called hybrid materials (Lutz and Phillips, 1983). Improvements in the technology of grinding and dispersion of fillers have produced highly filled materials with loading up to 87 mass% (70 vol.%) that are intended for the restoration of posterior teeth (Watts, 1992).

1.5 Polymerisation

Dental composites cure by a free radical polymerisation mechanism. In the case of the self-cure system the free radicals generated by the chemical interaction of benzoyl peroxide and an amine initiated polymerisation of methacrylate groups to form a cross linked polymeric matrix (Yearn, 1985; Ruyter, 1985).

In the case of visible light activated composites, diketone, usually camphorquinone, absorbs radiation energy at an appropriate wavelength and is transferred to an excited state (triplet state). The diketone should then combine with the reducing agent to form excited state of complex (exiplex), which breaks down to give free radicals.

$$\text{diketone} \xleftrightarrow{\text{Light}} \text{diketone triplet - state} \xrightarrow{\text{reducing agent}} \text{exiplex} \rightarrow \text{radicals (R)}$$

(McGinnis, 1975; Ruyter, 1985).

Each chain addition step in the polymerisation process requires a free radical, and thus it can be seen that the degree of conversion achieved depends not only on the particular chemistry of the formulation, but on the amount of suitable light energy which reaches the catalyst (Yearn, 1985). Unlike chemically cured composites, which cure more or less evenly throughout provided they are mixed efficiently, the light cured composites cure only where light reaches them. This means that surface layers nearest the source of radiation cure more efficiently than those deeper in the body of the material (Lee, *et al.*, 1976)

1.5.1 Polymerisation Mechanism

The principal chain-reaction steps involved subsequent to photo-activation process of the materials are given below, with the associated rate-constants (k):

Photo-sensitisation	$S \longrightarrow S^*$	
	$S^* + D \longrightarrow 2R^\bullet$	
Initiation $[k_i]$	$R^\bullet + M \longrightarrow RM^\bullet$	
Propagation $[k_p]$	$M^\bullet_n + M \longrightarrow M^\bullet_{(n+1)}$	
Termination $[k_t]$	$M^\bullet_n + M^\bullet_m \longrightarrow M_{(n+m)}$	

Inhibition / retardation [k_x] $M^{\bullet}_n + X \longrightarrow M_nX^{\bullet}$ [inactive]

$R^{\bullet} + X \longrightarrow RX^{\bullet}$ [inactive]

S and *S** represents the ground state and excited state of the photosensitiser; *D* denotes the photo-reducer (usually an amine), *M* the monomer and *X* the inhibitor, while $R^{\bullet}$ and $M^{\bullet}n$ are the initiator and polymer radicals. In the presence of certain chemicals, chains transfer is a further mechanistic possibility (Watts 1992).

1.6 Methods of Studying Efficiency (Degree of Conversion)

1.6.1 Fourier Transform Infra Red (FTIR)

The degree of conversion has been measured with infra-red (IR) spectroscopy and is seen to be in the range of 30 - 80% (Ruyter and Gyorosi, 1976; Ruyter and Svendsen, 1978; Asmussen, 1982a; Ruyter and Øysaed, 1987; Eliads, *et al.*, 1987; Lekka, *et al.*, 1989; Rueggeberg, *et al.*, 1990; Reuggeberg and Caughman, 1993; Yoshida and Greener, 1994; Park, 1996).

The infra-red technique is based on measuring the decrease in the carbon-carbon double bond absorbance at 1638 - 1636 cm^{-1} of the methacrylate monomer, that occurs during polymerisation. The quantities of remaining unreacted methacrylate groups are expressed as a percentage of the total amount of methacrylate groups in the unpolymerised materials. The measurement of degree of conversion by infra-red can be influenced by the technique or sample preparation. Cook and Johansson (1987), used infra-red spectroscopy to analyse ground samples of composites dispersed in potassium bromide powder and obtained a value for *Occlusin* composites about 58%. Ruyter and Øysaed, (1987), measured the degree of conversion of the same material in similar conditions of polymerisation and obtained a value of 73 %.

1.6.2 Hardness

The surface hardness reflects the extent of cure of the resin coupled with the amount and type of the inorganic particulate filler (Watts *et al.*, 1986). At greater depths below the

surface, the extent of resin polymerisation is reduced because of the lower intensities of light penetrating to these depths (Ruyter and Øysaed, 1982; Cook and Standish, 1983; Watts *et al.*, 1984).

The variation of microhardness with time reflects changes in the resin phase. However, the relationship between degree of conversion and microhardness of the resin is not invariably a simple linear correlation (Asmussen, 1982b; Ferracane, 1985).

The measurement for hardness of composite resins is an indirect method of evaluating the relative degree of polymerisation (Leung, *et al.*, 1983; Watts, *et al.*, 1984; Rueggeberg and Craig, 1988). The hardness and degree of conversion of light-activated composites decrease with depth from the exposed surface. This effect is caused by attenuation of light by the composite (Cook, 1980; McCabe and Carrick, 1989). In general, higher hardness values are an indication of more extensive polymerisation (Watts, *et al.*, 1984; Asmussen, 1982b).

1.6.3 Shrinkage Kinetics.

The time-dependence of shrinkage reflects the kinetics and mechanism of the self-limiting polymerisation process. This kinetics may also exhibit strong dependence on temperature, which is of practical significance in connection with the fabrication of composite inlays.

1.7 Methods of Studying Shrinkage

There are two general approaches to the determination of material shrinkage: volume dilatometry or non-volume dilatometric methods. Measurement by volumetric dilatometry has disadvantages with visible light cured materials (Hay and Shorthall, 1988; Watts and Cash, 1991a&b), although valuable data have been obtained by such methods (Soltesz, *et al.*, 1986; Penn, 1986). Non-volume dilatometric measurements are usually made of one-dimensional or possibly two-dimensional strain in a material by means of a contacting or non-contacting transducers (Watts and Cash, 1991b).

Polymerisation shrinkage or contraction has been measured by different methods:

Experiments for measuring volumetric shrinkage usually follow the basic pattern used by Smith and Schoonover, (1953), *viz.* a dilatometer with a mercury-filled capillary. The measurements are made indirectly by determination of linear height changes in a column of fluid connected to a reservoir surrounding the test substance. Because of problems of access to the light source, and opacity of mercury, it is more difficult to apply such methods to light-cured (VLC) materials and at the same time to ensure that the materials are cured throughout to the appropriate degree of conversion. Also such methods are somewhat inconvenient in that critical temperature control to (preferably) ± 0.1°C is mandatory because of thermal expansion/contraction of the surrounding fluid. Even then it may be difficult to correct for the effect of polymerisation exotherm on the fluid (Hay and Shortall, 1988).

Hegdahl and Gjerdet, (1977), measured the linear polymerisation contraction by using the arms of a strain gauge extensometer. The signal from the extensometer was amplified and continuously recorded on a stripchart recorder. The disadvantage of this method is that the measurements were started 2 min after commencement of mixing.

Wilson (1978), measured the polymerisation contraction by monitoring the distortion of a flexible steel blade attached to the surface of the setting composite.

A modified dilatometer was developed by deGee *et al.*, (1981). This device can measure the polymerisation shrinkage of setting materials independently of the sample design. It can also measure the polymerisation shrinkage of chemically cured as well as photoactivated materials.

A water dilatometer was developed by Bandyopadhyay, (1982), which avoided the toxic effects of mercury vapour. The measurement difficulties of this method could be the same as those of the mercury dilatometer.

Jorgensen *et al.*, (1985), and Munksgaard *et al.*, (1987), measured the wall-to-wall polymerisation contraction of a restoration using a light microscope.

Walls, *et al.*, (1988), developed Wilson's technique, (1978), for use with light-cured composites by replacing the steel blade with a length of glass capillary tubing which was attached to the pendent end of a minimal load transducer. They were positioned in the centre of a transparent glass cover slip overlying the material under test.

Feilzer *et al.*, (1989), determined the linear curing contraction from the start of the setting reaction, using a so-called linometer device. In this set-up linear contraction is determined by means of a contactless displacement transducer. This method determines the total of pre-gel plus post-gel shrinkage. It showed that when composite was sandwiched between two discs, the axial polymerisation contraction was a function of the distance between the disc and the diameter of the specimen. As the height of the specimen was increased, the axial contraction reduced to that of the linear polymerisation contraction.

Grajower and Guelmann, (1989), determined the dimensional change of glass polyalkenoate cements by means of a linear displacement transducer. The disadvantage of this technique was that shrinkage of the material was studied 8 min after the start of mixing, thus excluding an important part of the process.

Watts and Cash, (1991a), developed the basis of a deflection disc system that was used by Wilson (1978) and a related method used by Walls *et al.*, (1988). They used an indirect method of determination, in which they calculated the volumetric contraction from the 'post-gel' linear displacement of deflection of a disc-shaped specimen sandwiched between two glass plates, in which a resin composite disk is located in the centre of a brass ring and a linear variable displacement transducer (LVDT) in contact with the top surface of the upper flexible thin glass plate. This method, with some developments, was used in this study and the instrument is fully described in chapters 6 and 7.

A strain gauge was utilised by Sakaguchi *et al.*, (1991) and Versluis, (1994) to measure the linear polymerisation shrinkage of composite restorative materials. The strain gauge appears to be suitable for real-time measurement of the curing process and for the determination of post-gel shrinkage.

Fano *et al.*, (1997), measured the linear polymerisation shrinkage of microfilled composites by using a He-Ne scanning laser beam. It is a non-contact method.

Jafarzadeh-Kashi and Watts (1998) substituted the LVDT by a laser displacement transducer to measure the polymerisation shrinkage of different thicknesses of dentin bonding resins.

1.8 Factors Affecting Polymerisation

1.8.1 Light Intensity

The effectiveness of polymerisation of light-activated restorative materials is not only dependent on the chemistry of the material, concentration of initiator, the filler particle type, size and quantity (Peutzfeldt, 1994; Harrington *et al.*, 1996), but also dependent on the amount of suitable light energy which reaches the catalyst (Yearn, 1985), light intensity and exposure time (Feilzer, *et al.*, 1995a; Harrington, *et al.*, 1996), spectral distribution, and alignment of the light tip guide (Harrington *et al.*, 1996).

With the development of light sources of improved intensity, at least a 2 - 3 mm depth of material can be polymerised in 20 - 30 s irradiation. Intensity decreases within the body of the material because of absorption and scattering of the resin and filler particles and tooth substance. Greater depths can be polymerised using longer times, e.g. up to 4 mm after 40 s (Watts, 1992).

A minimum light intensity is required to fully activate polymerisation, *circa* 400-500 $mW.cm^{-2}$ (Watts *et al.*, 1984; Rueggeberg *et al.*, 1994).

1.8.2 Temperature effects on polymerisation efficiency

The question first arises, does the temperature generated from light-curing units significantly affect polymerisation? Masutani *et al.*, (1988), reported that a higher intensity light source is more effective in curing the resins than higher temperature generated by the light source. VLC lamps emit heat. The heat itself is a function of the lamp design and does not cause the resin composite cure to take place; the visible light emitted causes the material to cure (Goodis 1989&1993). However, if high intensity radiation produces a considerable temperature rise, this will significantly affect the cure process (Watts, 1999).

A number of clinical problems can occur during polymerisation of resin composite materials. External polymerisation of these materials (e.g. inlay restorations), by elevated temperatures, often with application of pressure or intense light can minimise these problems.

Since composite inlays are subjected to an additional curing cycle either by light and dry heat or by pressure, physical properties such as compressive strength, diametral tensile strength, toughness, dimensional stability, hardness, wear and colour stability are improved (Bausch *et al.*, 1981; Davidson *et al.*, 1981; Lutz *et al.*, 1984; Wendt, 1987a & b; Inoue *et al.*, 1988; Watts, 1990). Cook and Johannson, (1987) attributed that the post-curing temperature from 5 to 100°C causes additional polymerisation and an increase in strength and conversion of double bonds.

The higher temperature will accelerate and intensify the setting reaction, resulting in higher shrinkage rates and ultimate shrinkage values (Bausch, *et al.*, 1982; Penn, 1986).

The optimum duration of heat treatment of composite resins to achieve the best wear resistance was 125°C (Wendt 1989) and 150°C causes an increase in strength and stiffness (Asmussen and Peutzfeldt, 1990).

El-Hejazi, (1995), suggested that increasing the temperature at a constant light intensity increases the cure and the shrinkage. He found that with reduced light intensity to 20.8 % and increased temperature from 23°C to 60°C, shrinkage changed from 0.08 to 0.3 %, as compared with light intensity at 100 % when the shrinkage increased from an initial measured value at 23°C of 0.84 % to a final value of 1.86 % at 60°C.

1.9 Aim of the Study

The aim of this *in vitro* study was to investigate the factors affecting the polymerisation efficiency of resin-composites.

The output-light intensity produced from light units is considered one of the main factors that affect the polymerisation efficiency of the resin-composite materials. The temperature rises from these light sources may also effect the polymerisation of these materials (chapter

2 part I and II).

The availability of a dual-intensity mode of operation [10 s low intensity plus 30 s high intensity ("soft-start")] and a "full" intensity mode [40 s high] of the Elipar unit (Espé Dental AG) led us to study their effects on polymerisation efficiency. One of the criteria to be evaluated was whether any useful network-conversion (polymerisation) can be attained by the application of the 10 s low-intensity phase of the "soft-start" mode. The polymerisation efficiency of three representative resin-based restorative materials was studied by measuring the depth-of-cure (chapter 2 part III), exotherm (chapter 3), surface hardness (chapter 4) and degree of conversion (chapter 5).

The Elipar unit was used in these studies, with four modes of irradiation: "full" and "soft-start" and either 10 s or 40 s of low-intensity light. Some specimen groups were pre-conditioned at 37°C.

The "soft-start" and full intensity curing by the Elipar and XL3000 units were also used to study the polymerisation shrinkage-**strain** kinetics (chapter 7).

Finally, the polymerisation shrinkage-**stress** kinetics (chapter 8) were measured with a newly designed apparatus, based around a cantilever load cell. The materials were cured with "full" intensity and "soft-start" modes.

Chapter 2

Output Characteristics of "Soft-start" and Conventional 'Visible-Light' Polymerisation Units

Part I: Light Intensity Output from the Light Curing Units

Part II: Temperature Rises by Irradiation

Part III: Depth of Cure Produced in Composite Restoratives

Part I

Light Intensity Output from the Light Curing Units

2.I.1 Literature Review

2.I.1.1 Advantages of Visible Light Photo-Curing (VLC)

1. It is very much less damaging to soft tissues than ultra-violet radiation.
2. It is available from simple tungsten filaments (quartz halogen) lamps, rather than a mercury discharge lamps. Such lamps are quite stable in their output intensity for long periods of time.
3. It is well transmitted by both tooth tissue and by the resin and filler components so that a full cure can be effected rather more easily.
4. VLC curing units require no warm-up period.

2.I.1.2 Disadvantages of Photo-Curing

1. The chance of possible eye damage (retinal burns with visible light systems, corneal burns with ultraviolet systems). Some procedures, such as close viewing distances, direct view applications, and treating the anterior teeth, may increase the exposure to the user. It is recommended that protective eye glasses be worn to avoid this problem (Ellingson, *et al.*, 1986).
2. Difficulty in curing deep areas of restorations.
3. Heat generated could be harmful to the pulp.

2.I.1.3 Light Intensity and the Concept of "Soft-Start" Photo-polymerisation

The development of light-activated dental materials has increased the demand for light curing units with a light intensity output capable achieving maximum polymerisation of materials. The penetration of visible light into dental biomaterials is an essential factor in photoinitiation of the setting reaction of dental aesthetics (Watts and Cash, 1994).

The dental profession should demand a high and uniform quality of all curing units because the unit is one of the most important variables when light-activated materials are used (Hansen and Asmussen, 1993b)

Several studies have shown that the curing unit is of paramount importance in obtaining good clinical results with light-activated resins (Watts, *et al.*, 1984; Yearn, 1985; Moseley, *et al.*, 1986; Fan, *et al.*, 1987; Strang, *et al.*, 1987; Hansen and Asmussen, 1997). It has been found that in some circumstances a small change in intensity may result in significant changes in resin cure, deep within the bulk of the restoration (Rueggeberg, 1993). The proper wavelength range is essential for adequate polymerisation (Takamizu, *et al.*, 1988; Rueggeberg, 1993; Pires *et al.*, 1993; Unterbrink and Muessner, 1995). The duration of light exposure is another important factor in polymerisation (Rueggeberg and Jordan, 1993; Pires *et al.*, 1993). A high degree of conversion, which is primarily related to curing intensity and exposure time, is an important factor for the longevity of a restoration (Venhoven, *et al.*, 1993).

Nevertheless, in spite of the general emphasis on high light intensity, it has been pointed out that composites cured at low light intensity have a better marginal adaptation (Uno and Asmussen, 1991; Unterbrink and Muessner, 1995). The influence of different initial cure conditions, followed by final cure with full light intensity, on the physical properties and gap formation of light-cured composites was investigated by Mehl *et al.*, (1997). It was found that ***the initial cure with low light intensity, followed by final cure with high light intensity,*** significantly improves the marginal integrity of light-cured composite fillings. They also suggested that higher initial cure intensity does not allow enough flow to reduce internal stress, whereas a lower intensity may not activate enough initiator molecules to start an adequate reaction.

The above concept of low initial intensity followed by high final intensity has come to be termed "soft-start" photo-polymerisation. It is a major concern of this thesis to explain this phenomenon.

2.I.1.4 Characterisation of light–curing units performance

The assessment of light-curing units, can be either in isolation or in combination with a selected composite material (McCabe and Carrick, 1989). Measurement of the output from light-activated units has generally been performed with the use of a radiometer (Watts, *et al.*, 1984; Fan, *et al.,* 1987; Moseley, *et al.*, 1986; McCabe and Carrick, 1989; Hansen and Asmussen, 1993b; Peutzfeldt, 1994; Rueggeberg, *et al.*, 1994; Shortall, *et al.*, 1995a).

A number of factors may be causing the variation in the light source intensity. These include fluctuation in line voltage, bulb ageing, filter degradation, fibre optic guide wear, degradation, and breakdown of electrical components within the power supply of the light activation unit (Shortall *et al.,* 1995a; Martin 1998), contamination of the guide tip by resin-composites (Shortall *et al.,* 1995a; Dugan and Hartleb, 1989) and Repeated autoclaving may eventually cause some degradation, visible as a cloudy appearance of the light guide exit window (Shortall and Harrington, 1996).

2.I.2 Objectives

The objective of this part of the study was to evaluate the light intensity of two light-curing units, using a radiometer.

2.I.3 Materials and Methods

The light intensity delivered by an Elipar Highlight unit (Espé, Dental AG, Seefeld, Germany) and XL3000 light curing unit (3M, Dental Products, St. Paul, USA) were measured.

The light intensity from the Elipar Highlight light curing unit was measured with both high intensity and low intensity. Setting in the unit, intensity of the XL3000 unit was measured at the fixed standard condition (normal light intensity).

2.I.3.1 Elipar Highlight light curing unit

The Elipar unit (Fig. 2.I-1) is manufactured by "Espè Dental AG" with a variable light intensity. The light curing unit has a light guide with a 10 mm diameter, and the wavelength of emitted light also in the range 400-500 nm.

The Elipar Highlight features a "standard" light curing setting (mode) with full light power throughout the entire polymerisation period of 40 s and alternative "2 step mode". In the "2 step mode", the lighting intensity is low during the first 10 sec and then switches automatically to full light intensity for 30 s. Hence the 2-step mode, delivers "soft-start" conditions, as defined previously.

The unit is equipped with the following:

1. Light curing time can be changed to: 20, 40, or 60 seconds. If a 20 sec light curing time is selected while the unit is in "2 step mode", the mode automatically changes to "standard". If the setting is then changed to 40 or 60 sec, the "2 step mode" or "standard" can be selected by pressing the "2 step / standard" key.
2. The unit is equipped with a "Tester" in order to test the power available in the standard mode. A two-part indicator (white and green zones) shows whether or not the output power density is sufficient for reliable polymerisation.

2.I.3.2 XL3000 light curing unit

The XL3000 unit is lightweight, and has a light-guide (8 mm diameter). The wavelength of emitted light peaks at 400-500 nm. The full light power is emitted throughout the entire curing period. The unit is equipped with a changeable light curing time of 10, 20, 30, 40 s and XL (continuous light emission with a brief beep every 10 seconds).

2.I.3.3 The radiometer used for light intensity measurement

The light intensity was measured in mW, 20 sec after switch-on of the unit using a "Power Max 500A" radiometer (PM500A) (Molectron Detector Inc., Portland, OR, USA) and PM-3 Probe (Fig 2.I-1). Five repetitions were made in each cure.

The PM500A has an analogue display, and is battery operated. This display is 3.5" mirrored analogue meter, with two scales, 0-3 or 0-10. The probe connector informs the PM500A unit what probe type is connected. Each probe has a minimum and maximum useful range. The PM500A determines which ranges are valid based on which probe type it senses through the probe connector. If an invalid range is selected, the PM500A "pegs" the meter needle beyond full scale. By means of an analogue output and an A/D computer connection signals from the radiometer could be continuously measured over a 40 s (or longer) time period. Light intensity in mW was recorded at 20 s after switch-on of the units.

2.I.3.4 Protocol for measurement of the light intensity

The full intensity from both of the light curing units was measured under the following conditions:

1. **Direct measurement**: The light optic tip was exposed directly to the PM-3 probe. With the Elipar unit, this was done for both low and full intensity settings.
2. The intensity was exposed to the probe through **a 1 mm thickness of glass plate**.
3. The intensity was exposed to the probe through **a 3 mm thickness of glass plate**.
4. The intensity was exposed to the probe through **a 2 cm length of glass rod**.

5. The intensity was exposed to the probe through **a 1 mm thickness of glass plate and a 2 cm length of glass rod.**
6. The intensity was exposed to the probe through **a 3 mm thickness of glass plate and a 2 cm length of glass rod.**

2.I.3.5 Statistical analysis

One-way ANOVA was used to compare the intensity of the light curing units under the above conditions. It was followed by multiple comparison by the "Scheffè procedure" to evaluate the statistical significance difference at $p < 0.05$ between the different groups.

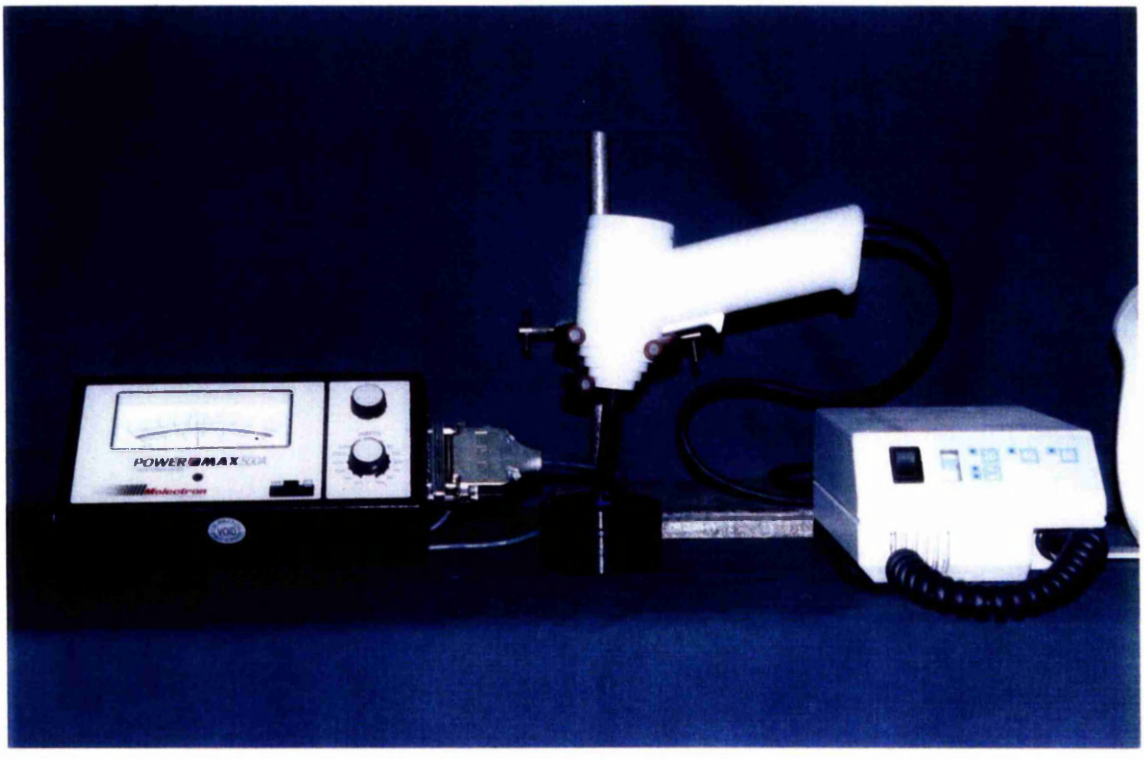

Fig 2.I-1: The Elipar light source and the radiometer used for measurement of light intensity

2.I.4 Results

Typical intensity/time recordings are illustrated in Figure 2.I.2. The results (mean values and standard deviations) for the light intensity of Elipar and XL3000 units are presented in Table 2.I-2, and graphically in Fig. 2.I-3. The full data are presented in Appendix I in CD.

Fig 2.I-3 shows the light intensity measurement with different measurement methods. The effective intensities were found to be attenuated by the increased thickness of the glass.

Statistical analysis showed a significant difference between the direct (non attenuated) light intensities measured for the Elipar (full intensity and low intensity) and the XL3000 units. The high intensity of the Elipar unit was significantly different ($p < 0.05$) from the high intensity of the XL3000 unit. The difference in the results between high intensity and low intensity of the Elipar unit were highly significant ($p < 0.05$). The low intensity was 13.7% of the high intensity. In other words, their effective low : high ratio was 1:7.

The following paragraphs next describe the statistical evaluation of the data on the attenuation of light by various glass plates or rods. This is considered separately for the Elipar (high and low settings) and XL3000 units:

(a) The direct irradiation of the high intensity of the Elipar unit was found significantly different to all of the attenuated values ($p < 0.05$). When 1 mm thick glass was used, the intensity fall by 23%. [Direct, 1 mm thick glass, 3 mm thick glass and 2 cm glass rod showed statistically significant differences to those measured with either 1 mm thick glass and 2 cm glass rod or 3 mm thick glass and 2 cm glass rod. No significant difference was found between the groups measured through 1 mm thick glass plus 2 cm glass rod and 3 mm thick glass plus 2 cm glass rod] (Table 2.I.3).

(b) The direct measurement of low intensity of the Elipar unit was found significantly different to the attenuated data ($p < 0.05$). When 1 mm thick glass was used, the intensity shows a significant difference to the rest of the measurement with greater

thickness of glasses. [1 mm thick glass showed a significant difference to those groups measured with 3 mm thick glass and 2 cm glass rod. 3 mm thick glass showed a significant difference to those groups measured with 3 mm thick glass and 2 cm glass rod. No significant different was found between the groups measured through 1 mm thick glass plus 2 cm glass rod and 3 mm thick glass plus 2 cm glass rod] (Table 2.I.4).

(c) The direct measurement of the light intensity of XL3000 was found significantly different to the attenuated data. When 1 mm thick glass was used, the intensity shows a significant difference to the rest of the measurements with greater thickness of glasses ($p = 0.000$). [1 mm thick glass showed a significant difference to those groups measured with 3 mm thick glass and 2 cm glass rod. 3 mm thick glass showed a significant difference to those groups measured with 3 mm thick glass and 2 cm glass rod. No significant difference was found between the groups measured through 1 mm thick glass plus 2 cm glass rod and 3 mm thick glass plus 2 cm glass rod] (Table 2.I.5).

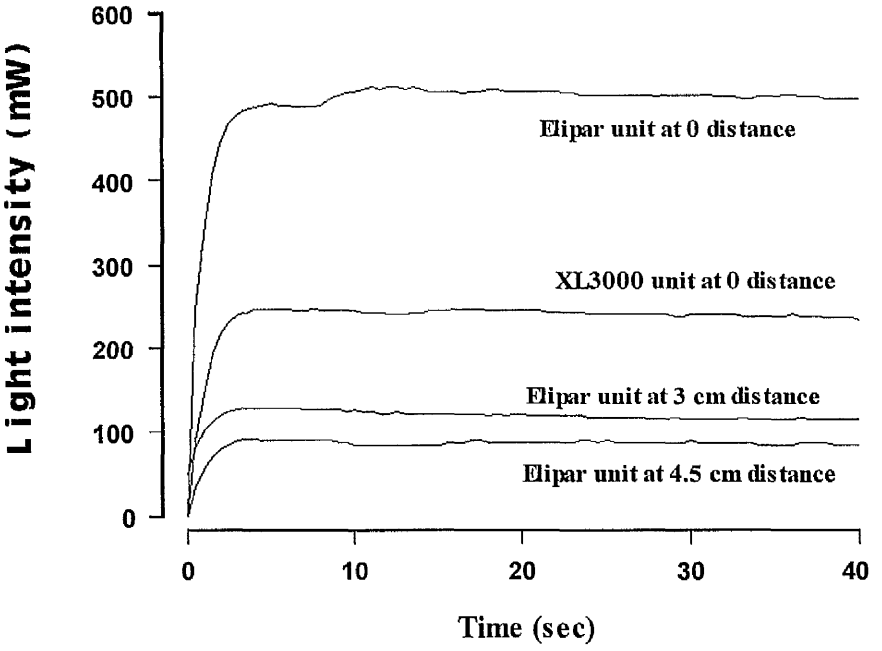

Fig. 2.I-2: The light output intensity events for Elipar and XL3000 units and the relationship between the light intensity with different distances from the radiometer probe.

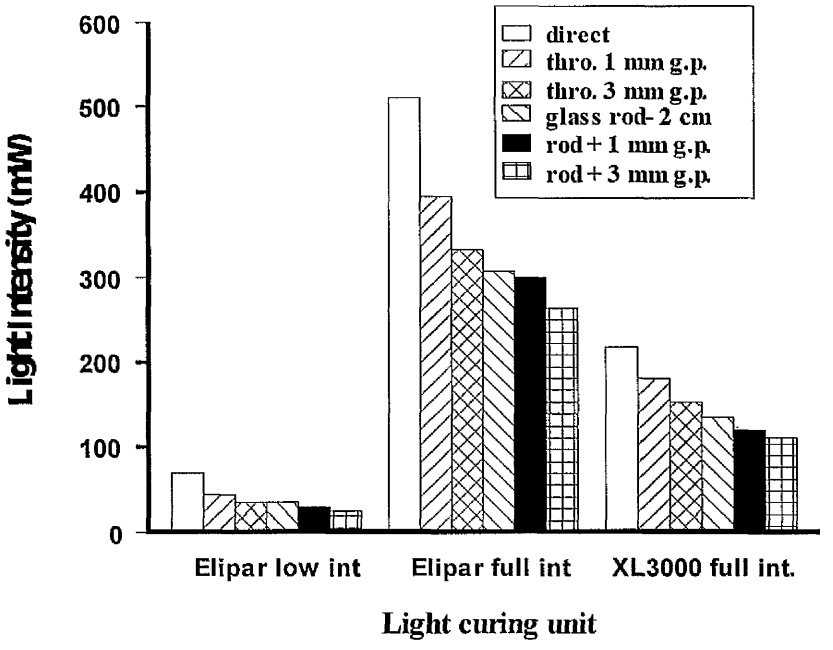

Fig. 2.I-3: Light intensity measurement of Elipar and XL3000 units, using different glass plate thicknesses (1 mm and 3 mm) and glass rod (2 cm).

Table 2.I-2: Light Intensity measurement of the light curing units (mW).

LCU	direct	thro 1 mm thick glass	thro 3 mm thick glass	thro 2 cm glass rod	thro glass rod+1 mm	thro glass rod+3 mm
Elipar (high int.)	510 (3.53)	395 (7.1)	333 (4.5)	308 (2.74)	300 (3.53)	264 (4.18)
Elipar (low int.)	70 (0)	44 (2.24)	35 (5)	34 (4.2)	29.6 (0.55)	25 (3.5)
XL3000	217 (6.7)	179 (4.2)	153 (4.5)	133 (4.47)	121 (2.24)	110 (3.53)

Table 2.I-3: Multiple comparison of means (Scheffè) for attenuated data for the high light intensity of Elipar unit.

Groups	Code	6	5	4	3	2	1
measure. Through 3 mm glass plate plus 2 cm glass rod	6						
measure. Through 1 mm glass plate plus 2 cm glass rod	5						
measure. Through 2 cm glass rod	4	*	*				
measure. Through 3 mm glass plate	3	*	*	*			
measure. Through 1 mm glass plate	2	*	*	*	*		
Direct measurement	1	*	*	*	*	*	

(*) Indicates significant differences at the level (p <0.05).

Table 2.I-4: Multiple comparison (Scheffè procedure) for attenuated data for the low intensity of the Elipar unit

Groups	code	6	5	4	3	2	1
measure. Through 3 mm glass plate plus 2 cm glass rod	Grp 6						
measure. Through 1 mm glass plate plus 2 cm glass rod	Grp 5						
measure. Through 2 cm glass rod	Grp 4	*					
measure. Through 3 mm glass plate	Grp 3	*					
measure. Through 1 mm glass plate	Grp 2	*	*	*	*		
Direct measurement	Grp 1	*	*	*	*	*	

(*) Indicates significant differences at the level (p <0.05).

Table 2.I-5: Multiple comparison (Scheffè procedure) of attenuated data for the high intensity of XL3000.

Groups	code	6	5	4	3	2	1
measurement through 3 mm glass plate plus 2 cm glass rod	Grp 6						
measurement through 1 mm glass plate plus 2 cm glass rod	Grp 5						
measurement through 2 cm glass rod	Grp 4	*					
measurement through 3 mm glass plate	Grp 3	*					
measurement through 1 mm glass plate	Grp 2	*	*	*	*		
Direct measurement	Grp 1	*	*	*	*	*	

(*) Indicates significant differences at the level (p <0.05).

2.I.5 Discussion

The effective light intensity can be measured in principle either directly by a radiometer or indirectly, by using light activated materials, measuring the depth of cure, surface hardness, and degree of conversion. The advantage of the radiometer method is that it gives an accurate quantitative value of light intensity at the effective wavelength (McCabe and Carrick, 1989).

Recently a number of light intensity meters (curing radiometers) have been marketed for dental use. They vary in design in respect to sensor aperture diameter, scale readings (analogue or digital) and units of measurement (arbitrary or mW/cm^2) (Shortall and Harrington, 1996).

The PM500A radiometer was chosen in this study to measure the light output intensity. The PM500A is an analogue power which combines speed and accuracy with versatility and ease of use. It features an easy-to-read analogue meter. This unit is under consideration by the ISO working group on powered polymerisation activations.

For the Elipar unit the full output intensity was 510 and the XL3000 unit 217 mW. These curing intensities were equivalent to 750 and 470 mW/cm^2 respectively, when they measured by Optilux radiometer (Optilux, Danbury, USA). It seems that the PM500 A possibly detects the blue light from 400 to 500 nm.

The light intensity decreased significantly when transmitted through the glass plates and rod. Thus the light intensity was absorbed, reflected, or scattered.

The light intensity emitted from the two studied light curing units was found reduced with the increased thickness of the glass plates used experimentally. As distance increases between the aperture window of the probe and the light exit of the light curing unit, thus reduces the intensity of the light (Fig. 2.I-2). This finding is in agreement with the findings of Pires *et al.*, (1993).

The exposure time and the light intensity play important factors in adequately polymerising composite resin materials. At the resin composite surface, sufficient light energy reaches and activates the photo-initiator camphorquinone, initiating polymerisation. Continuing exposure sustains the activation of photo-initiator molecules near the surface. Thus, duration of exposure is the most important factor in polymerisation of surface resin composite. However, because light is absorbed and scattered by composite resin, intensity decreases below the surface. Hence, intensity of the light source becomes a more critical factor in conversion (Rueggeberg and Jordan, 1993).

Different light intensities with the Elipar Highlight were obtained using different modes of exposure, including direct measurement 510 mW (100%). When light was exposed through various media (1 mm thick glass plate, 3 mm thick glass plate, 2 cm long glass rod, 1 mm thick glass plate with 2 cm glass rod, 3 mm thick glass plate with 2 cm glass rod), the intensities were reduced to 77.45% mW, 65.29% mW, 60.39% mW, 58.82% mW and 51.76% mW respectively.

The intensities obtained with the XL3000 unit using the same modes of exposure gave for direct measurement: 217 mW (100%). When light was exposed through the attenuating media (1 mm thick glass plate, 3 mm thick glass plate, 2 cm long glass rod, 1 mm thick glass plate with 2 cm glass rod and 3 mm thick glass plate with 2 cm glass rod) the intensities were reduced to 82.49% mW, 70.51% mW, 61.29% mW, 55.76% mW and 50.69% mW respectively.

The low light intensity of the Elipar unit was one seventh of full intensity. The question remains to what extent this low intensity can begin to polymerise the composite material? Can a "soft-start" approach reduce the polymerisation shrinkage-strain and thus reduce the shrinkage-stress?

The exposure time and the light intensity play important factors in adequately polymerising composite resin materials. At the resin composite surface, sufficient light energy reaches and activates the photo-initiator camphoroquinone, initiating polymerisation. Continuing exposure sustains the activation of photo-initiator molecules near the surface. Thus, duration of exposure is the more important factor in polymerisation of surface resin composite. However, because light is absorbed and scattered by composite resin, intensity decreases below the surface. Hence, intensity of the light source becomes a more critical factor in conversion (Rueggeberg and Jordan, 1993).

Different light intensities with the Elipar Highlight were obtained using different modes of exposure, including direct measurement 510 mW (100%). When light was exposed through various media (1 mm thick glass plate, 3 mm thick glass plate, 2 cm long glass rod, 1 mm thick glass plate with 2 cm glass rod, 3 mm thick glass plate with 2 cm glass rod), the intensities were reduced to 77.45% mW, 65.29% mW, 60.39% mW, 58.82% mW and 51.76% mW respectively.

The intensities obtained with the XL3000 unit using the same modes of exposure gave for direct measurement: 217 mW (100%). When light was exposed through the attenuating media (1 mm thick glass plate, 3 mm thick glass plate, 2 cm long glass rod, 1 mm thick glass plate with 2 cm glass rod and 3 mm thick glass plate with 2 cm glass rod) the intensities were reduced to 82.49% mW, 70.51% mW, 61.29% mW, 55.76% mW and 50.69% mW respectively.

The low light intensity of the Elipar unit was one seventh of full intensity. The question remains to what extent this low intensity can begin to polymerise the composite material? Can a "soft-start" approach reduce the polymerisation shrinkage-strain and thus reduce the shrinkage-stress?

2.I.6 Conclusions

1. The Elipar unit emitted higher output intensity than the XL3000 unit.
2. The low intensity setting of the Elipar unit was found to be 13% of full intensity, (ratio 1:7).
3. The light intensity decreased with increased glass thickness.

Part II

Temperature Rise by Irradiation

2.II.1 Literature Review

Visible light curing is accompanied by the production of heat (with a consequent rise in temperature) (Adamson, *et al.,* 1988), as well as the materials themselves emitting heat during the cure which is a matter of clinical interest since excessive heating will damage the pulp. The pulp must be protected against the thermal shock of some composite resins by the use of a liner (Watts *et al.*, 1983).

The temperature rise from the light sources was measured either in isolation or in combination with a dental biomaetrials by using a differential thermal analyser (DTA) (Adamson *et al.*, 1988; McAndrew *et al.*, 1987), and a thermocouple (Goodis *et al.*,1989 and 1993; Kanchanavasita *et al.,* 1996).

It was found that a significant temperature rise can take place beneath the cement lining during the light curing of overlying composite. The light is the source of much of this heat and the magnitude of the rise depends on the unit chosen (McAndrew *et al.*, 1987; Adamson *et al.*, 1988; Goodis *et al.,* 1989).

VLC lamps produce heat in dental materials, even with low light intensity. This phenomenon of the output of light curing unit has been noticed by many researchers (McCabe, 1985; Lloyd *et al.*, 1986; McAndrew *et al.*, 1987; Goodis *et al.*, 1993).

The visible light cure lamps varied in the amount of heat emitted (Goodis *et al.*, 1993) and the temperature rise increases with exposure time (Adamson *et al.*, 1988; Goodis *et al.,* 1989; Kanchanavasita *et al.,* 1996).

2.II.2 Objectives

The objective of this part of the study was to measure the temperature rise from two light curing sources with different intensities applied for time. The effect of using light attenuating glass plates was also to be investigated, because of the importance of this factor in polymerisation shrinkage strain and stress measurements, to be described later.

2.II.3 Materials and Methods

Two light curing units were investigated in this study. 1) Elipar Highlight and 2) XL3000.

The instrument used to measure the temperature rises from light sources was simple and gave direct measurement.

The tip of a type k thermocouple (CRS Components, Corby, UK) was secured onto a series of glass plates with tape. The tip of the thermocouple wire was left exposed to permit direct irradiation. The thermocouple was connected to a battery-powered amplifier and display unit, reading in °C. The light guide tip of the evaluated curing units was centrally positioned over the thermocouple tip (Fig 2.II-1).

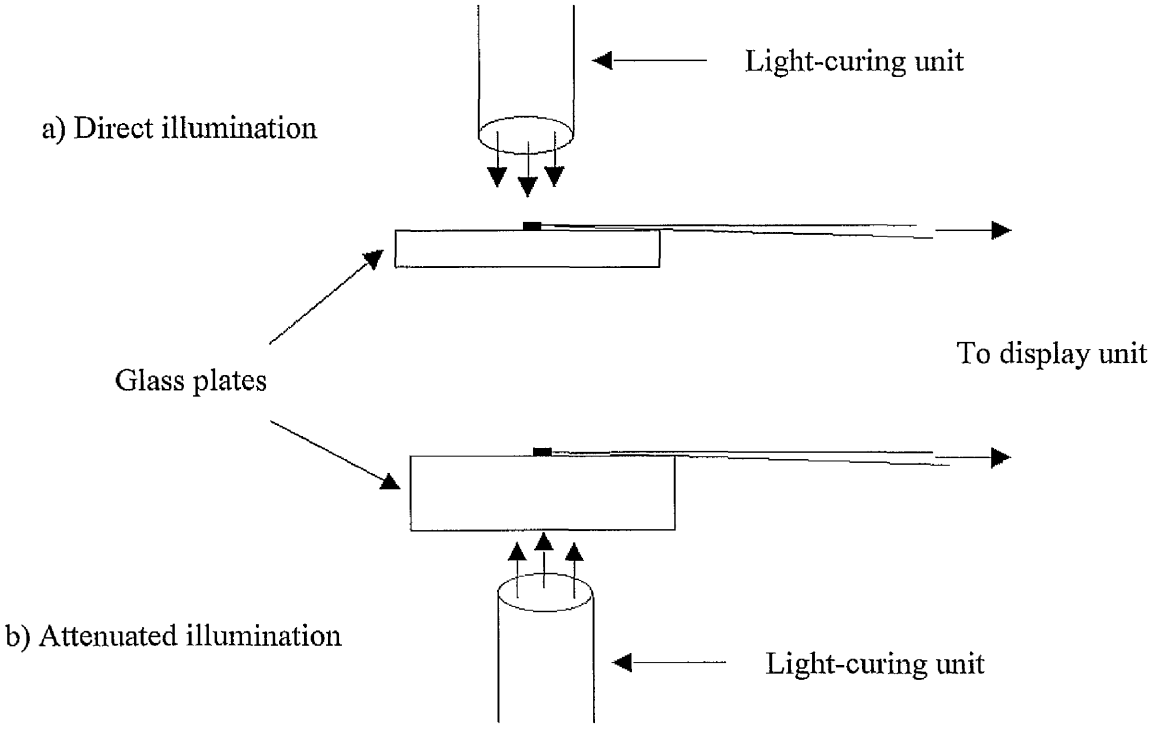

Fig. 2.II.1 Direct versus attenuated illumination of a thermocouple tip (type K) attached to a glass plate of thickness d (d = 1 mm or 3 mm). A glass rod was used in further experiments (not illustrated).

2.II.3.1 Measurement of the Temperature of the Light-Curing Units

The temperature of the light curing units was measured with the following attenuation conditions as follows:

1. The temperature was measured with the light exposed **directly on to the thermocouple tip**.
2. The temperature was measured through **a 1 mm thickness of glass plate.**
3. The temperature was measured through **a 3 mm thickness of glass plate.**
4. The temperature was measured through **a 1 mm thickness of glass plate and a 2 cm length of glass rod**.
5. The temperature was measured through **a 3 mm thickness of glass plate and a 2 cm length of glass rod**.

The temperature rise from Elipar unit were measured with low and high intensity settings. The XL3000 unit produced only a fixed light intensity, high intensity.

The measurements were performed at different exposure times, 10, 20, 30, 40, 60, 90, 120, and 180 sec. The measurement was repeated five times for each of the exposure times of the VLC and each light intensity. The temperature was allowed to return to room temperature ($23^{\circ}C \pm 1$) between each repeat.

2.II.3.2 Statistical Analysis

The data of the temperature rise from light sources due to increase in exposure time were statistically analysed using one-way analysis of variance (ANOVA) followed by the multiple comparison procedure (Scheffé) at $p < 0.05$.

2.II.4 Results

The mean values and standard deviations of the temperature rise from light curing units are presented graphically in Figs 2.II-2 to 2.II-4 and in Tables 2.II-1 to 2.II-3. The full data are represented in Appendix II in CD. The observed temperature rise can, of course, be directly interpreted as resulting from heat generation phenomenon.

Fig. 2.II-1 and Table 2.II-2 indicate that the heat generated from the Elipar source with full intensity increased with increased exposure duration and decreases with glass thickness. Direct exposure gave the greatest rises. The 1 mm thick glass plate reduced the temperature to 67% of the direct exposure with the Elipar curing unit for 40 s exposure. The result of the post hoc test (Scheffé) of the difference with increased time is shown in Table 2.II-4 ($p < 0.05$).

Fig. 2.II-3 and Table 2.II-2 show the temperature rise with low intensity light from the Elipar unit. The result of the post hoc test (Scheffé) of the effect of increased exposure time is shown in Table 2.II-5 ($p < 0.05$). The temperature rise increased with exposure time, in most cases.

The XL3000 light curing unit produced lower temperature rise than the Elipar Highlight at full intensity, (Fig. 2.II-4 and Table 2.II-3). Table 2.II.6 shows the statistical difference in the temperature rise with the increased irradiation time ($p < 0.05$).

The relationship between the light intensity and the temperature rise of the investigated light curing sources with different attenuation methods is demonstrated in Fig 2.II-5.

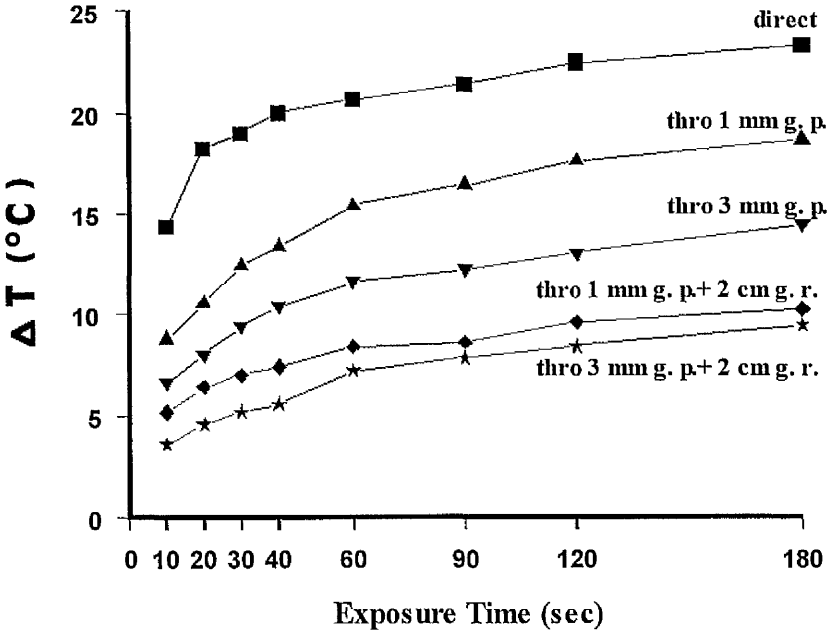

Fig. 2.II-2: Temperature rises produced by the Elipar unit with its full intensity setting. Where g. p. is glass plate and g. r. is glass rod.

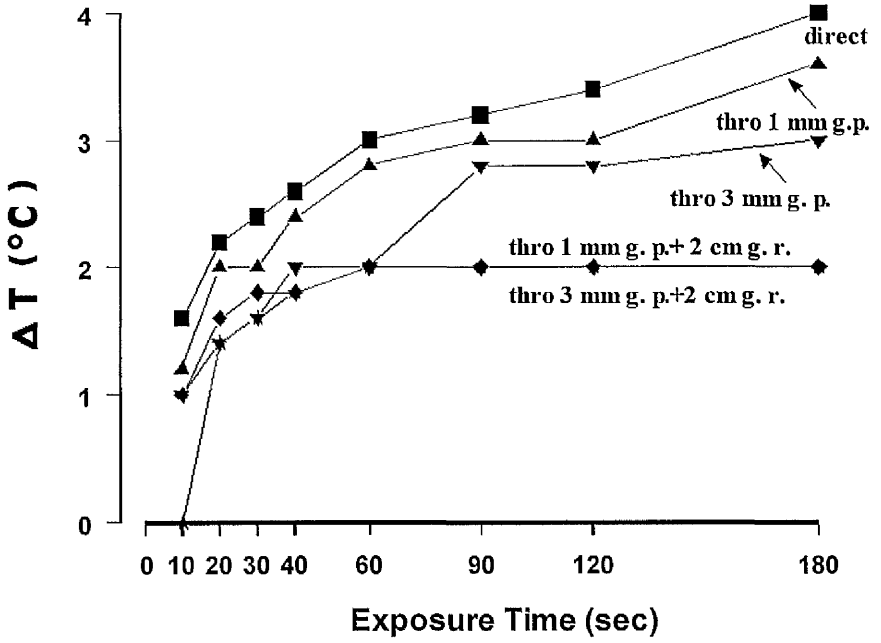

Fig. 2.II-3: Temperature rises produced by the Elipar unit with its low intensity setting.

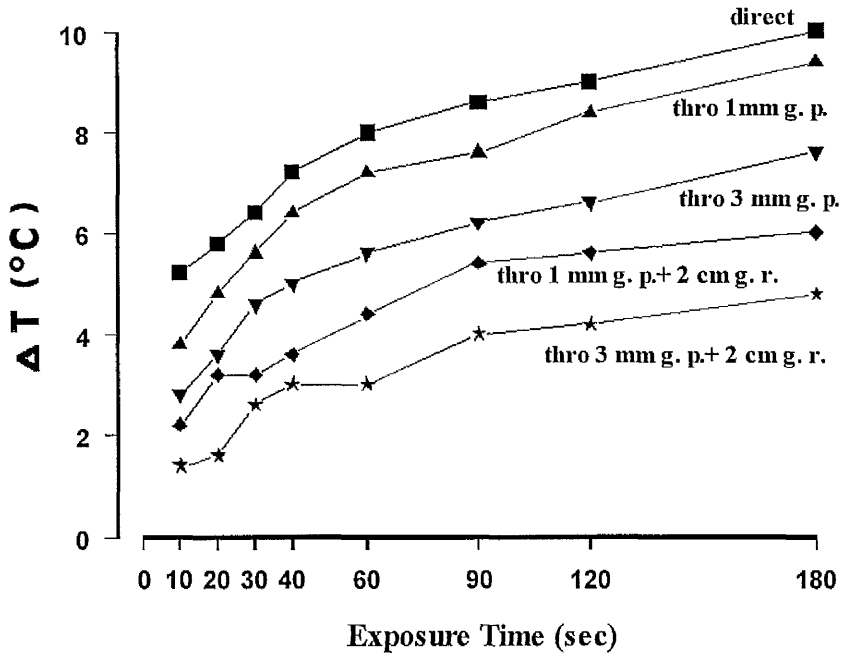

Fig. 2.II-4: Temperature rise produced by the XL3000 unit.

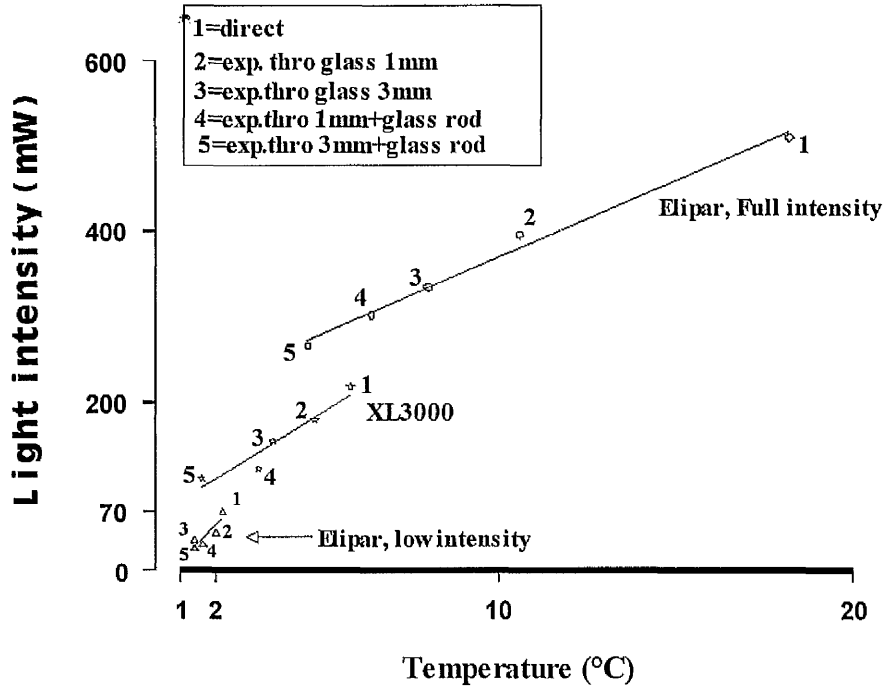

Fig. 2.II-5: Relationship between light intensity and temperature rise of the light-curing units.

Table 2.II-1: Mean values and SD (in parenthesis) of temperature increase "T" of the **Elipar unit with high light intensity**.

Time (sec)	Exposure method				
	1*	**2***	**3***	**4***	**5***
10	14.4 (0.89)	8.8 (0.45)	6.6 (0.54)	5.2 (0.45)	3.6 (0.5)
20	18.2 (1.64)	10.6 (0.55)	8 (0.71)	6.4 (0.55)	4.6 (0.55)
30	19 (1.58)	12.4 (0.55)	9.4 (0.55)	7 (0.71)	5.2 (0.45)
40	20 (1.58)	13.4 (0.55)	10.4 (0.55)	7.4 (0.55)	5.6 (0.55)
60	20.6 (1.14)	15.4 (0.55)	11.6 (0.55)	8.4 (0.55)	7.2 (0.45)
90	21.4 (0.89)	16.4 (0.54)	12.2 (0.45)	8.6 (0.55)	7.8 (0.45)
120	22.4 (0.89)	17.6 (0.45)	13 (0.71)	9.6 (0.55)	8.4 (0.55)
180	23.2 (0.82)	18.6 (0.55)	14.4 (0.55)	10.2 (0.45)	9.4 (0.45)

1* = direct exposure to thermocouple;

2* = exposure through 1mm thick glass plate;

3* = exposure through 3mm thick glass plate;

4* = exposure through 1mm thick glass plate with 2 cm glass rod;

5* = exposure through 1mm thick glass plate with 2 cm glass rod.

Table 2.II-2: Mean values and SD (in parenthesis) of temperature increase of the **Elipar unit with low intensity.**

Time (sec)	Exposure method				
	1*	**2***	**3***	**4***	**5***
10	1.6 (0.55)	1.2 (0.45)	1 (0)	1 (0)	0
20	2 (1)	2 (0)	1.6 (0.55)	1.4 (0.55)	1.4 (0.55)
30	2.4 (0.89)	2 (0)	1.8 (0.55)	1.6 (0.55)	1.6 (0.55)
40	2.6 (0.55)	2.4 (0.45)	2 (0)	1.8 (0.45)	1.8 (0.45)
60	3 (0)	3 (0)	2 (0)	2 (0)	2 (0)
90	3.2 (0.45)	3 (0)	2.8 (0.45)	2 (0)	2 (0)
120	3.4 (0.55)	3 (0)	2.8 (0.45)	2 (0)	2 (0)
180	4 (0.71)	3.6 (0.5)	3 (0)	2 (0)	2 (0)

1* = direct exposure to thermocouple;

2* = exposure through 1mm thick glass plate;

3* = exposure through 3mm thick glass plate;

4* = exposure through 1mm thick glass plate with 2 cm glass rod;

5* = exposure through 1mm thick glass plate with 2 cm glass rod.

Table 2.II-3: Mean values and SD (in parenthesis) of temperature increase of **XL3000 unit.**

Time (sec)	Exposure method				
	1*	**2***	**3***	**4***	**5***
10	5.2 (0.84)	3.8 (0.45)	2.8 (0.45)	2.2 (0.45)	1.4 (0.55)
20	5.8 (0.84)	4.8 (0.45)	3.6 (0.55)	3.2 (0.45)	1.6 (0.55)
30	6.4 (0.89)	5.6 (0.55)	4.6 (0.54)	3.2 (0.45)	2.6 (0.45)
40	7.2 (0.45)	6.4 (0.55)	5 (0.71)	3.6 (0.89)	3 (0)
60	8 (0.71)	7.2 (0.42)	5.6 (0.55)	4.4 (0.55)	3 (0)
90	8.6 (0.89)	7.6 (0.55)	6.2 (0.45)	5.4 (0.55)	4 (0)
120	9 (0.71)	8.4 (0.55)	6.6 (0.55)	5.6 (0.89)	4.2 (0.45)
180	10 (0.71)	9.4 (0.55)	7.6 (0.55)	6 (0.71)	4.8 (0.45)

1* = direct exposure to thermocouple;

2* = exposure through 1mm thick glass plate;

3* = exposure through 3mm thick glass plate;

4* = exposure through 1mm thick glass plate with 2 cm glass rod;

5* = exposure through 1mm thick glass plate with 2 cm glass rod.

Table 2.II-4: Multiple comparison (Scheffé) of exposure time on temperature rise from the Elipar unit, with high intensity.

Comparison of duration	Direct measurement	thro. 1 mm thick	thro. 3 mm thick	thro. 1 mm + 2 cm glasses	thro. 3 mm+ 2 cm glasses
10 vs 20					
10 vs 30		*	*		*
10 vs 40	*	*	*		*
10 vs 60	*	*	*	*	*
10 vs 90	*	*	*	*	*
10 vs 120	*	*	*	*	*
10 vs 180	*	*	*	*	*
20 vs 30					
20 vs 40		*	*		*
20 vs 60	*	*	*		*
20 vs 90	*	*	*	*	*
20 vs 120	*	*	*	*	*
20 vs 180	*	*	*	*	*
30 vs 40					
30 vs 60		*			
30 vs 90	*	*	*	*	*
30 vs 120	*	*	*	*	*
30 vs 180	*	*	*	*	*
40 vs 60					
40 vs 90				*	
40 vs 120		*	*	*	*
40 vs 180	*	*	*	*	*
60 vs 90					
60 vs 120					*
60 vs 180	*	*	*		*
90 vs 120					
90 vs 180		*	*		
120 vs 180					

(*) Indicates significant differences at the level $p < 0.05$.

Table 2.II-5: Multiple comparison (Scheffé) of exposure time on temperature rise from the Elipar unit, with low intensity.

Comparison of duration	Direct measurement	thro. 1 mm thick	thro. 3 mm thick	thro. 1 mm + 2 cm glasses	thro. 3 mm+ 2 cm glasses
10 vs 20					
10 vs 30		*		*	*
10 vs 40		*	*	*	*
10 vs 60		*	*	*	*
10 vs 90		*	*	*	*
10 vs 120	*	*	*	*	*
10 vs 180	*	*	*	*	*
20 vs 30					
20 vs 40					
20 vs 60		*			
20 vs 90		*	*		
20 vs 120		*	*		
20 vs 180	*	*	*		
30 vs 40					
30 vs 60					
30 vs 90					
30 vs 120			*		
30 vs 180		*	*		
40 vs 60					
40 vs 90					
40 vs 120					
40 vs 180		*	*		
60 vs 90					
60 vs 120					
60 vs 180			*		
90 vs 120					
90 vs 180					
120 vs 180					

(*) Indicates significant differences at the level $p < 0.05$.

Table 2.II-6: Multiple comparison (Scheffé) of exposure time on temperature rise from the XL3000 unit.

comparison of duration	Direct measurement	thro. 1 mm thick	thro. 3 mm thick	thro. 1 mm + 2 cm glasses	thro. 3 mm+ 2 cm glasses
10 vs 20					
10 vs 30		*	*		*
10 vs 40	*	*	*		*
10 vs 60	*	*	*	*	*
10 vs 90	*	*	*	*	*
10 vs 120	*	*	*	*	*
10 vs 180	*	*	*	*	*
20 vs 30					
20 vs 40		*	*		*
20 vs 60	*	*	*		*
20 vs 90	*	*	*	*	*
20 vs 120	*	*	*	*	*
20 vs 180	*	*	*	*	*
30 vs 40					
30 vs 60		*			
30 vs 90	*	*	*	*	*
30 vs 120	*	*	*	*	*
30 vs 180	*	*	*	*	*
40 vs 60					
40 vs 90				*	
40 vs 120		*	*	*	*
40 vs 180	*	*	*	*	*
60 vs 90					
60 vs 120					*
60 vs 180	*	*	*		*
90 vs 120					
90 vs 180		*	*		
120 vs 180					

(*) Indicates significant differences at the level $p < 0.05$.

2.II.5 Discussion

Underlying glass plates were used in the present experiments as a substrate in which to measure the temperature rise from the visible light sources. Different thicknesses of glass plates were used to discover how much the temperature rise can be minimised. The glass plates in the temperature rise measurements were also employed to determine factors influencing polymerisation shrinkage measurements, to be described later.

This simple experimental model gives information of relative, but not absolute clinical significance. That is, the ranking of temperature rise should be approximately the same intra-orally, but the actual temperature levels might differ significantly. Peak temperatures curve not attained until after 2 – 3 min irradiation, which is longer than normal clinical exposure.

The temperature rises decreased dramatically when the light was shone through different glass thicknesses, presumably due to the absorption or reflection of the light.

It was evident that the Elipar unit generated higher heat at its high intensity level. The heat emitted from the Elipar unit with its high intensity was found to be 20°C at 40 s. of exposure, when measured directly by the thermocouple. This heat was attenuated with the use of different glass thicknesses. With 1 mm thick glass and 3 mm thick glass, the heat emitted at 40 s duration was 13.4°C and 10.4°C respectively. The question remains to what extent can the increment of the restoration reduce the pulpal temperature rise from these units?

The Elipar generates a lower temperature rise with its low light intensity. This finding in agreement with (McCabe, 1985; Lloyd *et al.*, 1986; McAndrew *et al.*, 1987; Goodis *et al.*, 1993). This rise in temperature was decreased with increasing the glass plate.

It seems to be that the heat generated from the XL3000 unit is more acceptable. As seen from the results, with an exposure time of 20 sec to 60 sec the temperature increased from 5.8°C to 8°C, while with a glass thickness of 3 mm, the temperature ranged from

3.6°C to 5.6°C. This means temperature rise the heat reduced with increased glass thickness.

Increased exposure time will lead to increasing of rising temperature in the tooth at full light intensity for both of the tested light-curing units. This result coincides with the finding of Adamson *et al.*, (1988); Goodis *et al.*, (1989); Kanchanavasita *et al.*, (1996). This study also showed that the increased in light intensity linearly increases the temperature rise.

2.II.6 Conclusions

The temperature generated from the Elipar Highlight was higher than that generated from the XL3000 light curing unit. The longer the exposure time, the greater was the increase in the temperature rise up to 120 – 180 s.

Part III

Depth of Cure Produced by the Light-Curing Unit

5.III.1 Literature Review

The presence of partially polymerised or unpolymerised material is undesirable as it can lead to increased solubility and inferior mechanical properties (Buonocore and Davita, 1973; Lee, *et al.,* 1976), and failure of retention of the restoration (Young, 1977). Mechanically, the restoration may be compromised by the reduced strength and hardness of the resin (DeWald and Ferracane, 1987). In addition, uncured components may be leached from the restoration, causing pulpal damage (Young, 1977), local tissue irritation and possibly an increased potential for secondary caries (Inoue and Hayashi, 1982; DeLange, *et al.*, 1980).

Depth of cure can be defined as the level at which the hardness value is equivalent to at least 90% of the hardness at the surface of the composite (Skeeters, *et al.*, 1983). The method that has been most widely used for the evaluation of polymerisation efficiency of light-activated composite systems has been the measurement of depth of cure.

Several techniques have been used to measure the depth of cure of resin-composites, including microhardness profiles (DeLange *et al.*, 1980; Watts *et al.*, 1984; Matsumoto, *et al.*, 1986), a simple scrape test which involves scraping away uncured material and measurement of the length of the residual hard material (Leung, *et al.*, 1984; Hansen and Asmussen, 1993a); an optical assessment of the boundary between cured and uncured material detected by changes in translucency (Newmann, *et al.*, 1983); degree of conversion, measured by IR spectroscopy (DeWald and Ferracane, 1987) and a penetrometer technique whereby cylinders of composites contained in stainless steel moulds were irradiated from one end and then a penetrometer needle inserted into the other end under standard conditions (McCabe and Carrick, 1989; Harrington and Wilson, 1993; Shortall, *et al.*, 1995a and b).

2.III.1.1 Factors affecting the depth of cure

1. Chemical composition of the resin composite

Depth of cure is dependent upon the light permeability of the filler, as well as monomer composition and type and concentration of initiator, inhibitor, and accelerator in the resin materials (Nomoto and Hirasawa, 1992; Shortall, *et al.*, 1995b).

2. The type of resin composite filler

The transmission coefficient or attenuation factor of a composite is an indication of the reduction of photo-activating light intensity passing through the composites. Because of greater light scattering by the smaller filler particles, they have lower transmission coefficients and normally shallower depth of cure (Council on Dental Materials, 1982; Tirtha, *et al.*, 1982).

Curing depth is influenced by the shape of inorganic filler particles. Scattering and attenuation of light is generally considered to be less in spherical particle filled material than in splintered powder filled material (Tanoue, *et al.*, 1998a).

3. The intensity of the light source and irradiation time

Previous workers indicated that the depth of cure greatly depends upon light intensity (McCabe and Carrick, 1989; Harrington and Wilson 1993 and 1995; Peutzfeldt, 1994). As light passes through the bulk of composite to cause curing, it is absorbed and scattered. These result in an attenuation of light intensity as it passes through the restoration bulk (Rueggbereg, *et al.*, 1993). Hansen and Assmusen (1997) explained the relationship between the light intensity and the depth of cure by that the irradiation produces free radicals, which in their turn cause growth of polymer chains. The light penetrates the upper part of the resin, but absorption in the material prevents the light from reaching the deeper parts. The free radicals generated in the upper parts initiate polymerisation, but the polymerisation will not propagate in depth beyond a certain limit, so the deeper sections of the resin remain unpolymerised.

The recommended irradiation time for most of proprietary resins was 20 s, but many researchers have since recommended cure cycles of not less than 40 s in order to increase the conversion and the depth of cure (Swarts, *et al.*, 1983; Yearn, 1985; and Takamizu, *et al.*, 1988). However, the most essential variable for light-activated resins, both as to degree of conversion and depth of cure, is the curing unit itself (Watts, *et al.*, 1984; Yearn, 1985; Moseley, *et al.*, 1986; Fan, *et al.*, 1987; Takamizu *et al.*, 1988).

4. The proximity of the light unit

The relation between light intensity and distance of light-tip is dependent on several factors, one of which is the degree of divergence of the light beam leaving the exit window. With a completely parallel beam, the loss of intensity is minimal, whereas a highly diverging beam would give rise to significant reductions in intensity with distance (Hansen and Asmussen 1997).

5. Mould materials and dimensions

The depth of cure measurement was greater with using plastic moulds than those made in metal (Yearn, 1985; McCabe and Carrick, 1989). Harrington and Wilson (1993) also found that the depth of cure greater with using PTFE mould than those measured with using either stainless steel or Black Nylotron moulds and increased with increasing the size of the mould cavity.

2.III.2 Objectives

The purpose of this work was to assess the efficacy of soft-start polymerisation (low intensity followed by high intensity) on the depth of cure of different composite resin materials.

2.III.3 Materials and Methods

Three materials were examined in this study (Table 2.III-1).

Table 2.III-1: Composite resin materials used:

Material	Code	Batch No.	Filler size (μm)	Shade	Manufacturer
Z 100	**Z100**	5904A3	0.01 - 3.5	A3	3M Dental Products, St. Paul, USA
Charisma F	**CHRF**	055	0.02 - 2.0	A2	Heraeus Kulzer, Wehrheim, Germany
Pertac II	**PER2**	643081003	0.10 - 2.0	A3	Espé Dntal AG, Seefeld, Germany

The composite materials were packed into open ended split stainless steel moulds, 4 mm diameter and 6 mm high. Each mould was pressed between two celluloid strips and two glass slides to remove the excess material. The specimens were irradiated from the top surface of the mould with the Elipar light-curing unit for a determined time and light intensity. The tip of the light output was positioned at zero distance from the mould.

The irradiation time and light intensity were performed as follows:

1. 40 s. high light intensity.
2. "Soft-start" exposure (10 s. low light intensity + 30 s. high intensity).
3. 40 s. low light intensity.
4. 10 s. low intensity

2.III.3.1 Instrument used for measurement of depth of cure

The instrument used in this study consists of a penetrometer fitted with a digital meter which could be zeroed at any position within its total traverse. At the base of the movable part of the meter, a needle indentor of 0.5 mm diameter was mounted. The position of the needle can be determined in mm. Initially, the read-out was zeroed when the needle contacted the base of the specimen.

Five specimens per group, for each light intensity, from each material were prepared for depth of cure measurements. At 5 s from the end of the irradiation period, the specimens within the moulds were indented with the penetrometer needle (Fig 2.III-1) at the opposite end. The micrometer was used to displace the penetrometer needle within the specimen until it reached the hardened irradiated surface. The reading of the penetration was taken after 20 sec. The penetration result was subtracted from the mould height to determine the depth of cure. Measurements were made at the centre of the specimen.

2.III.3.2 Statistical Analysis

The values of the depth of cure were compared by two-factor analysis of variance (ANOVA) for the effect of the light intensities on the investigated materials. One-way ANOVA and, Scheffé multiple comparison tests were further performed for each investigated material.

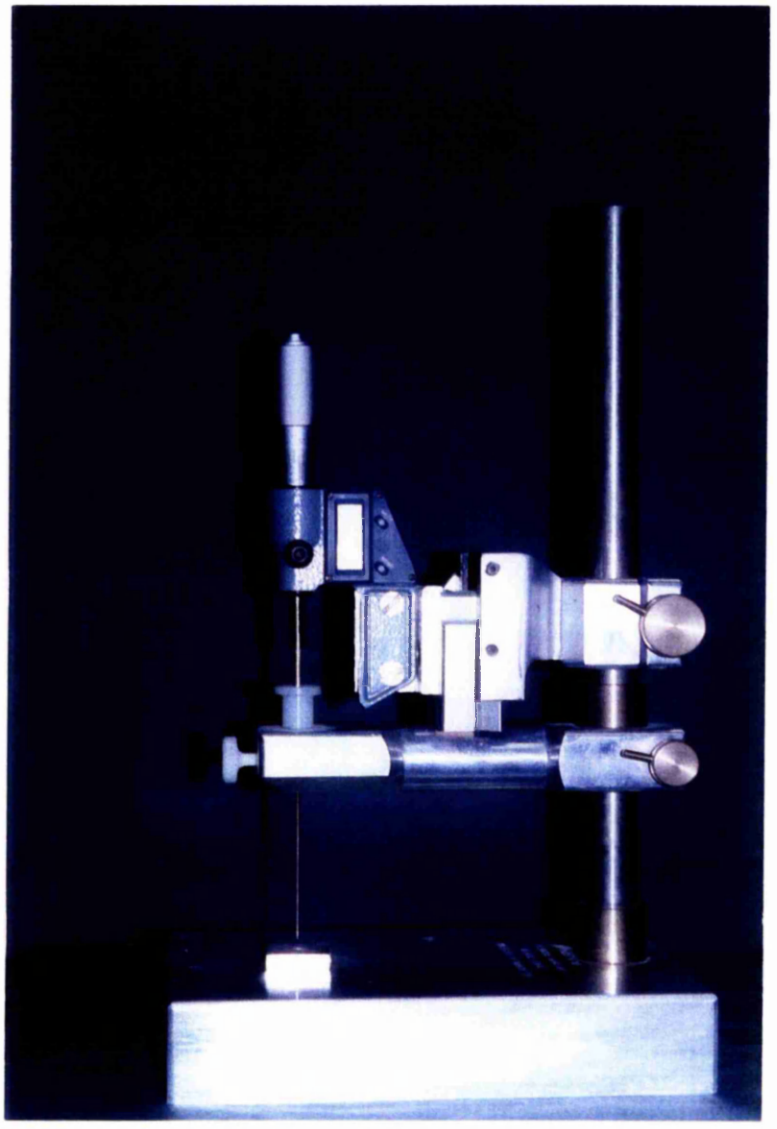

Fig. 2.III-1: The penetrometer instrument used to measure the depth of cure of the composite resin material.

2.III.4 Results

The mean values and standard deviations of the depth-of-cure of the investigated materials are represented in Tables 2.III-2 to 2.III-4 and the data also plotted graphically in Figs 2.III-2 to 2.III-4.

There were significant effects ($p < 0.05$) on the depth-of-cure of the investigated materials with the variation of the light intensities.

Table 2.III-6 and Fig. 2.III-2 demonstrate that the depth-of-cure of **Z100** was unaffected by the "soft-start" curing. There was no significant difference between those specimens cured with "soft-start" and high light intensity. The specimens cured by "soft-start" and high light intensity were significantly different to those cured with either 10 or 40 s low intensity. The depth-of-cure of samples cured with 10 and 40 s low intensity was significantly different.

Table 2.III-7 and Fig. 2.III-3 exactly the same picture was observed with **CHRF** except that depth-of-cure of samples that cured by 40 s low intensity was not significantly different than those which cured by 10 s low intensity.

The same similarities and differences between groups was apparent with **PER2** as was seen with **Z100**, as illustrated in Fig. 2.III-4 and the statistic is summarised in Table 2.III.8.

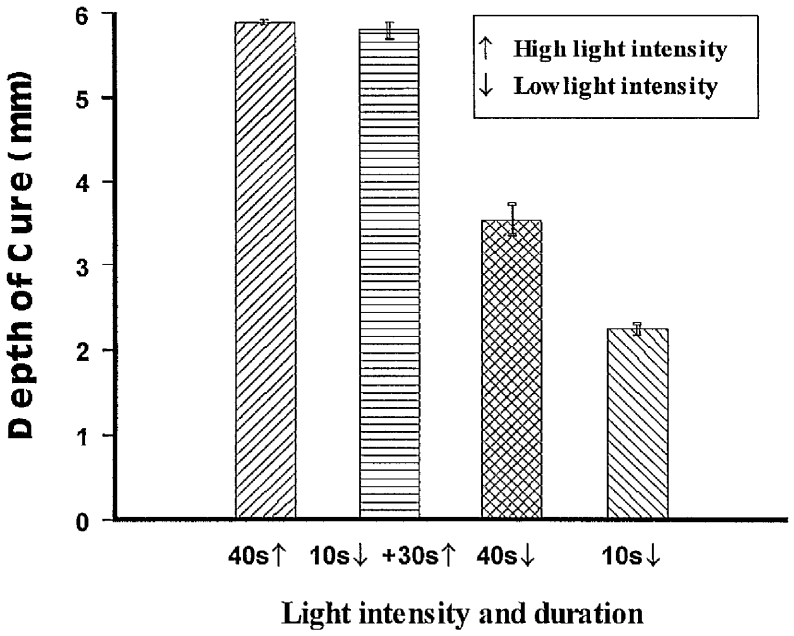

Fig 2.III-2: The effect of light intensity and duration on depth of cure of **Z100**.

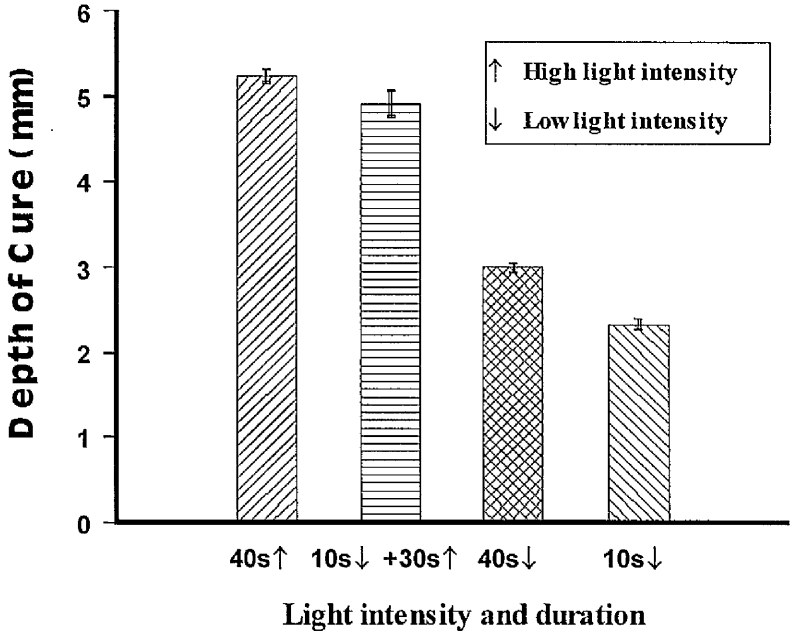

Fig 2.III-3: The effect of light intensity and duration on depth of cure of **CHRF**.

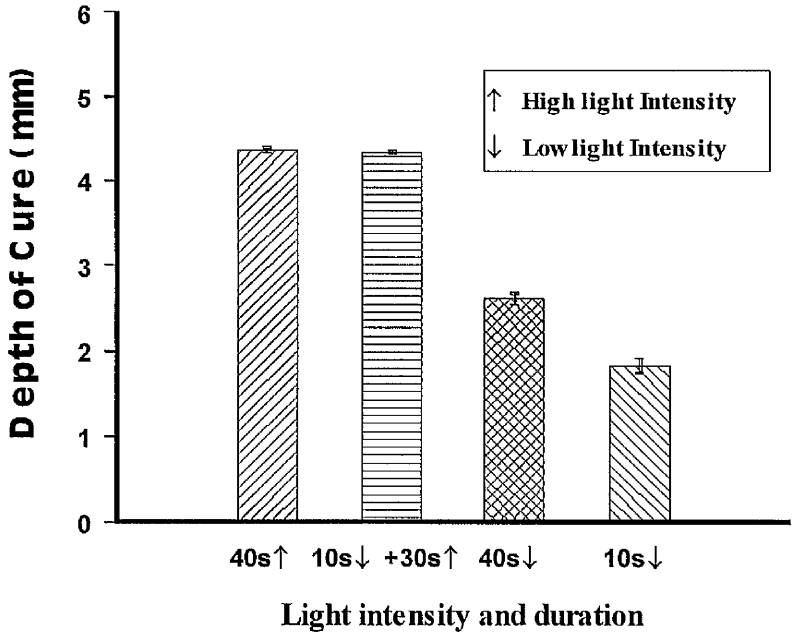

Fig 2.III-4: The effect of light intensity and duration on depth of cure of **PER2**.

Table 2.III-2: Depth of cure of **Z 100** with different light intensities and duration.

Sample No.	Light Intensity and Duration			
	40 s high int.	Soft-start	40 s low int.	10 s low int.
1	5.92	5.86	3.75	2.32
2	5.87	5.85	3.74	2.26
3	5.88	5.63	3.53	2.19
4	5.89	5.85	3.42	2.27
5	5.89	5.87	3.40	2.14
Mean	5.89	5.81	3.27	2.24
SD	0.02	0.01	0.17	0.07

Table 2.III-3: Depth of cure of **CHRF** with different light intensities and duration.

Sample No.	Light Intensity and Duration			
	40 s high int.	Soft-start	40 s low int.	10 s low int.
1	5.18	4.80	3.12	2.47
2	5.14	4.93	2.92	2.50
3	5.26	4.74	3.02	2.24
4	5.27	5.10	3.10	2.34
5	5.48	5.13	3.00	2.41
Mean	5.32	4.94	3.03	2.39
SD	0.12	0.17	0.08	0.10

Table 2.III-4: Depth of cure of **PER2** with different light intensities and duration.

Sample No.	Light Intensity and Duration			
	40 s high int.	Soft-start	40 s low int.	10 s low int.
1	4.49	4.36	2.60	1.90
2	4.48	4.34	2.72	1.91
3	4.54	4.34	2.92	1.91
4	4.40	4.29	2.60	1.94
5	4.34	4.34	2.64	1.98
Mean	4.45	4.33	2.70	1.93
SD	0.08	0.03	0.13	0.03

Table 2.III-5: Statistical analysis (2-Way ANOVA) of the effect of intensity of the material on depth of cure.

		Sum of Square	df	Mean Square	F	
Depth of cure	Main effects (Combined)	108.64	5	21.728	454.648	.000
	Material	10.561	2	5.280	110.489	.000
	Intensity	98.081	3	32.694	684.088	.000
	2-way interaction Material* Intensity	2.827	6	0.471	9.857	.000
	Model	111.47	11	10.134	212.035	.000
	Residual	2.294	48	4.779E-02		
	Total	113.76	59	1.928		

Table 2.III-6: Multiple comparison (Scheffe procedure) between depth of cure and the effect of light intensity for **Z100**.

Groups	code	4	3	2	1
10 s low intensity	Grp 4				
40 s low intensity	Grp 3	*			
Soft-start	Grp 2	*	*		
40 s high intensity	Grp 1	*	*		

Table 2.III-7: Multiple comparison (Scheffe procedure) between depth of cure and the effect of light intensity for **CHRF**.

Groups	code	4	3	2	1
10 s low intensity	Grp 4				
40 s low intensity	Grp 3				
Soft-start	Grp 2	*	*		
40 s high intensity	Grp 1	*	*		

Table 2.III-8: Multiple comparison (Scheffe procedure) between depth of cure and the effect of light intensity for **PER2**.

Groups	code	4	3	2	1
10 s low intensity	Grp 4				
40 s low intensity	Grp 3	*			
Soft-start	Grp 2	*	*		
40 s high intensity	Grp 1	*	*		

(*) denotes pairs of group significantly different at level ($p < 0.05$)

2.III.5 Discussion

The penetrometer technique was used to measure the depth of cure. Other workers have also used a penetrometer test method (McCabe and Carrick, 1989; Harrington and Wilson, 1993; Shortall, *et al.*, 1995a and b). Shortall, *et al.*, 1995a, argued that this test method is similar to the scrape test used in standards, in that they both measure the length of the cylinder of hardened material. The main difference is that the penetrometer can apply a constant force allowing consistency of the results.

The measurements were made near the walls of the cavity mould slightly lower than those at the centre. This is in agreement with McCabe and Carrick (1989) who used a penetrometer technique and found that the depth of cure decreased on moving toward the mould walls and that this reduction resulted in the 'bullet-like' shape of the end of the cure material.

The tip of the light curing unit was positioned at zero distance and completely parallel to the top surface of the composite resin, to obtain maximum polymerisation of the material and to avoid the problem of divergence of the light beam.

Some materials may be expected to be less affected by the efficiency of the light source than others. Three hybrid resin composite materials have been assessed in this study and found to vary substantially in performance compatibility with low intensity of the light. **Z100** may approach the ideal of having high depth of cure.

The depth-of-cure of this study reduced with reduced light intensity, whereas there was no significant difference between specimens, which cured by 40 s high light intensity and those cured by "soft-start". The fairly long exposure time could compensate for the early reduction in light intensity. For two materials (**Z100** and **PER2**), the depth-of-cure after 40 s low light intensity was found to be significantly greater than for samples exposed only to 10 s low light intensity. This result is in line with the work of McCabe and Carrick, (1989); Peutzfeld, (1994); Harrington and Wilson, (1993 and 1995). As shown in Tables III-6, 7, and 8, for **Z100** and **PER2**, there are significant differences between the

effects of low intensity for 40 s and 10 s duration. The difference was not significant for **CHRF**. This may by due to the differences in the type and concentration of the photo-initiator in these materials.

Z100 and **PER2** have the same shades (A3), which are darker than **CHRF** (A2). The depth of cure was higher in **Z100** and **CHRF** than **PER2**. The light transmission in **PER2** could be less than **CHRF**. This may be the reason **PER2** has a lower depth-of-cure. **Z100** is darker than **CHRF**, but has higher depth-of-cure. So, this could suggest that the depth of cure was less dependent upon the shade of the materials. Our finding in relation to the shade of the investigated materials, was in agreement with the finding of Ferracane and Greener, (1986) who noticed that the depth of cure of the darkest shade was equivalent to that of the lightest shade, supporting the view that depth of cure of light-activated composites may be less dependent upon shade than upon translucency.

The higher depth-of-cure of **Z100** may also be attributed to the filler size range 0.01 μm to 3.5 μm, which is slightly larger than **PER2** and **CHRF**. This may increase the transmission of the light to deeper areas. One more reason may be that **Z100** has a higher concentration of photoinitiator or light absorber.

Depth of cure is directly related to filler particle size in composite resins. The degree of scattering of light within the composite increases as the particle size of the filler in composite approaches the wavelength of the activating light. This scattering will reduce the amount of light that is transmitted through the composite. Maximum scattering occurs when particle diameters approach half the wavelength of the incident light, in this case 200 - 300 nm (Yearn, 1985).

DeWald and Ferracane, (1987), found that the larger particle and higher filler concentration of resin composites had the greatest depth of cure, since it was least affected by light scattering. They also found a lower depth of cure for microfine. The filler type, at all thicknesses, was found to be a significant factor influencing resin cure (Rueggeberg, *et al.*, 1993).

The degree of match and mis-match of the refractive indices of the filler and resin could influence depth of cure of composites. A close match provides a transparent composite facilitating transmission, while a gross mis-match produces an opaque material. In order to demonstrate this effect, refractive index match and mis-match composites were prepared by changing the ratio of monomer to comonomer. The depth of cure was increased from 2.3 mm in the refractive index mis-match, to 6 mm for the match (Yearn, 1985).

2.III.6 Conclusions

The initial cure of the composite materials with low intensity followed by high intensity did not reduce the depth-of-cure significantly with **Z100**, **CHRF** and **PER2** when compared with full intensity.

The Elipar unit has an effective lamp to cure the deep layer sufficiently with both 40 s full intensity or soft-start 10 s. followed by 30 s. full intensity.

Maximum depth-of-cure was obtained after 40 sec of high light intensity for all investigated materials: **Z100**, **CHRF** and **PER2**.

Prolonged curing time at low intensity can increase the depth-of-cure of composite resin materials.

Chapter 3

Comparison of "Soft-Start" and Conventional VLC Units by Exotherm Release during Polymerisation

3.1 Literature Review

Setting initiated by the action of visible light was first introduced into dentistry for composite filling materials, and its numerous inherent advantages soon led to widespread acceptance. However, polymerisation of these materials result in a temperature increase, which is caused by both the exothermic reaction process and the energy absorbed during irradiation (McCabe, 1985; Lloyd, *et al.,* 1986; Masutani, *et al.*, 1988; Smail, *et al.*, 1988).

The temperature rise in the deep part of the resin is presumably more important than that found in the surface layer (Hansen and Asmussen, 1993c). This temperature may cause pulpal damage (McCabe and Wilson, 1980; Watts *et al.,* 1983; Smail *et al.,* 1988; Hussey *et al.,* 1995). The pulp must be protected against the thermal shock of some resin composites by the use of a liner (Watts *et al.*, 1983). Since the heat passes through the liner materials during curing (McAndrew *et al.,* 1987; Adamson *et al.,* 1988; Smail *et al.,* 1988) the thickness of these materials should be increased to decreasing the temperature rise in the pulp chamber.

The exotherm reaction made by the material depends upon the product, ambient temperature (Masutani *et al.*, 1988; McCabe, 1985), and the thickness of the material (McCabe and Wilson, 1980; Lloyd *et al.,* 1986; Kanchanavasita, *et al.*, 1996). Other contributions made by the light depend upon exposure time, and characteristics of the light source (McCabe, 1985; Lloyd *et al.,* 1986; Adamson *et al.,* 1988; Kanchanavasita, *et al.*, 1996).

Several studies have investigated the heat emitted during the setting of the restorative dental materials by using different instrumentation. These include differential scanning calorimetry (DSC) (McCabe and Wilson, 1980), Differential thermal analysis (DTA) has been used by Lloyd, (1984); McCabe (1985); Lloyd *et al.,* (1986); Adamson *et al.*, (1988), thermocouple technique has been used by many researchers (Smail *et al.*, 1988; Stewart *et al.*, 1991;

Castelnuovo and Tjan, 1997; Goodis *et al.*, 1989) and a Thermovision 900 Infra-red scanning system was used by Hussey *et al.*, (1995).

In the study of McCabe (1985) a divided fiber optic system was used with the DTA instrument to separate the heat reaction of the composite from the temperature rise of the light source. The conclusion was that reproducible results were obtained from this method.

Kanchanavasita, *et al.*, (1996), investigated the temperature rise for two liner/base and two restorative type resin-modified glass ionomer cements and investigated the effects of factors such as specimen thickness, exposure time and environment temperature. They noticed that increasing the environmental temperature from 25°C to 37°C resulted in a decrease in the temperature rise either from light sources or dental biomaterials.

3.2 Objectives

It was the objective of this part of the study to investigate the exotherm during reaction of visible light cure resin composites and also to study the effect of the visible curing lights on the rise in temperature. The heating effect of the light sources was assessed by subjecting the cured material to a second identical exposure from the light sources.

1991; Castelnuovo and Tjan, 1997; Goodis *et al.*, 1989) and a Thermovision 900 Infra-red scanning system was used by Hussey *et al.*, (1995).

In the study of McCabe (1985) a divided fiber optic system was used with the DTA instrument to separate the heat reaction of the composite from the temperature rise of the light source. The conclusion was a reproducible results obtained from this method.

Kanchanavasita, *et al.*, (1996), investigated the temperature rise for two liner/base and two restorative type resin-modified glass ionomer cements and investigated the effects of factors such as specimen thickness, exposure time and environment temperature. They noticed that increasing the environmental temperature from 25°C to 37°C resulted in a decrease in the temperature rise either from light sources or dental biomaterials.

3.2 Objectives

It was the objective of this part of the study to investigate the exotherm during reaction of visible light cure resin composites and also to study the effect of the visible curing lights on the rise in temperature. The heating effect of the light sources was assessed by subjecting the cured material to a second identical exposure from the light sources.

3.3 Materials and Methods

Three visible light cured resin composite restorative materials were investigated in this study (Table 3-1).

Table 3-1: investigated materials.

Materials	Code	Batch No.	Manufacturer
Z 100	**Z100**	3021	3M Dental Products, St. Paul, USA
Pertac II	**PER2**	643081003	Espé, Dental AG, Seefeld, Germany
Solitaire	**SOL**	23	Heraeus Kulzer, Wehrheim, Germany

An insulating disc shaped polypropylene large block (diameter = 7 cm) was divided into two halves, the upper half containing holes (cavities) with different diameters and 3 mm height. The lower part of this apparatus was left flat, except for a 1 cm long groove, drilled from the edge toward the centre of the lower part to permit the exposed tip of a thermocouple to be inserted underneath the specimen being investigated. The two parts of the apparatus were connected together from the centre using a bolt. The 7 mm diameter cavity was chosen for this study. A thin polythene sheet was used above the thermocouple exposed tip to prevent bonding of the tested materials to the lower part of the apparatus. After insertion of the thermocouple tip, the two parts were tightened together by the bolt, to hold the thermocouple tip tightly in place.

Light-activated resin composites were packed into the mould cavity with great care to ensure that the composite was packed in close proximity to the thermocouple tip on each sample and to minimise the entrapment of air. Mylar strip was placed on top of the filled cavity surface and excess material was removed by pressing with a glass plate. Three groups of samples were prepared:

Group 1: irradiation 10 min after packing in cavity at 23°C for each composite material.

Group 2: 10 min storage at 12°C before curing for **Z100.**

Group 3: 10 min storage at 37°C before curing for **Z100.**

The Elipar unit and XL3000 light-activating units were used in this study. The light tip of the

selected curing units was placed directly on top of the specimens at 0 distance. For the Elipar unit two groups were cured at each temperature: the first group was irradiated for 40 s full light intensity and the second one cured by "soft-start". When the XL3000 unit was used, **Z100** was tested and all the groups were irradiated for 40 s normal light intensity.

The measurement of temperature rise was performed at the base of the resin composite. Temperature changes taking place during setting were recorded as a function of time. The temperature rise-time transients from the thermocouple output were obtained by measuring the output voltage by means of a rapid-response thermocouple amplifier. The amplifier output was connected to resident data acquisition software (BIOMAN) via an analog-to-digital converter (ADC) (Fig 3.1). Temperature readings recorded in ADC Units were converted to ^{o}C by means of the calibration coefficient determined. All measurements were carried out at room temperature ($23^{o}C \pm 1$)

Data are presented as *temperature/time peaks* and both *peaks areas* and *time-to-peak-temperatures* were determined.

The heating effect from the light was measured by subjecting the material to a second identical exposure from the light. Before proceeding with the second exposure (post-cure), the materials were allowed to return to the ambient temperature of $23^{o}C$. 15 min was allowed between the first and second exposure. The difference between the peak areas gives the net contributions produced by the resin composites. 'Un-Scan-It' software was used to perform this subtraction by calculating the area under each temperature/time curve.

In all 3 groups, measurements were repeated three times, undertaking the identical procedure with each new specimen.

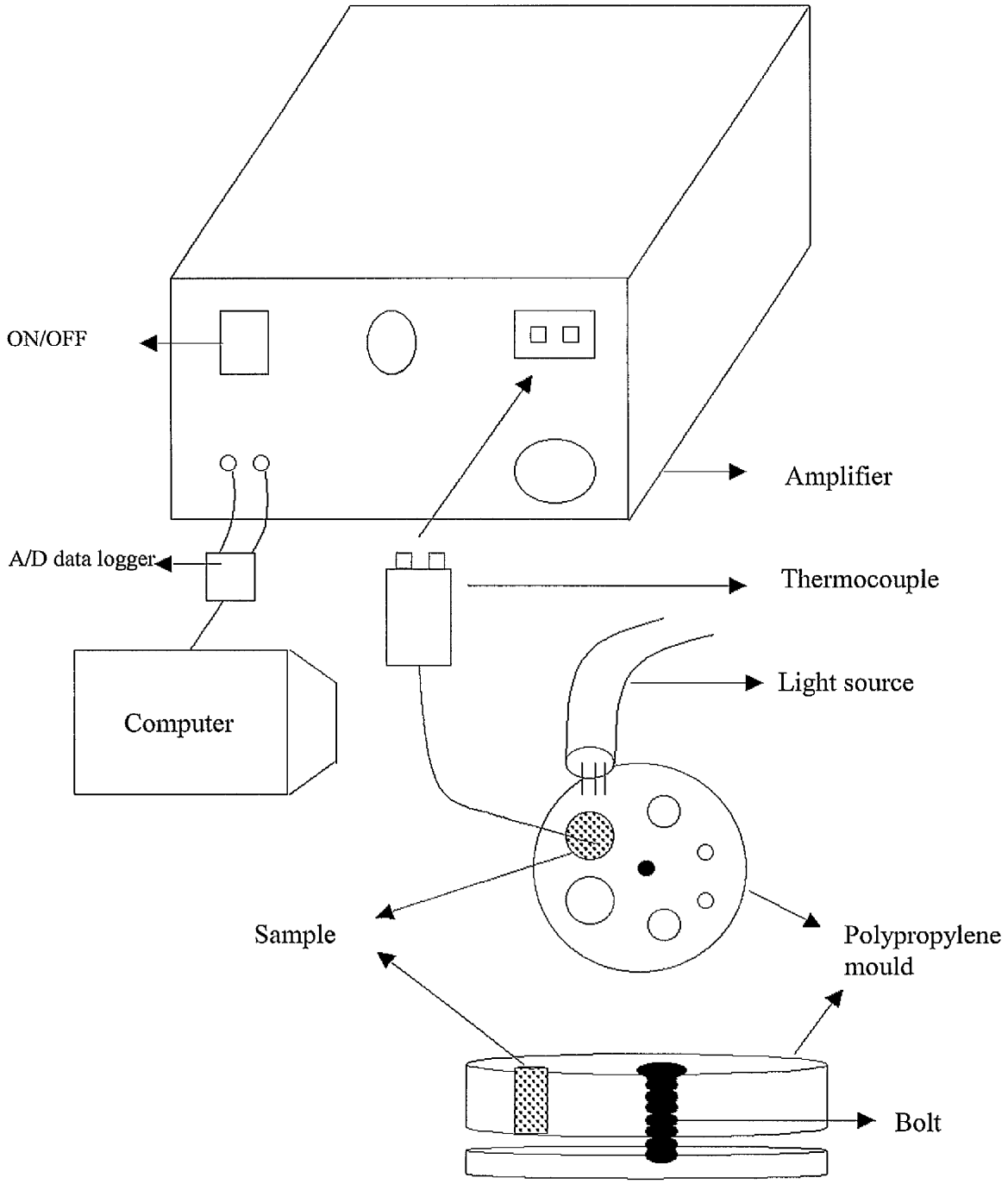

Fig 3-1: Apparatus used to measure exotherm reaction of the resin composites

3.3.1 Calibration of thermocouple

The type K thermocouple was first calibrated using warm and cold water baths and a sensitive Hg-in-glass thermometer. The thermocouple, connected to its amplifying unit, was linked to the data acquisition system via an A/D interface. The thermocouple tip and the thermometer were positioned in the cold water bath and data acquisition was triggered. Small quantities of warm water were added to the cold water at regular intervals and corresponding temperatures were read off from the thermometer when the system reached equilibrium. The procedure was repeated, from which a graph of temperature (°C) *versus* ADC (BIOMAN) units was plotted. The coefficient of calibration was then determined (Fig 3.2).

3.3.2 Statistical Analysis

For **Z100**, one-way ANOVA and the Scheffé multiple test was followed at $p < 0.05$, was used to analyse statistical differences between the three temperature results. For **SOL** and **PER2**, the un-paired sample t-Test of the difference was used for specimens cured by the Elipar unit using full light intensity and soft-start.

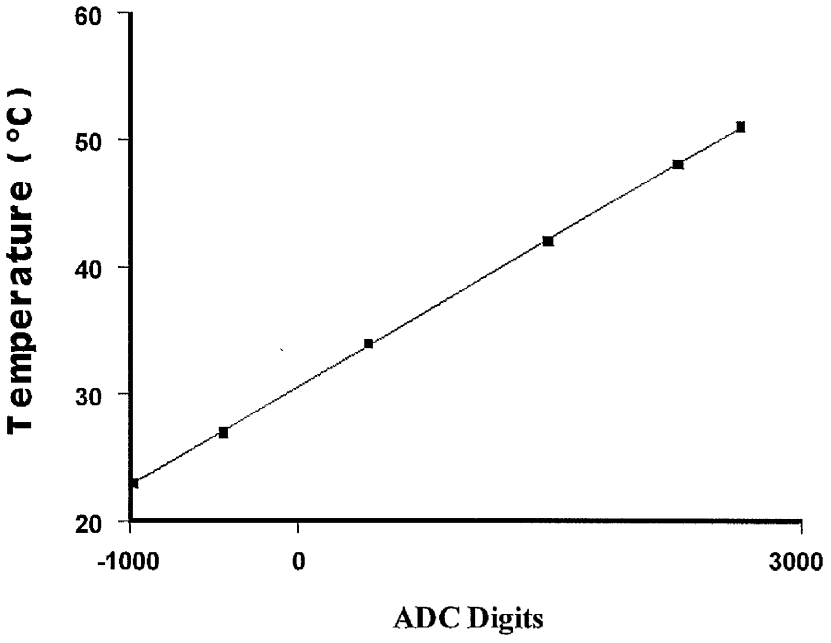

Fig 3-2: Voltage/temperature calibration factor calculation (1 °C / 133.6 ADC digits).

3.4 Results

The mean values and standard deviation of the exothermic reaction of the investigated materials are presented graphically in Figures 3-3 to 3-15 and the data are summarised in Tables 3-2 to 3-14. Table 3-15 presents additional data on time periods to reach the peak for initial cure. These tables present the peak areas of the investigated materials during light curing as well as the post-cure peak generated from the light curing unit. The net exotherm peak area was calculated by subtraction.

The time-to-peak decreased with increasing pre-cure temperature, which is readily understandable as the reaction is thermally activated, like the majority of chemical reactions.

The exotherm results of **Z100** for specimens stored at 12°C and cured with the XL3000 unit were found lower than those stored at 37°C or 23°C (Tables 3-2, 3 and 4). There was no significant difference between the groups ($p > 0.05$) (Table 3-16). Those specimens stored at 37°C which cured by full intensity from the Elipar unit provided lower temperatures than those stored at 12°C or 23°C (Tables 3-5, 6 and 7), and were statistically no difference (Table 3-16). On other hand with those specimens cured by "soft-start", those stored at 12°C were found slightly higher than those stored at 23°C or 37°C (Tables 3-8, 9 and 10). There was no statistical significant difference between these three temperatures (Table 3-16). Figures 3-2 to 3-10 show the exotherm results of **Z100**, graphically.

For **SOL** (Fig. 3-11 and 3-12) and **PER2** (Fig. 3-13 and 3-14), the exothermic reaction results were found higher with specimens cured by full intensity from the Elipar Highlight than those which cured by the "soft-start". Table 3-17 demonstrates the summary of the statistically significant difference (paired samples T-Test), between the two groups in the light cure mode. The statistical difference was significant for the two materials, 0.006 and 0.022 for **SOL** and **PER2**, respectively.

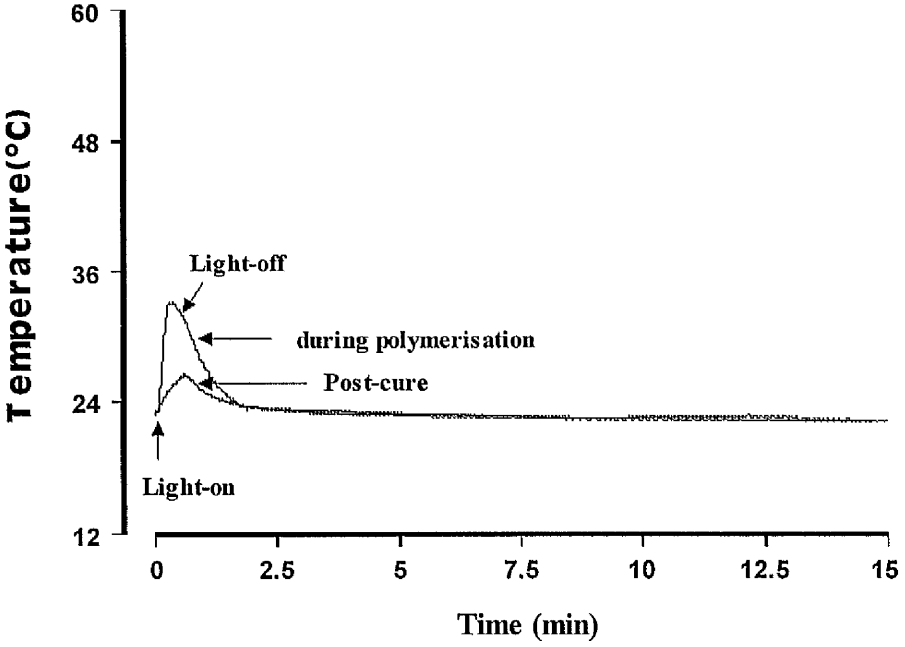

Fig 3-3: The exotherm reaction during polymerisation and 2nd light irradiation (post-cure) of **Z100**, after storage at **12°C** and cured by the **XL3000 unit**.

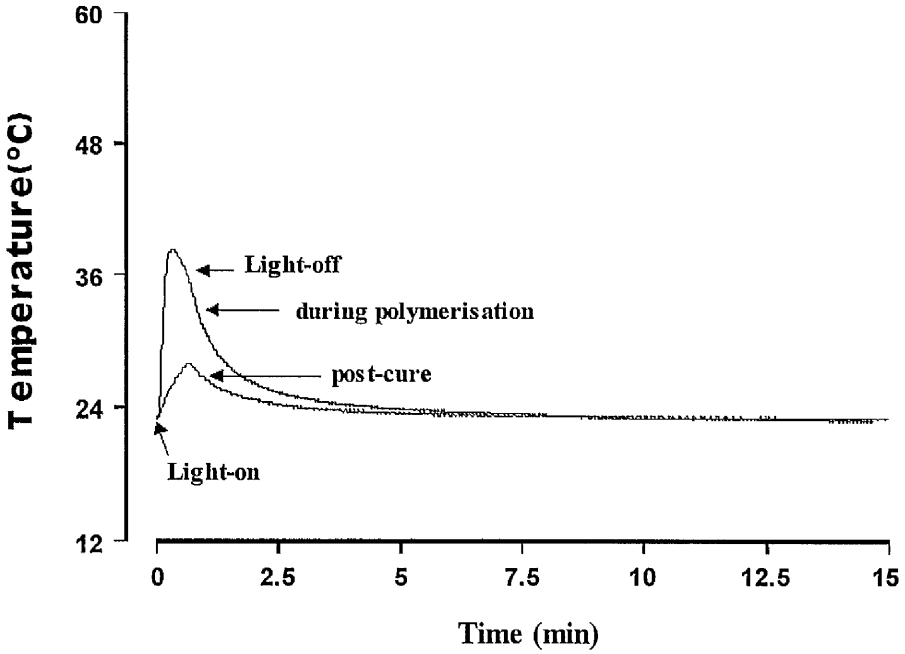

Fig 3-4: The exotherm reaction during polymerisation and 2nd light irradiation (post-cure) of **Z100**, after storage at **23°C** and cured by the **XL3000 unit**.

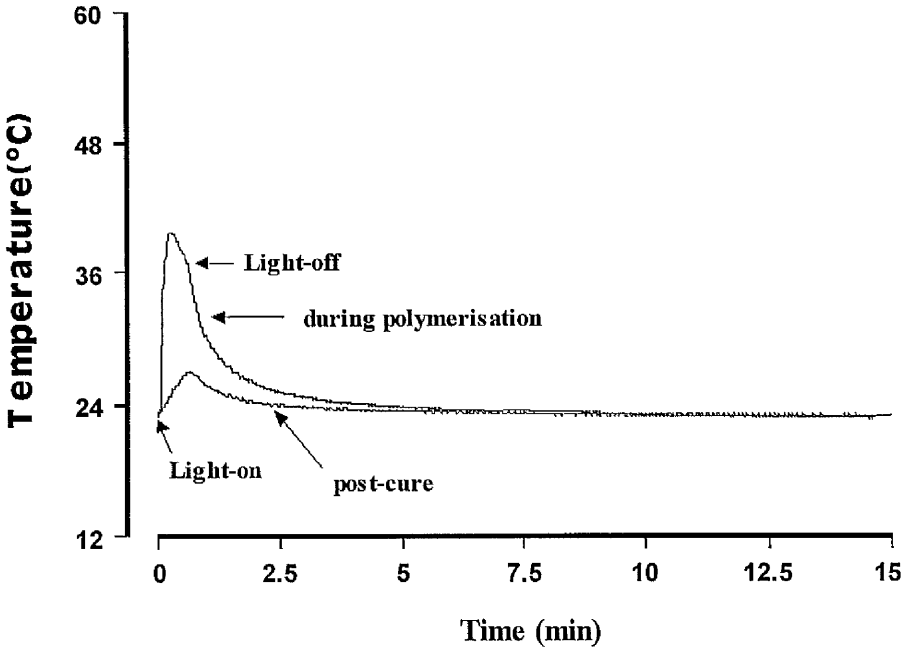

Fig 3-5: The exotherm reaction during polymerisation and 2nd light irradiation (post-cure) of **Z100**, after storage at **37°C** and cured by the **XL3000 unit.**

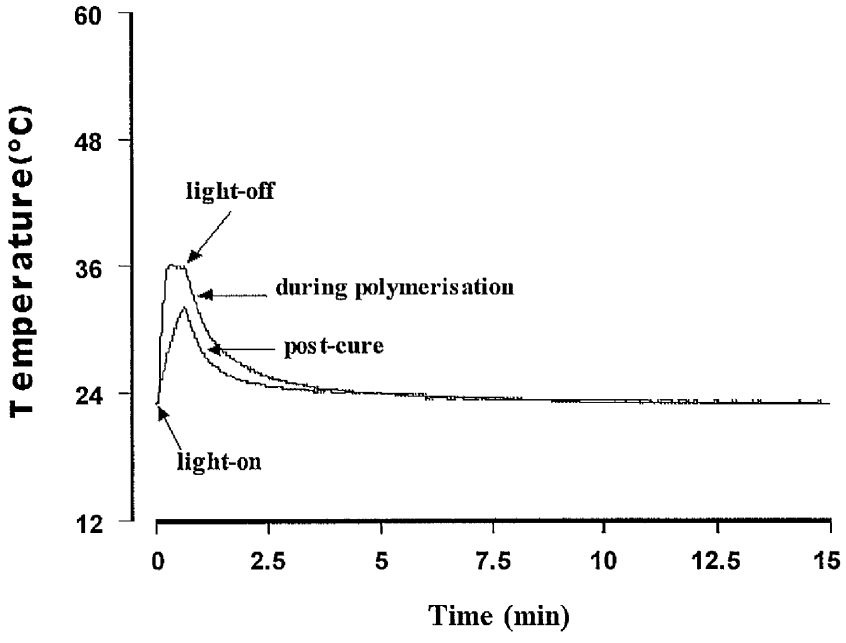

Fig 3-6: The exotherm reaction during polymerisation and 2nd light irradiation (post-cure) of **Z100**, after storage at **12°C** and cured with **full intensity by the Elipar unit.**

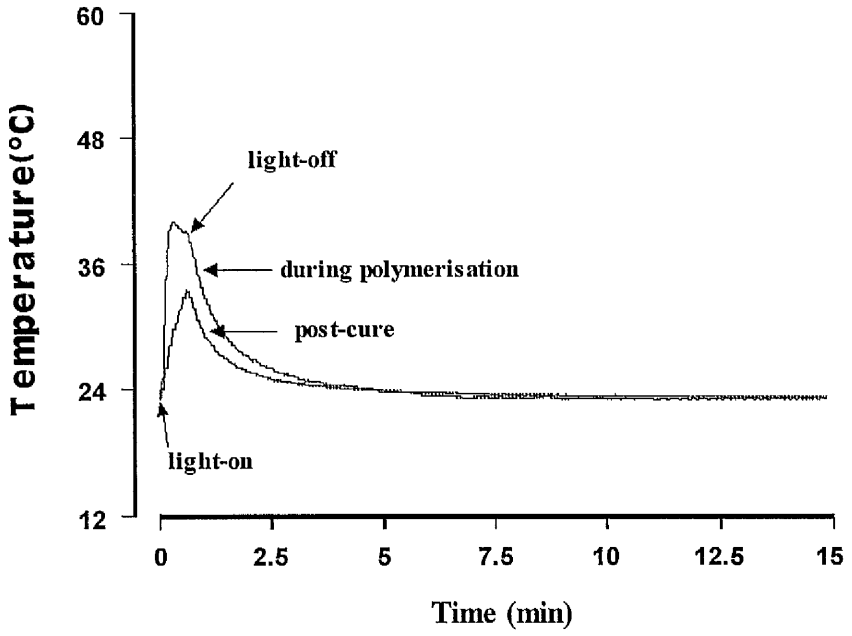

Fig 3-7: The exotherm reaction during polymerisation and 2nd light irradiation (post-cure) of **Z100**, at **23°C**, cured with **full intensity by the Elipar unit.**

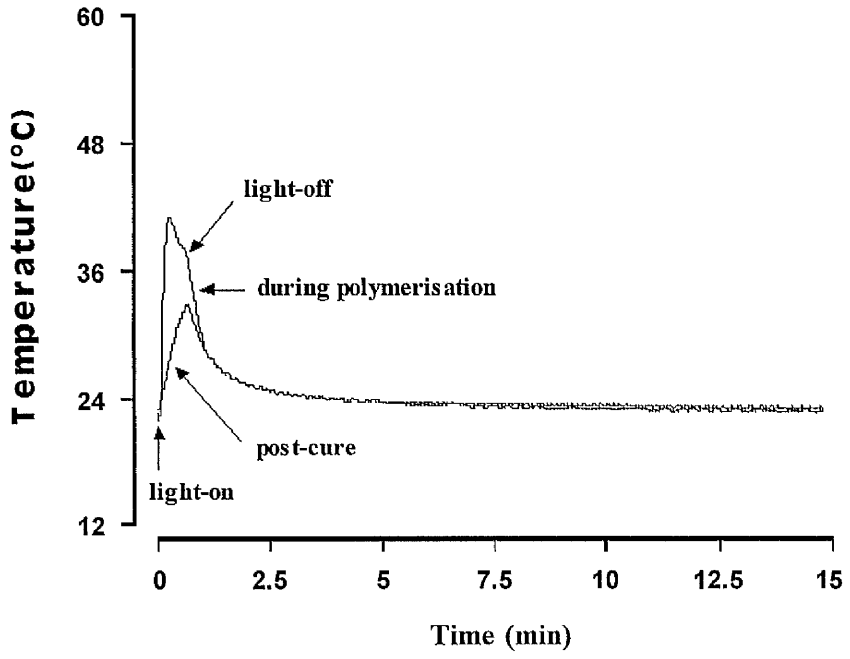

Fig 3-8: The exotherm reaction during polymerisation and 2nd light irradiation (post-cure) of **Z100**, after storage at **37°C** and cured with **full intensity by the Elipar unit.**

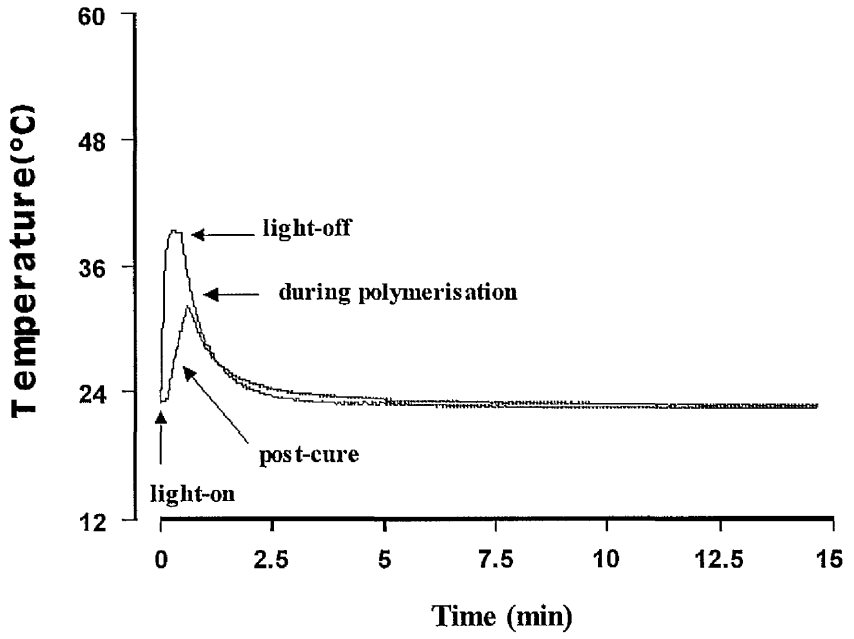

Fig 3-9: The exotherm reaction during polymerisation of and 2nd light irradiation (post-cure) of **Z100**, after storage at **12°C** and cure with **"soft-start" by the Elipar unit**.

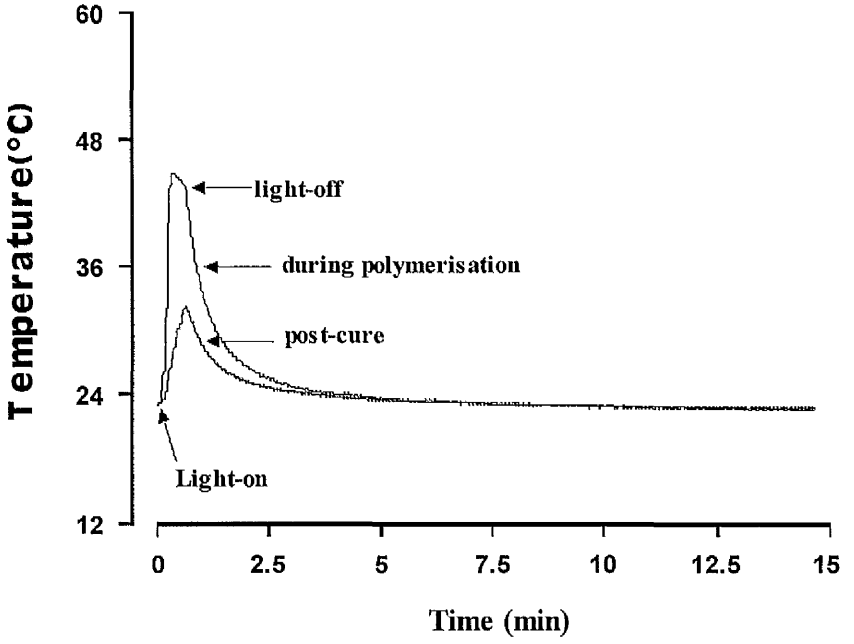

Fig 3-10: The exotherm reaction during polymerisation of and 2nd light irradiation (post-cure) of **Z100**, at **23°C** and cured with **"soft-start" by the Elipar unit**.

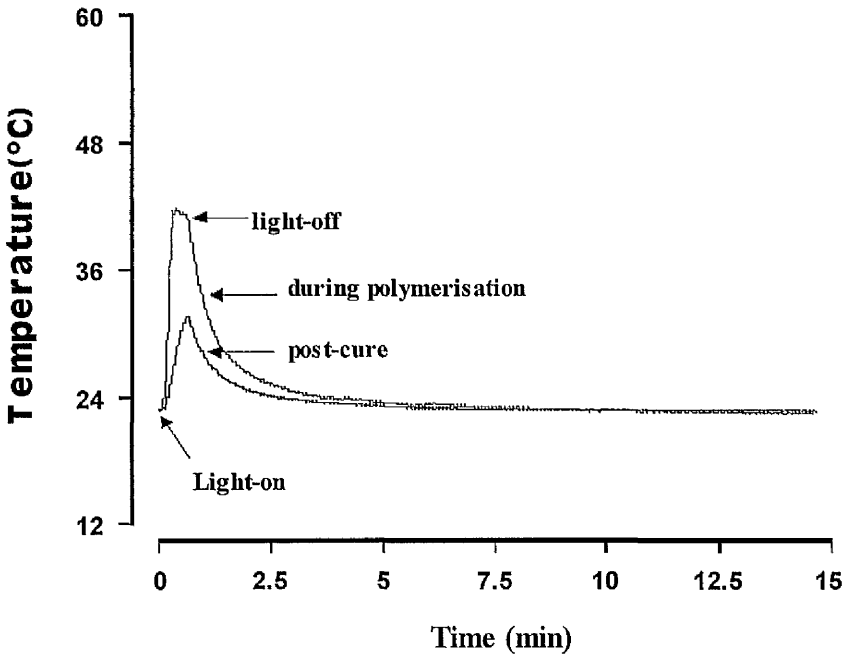

Fig 3-11: The exotherm reaction during polymerisation of and 2nd light irradiation (post-cure) of **Z100**, after storage at **37°C** and cured with **"soft-start" by the Elipar unit**.

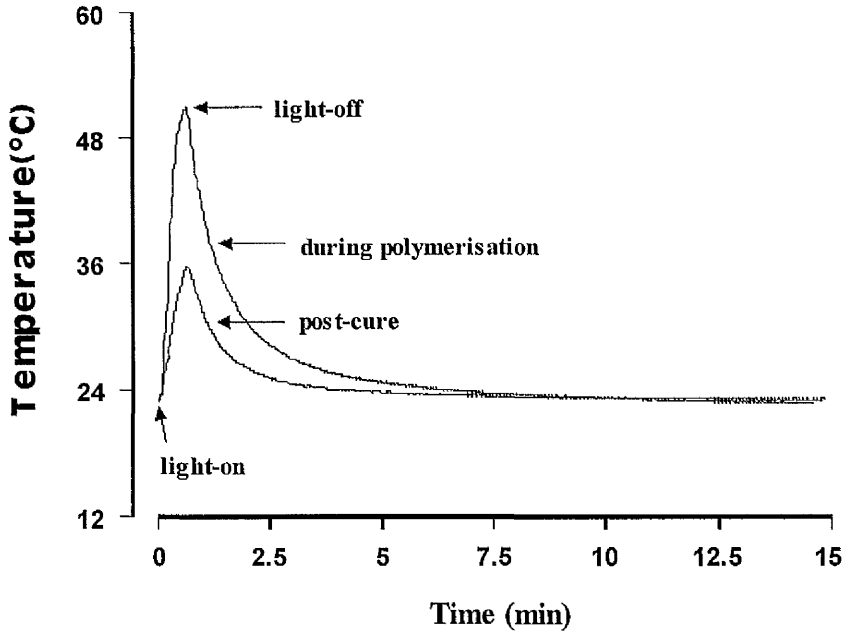

Fig 3-12: The exotherm reaction during polymerisation and 2nd light irradiation (post-cure) of **SOL**, at **23°C**, cured with **full intensity by the Elipar unit**.

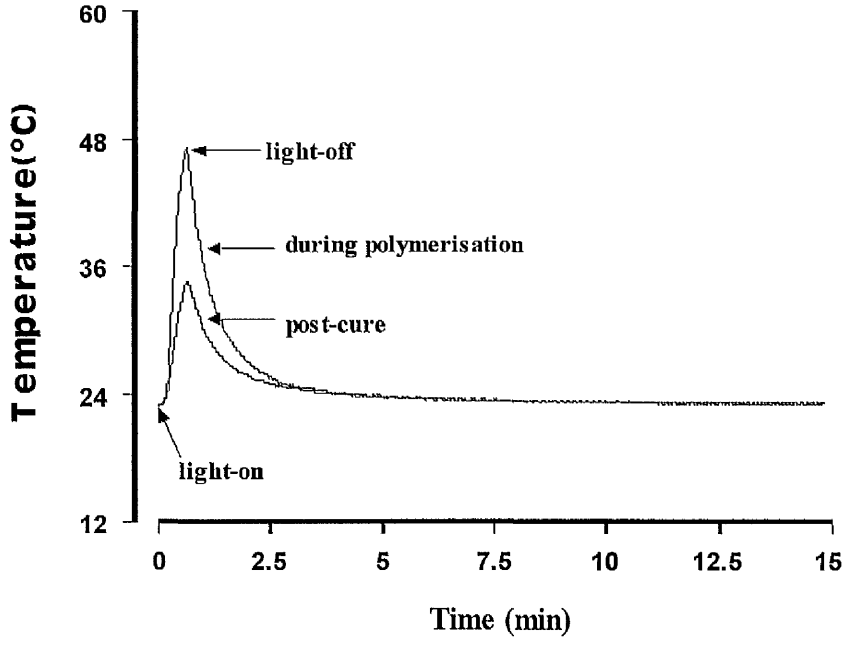

Fig 3-13: The exotherm reaction during polymerisation and 2nd light irradiation (post-cure) of **SOL**, at **23°C** and cured with **"soft-start" by the Elipar unit**.

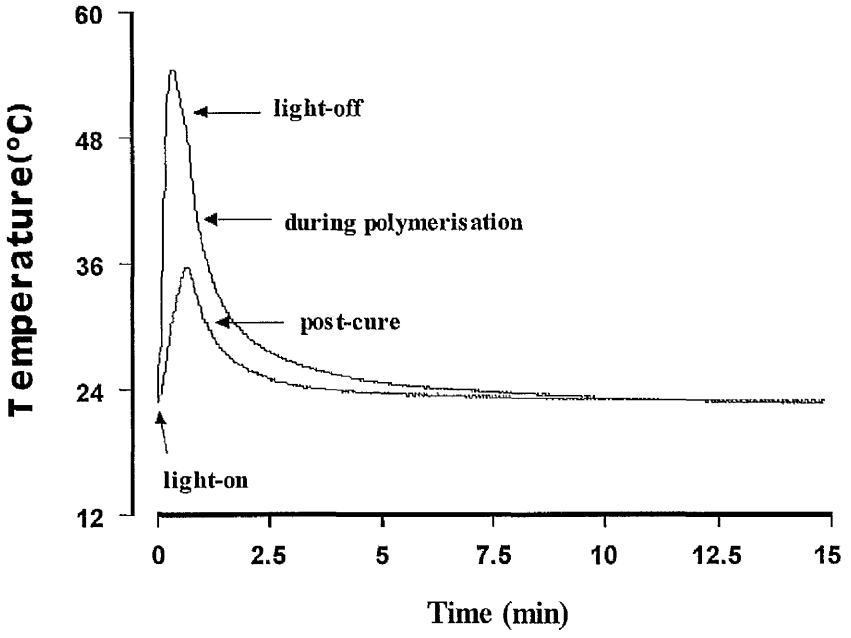

Fig 3-14: The exotherm reaction during polymerisation and 2nd light irradiation (post-cure) of **PER2**, at **23°C**, cured with **full intensity by the Elipar**.

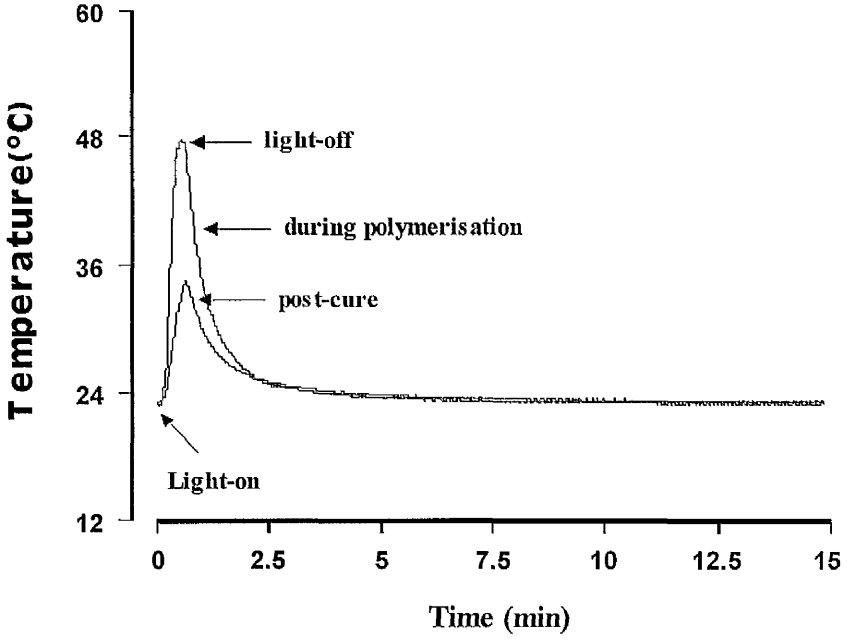

Fig 3-15: The exotherm reaction during polymerisation and 2nd light irradiation (post-cure) of **PER2**, at **23°C** and cured with **"soft-start" by the Elipar**.

Table 3-2: Peak areas (°C.min) produced by the exothermic reaction of **Z100** and heating by the XL3000 unit after 10 min storage at **12°C**.

Sample No.	Total peak area during polymerisation	Post-cure peak area	Net peak area due to exotherm alone
1	12.00	5.53	6.47
2	11.92	3.27	8.65
3	12.07	4.27	7.80
			Mean (SD) = 7.64 (1.1)

Table 3-3: Peak areas (°C.min) produced by the exothermic reaction of **Z100** and heating by the XL3000 unit at **23°C**.

Sample No.	Total peak area during polymerisation	Post-cure peak area	Net peak area due to exotherm alone
1	17.80	5.13	12.67
2	18.05	7.93	10.12
3	19.70	4.10	15.60
			Mean (SD) = 12.80 (2.7)

Table 3-4: Peak areas (°C.min) produced by the exothermic reaction of **Z100** and heating by the XL3000 unit after 10 min storage at **37°C**.

Sample No.	Total peak area during polymerisation	Post-cure peak area	Net peak area due to exotherm alone
1	16.90	6.44	10.46
2	18.50	5.23	13.27
3	16.00	7.80	08.20
			Mean (SD) = 10.64 (2.5)

Table 3-5: Peak areas (°C.min) produced by the exothermic reaction of **Z100** and heating by the Elipar with **full intensity** after 10 min storage at **12°C**.

Sample No.	Total peak area during polymerisation	Post-cure peak area	Net peak area due to exotherm alone
1	22.10	11.20	10.90
2	21.50	11.50	10.00
3	19.10	11.10	8.00
			Mean (SD) = 9.60 (1.5)

Table 3-6: Peak areas (°C.min) produced by the exothermic reaction of **Z100** and heating by the Elipar with **full intensity** at **23°C**.

Sample No.	Total peak area during polymerisation	Post-cure peak area	Net peak area due to exotherm alone
1	23.10	14.30	8.80
2	24.50	14.00	10.50
3	23.00	13.10	9.90
			Mean (SD) = 9.73 (0.86)

Table 3-7: Peak areas (°C.min) produced by the exothermic reaction of **Z100** and heating by the Elipar with **full intensity** after 10 min. storage at **37°C**.

Sample No.	Total peak area during polymerisation	Post-cure peak area	Net peak area due to exotherm alone
1	19.90	12.20	7.70
2	19.90	12.10	7.80
3	19.80	15.20	4.60
			Mean (SD) = 6.70 (1.8)

Table 3-8: Peak areas (°C.min) produced by the exothermic reaction of **Z100** and heating by the Elipar with **"soft-start"** after 10 min storage at **12°C**.

Sample No.	Total peak area during polymerisation	Post-cure peak area	Net peak area due to exotherm alone
1	20.30	12.30	8.00
2	19.80	11.10	8.70
3	22.90	10.80	12.10
			Mean (SD) = 9.60 (2.1)

Table 3-9: Peak areas (°C.min) produced by the exothermic reaction of **Z100** and heating by the Elipar with **"soft-start"** at **23°C**.

Sample No.	Total peak area during polymerisation	Post-cure peak area	Net peak area due to exotherm alone
1	25.10	11.20	13.90
2	20.70	10.90	9.80
3	25.20	11.30	13.90
			Mean (SD) = 12.50 (2.4)

Table 3-10: Peak areas (°C.min) produced by the exothermic reaction of **Z100** and heating by the Elipar with **"soft-start"** after 10 min storage at **37°C**.

Sample No.	Total peak area during polymerisation	Post-cure peak area	Net peak area due to exotherm alone
1	22.80	10.70	12.10
2	18.20	10.70	7.50
3	23.40	11.00	12.40
			Mean (SD) = 10.70 (2.7)

Table 3-11: Peak areas (°C.min) produced by the exothermic reaction of **SOL** and heating by the Elipar with **full intensity** at **23°C**.

Sample No.	Total peak area during polymerisation	Post-cure peak area	Net peak area due to exotherm alone
1	40.40	19.30	21.10
2	41.50	19.30	22.20
3	40.80	17.10	23.70
			Mean (SD) = 22.30 (1.3)

Table 3-12: Peak areas (°C.min) produced by the exothermic reaction of **SOL** and heating by the Elipar with **"soft-start"** at **23°C**.

Sample No.	Total peak area during polymerisation	Post-cure peak area	Net peak area due to exotherm alone
1	24.90	11.80	13.10
2	25.70	13.90	11.80
3	25.50	10.50	15.00
			Mean (SD) = 13.30 (1.6)

Table 3-13: Peak areas (°C.min) produced by the exothermic reaction of **PER2** and heating by the Elipar with **full intensity** at **23°C**.

Sample No.	Total peak area during polymerisation	Post-cure peak area	Net peak area due to exotherm alone
1	41.00	28.70	12.30
2	39.40	28.40	11.00
3	41.20	25.60	15.60
			Mean (SD) = 13.00 (2.4)

Table 3-14: Peak areas (°C.min) produced by the exothermic reaction of **PER2** and heating by the Elipar with **"soft-start"** at **23°C**.

Sample No.	Total peak area during polymerisation	Post-cure peak area	Net peak area due to exotherm alone
1	26.40	22.90	3.50
2	25.60	20.50	5.10
3	26.50	21.00	5.50
			Mean (SD) = 4.70 (1.0)

Table 3-15: The time (sec) to reach the temperature peak (SD in parentheses)

Material	Temp.	Full int. of Elipar	Soft-start of Elipar	XL3000
Z100	12°C	20.5 (3.1)	29.0 (6.9)	20.0 (0.0)
	23°C	17.7 (3.2)	21.0 (0.0)	19.5 (1.3)
	37°C	12.5 (0.0)	23.3 (1.4)	18.3 (3.2)
SOL	23°C	38.0 (0.0)	37.0 (0.0)	
PER	23°C	21.3 (0.6)	31.7 (0.3)	

Table 3-16: Statistical analysis (One-way ANOVA) of **Z100** between the three temperatures

Curing-light	Intensity	DF	Sum of sq.	Mean of sq.	F-Ratio	F-Pob.
3M	Normal	2	40.2481	20.1240	3.9775	0.0795
Elipar	Full	2	17.8156	8.9078	4.2712	0.0702
Elipar	Soft-start	2	13.2267	6.6133	1.1049	0.3904

Table 3-17: Summary of statistical analysis (un-paired samples T-Test) of **SOL** and **PER2**. The difference was performed between the results of full intensity and soft-start.

Material	Sig.
SOL	0.006
PER2	0.022

3.5 Discussion

Replacement of dentine by composite compromises the function of the dentine to protect the pulp since composites often have higher diffusivities (Watts *et al.*, 1987). Whereas lining is routinely placed below composite for other reasons, its role as a thermal barrier is of equal importance (McAndrew *et al.*, 1987). However, clinicians should be constantly aware of the potential thermal hazard to the dental pulp which might arise as the result of the use of visible-light cured lining materials in the restoration of deep cavities (Smail *et al.*, 1988).

The setting of the restorative materials was exothermic which produced a temperature rise. The evolution of heat started with the polymerisation process when the photons of the light energy activate the initiator to generate free radicals, which initiate the polymerisation process. This process continues with considerable velocity. Chain reactions continue until the monomer has been changed to polymer (Phillips, 1991).

The technique used in this study measured the heat produced from the light curing units as well as the exothermic heat of the light activating restorative materials. The second irradiation (post-cure) from the light unit was applied with each specimen, to differentiate between them. The presence of the thermocouple tip in the floor of the cavity mould makes it capable of recording temperature rise in the deep part of the resin-composites that may approximate to that in a clinical cavity.

In this study the polypropylene mould was used, due to its thermal insulating property and it may be reduce loss of heat from specimen. Secondly, the polypropylene mould possibly enhances curing at the depth of the cavity, by reflecting the visible-light.

The temperature/time peak was reached during exposure time. This finding coincided with the study of McCabe (1985); Lloyd, *et al.*, (1986); Adamson *et al.*, (1988). Lloyd, *et al.*, (1986) who observed that the temperature continues to rise almost linearly whilst the light is on.

SOL was found to have a very high exotherm with all the specimens either cured by full light intensity or soft-start from the Elipar unit. On the other hand **Z100** had the lowest exotherm. **PER2** had a higher exotherm result with full light intensity than those which cured by soft-start

irradiation. This means that the exotherm reaction varied with these three different materials of resin composites investigated. This finding was in agreement with the work of Lloyd, *et al.*, (1986); Adamson *et al.*, (1988) who noticed that a change in the exotherm was due to differences in composition.

The low level (1.6 °C) of temperature generated by the Elipar light source in the first 10 s could be a contributory factor towards low exotherm values in the specimens when treated with 10 s low light intensity plus 30 s high intensity.

The net peak area from the Elipar unit at the bottom of the resin composite with both full intensity or soft-start were 11.1 - 13.8 °C.min with **Z100**, 12.1 - 18.6 °C.min with **SOL** and 21.5 - 27.6 °C.min with **PER2**. This heat flow could be harmful to the pulp especially in deep cavities with a smaller amount of dentine remaining. The net peak areas from the XL3000 light curing unit ranged between 4.4 - 6.5 °C.min, which could be harmless to the pulp.

The results of **Z100** demonstrated that differences in temperature changes of the resin composites are caused by the differences in the light curing units used. The Elipar unit produces a greater temperature rise than the XL3000. At 40 sec irradiation, the Elipar unit was capable of creating a temperature rise of up to 20 °C when measured directly to the thermocouple and the XL3000 unit was capable of producing up to7.2 °C (Chapter 2 Part II).

The choice of light source has a substantial influence upon the temperature rise (McAndrew *et al.*, 1987). The differences in the temperature rises with the light curing units used may be due to the differences in the intensity of these light sources. The speed of the exothermic reaction of visible light resin composite materials increases with increasing intensity of the light source (Masutani *et al.*, 1988). The heat produced from VLC is a function of the lamp design and does not cause the composite resin cure to take place, the visible light emitted causes the material to cure (Goodis, *et al.*, 1989).

The results of exotherm of **Z100** for the specimens stored at 37 °C were found to be lower than those examined at 23 °C and with only some of those stored at 12 °C. This may be attributed to the fact that when the body has high temperature it can lose the heat faster than at low temperature; (Newton's law of cooling). This coincides with the finding of Kanchanavasita *et*

al., (1996).

3.6 Conclusions

1. The time to reach the peak temperature (inversely related to the rate of reaction) decreased with increased pre-cure temperature.

2. In **Z100**, the time-to-peak (rate of reaction) for specimens cured by the XL3000 light source was lower than those treated by soft-start from the Elipar Highlight, but greater than those cured by full intensity light.

3. The exotherm release increased during the irradiation time.

4. **SOL** has a greater net exotherm peak area than **Z100** and **PER2**.

Chapter 4

Comparative Evaluation of The Low Intensity Irradiation of Resin-Composites by Surface Hardness Measurements

4.1 Literature Review

The hardness of a material indicates the resistance to scratching (McCabe, 1990). The measurement for hardness of composite resins is an indirect method of evaluating the relative degree of polymerisation (Leung *et al.*, 1983 and Watts *et al.*, 1987; Rueggeberg and Craig, 1988) and as a method to evaluate the performance of light source (McCabe and Carrick, 1989).

The hardness of materials is commonly correlated with mechanical strength, rigidity, and resistance to intra-oral softening (Helvatjoglou *et al* 1991). The strength properties of restorative resin have been shown to depend on the composition of the monomer, filler (type, size and quantity) and on the type and amount of the polymerisation. It has been suggested that mechanical properties of resinous material are associated with the quantity of double bonds remaining in the polymer after polymerisation (Asmussen 1982b). Also the hardness varied according to the variation of time of exposure (DeLange, *et al.*, 1980; Watts *et al.*, 1984).

As has been pointed out by Pilo and Cardash, (1992), incomplete curing in the bulk of the restoration is analogous to a restoration composed of several different materials which differ greatly in their values of elastic modulus. Loading on the well-cured surface layer of the restoration which overlays an incompletely cured deeper portion may cause bending of the outer layer and inward displacement. This pattern of deformation predisposes to marginal fracture and open margins. Also, bulk restoration fracture, loss of anatomic form and marginal leakage may occur, other problems include secondary caries, adverse tissue reactions and pulpal irritation (Shortall, *et al.*, 1995b).

A stronger correlation between bottom surface hardness and light intensity has been established by Pires *et al.*, (1993). They noticed that the bottom surface hardness decreased with increasing distance of the curing tip from the specimen surface. As it is known that the

light is absorbed and scattered by the composite resin material, intensity of the light source is more critical for adequate conversion at increasing distances below the composite surface (Shortall, *et al.*, 1995a). Surface hardness is not an adequate clinical indicator of an adequately polymerized composite restoration, because even a very poor light source may produce a well-cured surface which conceals inadequately or even unpolymerised resin in the deeper parts of the cavity (Hansen and Asmussen, 1993a). The application of a high light intensity increased the curing depth of composite resins regardless of resin matrix composition (Tanoue, *et al.*, 1998a & b).

The surface hardness of dental composites is affected by the temperature (Bausch *et al.*, 1981, Hansen 1983, Greener *et al.*, 1984, Watts *et al.*, 1987). Watts *et al.*, (1986) confirmed that the increase in hardness is greater at 37 °C than at 20 °C, and materials stored in an aqueous environment at 37 °C were softened compared to dry samples. Hansen (1983) reported that temperature, water absorption and the contact time affect the surface hardness of dental composites with the aqueous media.

Poor solvent stability appears to be related to filler type as well as degree of conversion, since radiopaque glasses appear to be more easily hydrolysed in water than quartz (Watts, 1992). Söderholm (1983) and Øysaed and Ruyet (1986) have shown that all fillers leak Si in water, with quartz composites being more stable than those based upon Ba or Sr glasses.

4.2 Objectives

To evaluate the effect of two different light intensities emitted from the Elipar highlight unit on upper and lower surface hardness of resin composites.

To investigate whether the low intensity irradiation for 10 s achieves any measurable level of hardness from the zero value exhibited by the unset composite paste.

To study the effect of the post-cure temperature (37 °C) on the hardness of the resin composite materials cured at low intensity to see if the temperature can compensate for deficiency in the light intensity.

4.3 Materials and Methods

Plastic moulds 2.5 mm deep with a hole 5 mm in diameter were used. Three resin composite materials are listed in Table 4-1 and were cured using the Elipar Highlight unit.

Table 4-1: Resin composite materials were investigated

Materials	Code	Batch No.	Manufacturer
Z100	**Z100**	3021	3M Dental Products, ST. Paul, USA
Pertac II	**PER2**	643081003	Espé, Dental AG, Seefeld, Germany
Charisma	**CHR**	049	Heraeus Kulzer, Wehrheim, Germany

5 groups from each material were examined:

Group 1. Irradiated for 40 s high light intensity and stored dry at 23 °C.

Group 2. Irradiated for 10 s. low light intensity and stored dry at 23 °C.

Group 3. Irradiated for 10 s. low light intensity and stored wet in deionized water at 23 °C.

Group 4. Irradiated for 10 s. low light intensity and stored dry at 37 °C.

Group 5. Irradiated for 10 s. low light intensity and stored wet in deionized water at 37 °C.

The moulds were covered with cellulose acetate matrix strips then by a glass microscope slide at both sides. Hand pressure was applied to remove the excess material. The specimens were irradiated from the top surface and stored for ageing times 5, 60 min, 24 hrs, 1 wk, 1 month, and 3 months, before the measurements were taken. ***The hardness of each group was measured at five different sites on each of the top and lower surfaces on each specimen, and the mean value calculated.*** For each group of experiments, the hardness was taken as the mean value obtained from the three specimens.

4.3.1 Specimen Measurement

The hardness was measured using a Wallace Hardness Instrument (H. W. Wallace Co. Ltd., Croydon, England) (Fig 4-1). This measures directly and accurately the depth of penetration of a Vickers Pyramid Diamond Indenter into the specimen. The instrument consists basically of an indenter and a means of applying a primary load (1 gram) followed by a secondary load (300 grams), to the indenter. The specimen was mounted on the table of the instrument using

a vacuum device and indentation was measured by raising the table until the indenter was returned to the position it occupied before the secondary load was applied. The movement of the table is equal to the depth of indentation. The Wallace numbers or penetration depths were taken with the load applied for 15 sec. These surface penetration depths were re-expressed as hardness in the reciprocal unit (mm^{-1}), so that the resultant parameter increased with increasing hardness. Thus, the smaller the indentation, the larger is the hardness number, and the harder is the material.

The stresses under the indenter are rather complicated, the key feature is that plastic deformation is required to obtain a permanent deformation that can be measured. The Vickers indenter in the Wallace Micro Indentation Instrument is a square pyramid, and the shape of indentation is identical at all loads and hardnesses. The area of indentation is calculated, from the depth of indentation to obtain the surface hardness number. The angle 136° arises from the angle between opposing faces of the pyramid. It can be seen that the surface hardness is inversely proportional to the square of the depth of indentation in the materials.

4.3.2 Statistical Analysis

The data of the surface hardness of the three investigated materials were statistically analysed using 4-way analysis of variance (ANOVA). The independent variables were light intensity [two levels (full intensity and low intensity)], temperatures [two levels (23°C and 37°C)], storage [two levels (dry and wet)], ageing time [six levels (5 min, 1 hr, 24 hr, 1 wk, 1 month and 3 months)]. One-way ANOVA followed by the Scheffé procedure were further performed to detect any significant difference in ageing time for each tested group and each tested surface at $p < 0.05$.

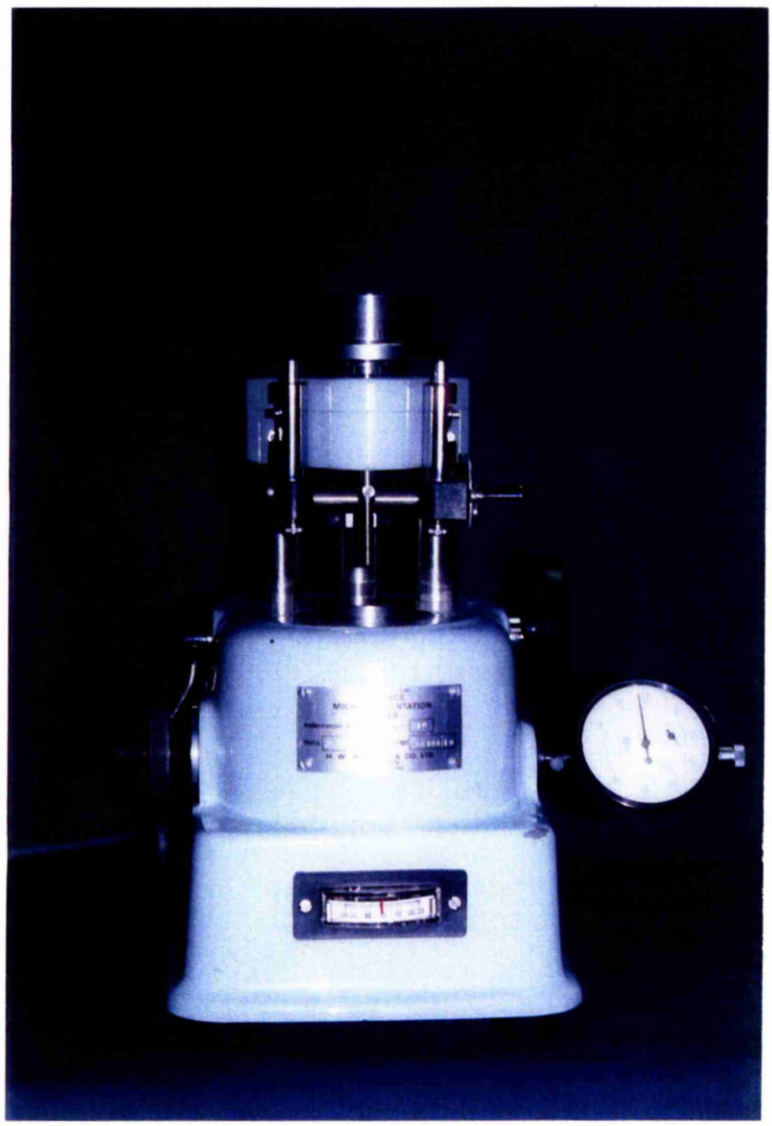

Fig 4-1: Wallace Hardness Instrument.

4.4 Results

The mean values and standard deviations of surface hardness results are plotted graphically in Figs 4 - 3 to 4 – 5 and presented in Tables 4 - 2 to 4 - 4.

The hardness development of each surface (top and bottom) of **Z100** material is presented in Fig. 4-3 and Table 4-2. The surface hardness was significantly increased with ageing time ($p < 0.05$). The specimens treated with full intensity were found to have the highest surface hardness either on top or lower surfaces. The surface hardness was increased with temperature (37°C). The temperature (37°C) improved the hardness by 21% in dry condition and 15% in wet storage. Low intensity was compensated to some degree by elevated temperature (37°C) especially in dry storage. The statistical analysis were summarized in Tables 4-5 and 4-6.

Fig 4-4 and Table 4-3 demonstrate the development of the surface hardness of **PER2**. The hardness (top and bottom) significantly increased with time for the specimens cured by 40 s high intensity ($p < 0.05$). For specimens cured by 10 s low intensity, the surface hardness was low at top surfaces and nil (zero) at bottom surfaces. The temperature (37°C) slightly improved the hardness for specimens cured by 10 s low intensity. The surface hardness of specimens stored wet was lower than those stored dry. Tables 4-7 and 4-8 show the statistical analysis the hardness with the ageing time.

Table 4-4 and Fig. 4-5 present the development of the surface hardness of **CHR** with ageing time and with other variables (intensity, storage, and temperature). The highest microhardness was obtained from the specimens which cured by full light intensity, then the specimens cured by low intensity and stored at 37°C, whether dry or wet. The same principle was found with **CHR**, in that the greatest increase in hardness after cessation of the activating light was found at the first week. The statistical analyses were demonstrated in Tables 4-9 and 4-10.

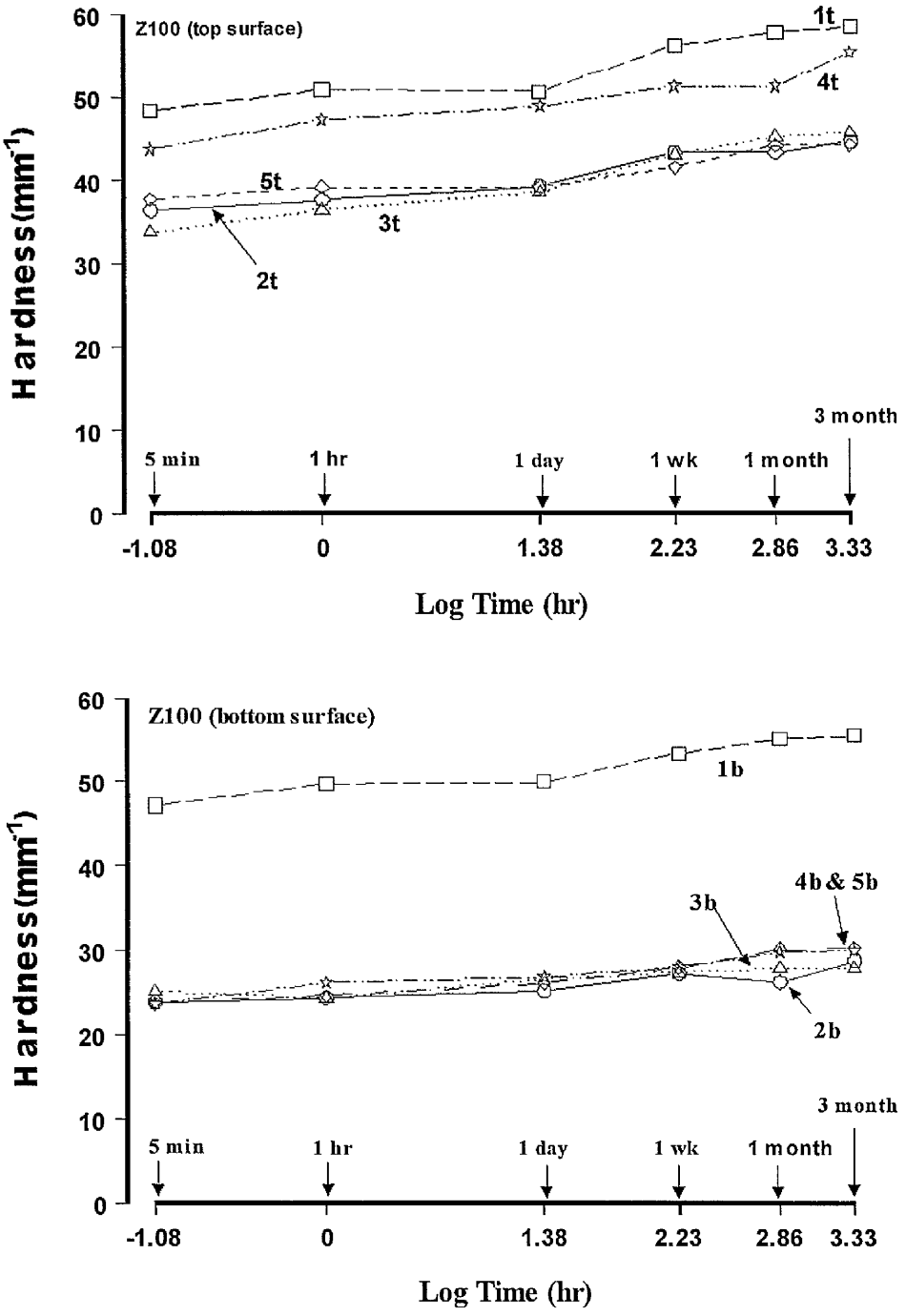

Fig 4-3: Hardness development of **Z100** material. Specimens cured and stored in different conditions:

1t) Top surface, full intensity, 23°C, dry.
2t) Top surface, low intensity, 23°C dry.
3t) Top surface, low intensity, 23°C wet.
4t) Top surface, low intensity, 37°C dry.
5t) Top surface, low intensity, 37°C wet.

1b) Bottom surface, full intensity, 23°C dry.
2b) Bottom surface, low intensity, 23°C dry
3b) Bottom surface, low intensity, 23°C wet.
4b) Bottom surface, low intensity, 37°C dry.
5b) Bottom surface, low intensity, 37°C wet.

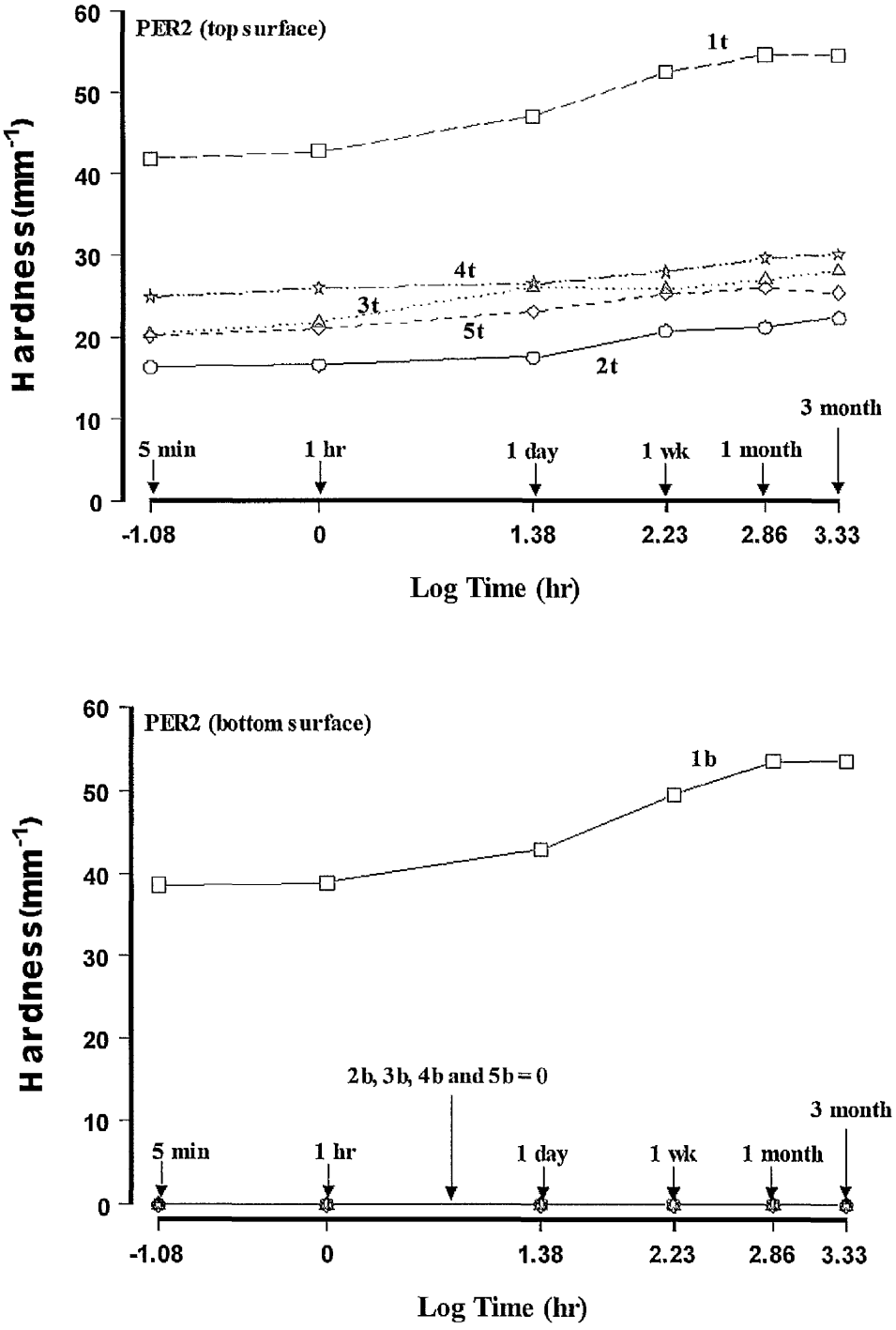

Fig 4-4: Hardness development of **PER2** material. Specimens cured and stored in different conditions:

1t) Top surface, full intensity, 23°C, dry.
2t) Top surface, low intensity, 23°C dry.
3t) Top surface, low intensity, 23°C wet.
4t) Top surface, low intensity, 37°C dry.
5t) Top surface, low intensity, 37°C wet.

1b) Bottom surface, full intensity, 23°C dry.
2b) Bottom surface, low intensity, 23°C dry
3b) Bottom surface, low intensity, 23°C wet.
4b) Bottom surface, low intensity, 37°C dry.
5b) Bottom surface, low intensity, 37°C wet.

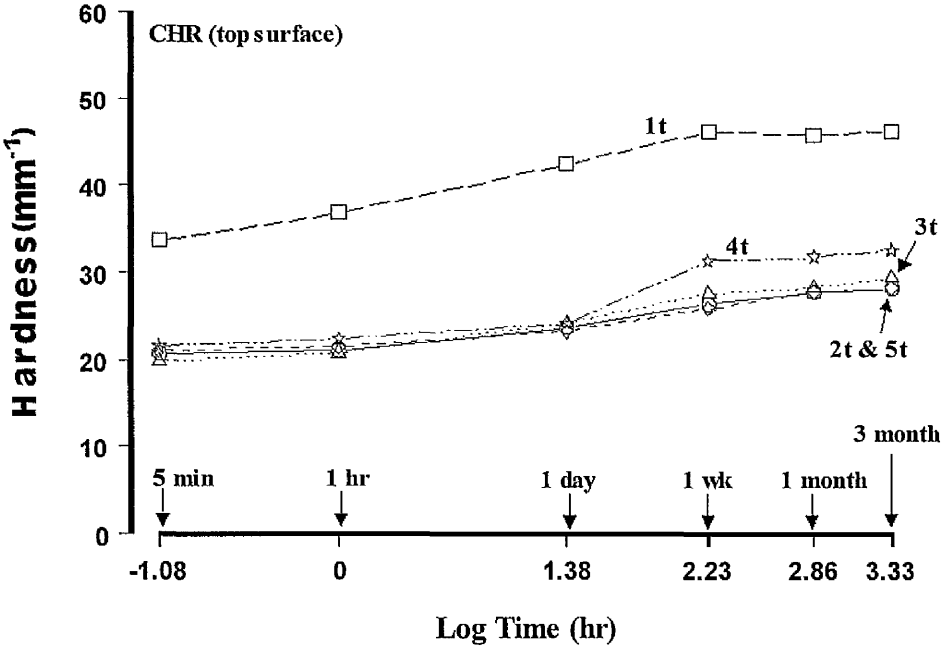

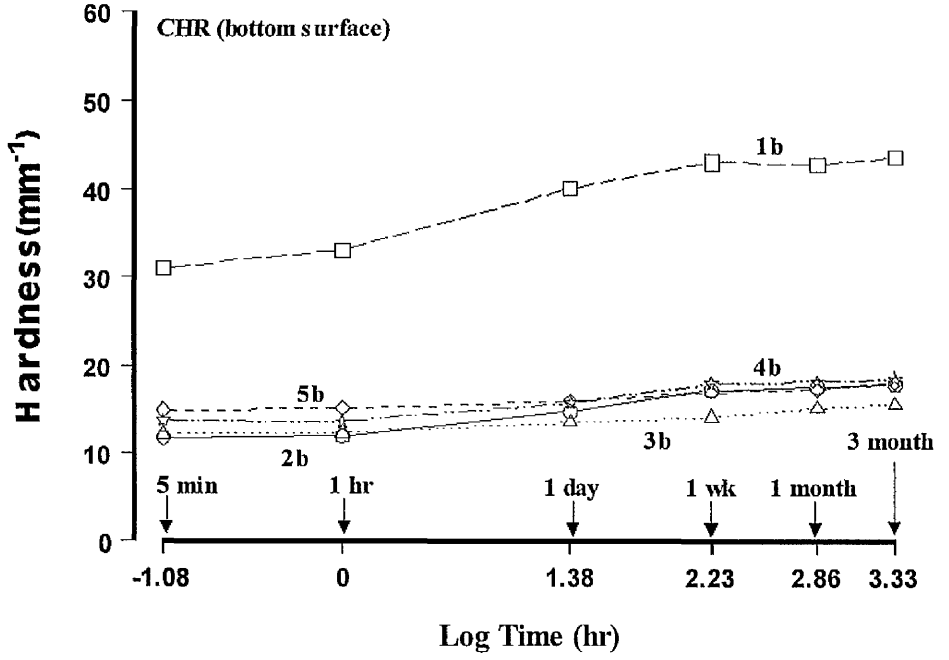

Fig 4-5: Hardness development of **CHR** material. Specimens cured and stored in different conditions:

1t) Top surface, full intensity, 23°C, dry.
2t) Top surface, low intensity, 23°C dry.
3t) Top surface, low intensity, 23°C wet.
4t) Top surface, low intensity, 37°C dry.
5t) Top surface, low intensity, 37°C wet.

1b) Bottom surface, full intensity, 23°C dry.
2b) Bottom surface, low intensity, 23°C dry
3b) Bottom surface, low intensity, 23°C wet.
4b) Bottom surface, low intensity, 37°C dry.
5b) Bottom surface, low intensity, 37°C wet.

Table 4-2: Mean values and SD (in parenthesis) of surface hardness of **Z100.**

Storage	Temp.	Cure	Surface Tested	Time	Mean	(SD)	% of hardness increase
Dry	23°C	Full light Intensity	Top	5 min	48.41	(3.18)	16.91 %
				1 hr	50.90	(4.20)	
				1 day	50.59	(3.00)	
				1 week	56.03	(2.04)	
				1 month	57.67	(0.45)	
				3 months	58.26	(1.40)	
Dry	23°C	Full light Intensity	Lower	5 min	47.10	(2.60)	15.04 %
				1 hr	49.63	(1.40)	
				1 day	49.82	(1.80)	
				1 week	53.30	(5.00)	
				1 month	54.97	(4.00)	
				3 months	55.44	(3.30)	
Dry	23°C	10 s Low intensity	Top	5 min	36.46	(1.50)	18.23 %
				1 hr	37.64	(1.50)	
				1 day	39.23	(0.84)	
				1 week	43.28	(2.34)	
				1 month	43.27	(2.20)	
				3 months	44.59	(4.90)	
Dry	23°C	10 s Low intensity	Lower	5 min	23.84	(1.30)	17.05 %
				1 hr	24.32	(1.50)	
				1 day	25.15	(0.85)	
				1 week	27.20	(1.97)	
				1 month	26.22	(1.12)	
				3 months	28.74	(2.30)	
Wet	23°C	10 s Low intensity	Top	5 min	33.70	(2.30)	26.07 %
				1 hr	36.50	(2.60)	
				1 day	38.53	(2.55)	
				1 week	43.02	(3.10)	
				1 month	45.16	(2.10)	
				3 months	45.58	(4.80)	
Wet	23°C	10 s Low intensity	Lower	5 min	25.14	(0.23)	9.57 %
				1 hr	24.32	(0.85)	
				1 day	26.53	(0.89)	
				1 week	27.39	(1.39)	
				1 month	27.78	(1.80)	
				3 months	27.80	(1.30)	
Dry	37°C	10 s Low intensity	Top	5 min	43.80	(2.66)	20.80 %
				1 hr	47.25	(2.80)	
				1 day	48.80	(7.60)	
				1 week	51.20	(2.60)	
				1 month	51.20	(0.61)	
				3 months	55.30	(4.50)	
Dry	37°C	10 s Low intensity	Lower	5 min	23.70	(5.10)	20.87 %
				1 hr	26.15	(4.20)	
				1 day	26.80	(3.80)	
				1 week	27.97	(0.60)	
				1 month	29.79	(0.80)	
				3 months	29.95	(0.62)	
Wet	37°C	10 s Low intensity	Top	5 min	37.72	(0.87)	14.63 %
				1 hr	39.21	(0.85)	
				1 day	39.10	(4.20)	
				1 week	41.50	(1.80)	
				1 month	44.11	(1.94)	
				3 months	44.18	(0.68)	
Wet	37°C	10 s Low intensity	Lower	5 min	23.70	(1.40)	21.15 %
				1 hr	24.64	(1.40)	
				1 day	26.05	(3.10)	
				1 week	28.01	(2.70)	
				1 month	30.05	(2.27)	
				3 months	30.16	(1.00)	

Table 4-3: Mean values and SD (in parenthesis) of surface hardness of **PER2**.

Storage	Temp.	Cure	Surface Tested	Time	Mean	(SD)	% of hardness increase
Dry	23°C	Full light Intensity	Top	5 min	41.88	(2.00)	24.77 %
				1 hr	42.70	(2.40)	
				1 day	47.03	(2.82)	
				1 week	52.25	(2.80)	
				1 month	54.45	(2.60)	
				3 months	54.34	(1.04)	
Dry	23°C	Full light Intensity	Lower	5 min	38. 67	(1.25)	27.72 %
				1 hr	38.90	(1.08)	
				1 day	43.04	(3.51)	
				1 week	49.50	(1.50)	
				1 month	53.37	(0.83)	
				3 months	53.50	(2.08)	
Dry	23°C	10 s Low intensity	Top	5 min	16.36	(0.92)	26.47 %
				1 hr	16.64	(0.60)	
				1 day	17.49	(1.34)	
				1 week	20.70	(5.80)	
				1 month	21.12	(7.60)	
				3 months	22.25	(7.60)	
Dry	23°C	10 s Low intensity	Lower	5 min	0.0		00
				1 hr	0.0		
				1 day	0.0		
				1 week	0.0		
				1 month	0.0		
				3 months	0.0		
Wet	23°C	10 s Low intensity	Top	5 min	20.40	(2.40)	26.97 %
				1 hr	21.84	(2.30)	
				1 day	26.03	(0.81)	
				1 week	25.71	(2.06)	
				1 month	26.85	(1.60)	
				3 months	27.94	(1.70)	
Wet	23°C	10 s Low intensity	Lower	5 min	0.0		00
				1 hr	0.0		
				1 day	0.0		
				1 week	0.0		
				1 month	0.0		
				3 months	0.0		
Dry	37°C	10 s Low intensity	Top	5 min	24.90	(1.90)	16.94 %
				1 hr	25.90	(2.35)	
				1 day	26.45	(3.04)	
				1 week	27.85	(1.90)	
				1 month	29.46	(2.70)	
				3 months	29.98	(2.10)	
Dry	37°C	10 s Low intensity	Lower	5 min	0.0		00
				1 hr	0.0		
				1 day	0.0		
				1 week	0.0		
				1 month	0.0		
				3 months	0.0		
Wet	37°C	10 s Low intensity	Top	5 min	20.15	(1.16)	20.42 %
				1 hr	21.05	(1.47)	
				1 day	23.08	(2.90)	
				1 week	25.20	(2.70)	
				1 month	25.83	(2.60)	
				3 months	25.32	(1.70)	
Wet	37°C	10 s Low intensity	Lower	5 min	0.0		00
				1 hr	0.0		
				1 day	0.0		
				1 week	0.0		
				1 month	0.0		
				3 months	0.0		

Table 4-4: Mean values and SD (in parenthesis) of surface hardness of **CHR**.

Storage	Temp	Cure	Surface Tested	Time	Mean	(SD)	% of hardness increase
Dry	23°C	Full light Intensity	Top	5 min	33.6	(1.21)	27.00 %
				1 hr	36.7	(2.06)	
				1 day	42.3	(1.16)	
				1 week	46.03	(2.22)	
				1 month	45.74	(2.90)	
				3 months	46.03	(2.20)	
Dry	23°C	Full light Intensity	Lower	5 min	31.05	(0.52)	29.00 %
				1 hr	33.09	(1.17)	
				1 day	40.15	(2.80)	
				1 week	43.10	(2.60)	
				1 month	42.83	(2.80)	
				3 months	43.73	(2.40)	
Dry	23°C	10 s Low intensity	Top	5 min	20.70	(1.66)	26.47 %
				1 hr	21.09	(1.71)	
				1 day	23.70	(1.82)	
				1 week	26.30	(1.60)	
				1 month	27.70	(2.30)	
				3 months	28.15	(2.20)	
Dry	23°C	10 s Low intensity	Lower	5 min	11.76	(0.83)	37.93 %
				1 hr	11.90	(0.89)	
				1 day	14.70	(0.47)	
				1 week	17.14	(2.23)	
				1 month	17.56	(2.23)	
				3 months	17.82	(1.85)	
Wet	23°C	10 s Low intensity	Top	5 min	19.90	(0.96)	31.99 %
				1 hr	20.78	(0.86)	
				1 day	24.23	(1.73)	
				1 week	27.50	(1.10)	
				1 month	28.24	(1.24)	
				3 months	29.26	(1.60)	
Wet	23°C	10 s Low intensity	Lower	5 min	12.10	(0.84)	22.44 %
				1 hr	12.33	(0.72)	
				1 day	13.50	(0.74)	
				1 week	14.10	(0.58)	
				1 month	15.17	(1.16)	
				3 months	15.60	(1.18)	
Dry	37°C	10 s Low intensity	Top	5 min	21.60	(2.60)	33.54 %
				1 hr	22.40	(2.60)	
				1 day	24.13	(3.50)	
				1 week	31.21	(1.71)	
				1 month	31.66	(2.44)	
				3 months	32.50	(4.10)	
Dry	37°C	10 s Low intensity	Lower	5 min	13.70	(1.40)	29.94 %
				1 hr	13.64	(0.55)	
				1 day	15.70	(0.73)	
				1 week	17.90	(0.68)	
				1 month	18.19	(0.65)	
				3 months	18.43	(0.69)	
Wet	37°C	10 s Low intensity	Top	5 min	21.07	(1.19)	25.06 %
				1 hr	21.50	(1.44)	
				1 day	23.30	(2.40)	
				1 week	25.81	(3.11)	
				1 month	27.75	(3.40)	
				3 months	28.13	(2.60)	
Wet	37°C	10 s Low intensity	Lower	5 min	14.90	(1.38)	17.63 %
				1 hr	15.11	(1.36)	
				1 day	15.90	(0.37)	
				1 week	16.94	(0.97)	
				1 month	17.29	(0.90)	
				3 months	18.09	(1.20)	

Table 4-5: Statistical analysis (Scheffé test) of top surfaces **Z100** at different ageing times.

Time	Full int., 23°C, dry	Low int., 23°C, dry	Low int., 23°C, wet	Low int., 37°C, dry	Low int., 37°C, wet
5 min – 1 hr					
5 min – 1 day			*		
5 min – 1 wk	*	*	*	*	*
5 min – 1 month	*	*	*	*	*
5 min – 3 months	*	*	*	*	*
1 hr - 1 day					
1 hr - 1 wk	*	*	*		
1 hr - 1 month	*	*	*		*
1 hr - 3 months	*	*	*	*	*
1 day - 1 wk	*	*	*		
1 day - 1 month	*	*	*		*
1 day - 3 months	*	*	*	*	*
1 wk - 1 month					
1 wk - 3 months					
1 month - 3 months					

(*) Indicates significant differences at the level $p < 0.05$.

Table 4-6: Statistical analysis (Scheffé test) of Bottom surfaces **Z100** at different ageing times.

Time	Full int., 23°C, dry	Low int., 23°C, dry	Low int., 23°C, wet	Low int., 37°C, dry	Low int., 37°C, wet
5 min – 1 hr					
5 min – 1 day					
5 min – 1 wk	*	*	*	*	*
5 min – 1 month	*	*	*	*	*
5 min – 3 months	*	*	*	*	*
1 hr - 1 day			*		
1 hr - 1 wk		*	*		*
1 hr - 1 month			*	*	*
1 hr - 3 months	*	*	*	*	*
1 day - 1 wk					
1 day - 1 month	*				*
1 day - 3 months	*	*			*
1 wk - 1 month					
1 wk - 3 months					
1 month - 3 months		*			

(*) Indicates significant differences at the level $p < 0.05$.

Table 4-7: Statistical analysis (Scheffé test) of top surfaces **PER2** at different ageing times.

Time	Full int., 23°C, dry	Low int., 23°C, dry	Low int., 23°C, wet	Low int., 37°C, dry	Low int., 37°C, wet
5 min – 1 hr					
5 min – 1 day	*		*		*
5 min – 1 wk	*		*	*	*
5 min – 1 month	*		*	*	*
5 min – 3 months	*	*	*	*	*
1 hr - 1 day	*		*		
1 hr - 1 wk	*		*		*
1 hr - 1 month	*		*	*	*
1 hr - 3 months	*	*	*	*	*
1 day - 1 wk	*				
1 day - 1 month	*			*	
1 day - 3 months	*			*	*
1 wk - 1 month					
1 wk - 3 months					
1 month - 3 months					

(*) Indicates significant differences at the level $p < 0.05$.

Table 4-8: Statistical analysis (Scheffé test) of lower surfaces **PER2** at different ageing times.

Time	Full int., 23°C, dry	Low int., 23°C, dry	Low int., 23°C, wet	Low int., 37°C, dry	Low int., 37°C, wet
5 min – 1 hr					
5 min – 1 day	*				
5 min – 1 wk	*				
5 min – 1 month	*				
5 min – 3 months	*				
1 hr - 1 day	*				
1 hr - 1 wk	*				
1 hr - 1 month	*				
1 hr - 3 months	*				
1 day - 1 wk	*				
1 day - 1 month	*				
1 day - 3 months	*				
1 wk - 1 month	*				
1 wk - 3 months	*				
1 month - 3 months					

(*) Indicates significant differences at the level $p < 0.05$.

Table 4-9: Statistical analysis (Scheffé test) of top surfaces **CHR** at different ageing times.

Time	Full int., 23°C, dry	Low int., 23°C, dry	Low int., 23°C, wet	Low int., 37°C, dry	Low int., 37°C, wet
5 min – 1 hr					
5 min – 1 day	*	*	*		
5 min – 1 wk	*	*	*	*	*
5 min – 1 month	*	*	*	*	*
5 min – 3 months	*	*	*	*	*
1 hr - 1 day	*	*	*		
1 hr - 1 wk	*	*	*	*	*
1 hr - 1 month	*	*	*	*	*
1 hr - 3 months	*	*	*	*	*
1 day - 1 wk		*	*	*	
1 day - 1 month		*	*	*	*
1 day - 3 months	*	*	*	*	*
1 wk - 1 month					
1 wk - 3 months					
1 month - 3 months					

(*) Indicates significant differences at the level $p < 0.05$.

Table 4-10: Statistical analysis (Scheffé test) of lower surfaces **CHR** at different ageing times.

Time	Full int., 23°C, dry	Low int., 23°C, dry	Low int., 23°C, wet	Low int., 37°C, dry	Low int., 37°C, wet
5 min – 1 hr					
5 min – 1 day	*	*	*	*	
5 min – 1 wk	*	*	*	*	*
5 min – 1 month	*	*	*	*	*
5 min – 3 months	*	*	*	*	*
1 hr - 1 day	*	*	*	*	
1 hr - 1 wk	*	*	*	*	*
1 hr - 1 month	*	*	*	*	*
1 hr - 3 months	*	*	*	*	*
1 day - 1 wk		*		*	
1 day - 1 month		*	*	*	*
1 day - 3 months	*	*	*	*	*
1 wk - 1 month			*		
1 wk - 3 months			*		
1 month - 3 months					

(*) Indicates significant differences at the level $p < 0.05$.

4.5 Discussion

In this work, the surface hardness of the resin composites was measured after polymerisation using a Wallace hardness instrument. This measures the depth of penetration of a Vickers diamond, but we express the data as reciprocal penetration (mm^{-1}). The principle of this tester is that the indenter remains in contact with the specimen during the dwell time and also whilst the measurement is made. Therefore no recovery is possible, which may occur in tests on polymers where the indenter is removed before measurement.

Vickers hardness is normally measured following removal of the indenter from the material. While the resultant figure indicates permanent deformation (the Wallace value gives permanent plus elastic deformation), optical determination of the residual indentation in the test material is difficult, especially in composite resin materials. The permanent deformation in the surface resulted from local plastic flow. The plastic flow in resin composites occurs most readily in the resin phase (Watts, *et al.*, 1987).

In this study, a number of factors were found to affect the surface hardness of the resin composite materials. These included the light intensity; temperature; ageing time and water storage.

Polymerisation is not an immediate process, but it is continuous and constant even after the removal of the light source (Hansen, 1983). The variation of microhardness with time reflects changes in the resin phase. These changes may correlate with the time variation of residual methacrylate groups in the resin. However the relationship between degree of conversion and microhardness of the resin, invariably is not a simple linear correlation (Assmusen, 1982b; Ferracane, 1985). The increase in surface microhardness with time means that an appreciable concentration of free radicals persist in the system after cessation of light irradiation (Ledwith, 1977). The results of this part in agreement with the findings of Watts, *et al.*, (1987) on the time scale of the surface hardness increase.

Increases in hardness and degree of conversion following prolonged exposure are explained by the elevated rates of free radical formation from the photoinitiator-amine exiplex (Eliades, *et al.*, 1987). Increasing the exposure time of the resin composites to the curing light results in an increase in the hardness. This phenomenon was found in the measurement of the depth of cure (Chapter 2, Part III), when the duration time of the low intensity was increased to 40

seconds. The depth of cure was found to be greater than when the investigated materials were cured for only 10 sec. Therefore, increase in the exposure time can increase the degree of the conversion of the resin composites. This property will be more fully explained in the study of degree of conversion (Chapter 5).

Higher light output provided greater hardness of light-cured composite resins. It is indicated from the results obtained that surface hardness was achieved at the end of the light irradiation time. Particularly so when the materials were cured by full light intensity, but also when irradiated by low light intensity and stored at an elevated temperature (37 °C), there was an increase in the hardness due to the increase in the extent of cure. The effect of light intensity on the surface hardness of the resin composite materials was significantly noticed. This is in agreement with the findings of several researchers (Yearn, 1985; Hansen and Asmussen, 1993a; Tanoue, *et al.*, 1998c).

As presented in the results, the hardness of the bottom surfaces were lower than the top surfaces. When the resin composites were cured by full light intensity, the hardness of the lower surfaces was less affected. Nevertheless, the hardness of top or bottom surfaces varies between the different resin composite brands, even if the same light curing unit and light intensity are used. The low intensity of light (10 s) of the Elipar highlight was not sufficient to completely polymerise the investigated materials. Particularly with **PER2**, the hardness of the bottom surface was found to be nil and there was no improvement in this material with storage time even at 37°C. This may be attributed to the effect of composition and chemistry of this material. From these results we can say that the hardness is a good predictor for the degree of conversion of the resin composites and exhibits the ability of the light to polymerise the materials.

The Elipar unit used in this study was found to polymerise the resin composites investigated efficiently when full light intensity was used, but the low intensity greatly influenced the flow of the restorative materials and it is suitable to use for "soft-start" polymerisation. At greater depths below the surface, the extent of resin polymerisation is reduced because of the lower intensities of light penetrating to these depths (Ruyter and Øysaed, 1982; Cook and Standish, 1983; Watts, *et al.*, 1984).

Elevated temperature to 37 °C cannot completely compensate the lack of light intensity, but

it can improve the cure of the composite resin to some degree. The microhardness of the resin composites investigated cured by low intensity and stored dry at 37 °C, were higher than those stored at 23 °C either dry or wet. **Z100** was the material most improved by post-cure heat at 37°C, while with **PER2** the least improvement was observed. The increase in temperature could not change in the polymerisation of **PER2** at the bottom surface, but a slight change was noticed at the top surface. In general, it is suggested that the increase in temperature can improve the degree of polymerisation of some brands of resin composite restorative materials. This results in agreement with the findings of Hirabayashi, *et al.*, (1993). McCabe, (1985), reported that a greater degree of conversion was achieved at 37°C compared to 23°C, particularly at short exposure times. As conversion proceeds, the glass transition temperature of the resin increases until it reaches the temperature of the polymerising material. Further conversion then becomes difficult as the mobility of the polymer and monomer molecules is greatly reduced. The reaction rate depends upon the segmental mobility in the resin phase, which is thermally activated at increased temperatures (Watts, *et al.*, 1986 and 1987). The reactivity of the radicals is affected by the viscosity of the matrix, which determines the mobility of the polymer radicals. The high temperature may lead to an enhanced mobility of dimethacrylate monomers and a greater flexibility of the chains in the network (Kildal and Ruyter, 1994).

Composite materials are known to absorb a small percentage of water (Braden, *et al.*, 1976) which changes the magnitude of some physical properties (Watts, *et al.*, 1987). Since hardness is a surface property, then the effects of water sorption on the material surface should occur much more rapidly than the bulk. In composites, bulk equilibrium is not attained in 1 week (Swarts, *et al.*, 1982) and may take as much as 30 days (Fan, *et al.*, 1985). Normally the changes observed are that water sorption decreases the microhardness, whether stored in 23°C or 37°C. Longer storage of the resin composites in water may reach the stabilisation stage, and it is possible that microhardness decreases. In this study, the microhardness was found almost linear from one month to 3 months. This may give an indication that the microhardness will decrease after 3 months. These results are in agreement with Helvatjoglou, *et al.*, (1991) who found that the hardness of wet, light-cured specimens of composite restorative materials progressively increased for 4 weeks followed by stabilisation or decrease.

As mentioned in "Methods", the mould depth used was 2.5 mm, in correlation with the results of the depth of cure of the investigated materials **Z100**, **PER2** and **CHR F**, when cured by 10

s low intensity, (2.24 mm, 1.93 mm and 2.39 mm respectively). Thus, a low level of polymerisation (hardness) at the bottom surfaces was found for **Z100** and **CHR**, but for **PER2** it was found nil at all points in the time scale (from 5 min to 3 months). It is obvious that the low intensity light does not easily reach the deep areas of this resin restorative material.

The hardness of **Z100** was found higher than **CHR** and **PER2**. This may be attributed to the filler size of **Z100** (0.1 – 3.5 μm) which is slightly larger than **CHR** and **PER2** (0.1 – 2 μm).

4.6 Conclusions

- The upper and lower surface hardness varied between these resin composite products.

- The hardness of the group cured by full intensity was significantly higher than those cured by low intensity. Thus, the investigated materials are greatly affect by variation in the light intensity.

- The hardness was low at the bottom surfaces, due to the attenuation in the light intensity by the resin composites.

- The low intensity irradiation produced significant cure of the material as shown by the finite hardness values attained.

- The post-cure temperature significantly increased the hardness rate of **Z100** when stored dry at 37°C for the longer storage times.

- The increase in hardness of the investigated materials is greater at 37°C than 23°C.

Chapter 5

Comparative Evaluation of the Low-Intensity "Soft-Start" Irradiation of Resin-Composites by Degree of Conversion Measurements

5.1 Literature Review

The degree of conversion (DC) of resin materials is defined by the extent to which carbon double bonds (C=C) are converted into carbon single bonds (C-C).

It is preferable for a dental restorative resin to convert all of its monomer to polymer during its polymerisation reaction. However, dimethacylate monomers undergo extensive cross-linking on polymerisation with considerable residual unsaturation in the final product. This ranges from 25-45 %, or degree of conversion (DC) ranging from 55 - 75 % (Ferracane and Greener, 1984 and 1986; Eliades *et al.*, 1987; Ruyter and Øysæd, 1988).

Cross-linking of the dimethacrylate occurs when polymer chains are joined together by chemical bonds and this has a profound effect on the properties of the polymer (Phillips, 1991). The unconverted methacrylate groups must reside in the polymer network either as residual monomer or (a majority) as pendant side chains (PSC), which extend from the main chains by virtue of having reacted at only one end of the difunctional molecule. A further possibility is a cyclisation reaction. As residual monomers, these molecules function as plasticizing agents which can reduce the properties of the polymer network. This occurs until such time as the monomers leach from the composite into the oral environment. Pendant side chains will act as permanent plasticizers in the composite (Watts, 1992).

The conversion of dental resins has been evaluated by Infrared (IR) Spectroscopy (Ruyter and Svendsen, 1978; Ruyter and Øysæd,1982; Ferracane and Greener, 1984; Eliades *et al.*, 1987; Rueggeberg and Craig, 1988; Rueggeberg and Caughman, 1993; Ferracane, *et al.*, 1997; Bagis

and Reuggeberg, 1997; Loza-Herrero, *et al.*, 1998). The unpolymerised carbon-carbon double bonds give rise to an infrared (IR) absorption at 1638 cm^{-1}, which enables determination of DC (Watts, 1992). The rate at which the height of carbon double bonds (C = C) of this peak reduces, gives a direct indication of the rate of consumption of double bonds in the setting reaction (McCabe, 1992).

The nature of the unpolymerised resin is of considerable concern, especially in terms of deleterious effects on the mechanical properties and dimensional stability of the restoration (Cox *et al.*, 1987). The presence of unreacted molecules, or poorly polymerised resin, at the base of a light cured composite restoration, has several undesirable features. Mechanically, the restoration may be compromised by the reduced strength and hardness of the resin. In addition, unreacted components may be leached from the restoration, causing local tissue irritation and possibly an increased potential for secondary caries (DeWald and Ferracane, 1987). To avoid these damaging effects, the DC must be increased in order to produce stiffer and more durable resins (Watts, 1992).

For a given VLC product the DC depends upon the light intensity reaching the composite surface, the time of exposure, (Watts, 1992; Rueggeberg, *et al.*, 1993; Feilzer, *et al.*, 1995a; Harrington, *et al.,* 1996), and the thermal energy within the system, as determined principally by the ambient temperature (Watts, 1992).

Loza-Herrero, *et al.*, (1998), reported on the free radicals created during initial light curing. They found that the number of these remaining free radicals may be too low to provide for additional conversion of monomer in post-cure-heated specimens, but that this is dependent upon the time after initial light-curing at which the specimen is exposed to heat treatment. The effect of post-cure heat was a significant increase in the DC of the restorative composite resins. Also this was studied by other researchers (Ferracane, *et al.*, 1997; Bagis and Reuggeberg, 1997).

5.2 Introduction to FT-IR Spectroscopy

5.2.1 Infrared Spectrometer

When a material is expose to infrared radiation, some of the infrared energy is absorbed and the rest will be transmitted. If we place a detector that is sensitive to infrared radiation in the path of the transmitted beam, we can determine how the beam has changed. The C = C in the dimethacrylate can absorb the precise amount of radiation energy near 1637 cm^{-1} which causing a characteristic stretching vibration of the molecule. This is the basic principle of an infrared spectrometer.

Fourier Transform Infrared (FT-IR) spectrometer operates under the same general principle as the simple spectrometer. Its mechanisms are housed in two basic components: 1) an optical bench and 2) a computer.

5.2.1.1 Components of the Optical Bench

The optical bench measures the intensity of a specially encoded infrared beam after it has been passed through a sample. The resulting signal, called an "*interferogram*", contains information about all frequencies present in the beam. The optical bench consists of (Fig 5-1):

5.2.1.1.1 The Source

The heated *source* emits infrared radiation. The source in an FT-IR spectrometer is extremely stable. If allowed sufficient time to heat up thoroughly, it produces the same pattern of intensities over its defined frequency range no matter when they are measured. The infrared beam leaves the source and is deflected off a mirror. The mirror directs the beam into the interferometer where spectral encoding takes place.

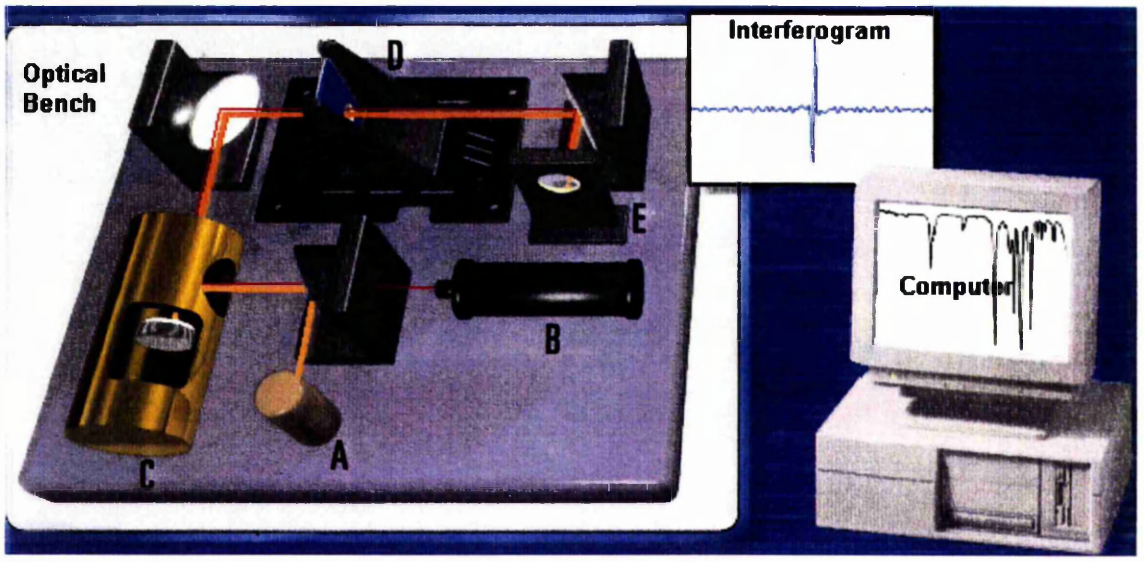

Fig 5-1: Components of optical bench of the FT-IR connected to the computer. (A) the source of the IR, (B) the laser, (C) interferometer, (D) specimen holder and (E) the detector. The yellow line indicates the emission of the IR from the source and the red line indicates the laser path.

5.2.1.1.2 Interferometer

Inside the interferometer, the beam is immediately split into two paths by the beamsplitter. Each path leads to a mirror, which simply sends the beam back to the beamsplitter, where it is recombined. This configuration causes the beams to interfere with each other constantly as the beams are recombined. These two mirrors are:

1. The *fixed mirror* is attached to the interferometer housing so it always reflects the beam from the same place.
2. The *moving mirror* travels back and forth along a precisely controlled track reflecting the beam from a position that is constantly changing. This movement causes the intensity of the recombined beam to change constantly. The change in intensity is different for each frequency of radiation. This movement is called "scanning" because it allows us to gather information about, or "scan", all frequencies of the beam.

5.2.1.1.3 The Detector

The infrared beam exits the interferometer and is reflected by a couple of mirrors before it reaches the detector. However, the detector in an infrared spectrometer detects infrared light, which is invisible to the human eye.

The detector produces an electrical signal in response to the encoded radiation striking it. The detector measures the total intensity of infrared radiation reaching it across all frequencies. This measurement is read many times per second to generate the interferogram.

The interferogram records the total intensity of infrared radiation reaching the detector at each position of the moving mirror. The intensity of the radiation detected at a given mirror position along the X-axis is indicated by the height of the curve at that point.

A new interferogram is produced each time the moving mirror travels the length of its track (completes one scan). If we collect more than one scan, the computer adds the individual interferogram together and presents the average of all of the data (because it tends to reduce the noise level of the resulting spectrum). An interferogram can be generated regardless of

whether or not a sample is present.

An interferogram is first generated by recording the amount of radiation reaching the detector over time. This is called the *Background Interferogram* because it shows the energy passing through the components of the *optical bench.*

The sample is then placed in the path of the encoded infrared beam. The encoded (recombined) infrared beam interacts with the sample, where certain frequencies may be absorbed or partially absorbed. As a result, the beam that comes out of the sample is different from the one that went in. The strength of the absorptions are determined by the sample's chemical makeup.

5.2.1.1.4 The Laser

A laser is an intense beam of light energy that is of one specific frequency. Lasers are created by passing a beam of light energy through molecules that have been artificially excited. The beam picks up energy from the charged molecules, which increases the beam's intensity.

The laser produces a single frequency of red light that follows the same path as the infrared radiation. The laser calibrates the instrument internally.

The frequency of the laser beam is known to great accuracy. As the laser beam passes through the interferometer and beamsplitter, it undergoes the same interference that occurs with the infrared beam. The cycles of the encoded laser beam are used as a sampling clock. The clock determines the number of times the detector is read during a scan and the precise location of the moving mirror at each reading. This ensures the accuracy of each frequency measurement and explains what is meant by "internal calibration".

The laser also ensures that the readings taken during multiple scans are precisely synchronized, which maintains instrument precision. Because the laser beam is visible and travels through the focal point of the infrared beam, it is useful for aligning accessories and extremely small samples.

5.2.1.2 The Computer

The information contained in the background and sample interferograms is transmitted to the computer, where further processing takes place to produce the spectrum.

The computer decodes the interferogram data to obtain an energy curve. The energy curve shows the intensity of the radiation reaching the detector at each frequency.

The background energy curve (also called a "background signal-beam") establishes the energy distribution of the beam before it reaches the sample. The computer reads the interferogram, which shows the total amount of infrared radiation that reached the detector at each position of the moving mirror. Each time the intensity is measured, the difference in the path lengths of the two beams is precisely calculated. A complex mathematical calculation, called a *Fast Fourier Transform,* is used to determine the intensity of each frequency that reached the detector during the scan.

Since FT-IR spectrometers use the same beam to measure the background and sample, these graphs are often termed "single-beam energy curves" or "single-beam spectra". The single-beam technology works well in FT-IR spectroscopy because the source used in an FT-IR spectrometer is extremely stable.

The computer divides the sample single-beam by the background single-beam. The result is a transmission spectrum, which shows the change in intensity at each frequency that is due solely to absorption by the sample.

5.3 Quantitative Analysis

To ensure quantitative conditions for the infrared spectroscopic procedure, the absorbance measurement must follow Beer-Lambert Law. Thus, the variation of light intensity on passing through an absorbing medium may be expressed in terms of the law (Bower and Maddams, 1989):

$$A = log\ (I_o / I) = \epsilon cl \qquad \text{----------} \qquad Eq.\ 1$$

where A is the absorbance; I is the incident light intensity at a depth l in the absorbing medium; c is the concentration of the absorbing species; and ϵ is a constant for the material termed the absorptivity or extinction coefficient. Values of absorbance range from zero when there is no absorption $(I=I_o)$ to infinity when there is complete absorption of the incident radiation $(I=0)$. Most spectrometers display the spectrum as percentage transmittance against wavenumber. Transmittance is defined as:

$$T = I / I_o \qquad \text{----------} \qquad Eq.\ 2$$

so that percentage transmittance:

$$\%T = 100\ (I / I_o) \qquad \text{----------} \qquad Eq.\ 3$$

and absorbance:

$$A = log\ (1 / T) \qquad \text{----------} \qquad Eq.\ 4$$

5.4 Objectives

To study the effect of the different light intensities and durations of the Elipar unit on the degree of conversion of representative resin composites.

5.5 Materials and Methods

Three composite resin materials were investigated in this study (Table 5-1) using the Elipar Highlight light-curing unit.

Table 5-1: The resin composite materials investigated

Material	Code	Batch No.	Filler size (μm)	Shade	Manufacturer
Z100	**Z100**	5904A3	0.01 - 3.50	A3	3M Dental Products, USA
Charisma F	**CHRF**	055	0.02 – 2.00	A2	Heraeus Kulzer, Wehrheim
Pertac II	**PER2**	643081003	0.10 – 2.00	A3	Espé Dntal AG, Germany

A small amount of the materials was placed between two thin polythene sheets. The polythene sheets, including the material, were placed between two plastic blocks and then a G-type clamp was used to compress the material to obtain as thin a film as possible. A micrometer dial gauge (Mitotoyo Co, Tokyo, Japan) was used to measure the film thickness of the specimens. This was done by measuring the two sheets before and after the material was inserted and taking the difference to be the film thickness of the specimen. The thickness of the specimens ranged from 40 - 70 μm. The spectra of the polythene sheet was shown in Fig 5-2.

Five groups of specimens were prepared for this experiment:

Group 1. Composite materials were measured uncured. The results were to be used as 100 % unreacted carbon-carbon double bond of the monomer.

Group 2. Specimens were cured for 40 sec full light intensity.

Group 3. Specimens were cured for 10 sec low light intensity followed by 30 sec full light intensity.

Group 4. Specimens were cured for 40 sec low light intensity.

Group 5. Specimens were cured for 10 sec low light intensity.

The measurements were obtained at ageing times of 5, 60 min, 24 hrs, 1 week, 1 month and 3 months. The specimens were stored dry and dark in a light-tight drawer. Seven specimens

(n = 7) were used for each set of each material.

Fourier Transform Infra-red (FTIR) Spectroscopy via an ATI Mattson Genesis Series FTIR Spectrometer was used to analyse the unreacted methacrylate groups. The specimens were placed in the sample compartment of the FTIR instrument, and the spectra were obtained using 10 scans at a resolution of 4 cm^{-1}. The wavenumber range from 2000 to 550 cm^{-1} was scanned first and then the range of 1680 to 1550 cm^{-1} was expanded to facilitate the calculation of the interesting area. The spectra were collected initially as the transmission and then converted to absorbance.

5.5.1 Determination of the Percent of Unreacted Methacrylate from Groups Transmission FTIR

The monomer conversion of each specimen was determined by monitoring the ratio of the absorbance of the aliphatic carbon double bond (C = C) peak (1637 - 1638 cm^{-1}) to that of the aromatic (C...C) absorbance peak (1607 - 1608 cm^{-1}) for the investigated materials, uncured and cured specimens (Ruyter and Svendsen, 1978; Rueggeberg *et al.*, 1990; Rueggeberg and Caughman, 1993). A decrease in this ratio indicated that, as compared to the uncured material, aliphatic C = C was transmitted to polymer product. The aromatic peak is used as an internal reference so that component concentrations did not need to be determined. The absorbance of this group can be used as a reference because it does not react during polymerisation and therefore should not change in its concentration. If polymerisation has progressed totally, the aliphatic C = C peak would completely disappear with respect to the aromatic peak (Rueggeberg and Caughman, 1993). The percent of monomer converted into polymer was calculated for each specified time, using the standard baseline technique (Fig 5-3). The mean conversion for each resin at each time and cure condition was determined.

Therefore, the residual unreacted methacrylate groups for these materials was evaluated using the following equation:

$$\%\ \text{of unreacted (C = C)} = \frac{\left[(\text{Abs C = C}) / (\text{Abs C...C})\right]_{polymer}}{\left[(\text{Abs C = C}) / (\text{Abs C...C})\right]_{monomer}} \times 100$$

5.5.2 Statistical Analysis

Two-way statistical analysis was used to demonstrate the effects of light intensity and time on the DC of the investigated resin-composites. One-way ANOVA followed by Scheffé procedure were performed to detect significant difference between the light intensities at $p < 0.05$.

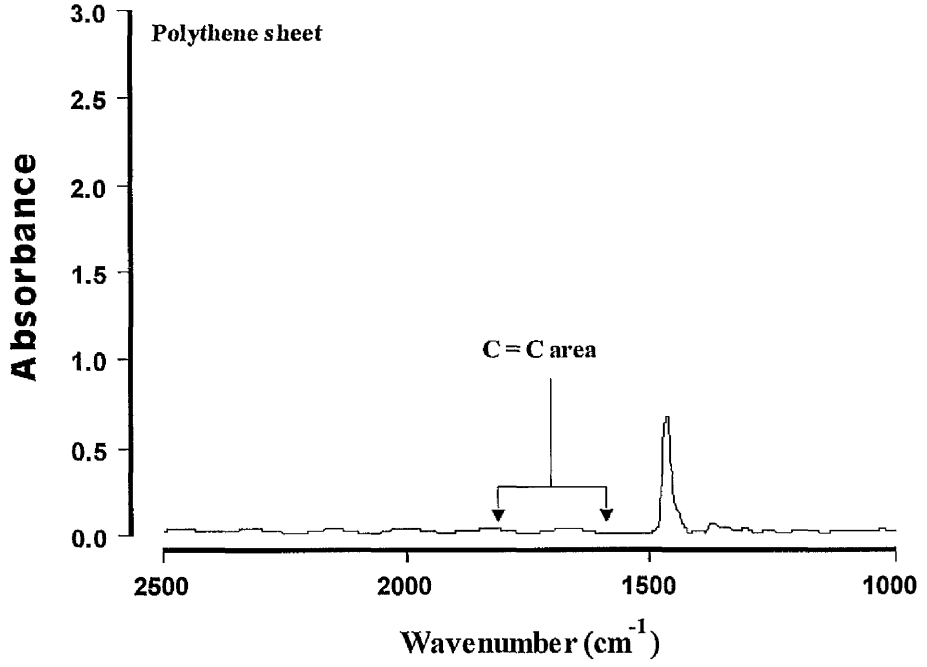

Fig 5-2: Spectra of the polythene sheet.

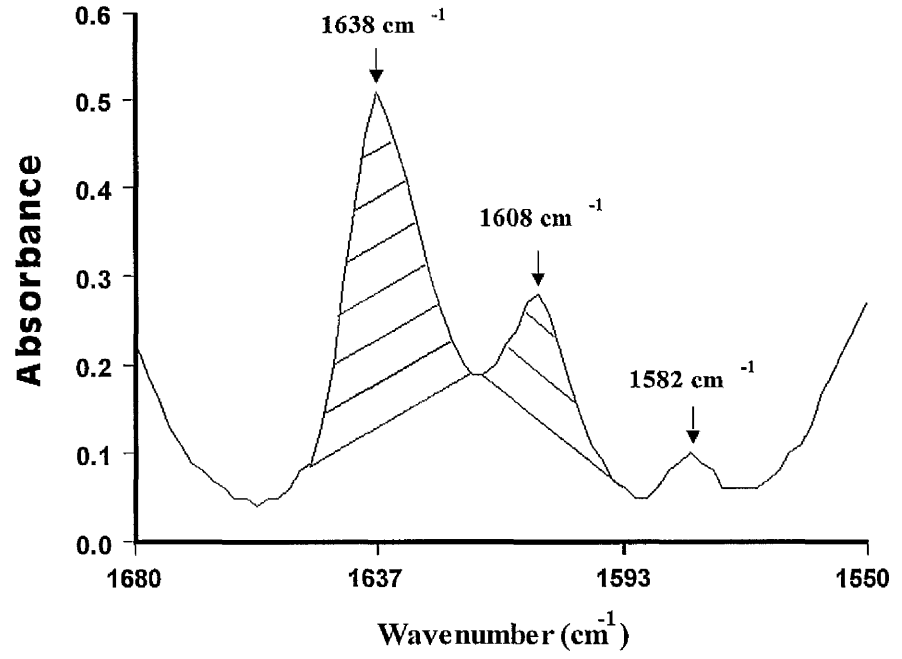

Fig. 5-3: Calculation of peak area of the unreacted carbon double bond (C=C).

5.6 Results

Full transmission FT-IR absorbance spectra before and after polymerisation of the resin composites investigated are shown in Fig. 5-4, 5-5 and 5-6. The absorption bands at 1637, 1638, 1637 cm^{-1} represent the methacrylate C=C stretching vibrations, while 1608, 1608 and 1607 cm-1 represent the aromatic C...C stretching vibration for **Z100**, **CHRF** and **PER2** respectively. The mean values and standard deviation are plotted graphically in Figs. 5-6 to 5-8 and presented in Tables 5-2 to 5-4. The whole data are listed in appendix IV in CD. There was gradual increase in DC with ageing time for the composite materials investigated.

Using two-way ANOVA, the effect of light intensity and time on **Z100** DC were highly significant ($p = 0.000$). However, the interaction between these two factors was not significant ($p = 0.987$). Specimens cured at 40 s high intensity were found to be not significantly different ($p > 0.05$) to those cured by "soft-start". But these groups were significantly different ($p = 0.0000$) to those cured by 40 or 10 s low intensity (Table 5-5) (Fig 5-7).

With **CHRF**, two-way ANOVA, the effect of light intensity and time on DC were highly significant ($p = 0.000$). However, the interaction between these two factors was highly significant ($p = 0.000$). The effect of light intensity on DC was found to be not significantly different ($p > 0.05$) for specimens cured by 40 s high intensity with those cured by soft-start. Specimens cured by 40 s high intensity and soft-start were found to be significantly different ($p = 0.000$) to those cured by 40 or 10 s low intensity (Table 5-6) (Fig 5-8).

Similar statistical tests were carried out on **PER2**. In this case, the influence of light intensity on DC was highly significant ($p = 0.000$) as was the influence ageing time ($p = 0.000$). However, the interaction between these two factors was not significant ($p = 0.760$). Table 5-7 demonstrates the analysis for the effect of different light intensity on DC. Specimens cured by 40 s high intensity were found to be not significantly different ($p > 0.05$) to those cured by soft-start. These two groups were found to be significantly different to those cured by 10 s low intensity. The specimens cured by 40 s low intensity were found to be not significantly different ($p = 0.000$) to those cured by 10 s low intensity (Fig 5-9).

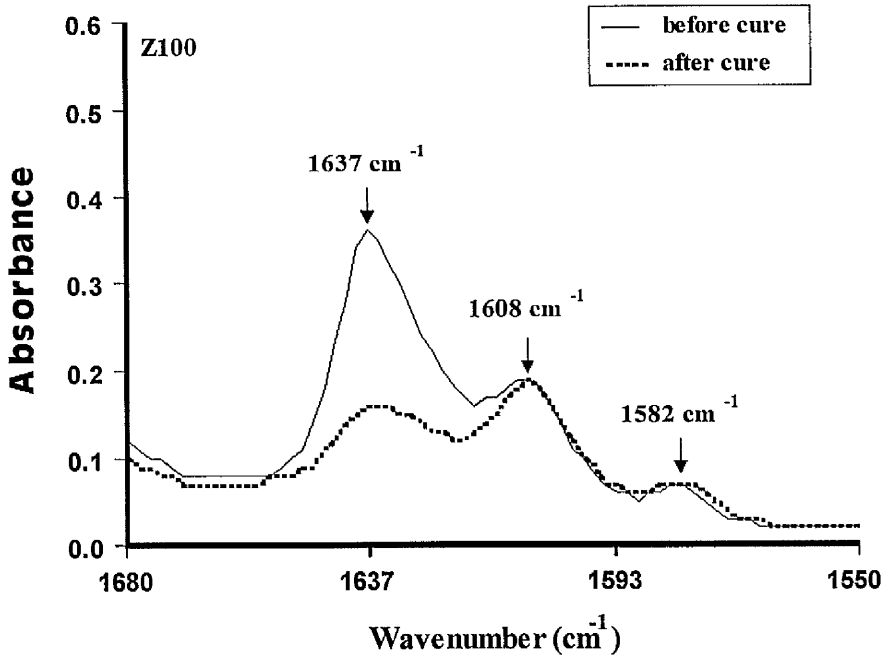

Fig 5-4: FTIR absorbance of **Z100**, before and after cure.

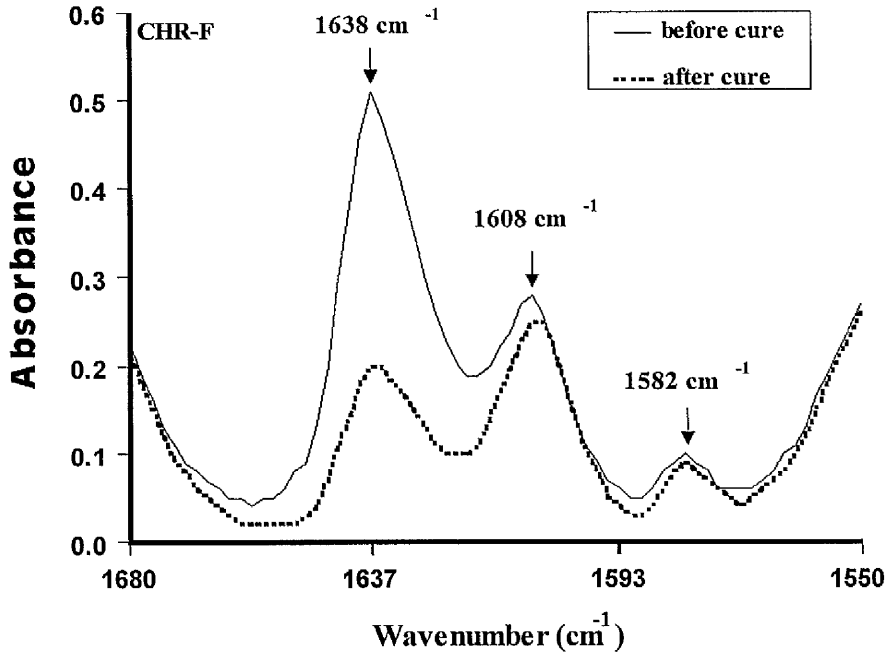

Fig 5-5: FTIR absorbance of **CHRF**, before and after cure.

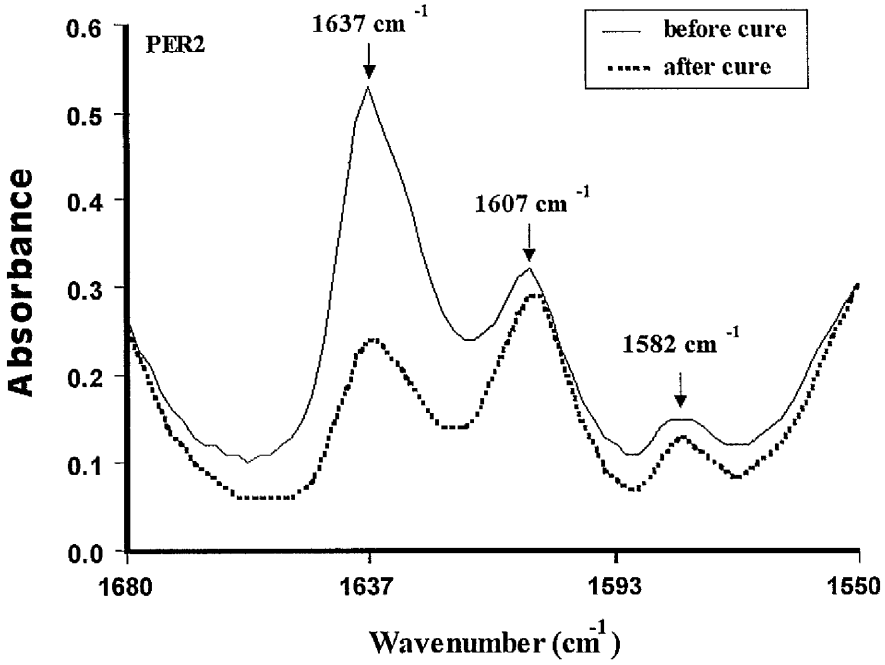

Fig 5-6: FTIR absorbance of **PER2**, before and after cure.

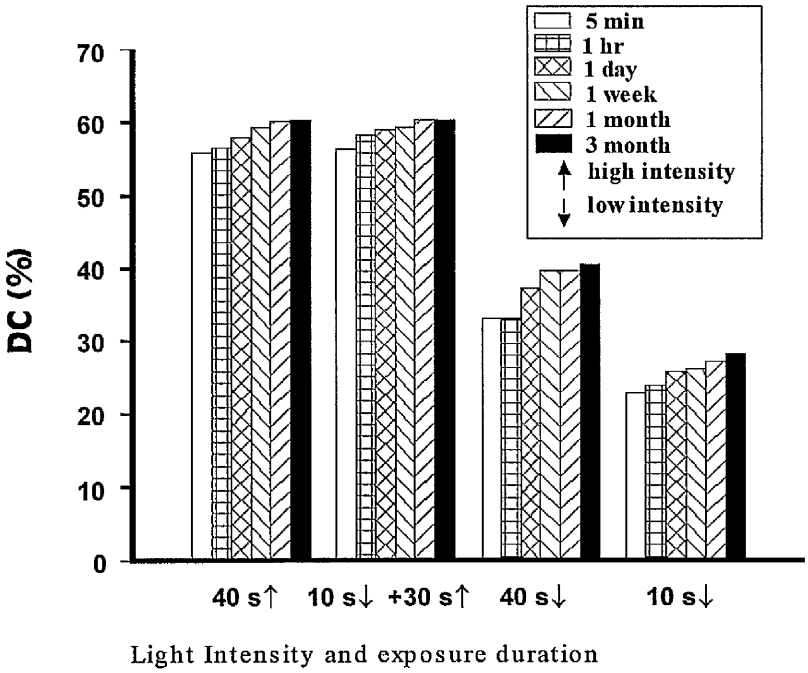

Fig. 5-7: Degree of conversion of **Z 100**, cured by different light intensities.

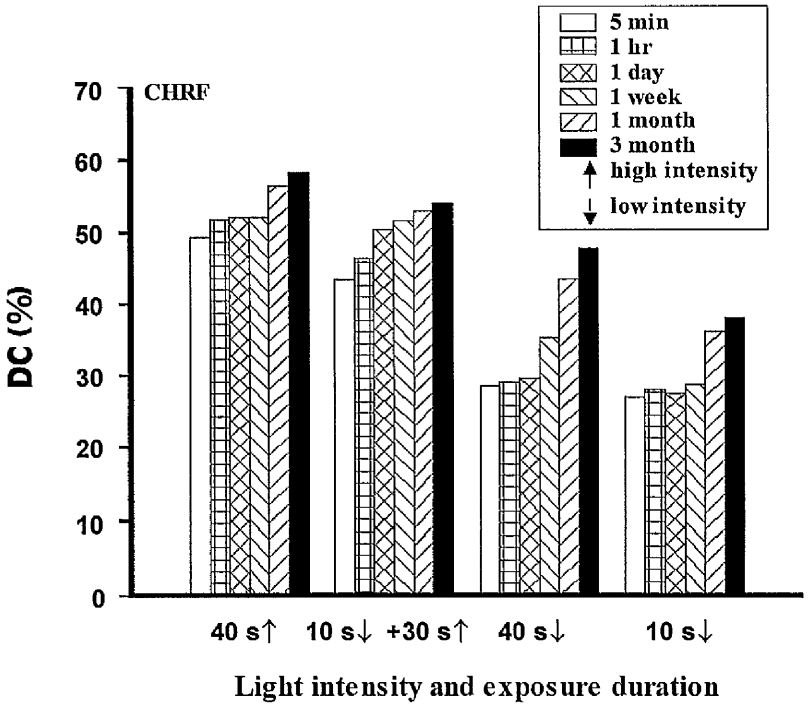

Fig. 5-8: Degree of conversion of **CHRF**, cured by different light intensities

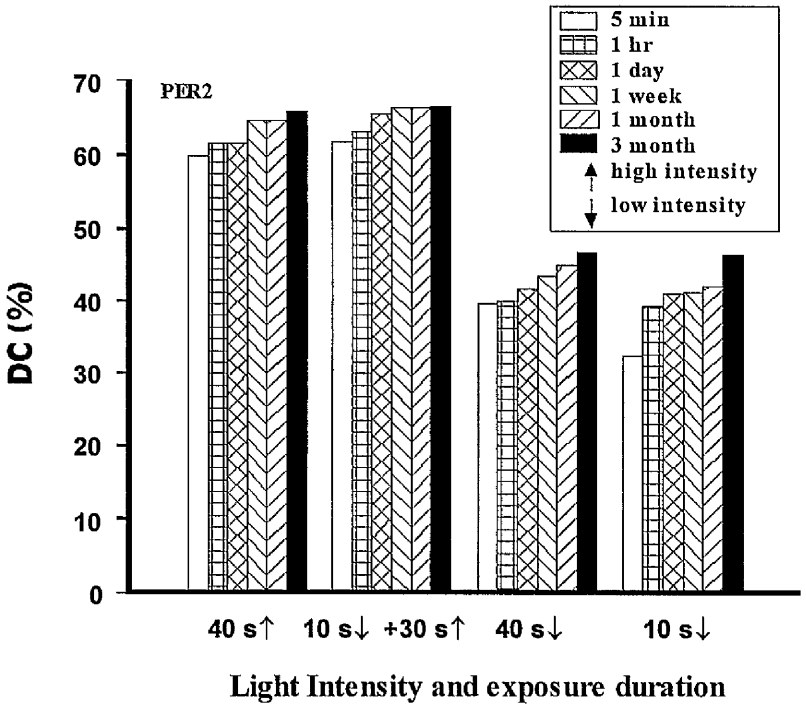

Fig. 5-9: Degree of conversion of **PER2**, cured by different light intensities.

Table 5-2: Mean values and SD (in parenthesis) of DC (%) of **Z100**.

Light intensity	Time					
	5 min	1 hr	1 day	1 week	1 month	3 month
40 s full intensity	55.67 (5.74)	56.67 (3.13)	57.78 (1.67)	59.13 (5.39)	60.06 (3.07)	60.35 (2.42)
Soft-start	56.24 (2.44)	58.04 (2.52)	58.96 (0.68)	59.32 (0.92)	60.22 (1.54)	60.29 (1.77)
40 s low intensity	33.10 (2.74)	33.19 (4.59)	37.22 (8.06)	39.49 (5.49)	39.53 (3.11)	40.28 (2.21)
10 s low intensity	22.76 (4.23)	23.94 (6.09)	25.97 (3.45)	26.01 (2.94)	27.15 (2.66)	28.19 (2.87)

Table 5-3: Mean values and SD (in parenthesis) of DC (%) of **CHRF**.

Light intensity	Time					
	5 min	1 hr	1 day	1 week	1 month	3 month
40 s full intensity	49.38 (3.14)	51.76 (2.74)	51.90 (4.17)	52.01 (3.75)	56.35 (2.03)	58.14 (1.48)
Soft-start	43.30 (0.93)	46.36 (3.35)	50.27 (4.65)	51.36 (5.45)	52.74 (2.69)	53.83 (0.51)
40 s low intensity	28.67 (3.10)	29.17 (2.82)	29.61 (3.80)	35.15 (5.89)	43.35 (2.14)	47.70 (3.45)
10 s low intensity	26.85 (4.19)	27.88 (4.64)	27.58 (3.26)	28.82 (6.31)	36.18 (2.87)	37.91 (3.09)

Table 5-4: Mean values and SD (in parenthesis) of DC (%) of **PER2**.

Light intensity	Time					
	5 min	1 hr	1 day	1 week	1 month	3 month
40 s full intensity	59.65 (3.85)	61.32 (3.06)	61.32 (3.20)	64.71 (4.71)	64.71 (4.18)	65.58 (1.87)
Soft-start	61.69 (5.54)	62.99 (0.84)	65.40 (3.59)	66.24 (3.13)	66.24 (3.13)	66.63 (1.83)
40 s low intensity	32.19 (7.49)	39.59 (12.08)	41.86 (11.62)	43.32 (9.26)	44.90 (7.03)	46.47 (2.97)
10 s low intensity	39.98 (5.35)	39.33 (8.74)	40.91 (4.02)	41.10 (3.91)	42.12 (4.26)	46.29 (4.37)

Table 5-5: Multiple comparison (Scheffé procedure) between DC and the effect of light intensity for **Z 100**.

Groups	code	4	3	2	1
10 s low intensity	Grp 4				
40 s low intensity	Grp 3	*			
Soft-start	Grp 1	*	*		
40 s full intensity	Grp 2	*	*		

Table 5-6: Multiple comparison (Scheffé procedure) between DC and the effect of light intensity for **CHRF**.

Groups	code	4	3	2	1
10 s low intensity	Grp 4				
40 s low intensity	Grp 3	*			
Soft-start	Grp 2	*	*		
40 s full intensity	Grp 1	*	*		

Table 5-7: Multiple comparison (Scheffé procedure) between DC and the effect of light intensity for **PER2**.

Groups	code	4	3	2	1
10 s low intensity	Grp 4				
40 s low intensity	Grp 3				
Soft-start	Grp 1	*	*		
40 s full intensity	Grp 2	*	*		

(*) denotes pairs of group significantly different at level ($p < 0.05$).

5.7 Discussion

The monomer resins always contain components from the initiator system. In addition, the resins may contain additives like inhibitors, UV stabilisers and plasticisers. The components are present in small quantities and give minor contributions to the IR spectra of the resin (Ruyter and Øysaed, 1988).

The advantages to use Fourier Transform infrared (FTIR) spectroscopy in this part of the study include better signal-to-noise ratios and the ability to record complete spectra in very much shorter time scales. It typically takes a few seconds rather than several minutes to collect the transmittance spectra. Also the sensitivity of the instrument is one of the advantages of FTIR. This achieved when multiple scans are collected, the spectrometer adds them together and uses their average values to create the infrared spectrum. This is called "signal average" and the spectrometer does it automatically. Signal averaging can improve instrument sensitivity because signals produced by the sample are constant, while noise, due to instrument components and electronics, is random (averaged noise gets smaller as scans added). Further advantage that the FT-IR spectrometers are able to determine with great accuracy the frequencies at which a sample absorbs IR and to measure the same sample again and again with no shift in peak position. This high degree of reliability is due to the laser, which determines when the detector is read during a scan and the precise location of the moving mirror at each reading. The spectrometer uses the laser's frequency value as a reference when measuring the intensity of each frequency produced by the infrared source.

5.7.1 Sampling Technique

The DC in this study was not measured at different depths of the cured composite resin materials, so we preferred to use the thin film method between two polythene sheets. The thin film technique was used, as described in the 'Methods', rather than another technique such as a thin film between two NaCl plates, or KBr or ATR methods.

Use of the thin film technique indicates the measurement of the DC at the surface of the cured sample and could give a proper indication of the effect of light intensity on the extent of the cure. Even though the restorative composite resin materials contain filler particles, the thin film

technique can still provide useful and reproducible results for DC. The thin film technique has been used by many previous researchers (Asmussen, 1982a; Ferracane and Greener, 1984; Caughman *et al.*, 1991).

The reason for using thin polythene sheets in this study is that the spectra of these sheets would not interfere with the spectra of the investigated materials (Fig.5-6). So these sheets act as a window for those aliphatic and aromatic peaks. Also these sheets were chosen instead of NaCl crystal plates due to the difficulty of detaching the two NaCl plates from each other after cure, which may destroy the NaCl plates (Al-Hindi 1995).

In KBr method, the cured resin composites need milling to obtain resin powder. The milling procedure may generate some heat, which may alter the results of the tested material. As it is known, the temperature rise can gave better polymerisation. Ferracane and Greener (1984), concluded that the degree of cure for the unfilled resins via KBr pellet technique was slightly greater than that found with the film technique, possibly due to a localised heating effect during grinding of the specimen.

The ATR technique cures the sample over the crystals to obtain the value of the DC. However, the proposal of this study was to measure the DC of the resin composite materials over different ageing times. So the disadvantage of these crystals is that they cannot be used for one sample over months. One more problem with the use of ATR is the difficulty of removing the resin sample after cure, which may lead to scratching the crystal.

5.7.2 Light Intensity Variable

As explained in the introduction, the effectiveness of the polymerisation of light-activated restorative materials is not only dependent on the chemistry of the material; concentration of initiator; the filler particle type; size and quantity (Peutzfeldt, 1994; Harrington *et al.*, 1996), but also dependent on the amount of suitable light energy which reaches the catalyst (Yearn, 1985), light intensity and exposure time (Watts, 1992; Rueggeberg, *et al.*, 1993; Feilzer, *et al.*, 1995a; Harrington, *et al.*, 1996), spectral distribution, and alignment of the light tip guide (Harrington *et al.*, 1996).

It is expected that the DC increases with increased light intensity. As shown in the results, with all investigated materials, the DC was found to be higher with the specimens cured at 40 s full intensity and soft-start. The DC decreased with reduced light intensity, either at 40 s or 10 s exposure. When the low intensity curing time increased to 40 s, the DC was improved slightly. The initial light exposure will cause a rapid increase in conversion of the resin, resulting in a viscous gel (Reuggeberg and Caughman, 1993).

The first 10 s low intensity in the soft-start polymerisation does not reduce the final results of the DC, due to the further 30 s cure by full intensity.

From the results obtained in this study it was found that the DC of **Z100** and **PER2** specimens, when cured by 40 s full intensity, were equivalent to those cured by soft-start. The results for these two materials can verify this finding. The DC of **Z100** and **PER2** cured by soft-start was actually slightly higher than those cured by 40 s full intensity.

The DC of **CHRF** is slightly affected by the soft-start cure. The results of the specimens cured by soft-start were lower than those cured by 40 sec high intensity, but there was no significant difference.

Rueggeberg and Jordan, (1993), suggested that the polymerisation of the surface was more dependent upon duration than intensity of exposure. Our findings show that the degree of cure was greatly affected by both the duration of exposure and light intensity. In our study the light tip was at 0 distance from the sample surface, and the light intensities used were both high and low. Rueggeberg and Jordan, (1993), used fixed light intensity source with the actual intensity differences resulting from increasing distances of the light tip from the sample surface. It was found in this study that the DC was affected by the different light intensities. On the other hand, the effect of the duration of exposure on degree of cure was in agreement with their findings.

The results of **Z100** and **CHRF**, treated by either 40 sec full intensity or soft-start, were in agreement with the findings by Park, (1996). He measured the DC in various layers, and he used 60 sec to cure the investigated materials. For comparison with our study, the top layer near to the light curing tip was chosen from his study. He found the DC of **Z100**, and **CHRF**,

after three days storage in the dark was 47 % and 53 %, respectively. In our study the DC of **Z100** was 55.6 % for 40 sec full intensity, and 56.2 % for soft-start. The DC of **CHRF** was 49.4 % for 40 s. full intensity, and 43.3 % for soft-start.

5.7.3 Ageing Time Variable

The DC was found to be increased with ageing time. This increase was found to be slow, and most of the polymerisation process occurred in the first 40 sec of light activation. The results of the present work coincide with the findings of Loza-Herrero, *et al.*, (1998). As mentioned above, free radicals remain after initial curing, and these can enhance the post-cure reaction.

5.7.4 Effect of Composition of the restorative resin-composites

The presence of TEGDMA in different percentages can vary the viscosity of the resins. The lower viscosity of the more diluent resin may allow for an enhanced mobility of reactive groups during the polymerisation process, leading to a greater degree of polymerisation (Assmusen, 1982a; Ferracane and Greener, 1984). Therefore, composites which included greater amounts of TEGDMA showed a greater DC (Imazato, *et al.*, 1995). Thus, the conversion of resin composites with BisGMA/TEGDMA mixture was fairly efficient, even with minimal light energy input (Ferracane *et al.*, 1997).

The filler does not take part in the polymerisation process, but it can be an important factor during the activation of the material with a visible light activation unit (Yearn, 1985; Watts, 1992). However, the filler seems to have no effect on our thin film sampling technique.

This study was carried out at room temperature (23°C), but we can say that the remaining double bonds are decreased with the post-cure heat. The effect of post-cure heat was studied by Ferracane, *et al.*, 1997; Bagis and Reuggeberg, 1997; Loza-Herrero, *et al.*, 1998. Any increased conversion obtained after heat treatment may be due to the reaction of previously unreacted residual monomers (Loza-Herrero, *et al.*, 1998).

5.8 Conclusions

- The DC of the investigated composite resin materials gradually increased with ageing time.

- The DC decreased dramatically with reduced light intensity. Nevertheless conversions in the range 30% were obtained with the low intensity exposure and there rose gradually to *circa* 40%.

- The DC of **Z100** and **PER2** was not affected by the soft-start cure. The results were found to be slightly higher than those cured by 40 sec full intensity. This difference was not significant.

- Soft-start cure did slightly affect the DC of **CHRF**. The results were lower than those cured by 40 s full intensity.

Chapter 6
Polymerisation Shrinkage-Strain "Bonded-Disk" Method Development

6.1 Introduction

The majority of polymerisation and setting reactions result in contraction of the material during the setting phase.

Polymerisation shrinkage of composite resins, particularly contraction in a direction normal to the interface of the material with dental tissues, is of critical importance (Davidson, 1985).

Wilson (1978), measured polymerisation contraction by monitoring the distortion of a flexible steel blade attached to the surface of the setting composite. Walls, *et al.*, (1988), developed Wilson's technique (1978) for use with light-cured composites by replacing the steel blade with a transparent glass cover slip. Further development of this technique was made by Watts and Cash (1991a&b). This development consisted particularly of the construction of an apparatus to consistently align the measurement assembly, so as to place the anvil of the displacement transducer precisely above the centre of the support ring and specimen disc. The support ring was adhesively bonded onto a rigid glass microscope slide (75 mm length x 25 mm width x 1 mm diameter).

The present work is an extension of the methodology proposed by Watts and Cash (1991a&b). This extension in this methodology consists of measuring the polymerisation shrinkage of the resin composites by substituting the glass microscope slide with thicker glass plates and studying the amount of micro-distortion of the glass plates, by heating from the light source and /or the heating anvil during the experimental work.

6.2 Materials and Methods

6.2.1 Instrument Design

The apparatus was as used by Watts and Cash (1991) and further modified by these authors to allow resin specimens to be environmentally heated to maintain a steady temperature throughout each test cycle, so that resin cure kinetics *versus* temperature could be determined.

The apparatus (Fig 6-1) consisted of an aluminium stand incorporating a horizontal table and capable of clamping a Linear Variable Displacement Transducer (LVDT) (GT 2000, RDP Electronics, Wolverhampton, UK), in the alignment with a disc shaped specimen. A clinical fibre optic unit was positioned below the table by an adjustable clamp. A brass "anvil" approximately 40 mm diameter was positioned in a recess in the horizontal table.

The anvil, acted as a measuring surface, which was electrically heated by two high power electrical resistors fitted to the underside and embedded in an epoxy resin. The temperature was monitored *via* a calibrated thermocouple tip inserted in a hole drilled into the rim. When connected to an electrical supply, the table insert was heated due to the power dissipated in the resistors. The insert was constructed so as to be a loose fit into the stand, so that it was thermally decoupled from the stand (Figure 6-1).

In the "bonded disk" technique for composite shrinkage, it has been assumed hitherto that the lower rigid glass plate is completely rigid and is unaffected by the light. A series of experiments was devised to investigate any necessary correction terms arising from these factors. For comparison, it should be noted that a typical displacement arising from composite shrinkage is about 30 μm.

The experiments consisted in using the shrinkage instrument without any composite specimens and the LVDT probe resting on the upper glass surface. The glass plate was positioned either before or after the anvil was heated to a series of steady temperatures: 23, 37, 45 and 60 °C. At a given steady temperature a recording was made for a minimum

of 8 min during which the light-unit was illuminated directly below the glass plate. Expansion effects due to irradiant heating were re-evaluated.

Two types of rigid glass plates were investigated in this study, 1 mm and 3 mm thick. These were 75 mm long and 25 mm wide.

The procedure for measuring the polymerisation shrinkage strain of the resin composites is explained in detail in the next chapter (Chapter 7).

6.2.2 Calibration of the LVDT

For calibration of the LVDT, the transducer was lightly clamped in a horizontal stand, opposed by a modified and calibrated digital micrometer (Mitutoyo, Tokyo, Japan), with a display accuracy of 1 μm. The transducer armature was displaced by the micrometer armature through known increments while the transducer output voltage was recorded in the memory store of the data-recording system (Fig 6-2). The voltage/displacement calibration factor was then calculated by linear regression ($r \approx 0.9999$). The transducer was calibrated periodically throughout the course of the work.

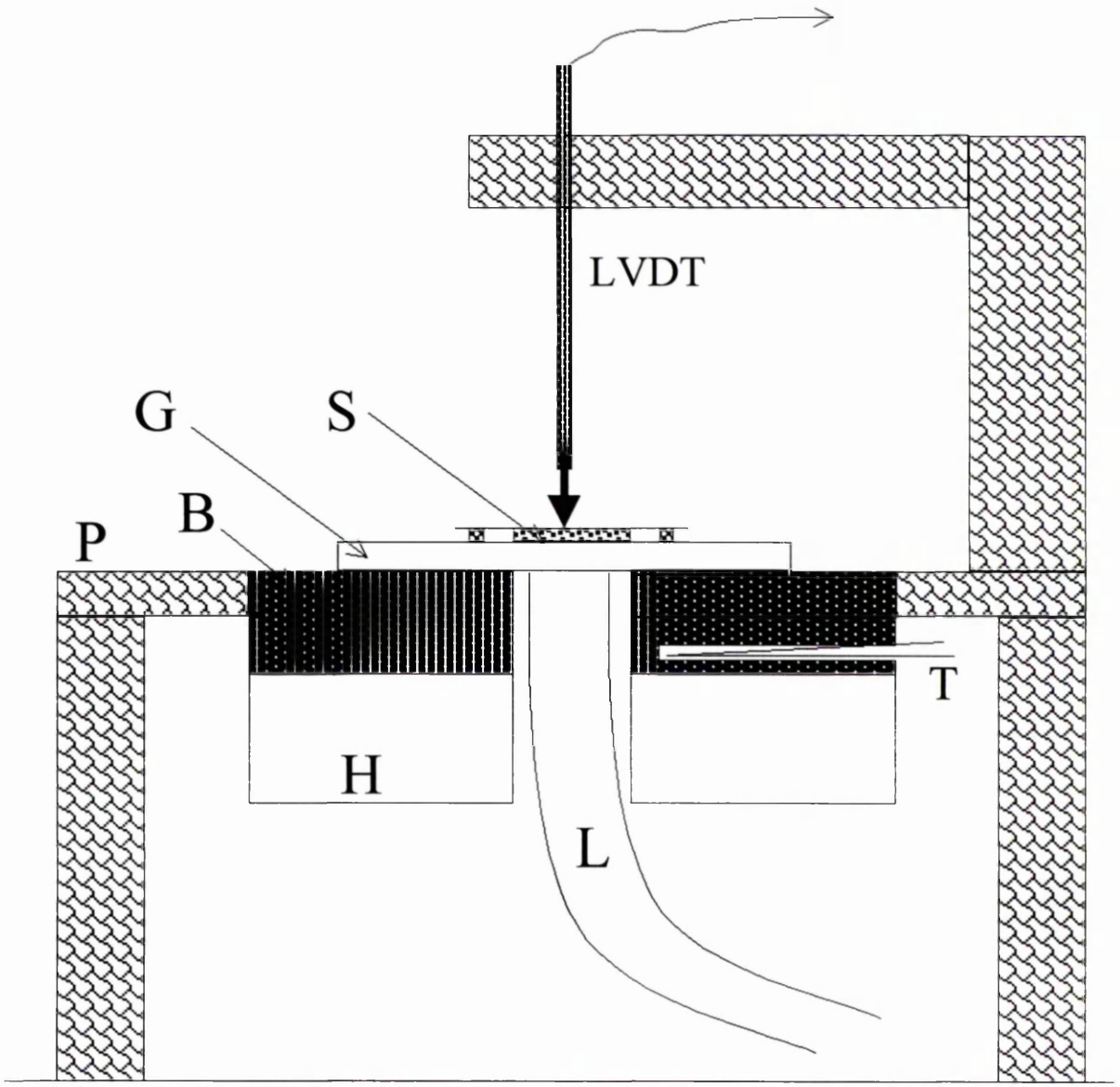

Fig 6-1: Shrinkage Strain Apparatus:
A platform (P) incorporated a brass insert (B), on which rested a 3 mm thick glass plate (G). On the plate was a square cross-section metal ring, within which the specimen (S) was centrally located. Resting on the specimen and ring was a glass cover slip of thickness 0.1 mm. The cover slip was lightly contacted by the probe of a linear variable displacement transducer (LVDT), connected to a data-acquisition system. The brass insert was heated from below (H) and the temperature recorded by a thermocouple (T).

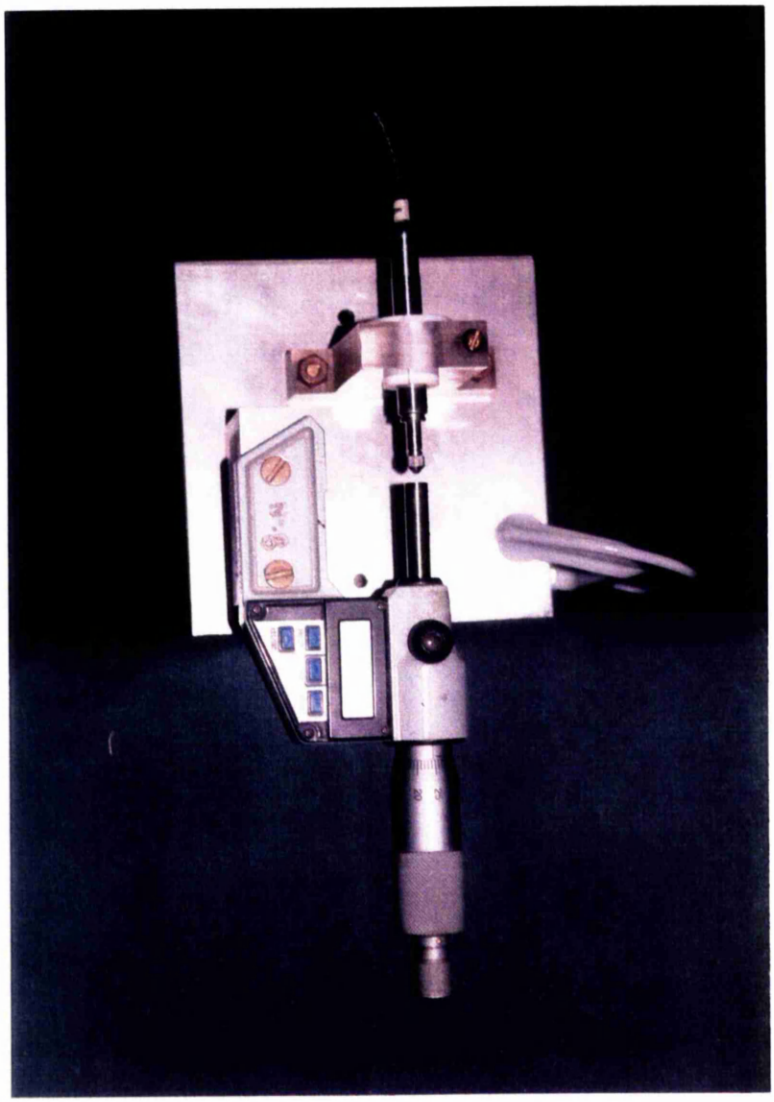

Fig 6-2: Calibration device

6.3 Results

The data of the effect of the heat generated from the light sources are presented in Figures 6-3 to 6-7.

Fig 6-3 shows the displacement arising from the thermal expansion of the 1 mm glass plate, to reach an equilibrium strain value. The plate was heated with the brass anvil. The displacement was ≈ 0 at 23°C, 0.83 μm at 37°C, 1.89 μm at 45°C, and 5.5 μm at 60°C. The maximum deflection for these plates was obtained after 19 min.

The maximum displacement of 3 mm thick glass plates (Fig 6-4) was found to be 0 at 23°C, 1.4 μm at 37°C, and 1.4 μm at 60°C. These deflections were obtained after 30 min.

Further data for glass displacements were obtained when the brass anvil was pre-heated until the required temperature was reached and then the glass plates were placed onto it for a displacement study (Fig 6-5).

Light curing has an extra effect on glass plate displacement (Fig 6-6). This increase in displacement was found to be 0.40 μm for 3 mm thick glass and 0.54 μm for 1 mm glass plate. By increasing the temperature of the brass anvil, the relative effect of the curing light decreased (Fig 6-7). For example 3 mm glass plate displaced 0.40 μm at 60°C and a further 0.72 μm at 23°C. This probably arises from Newton's law of cooling.

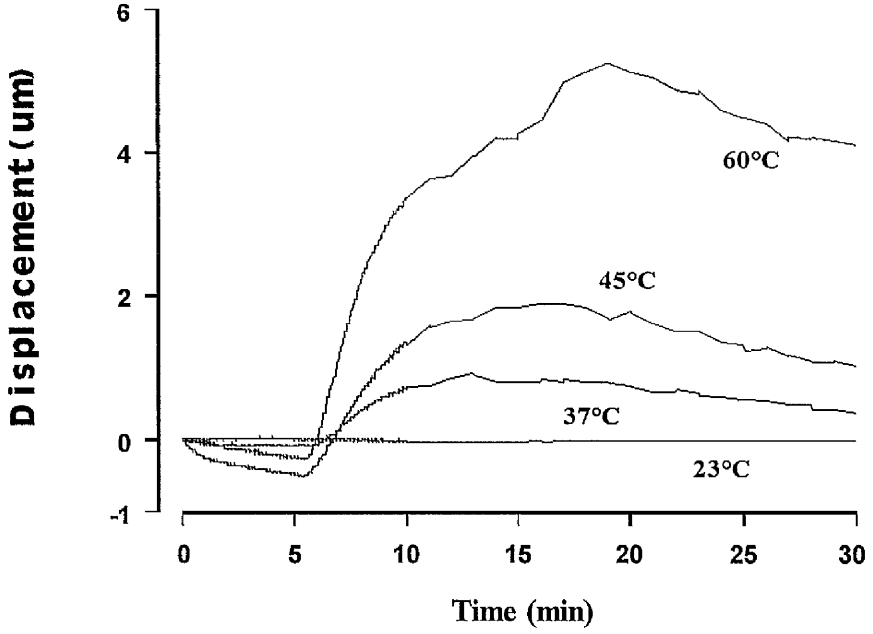

Fig 6-3: Effect of different temperatures on displacement of a 1 mm thick glass plate supported on the brass 'anvil', which was heated from time = 0 to reach the equilibrium temperature.

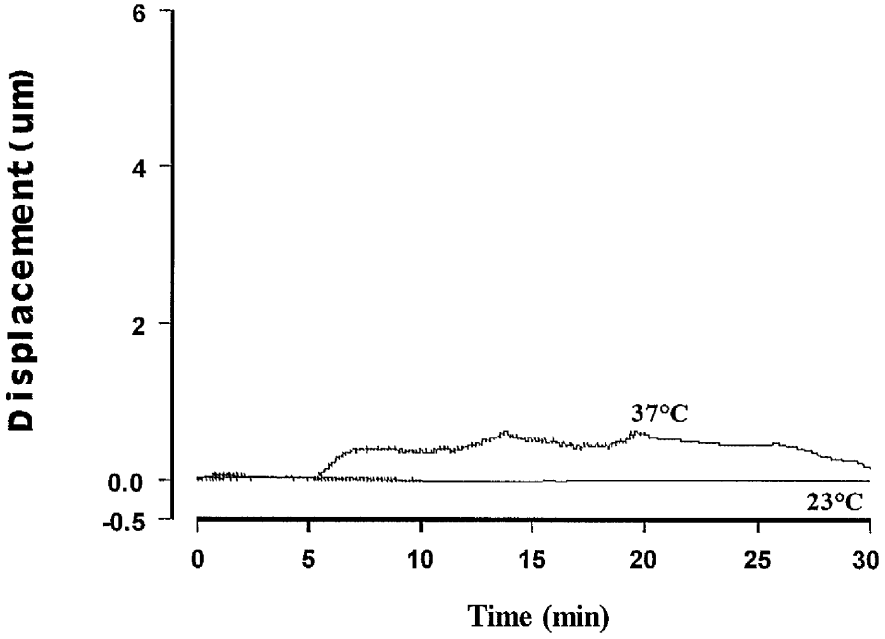

Fig 6-4: Effect of different temperatures on displacement of a 3 mm thick glass plate supported on the brass 'anvil', which was heated from time = 0 to reach the equilibrium temperature.

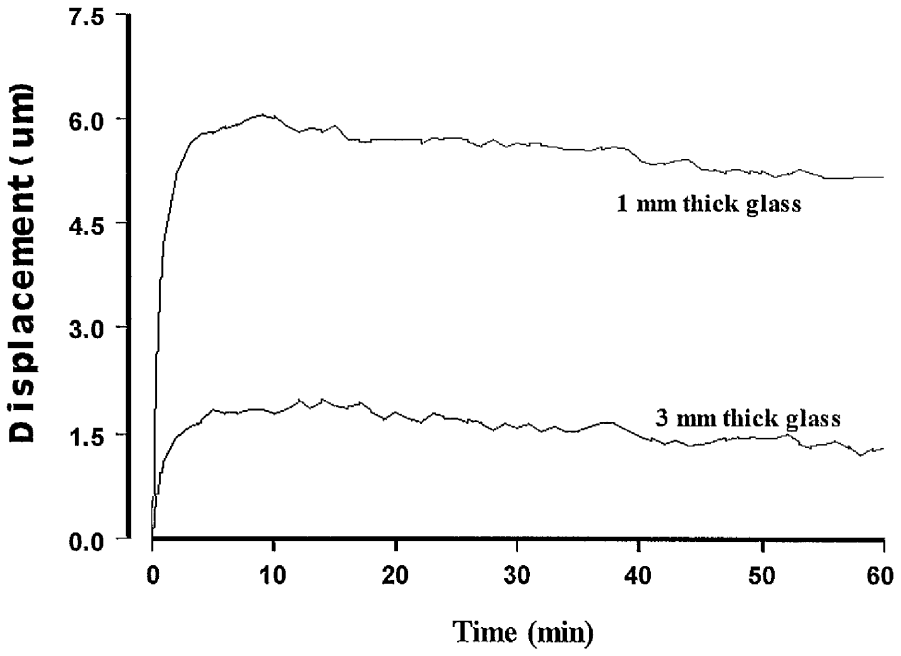

Fig 6-5: Displacement due to thermal expansion of a 1 mm and a 3 mm thick glass plates. The brass anvil was pre-heated to 60°C, then the glass was placed on top of the brass anvil at t = 0.

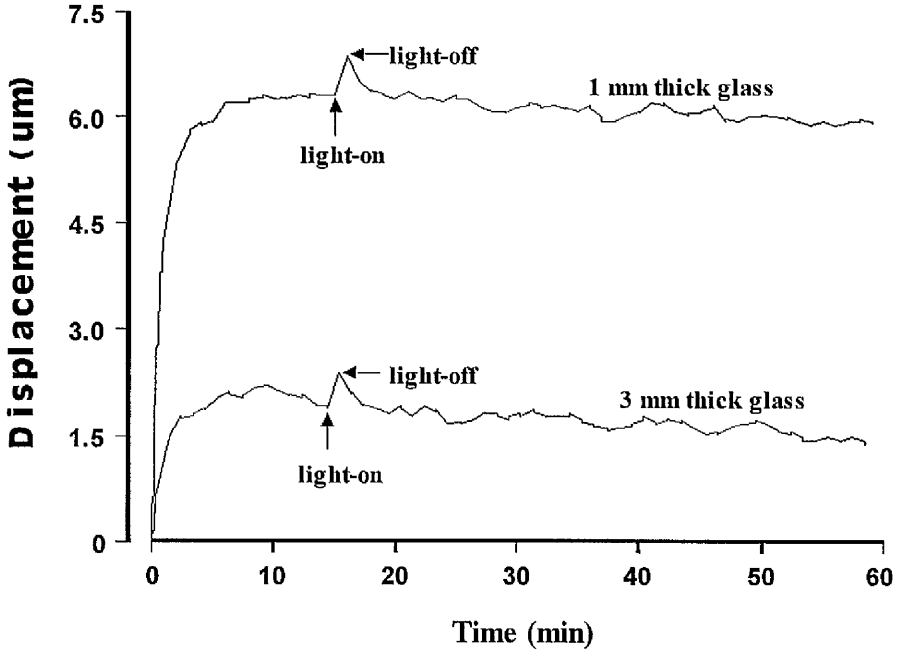

Fig 6-6: Displacement of 1 and 3 mm thick glass plates due to thermal expansion, with the superimposed effect of light irradiation. The brass anvil was pre-heated to 60°C, then the glass was placed on top of the brass anvil at t = 0.

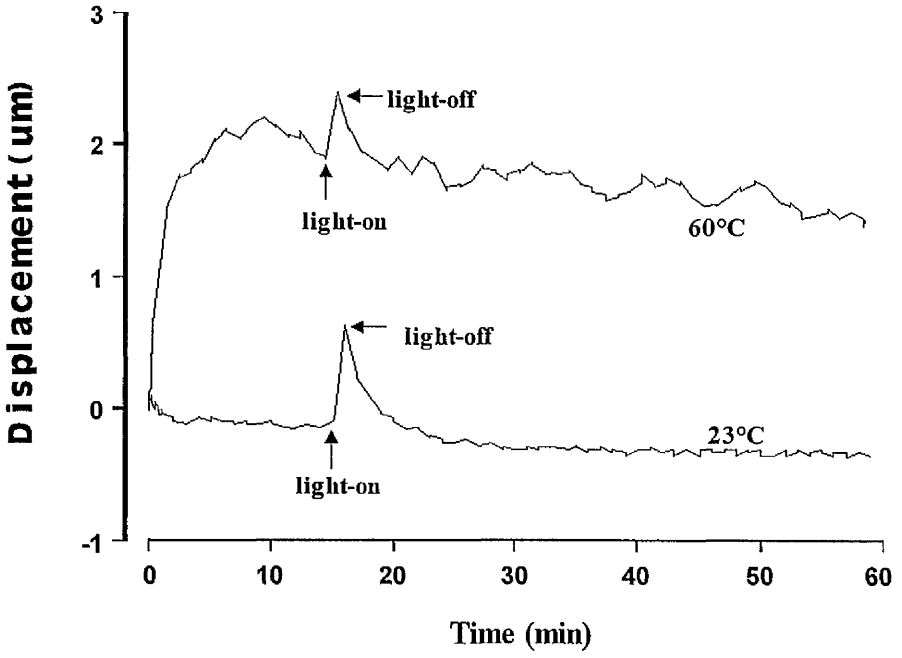

Fig 6-7: Displacement of 3 mm thick glass plate due to thermal expansion, with the superimposed effect of light irradiation. The brass anvil was pre-heated to the indicated temperature then the glass plate was placed on top of the brass anvil at t = 0.

6.4 Discussion

Two factors can possibly affect the original shape of the glass plates used in this method:

1. Thermal expansion of the glass.
2. Deflection or bending due to stress.

It is desirable to point out to that the elasticity of a material is the property by which a body returns to its original shape after removal of the load. From Hooke's law:

$$E = \sigma / \varepsilon \qquad \text{Eq. 1}$$

Where σ is stress and ε is strain and E is elastic modulus. The body is perfectly elastic if it returns to its original shape completely after unloading; it is partially elastic if the deformation produced by the external forces does not disappear completely after unloading. In the case of a perfectly elastic body the work done by the external forces during deformation is completely transformed into potential energy of strain (i.e. the small temperature changes which usually accompany elastic deformation and the corresponding heat exchange with the surroundings are neglected in this consideration). In the case of a partially elastic body, part of the work done by the external forces during deformation is dissipated in the form of heat, which is developed in the body during the non-elastic deformation (Timoshenko, 1980).

Expansion (factor one) of the glass plate due to changes in temperature may have the same effect as changes in lengths. If the temperature of the glass plate is raised from T_o to T and thermal expansion is prevented by fixing the ends, there will be produced in the glass plate compressive stresses, whose magnitude may be calculated from the condition that the length remains unchanged. Let α denote the coefficient of thermal expansion and σ the thermal stress produced by the reactions. We substitute ε in equation 1 with $\alpha\ (T_o - T)$. Then the equation for determining σ will be

$$\alpha\ (T_o - T) = \sigma / E \qquad \text{Eq. 2}$$

From which

$$\sigma = E \,.\, \alpha\,(T_o - T) \qquad \text{Eq. 3}$$

where $\alpha\,(T_o - T)$ is the thermal strain, ε_T.

Increasing temperature causes expansion and thus a positive strain, while decreasing temperature results in contraction and negative strain. An important feature about this behaviour is that if there is no restraint on the material there can be strain unaccompanied by stress. However, if there is any restriction on free change in size, then a thermal stress will result. The total strain in a body experiencing thermal stress may be divided into two components, the strain associated with the stress, ε_σ, and the strain resulting from the temperature change, ε_T (Benham *et al*, 1998). Thus

$$\varepsilon = \varepsilon_\sigma + \varepsilon_T \qquad \text{Eq. 4}$$

Hence

$$\varepsilon = (\frac{\sigma}{E}) + [\alpha(T_o - T)] \qquad \text{Eq. 5}$$

Deflection or bending (factor two) of the glass plate is possible. During the setting reaction of the material, there are some stresses generated, which may lead to deflection of the glass plates. The deflection can be of some importance in the case of thin glass plates, but in the case of a thick plate the deflection is small. This deflection should increase with decreasing thickness of the plate and decrease with increasing thickness. The maximum deflection should not exceed a certain limit. The glass plates are rectangular cross section and they are simply supported from underneath. It is necessary to refer to the moment of inertia (I_z) of these plates

$$I_z = \frac{bh^3}{12} \qquad \text{Eq. 6}$$

Where ***b*** is the width and ***h*** is the height or thickness of the rectangular cross section. The maximum deflection (y_{max}) of the glass plate is evidently at the middle of the span. This is given by the following equation:

$$y_{max} = (\frac{5}{384}) \times (\frac{ql^4}{E.I_z}) \qquad \text{Eq. 7}$$

Where ***q*** denotes the force on the plate, ***l*** is the length of the support of the glass plate. From equations 6 and 7 the maximum deflection will be:

$$y_{max} = (\frac{5 \times 12}{384}) \times (\frac{ql^4}{E.bh^3}) \qquad \text{Eq. 8}$$

It is noticed that maximum deflection increases with *decreasing* the thickness of the glass plate and it decreases with increasing the thickness (Timoshenko, 1980).

We cannot ignore the importance of the light intensity on the setting of the resin composite materials. Increasing the light intensity will tend to increase the degree of the conversion and hence, the polymerisation shrinkage of the materials will increase.

The light intensity was reduced with increasing thickness of the glass plate (Chapter 2, Part I), which could be considered a factor which could change the values for polymerisation shrinkage of the resin composites when irradiated through the glass plate. The polymerisation shrinkage of the resin composite materials generates stresses that could cause bending of the glass plate. So for measurement with 1 mm thin glass plates the bending will may be greater than for those of the 3 mm thick glass plate.

6.5 Conclusions

It is concluded that the glass plate can be affected by the heat generated from the lamp of the light source, apparatus and investigated material during setting, which may affect the results of polymerisation shrinkage of the resin composites.

The developed method of this study gave reproducible results. The temperature apparently affected the glass plates. Therefore, the apparent values for shrinkage of resin composites may be slightly affected. The increase of the "ambient" (anvil) temperature will lead to thermal expansion of the glass plates. Further heat was produced from light-curing sources, which could contribute to the thermal expansion of the glasses. The thinner glass may be more affected

Consequently, in the investigation of the polymerisation shrinkage of the resin composites with increasing temperature, it is advisable to pre-heat the apparatus to the required temperature. Then the glass plate with loaded sample should be placed pre-test for 3 – 5 min to thermally and mechanically equilibrate. Pre-heating the specimen before measurement ensures that the setting and shrinkage behaviour occur at the required temperature.

Chapter 7

Polymerisation Shrinkage-Strain of Resin Composites with Conventional and "Soft-Start" Light Irradiation

7.1 Literature Review

An inherent disadvantage of dental composite restorative materials is that they shrink during polymerisation (Watts 1996). It is obviously undesirable for a restorative material to contract excessively during setting as its adaptation to the cavity walls would be impaired (Walls *et al.*, 1988).

The molecular origins of shrinkage lie in the conversion of the monomer molecules into a polymer network. This is accompanied by a closer packing of the molecules, which leads to bulk contraction (Venhoven *et al.*, 1993; Davidson and Feilzer, 1997).

The polymerisation of the resin matrix initially produces a gelation in which the restorative material is transformed from a viscous-plastic into a rigid-elastic phase. The gel point is defined as the moment at which the material can no longer provide viscous flow to keep up with the curing contraction (Davidson and Feilzer, 1997).

Following the onset of cure, the post-gelation rigid contraction is the factor of clinical significance. Flow may compensate for the effects of shrinkage during the pre-gelation phase. VLC composites reach the gel point rapidly (Watts, 1992).

The volumetric curing contraction determinations are basically "free" shrinkage measurements and therefore offer total (pre- and post-gel) curing contraction (Lai and Johnson, 1993; Attin *et al.*, 1995), while the dimensional changes in linear curing contraction determinations are more or less as a post-gel curing phenomenon (Walls *et al.*, 1988; Watts and Cash, 1991a).

The shrinkage rate and the degree of shrinkage of a direct restorative material depend on

many factors. These factors are the monomer system and the concentrations of the catalyst and/or initiating system. Other important factors are the amount of filler, filler type, size and coating (Feilzer, *et al.,* 1988).

Four variables influence polymerisation contraction, which would affect the reduction in the quantity of volumetric polymerisation contraction within the composites system (Walls et al., 1988), these are:

(a) The size of the molecule undergoing polymerisation. The larger the molecule before polymerisation, the lower the contraction.

(b) As the filler loading rises, the polymerisation contraction falls. Towards the upper limit of filler fraction, diluent monomers are generally added to reduce resin viscosity in order to enhance the filler loading and a greater shrinkage is associated with the smaller diluent monomers (Watts, *et al.,* 1986; Watts, 1991b).

(c) Degree of polymerisation or conversion: As the degree of conversion rises, the resin will undergo greater contraction. Optimum DC and minimal polymerisation shrinkage are generally maintained as goals (Walls *et al.*, 1988).

(d) The nature of the resin undergoing polymerisation. Molecules which polymerise via a ring-opening mechanism would either undergo minimal volumetric change or even expand during setting (Walls *et al.*, 1988).

Progress towards elimination or reduction of polymerisation contraction, by synthesis of monomers that expand upon polymerisation has been investigated (Stansbury, 1990; Eick *et al.*, 1993). An alternative approach is the application of secondary curing to composite (Watts, 1990; Dionysopoulos and Watts, 1989).

The technique employed during clinical placement of the material can be varied to minimise the effect of contraction, (Watts, *et al.*, 1986; Jensen and Chan, 1985; Ikemi and Nomoto, 1994).

It is pointed out that composites cured at low light intensity have a better marginal adaptation. This procedure, however, leads to inferior material properties, e.g. for microhardness, compressive strength, flexural strength, etc caused by modest conversion of double bonds (Unterbrink and Muessner 1995; Uno and Asmussen 1991).

Another way to minimise the wall-to-wall contraction is to allow flow of composite resin during setting by means of controlled polymerisation. This can be done by prepolymerisation at low light intensity followed by final cure at high light intensity (Mehl *et al.*, 1997).

Polymerisation shrinkage may cause adhesive or cohesive failure and interfacial gap formation around the margins of the cavity, resulting in microleakage which will lead to pulpal irritation, thermal sensitivity and secondary caries (Asmussen, 1975; Lee *et al.*, 1976; Bausch *et al*, 1982; Causton, *et al.*, 1985, Rees and Jacobsen, 1989; Watts, 1992; Retief, 1994).

7.2 Objectives

It was the objective of this part of the study to investigate the effect of three variables on the polymerisation shrinkage:

I. The effect of different light sources.
II. Soft-start irradiation produced from the Elipar Highlight unit.
III. The effect of different temperatures.

7.3 Materials and Methods

The restorative materials examined in this study are listed in Table 7-1, and their polymerisation shrinkage were determined using an apparatus described in details in the previous chapter (Chapter 6).

Table 7-1: VLC composite materials investigated.

Materials	Code	Batch No.	Manufacturer
Charisma	**CHR**	049	Heraeus Kulzer, Wehrheim, Germany
Charisma F	**CHRF**	28	
Solitaire	**SOL**	23	
Lite Fil II	**LF2**	109598	Shofu, Japan
Pertac II	**PER2**	643081003	Espé Dental AG, Seefeld, Germany
Tetric Ceram	**TETC**	823365	Ivoclar-Vivadent, Liechtenstein
P-50	**P50**	9350	3M Dental Products, St. Paul, USA
Z100	**Z100**	3021	

7.3.1 Light Intensity and Temperature Variables

The following variables were investigated, using the selection of materials indicated.

7.3.1.1 Two different light-cure units

Z100 and **CHR** were compared, using different light sources (Elipar and XL3000).

7.3.1.2 Soft-start versus full intensity

Four materials (**CHR**, **LF2**, **PER2**, and **Z100**) were cured by soft-start (group 1) and by full

intensity (group 2), with the Elipar unit.

7.3.1.3 Temperature increase to 37 °C

Six materials (**CHR, CHRF, P50, SOL, TET,** and **Z100**) were cured with the XL3000 unit at 23°C (room temperature) and 37°C (human body temperature). The temperature was elevated in the apparatus using an electrical supply (mentioned above, 6.2.1).

7.3.2 Test Procedure

A disc-shaped specimen, about 7 x 1.5 mm, was placed at the centre of a square cross-section brass ring, internal diameter 16 mm and height 1.5 mm, adhesively bonded onto the modified rigid glass plate, 74 x 25 x 3 mm. The top edge of the ring and a disc specimen were covered by a flexible 22 mm square glass cover-slip, thickness 0.1 mm (type 0, Chance-Propper Ltd., Warley, UK), (Fig 7-1). A centrally aligned LVDT was positioned over the centre of the cover-slip. The transducer was used without a spring, relying upon the self-weight (*circa* 9 g) of the probe to maintain contact. Cure was initiated from below by transillumination of the glass plate beneath the specimen.

The cover slip deflects as shrinkage takes place, and the deflection at the centre of the cover-slip was monitored over time by the calibrated LVDT (sensitivity < 0.1 μm). The LVDT was connected to a signal conditioning unit (type E307-3, RDP Electronics, Wolverhampton, UK) and a PC transient data-recorder. Zero of the shrinkage-measurement period was taken as the concurrently recorded moment of lamp illumination.

The shrinkage deflection in μm of the cover slip and specimen ($\Delta L = L_o - L$), was determined from the data via a voltage/displacement calibration, where L_o is the original specimen thickness and L is the final thickness. The percent shrinkage [$(\Delta L / L_o) \times 100$] was calculated as a function of time. However, since the cover slip deforms in a "dinner-plate" pattern as shrinkage takes place, the procedure essentially determines volumetric contraction constrained into 1-D of disk specimen. Each measurement was repeated twice (n = 3).

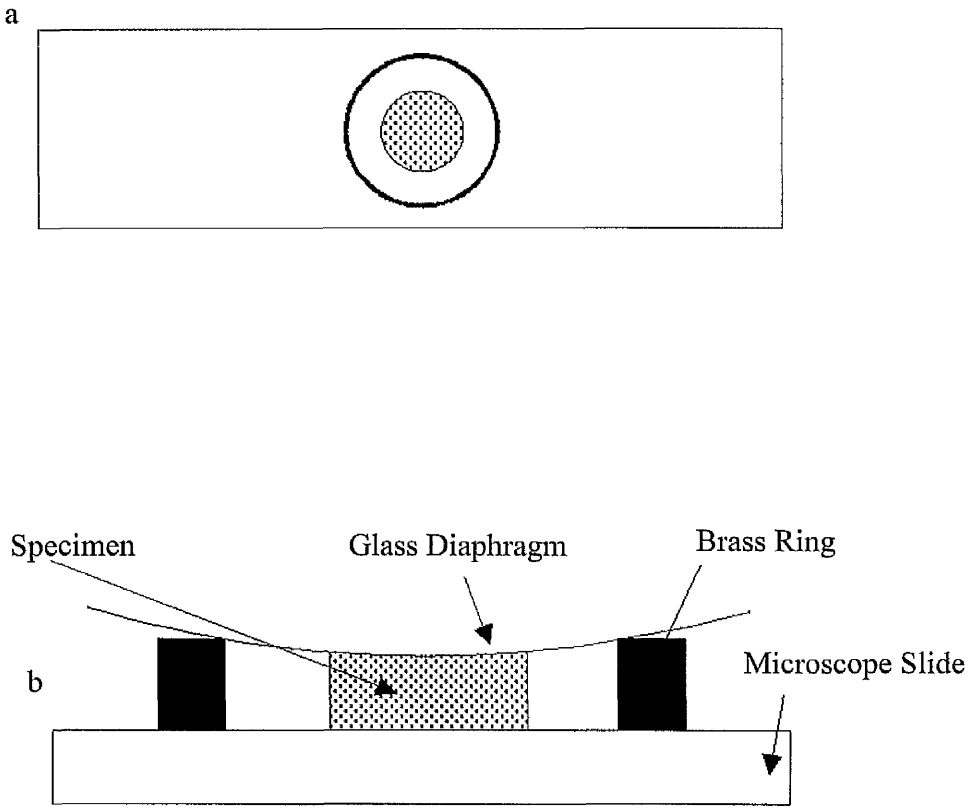

Fig. 7-1: Disc specimen mounted to the rigid glass plate at the centre of the brass-supporting ring: (a) Plan view; (b) elevation, with glass diaphragm in position.

7.3.3 Statistical Analysis

The time-dependence of polymerisation shrinkage was analysed with one-way ANOVA followed by multiple comparison (Scheffé procedure). One-way ANOVA and Scheffé multiple comparison were also used to differentiate statistically between the materials investigated when cured by soft-start polymerisation or full intensity and when measured at different temperatures 23°C and 37°C.

7.4 Results

Full data of the time-dependence of polymerisation shrinkage strain of the investigated materials are tabulated in Appendix V in CD.

7.4.3 Effect of two different light cure units on shrinkage

The XL3000 and the Elipar units have different intensity of light, but they have the same wavelength (400-500 nm). The polymerisation shrinkage strain of **Z100** and **CHR** was slightly lower with XL3000 to those cured by Elipar. However, There was no statistically significant difference between the use of the Elipar and XL3000 units. The data of the two materials were presented in Table 7-2 and plotted graphically in Figures 7-2 and 7-3.

Table (7-2): Mean values (SD in parenthesis) of the effect of two different light cure units on shrinkage (%).

Mat	Light unit	10 s	20 s	30 s	40 s	1 min	5 min	10 min	20 min
CHR	XL3000	1.13 (0.06)	1.68 (0.04)	1.92 (0.02)	2.05 (0.02)	2.20 (0.03)	2.40 (0.03)	2.48 (0.03)	2.56 (0.02)
	Elipar	1.20 (0.08)	1.72 (0.02)	1.95 (0.05)	2.09 (0.06)	2.23 (0.07)	2.47 (0.09)	2.56 (0.10)	2.63 (0.10)
Z100	XL3000	1.32 (0.03)	1.94 (0.03)	2.16 (0.02)	2.31 (0.03)	2.42 (0.03)	2.59 (0.09)	2.64 (0.09)	2.68 (0.09)
	Elipar	1.67 (0.07)	2.07 (0.07)	2.23 (0.07)	2.33 (0.06)	2.43 (0.06)	2.62 (0.04)	2.70 (0.04)	2.78 (0.04)

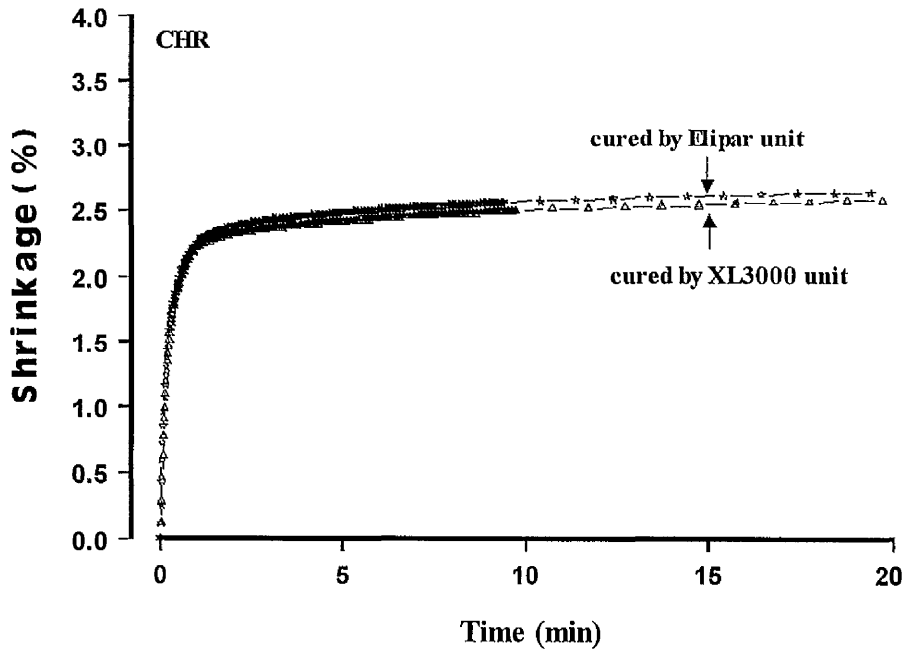

Fig 7-2: Effect of the XL3000 and the Elipar units on polymerisation shrinkage of **CHR**.

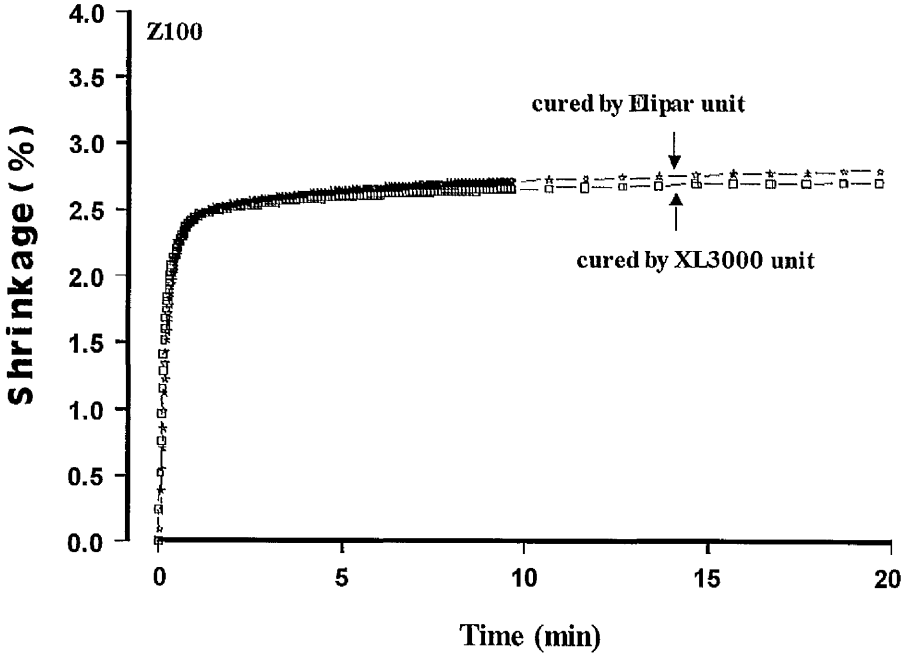

Fig 7-3: Effect of the XL3000 and the Elipar units on polymerisation shrinkage of **Z100**.

7.4.2 Soft-Start versus full intensity effects on shrinkage

The mean values and standard deviation of the polymerisation shrinkage strain are represented in Table 7-3. The data are plotted graphically in Figures 7-4 to 7-9.

For soft-start polymerisation, Table 7-4 shows one-way ANOVA of the time dependence of polymerisation shrinkage and Table 7-5 compares means between the increased time by using the Scheffé procedure at $p < 0.05$.

For full intensity polymerisation, Table 7-8 shows one-way ANOVA the time dependence of polymerisation shrinkage and Table 7-9 compares means between the increased time by using Scheffé procedure at $p < 0.05$.

In both cure modes, it was noticed that there were significant differences between 10 s and 40 s, and 40 s (the end of cure) and the maximum shrinkage time of 20 min for all investigated materials. In soft-start polymerisation there were significant difference between 40 s and 1 min for **CHR**, **LF2**, **PER2**, and **Z100**. On the other hand, in full intensity polymerisation there were significant differences between 40 s and 1 min for **CHR**, **LF2** and **PER2**, but no significant difference for **Z100**.

Table 7-6 indicates the one-way statistical analysis of polymerisation shrinkage between the materials cured by soft-start polymerisation. Table 7-7 demonstrates the comparisons between the means (Scheffé procedure). There were significant differences between **PER2** and **LF2** and **CHR**, between **Z100** and **LF2** and between **CHR** and **LF2** (Fig 7-8).

Table 7-10 indicates the one-way statistical analysis of polymerisation shrinkage between the materials cured by full intensity polymerisation. Table 7-11 demonstrates the comparisons between the means (Scheffé procedure). With this cure mode there were statistical differences between **PER2** and **LF2**, **CHR** and **Z100**. Also there was a significant difference between **Z100** and **LF2**, and between **CHR** and **LF2** (Fig 7-9).

Table 7-3: Mean values and SD (in parenthesis) of the effect of **Soft-start** and **full intensity** on polymerisation shrinkage strain (%) of the investigated resin composites

Mat.	Curing mode	10 s	20 s	30 s	40 s	1 min	5 min	10 min	20 min
CHR	Soft-start	0.01 (0.01)	0.02 (0.01)	0.52 (0.07)	1.45 (0.03)	1.99 (0.06)	2.36 (0.08)	2.45 (0.08)	2.54 (0.08)
	Full int.	1.20 (0.08)	1.72 (0.02)	1.95 (0.05)	2.09 (0.06)	2.23 (0.07)	2.47 (0.09)	2.56 (0.10)	2.63 (0.10)
LF2	Soft-start	0.01 (0.02)	0.01 (0.02)	0.09 (0.03)	0.51 (0.04)	1.09 (0.05)	1.49 (0.05)	1.59 (0.06)	1.69 (0.06)
	Full int.	0.36 (0.02)	0.75 (0.01)	1.03 (0.02)	1.23 (0.02)	1.37 (0.02)	1.62 (0.02)	1.71 (0.03)	1.80 (0.02)
PER2	Soft-start	0.00	0.01 (0.01)	0.63 (0.15)	1.71 (0.06)	2.37 (0.06)	2.70 (0.07)	2.76 (0.08)	2.81 (0.10)
	Full int.	1.79 (0.02)	2.19 (0.01)	2.39 (0.01)	2.54 (0.01)	2.64 (0.01)	2.79 (0.01)	2.84 (0.02)	2.89 (0.03)
Z100	Soft-start	0.03 (0.02)	1.30 (0.06)	1.92 (0.05)	2.15 (0.03)	2.34 (0.04)	2.52 (0.07)	2.58 (0.08)	2.63 (0.09)
	Full int.	1.67 (0.07)	2.07 (0.07)	2.23 (0.07)	2.33 (0.06)	2.43 (0.06)	2.62 (0.04)	2.70 (0.04)	2.78 (0.04)

(A)

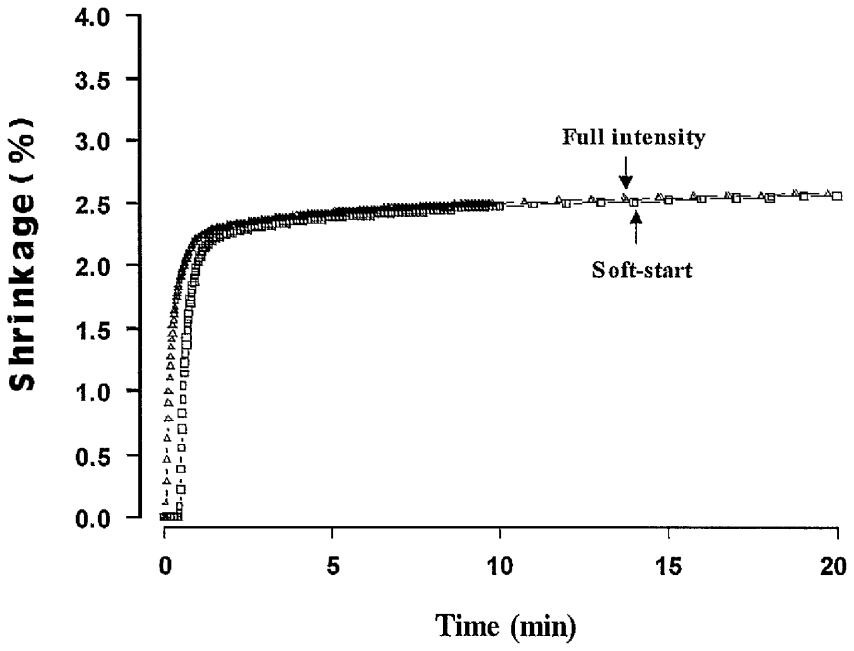

(B)

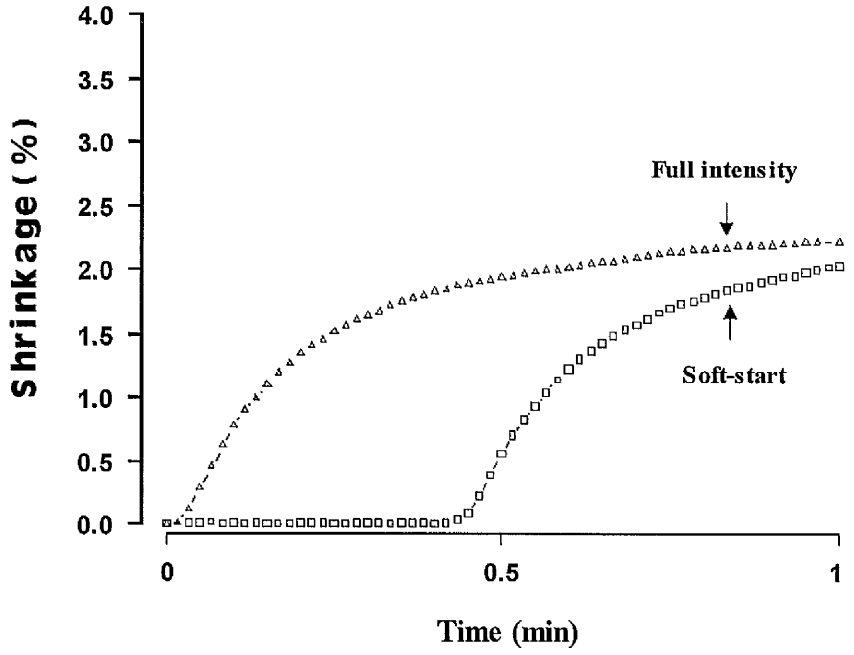

Fig 7-4: Polymerisation shrinkage-strain of **CHR**, cured by soft-start and full intensity. (A) full scale and (B) expanded scale for 1 min.

(A)

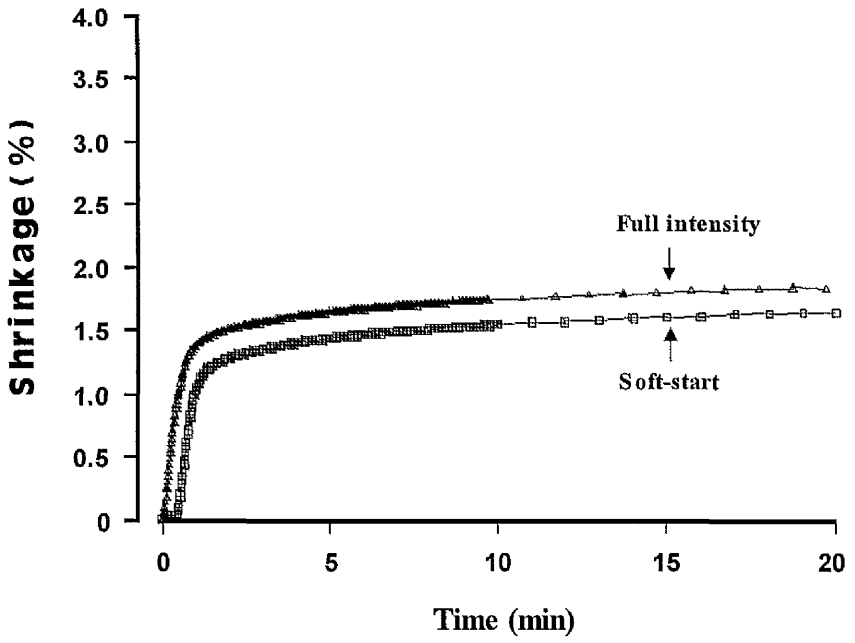

(B)

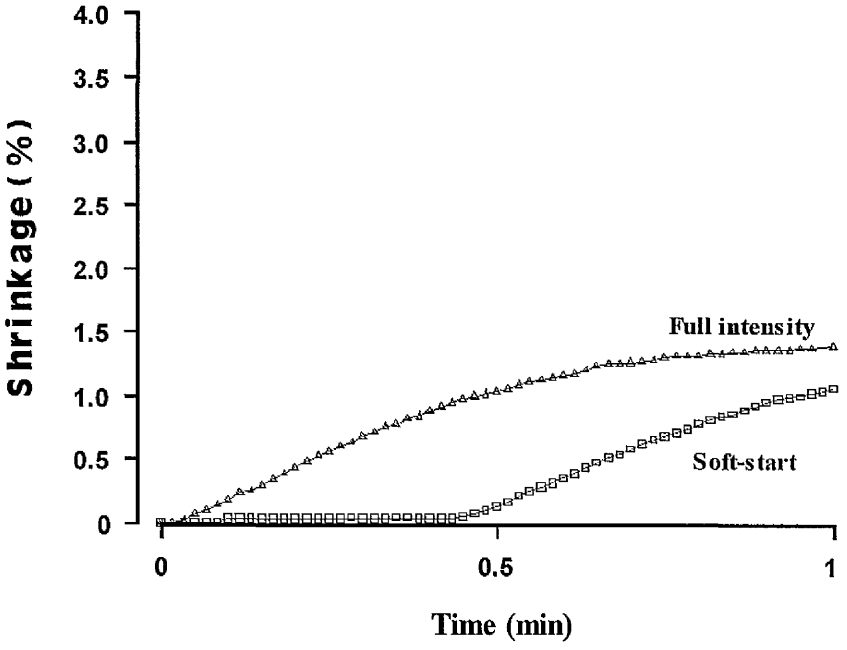

Fig 7-5: Polymerisation shrinkage-strain of **LF2**, cured by soft-start and full intensity. (A) full scale and (B) expanded scale for 1 min.

(A)

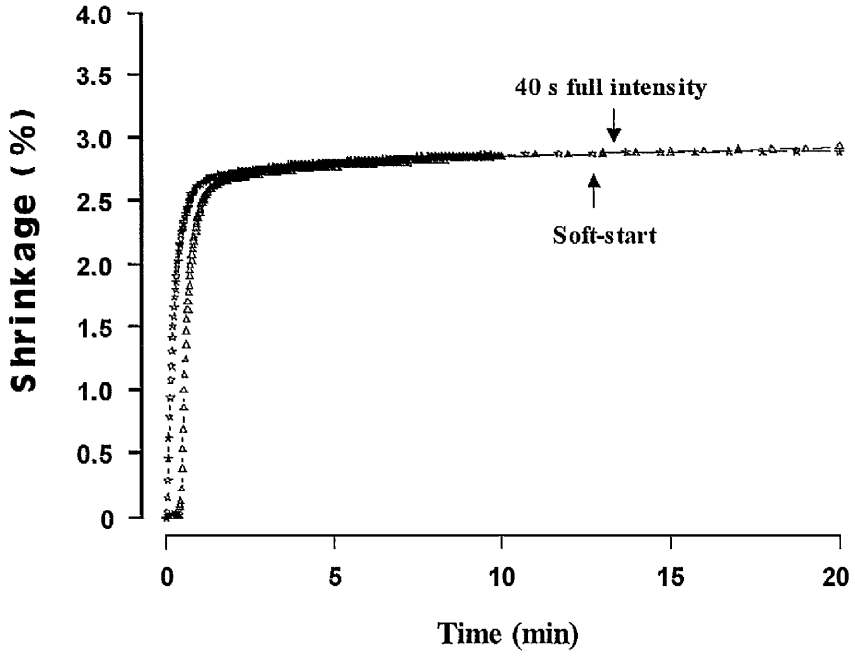

(B)

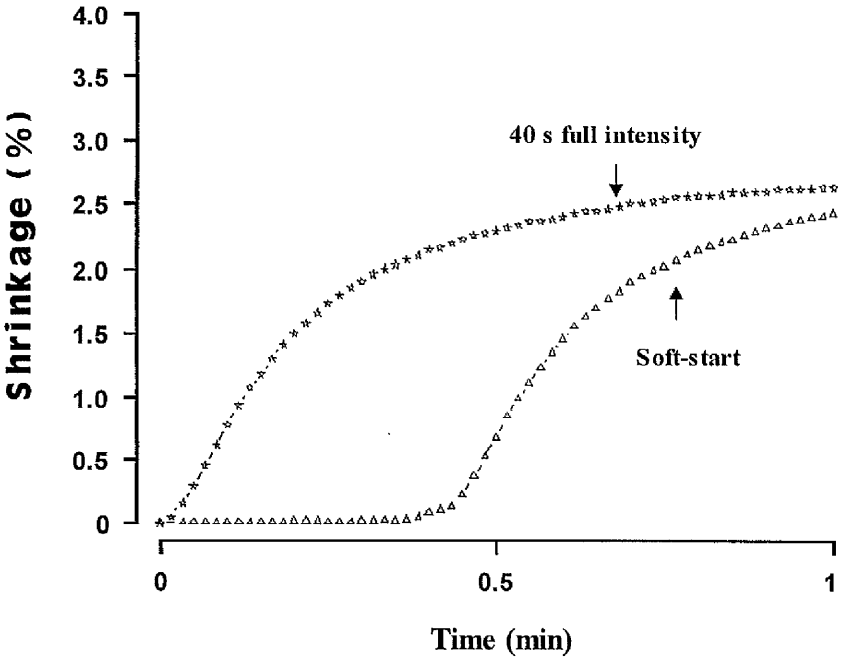

Fig 7-6: Polymerisation shrinkage strain of **PER2**, cured by soft-start polymerisation and full intensity. (A) full scale and (B) expanded scale for 1 min.

(A)

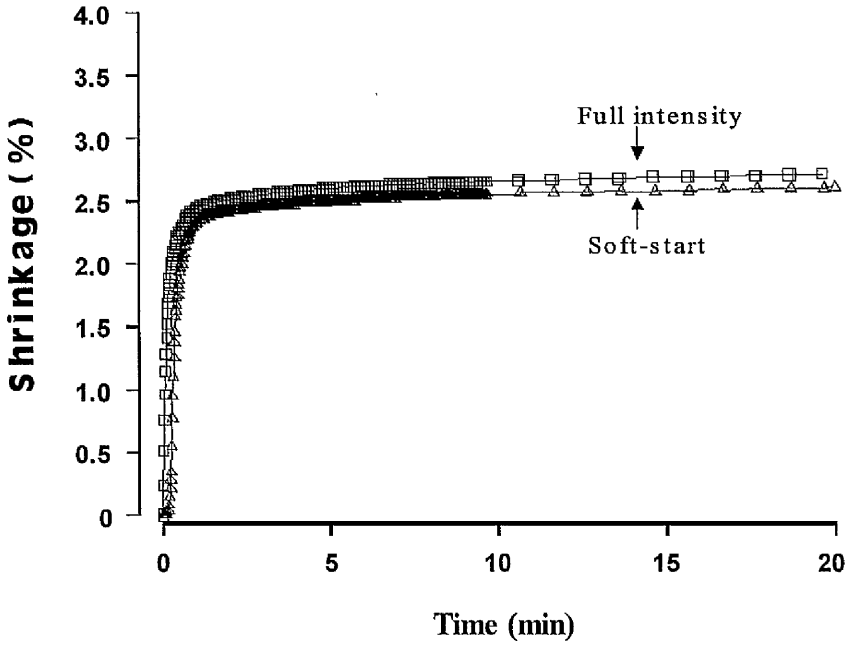

(B)

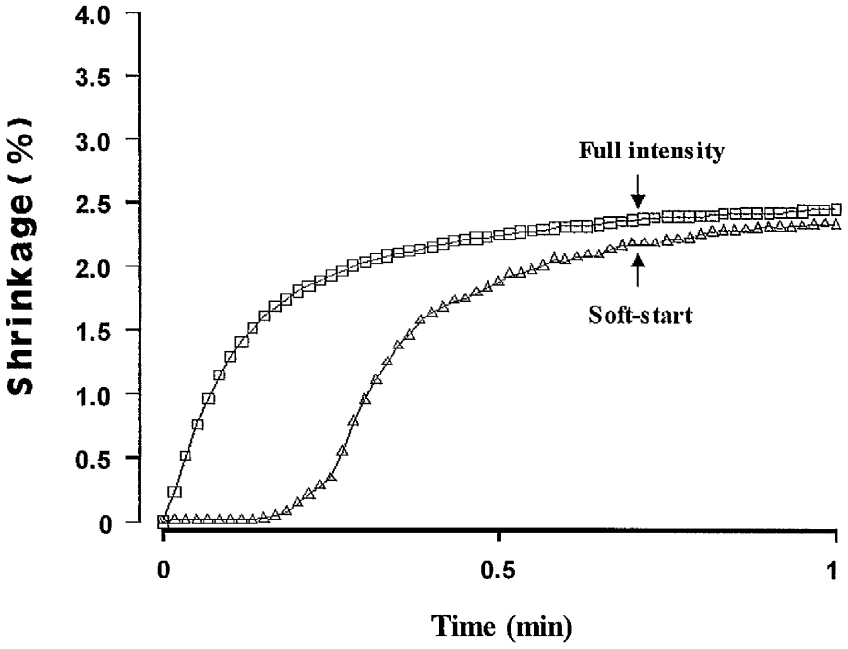

Fig 7-7: Polymerisation shrinkage strain of **Z100**, cured by soft-start polymerisation and full intensity. (A) full scale and (B) expanded scale for 1 min.

(A)

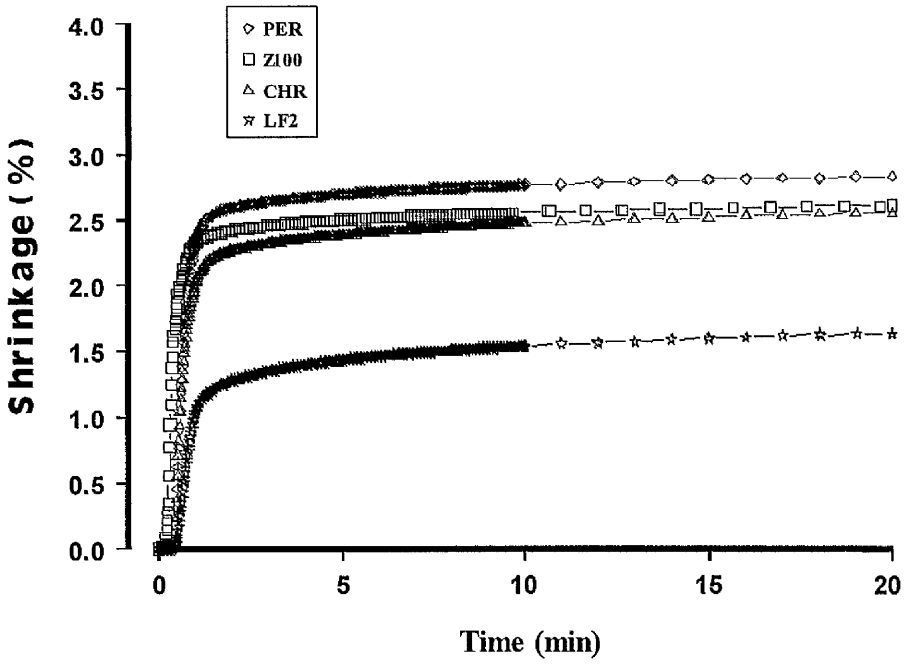

(B)

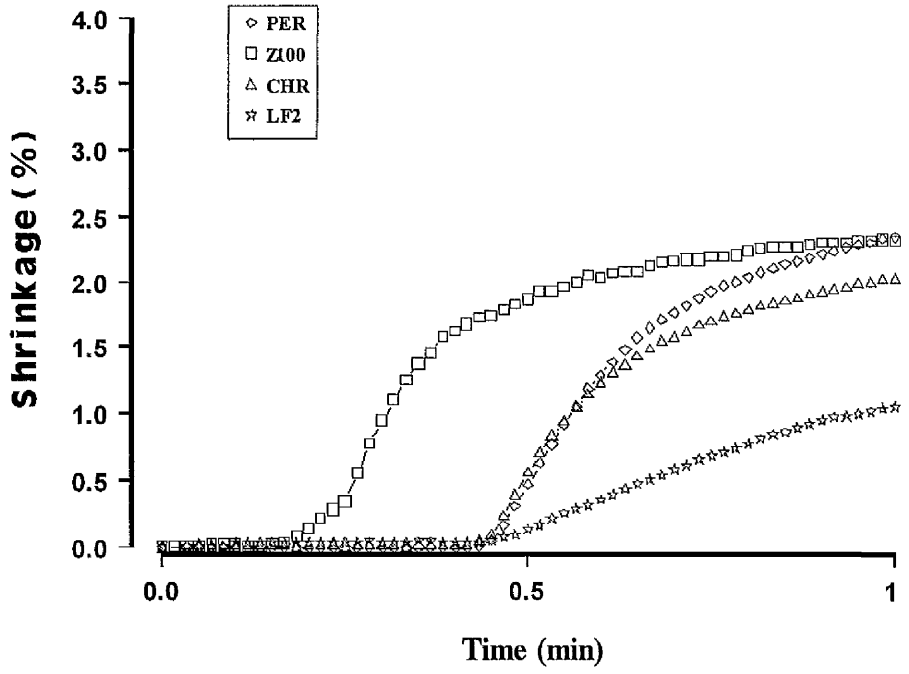

Fig 7-8: Polymerisation shrinkage strain of Four resin composite materials, cured by **soft-start polymerisation**. (A) full scale and (B) expanded scale for 1 min.

(A)

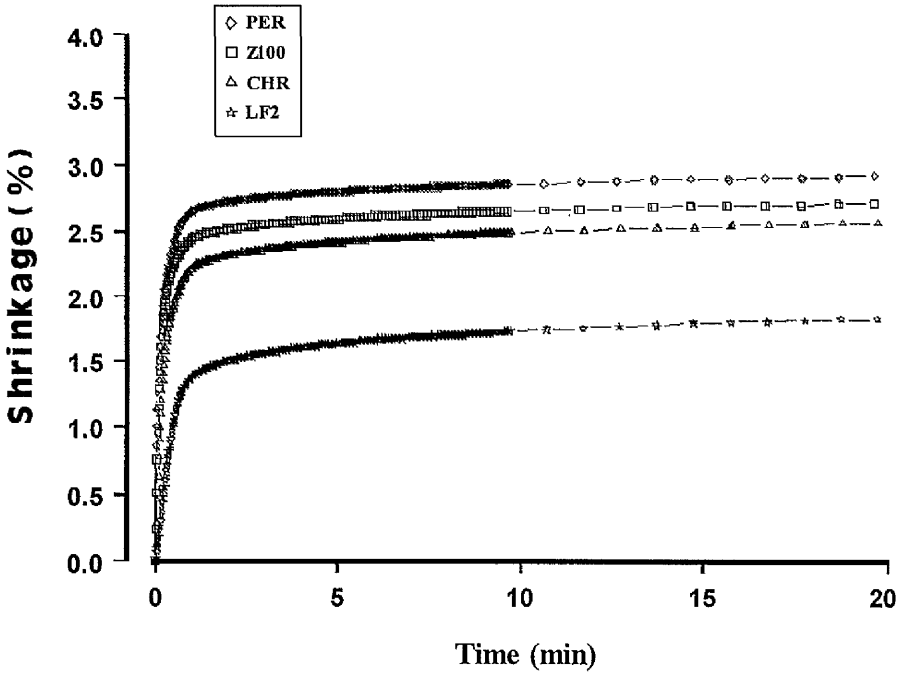

(B)

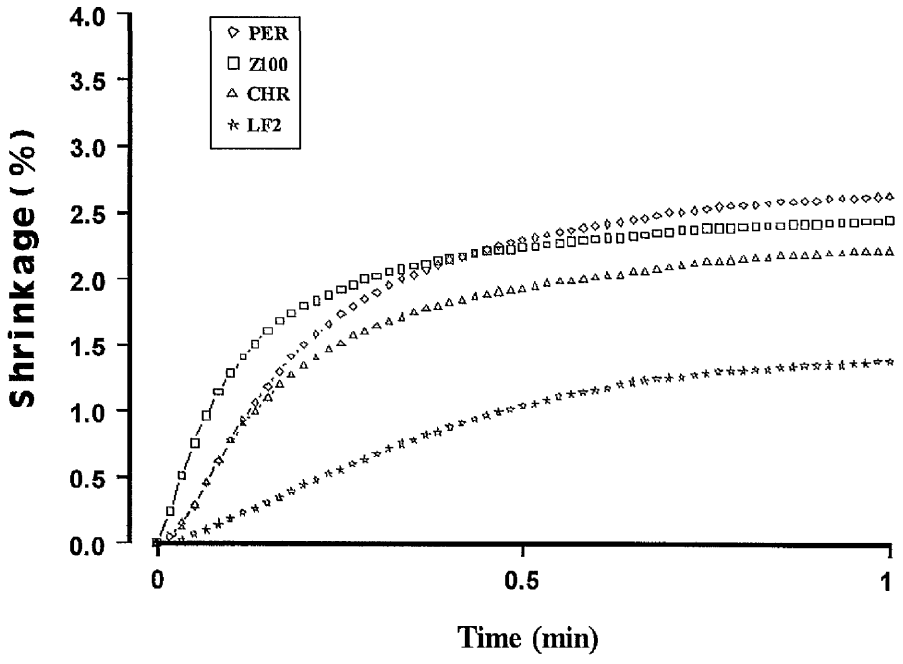

Fig 7-9: Polymerisation shrinkage strain of Four resin composite materials, cured by **Full intensity**. (A) full scale and (B) expanded scale for 1 min.

Table 7-4: One-way ANOVA of polymerisation shrinkage-strain of VLC materials when cured by **soft-start polymerisation**. The analysis was performed at different times.

Material	D.F.	Sum of Square	Mean Squares	F Ratio	F Prob.
CHR	7	24.8888	3.5555	1043.3315	0.0000
LF2	7	11.4433	1.6348	868.0149	0.0000
PER2	7	31.9117	4.5558	715.1089	0.0000
Z100	7	16.5282	2.3612	685.2263	0.0000

Table 7-5: Comparison of means (Scheffé procedure) of shrinkage strain at different times for the investigated materials

Time	CHR	LF2	PER2	Z100
10s – 20s				*
10s – 30s	*		*	*
10s – 40s	*	*	*	*
10s – 1 min	*	*	*	*
10s – 5 min	*	*	*	*
10s – 10 min	*	*	*	*
10s – 20 min	*	*	*	*
20s – 30s	*		*	*
20s – 40s	*	*	*	*
20s – 1 min	*	*	*	*
20s – 5 min	*	*	*	*
20s – 10 min	*	*	*	*
20s – 20 min	*	*	*	*
30s – 40s	*	*	*	*
30s – 1 min	*	*	*	*
30s – 5 min	*	*	*	*
30s – 10 min	*	*	*	*
30s – 20 min	*	*	*	*
40s – 1 min	*	*	*	
40s – 5 min	*	*	*	*
40s – 10 min	*	*	*	*
40s – 20 min	*	*	*	*
1 min – 5 min	*	*	*	
1 min – 10 min	*	*	*	*
1 min – 20 min	*	*	*	*
5 min – 10 min				
5 min – 20 min		*		
10 min – 20 min				

(*) Indicates significant differences at the level $p < 0.05$.

Table 7-6: One-way ANOVA of polymerisation shrinkage strain of VLC materials when cured by **Soft-satart polymerisation**. The analysis was performed between the different materials.

Source	D.F.	Sum of Square	Mean Squares	F Ratio	F Prob.
Between groups	3	2.2178	0.7393	100.5790	0.0000
Within groups	8	0.0588	0.0073		
Total	11	2.2766			

Table 7-7: Comparison of means (Scheffé procedure) of shrinkage strain between the materials investigated.

Materials	**LF2**	**CHR**	**Z100**	**PER2**
LF2				
CHR	*			
Z100	*			
PER2	*	*		

(*) Indicates significant differences at the level $p < 0.05$.

Table 7-8: One-way ANOVA of polymerisation shrinkage strain of VLC materials when cured by **Full intensity**. The analysis was performed at different times.

Material	D.F.	Sum of Square	Mean Squares	F Ratio	F Prob.
CHR	7	4.7909	0.6844	641.6339	0.0000
LF2	7	5.2756	0.7537	1987.6609	0.0000
PER2	7	2.9818	0.4260	2044.6371	0.0000
Z100	7	2.4239	0.3463	65.7486	0.0000

Table 7-9: Comparison of means (Scheffé procedure) of shrinkage strain at different time for the investigated materials

Time	CHR	LF2	PER2	Z100
10s – 20s	*	*	*	*
10s – 30s	*	*	*	*
10s – 40s	*	*	*	*
10s – 1 min	*	*	*	*
10s – 5 min	*	*	*	*
10s – 10 min	*	*	*	*
10s – 20 min	*	*	*	*
20s – 30s	*	*	*	
20s – 40s	*	*	*	*
20s – 1 min	*	*	*	*
20s – 5 min	*	*	*	*
20s – 10 min	*	*	*	*
20s – 20 min	*	*	*	*
30s – 40s	*	*	*	
30s – 1 min	*	*	*	
30s – 5 min	*	*	*	*
30s – 10 min	*	*	*	*
30s – 20 min	*	*	*	*
40s – 1 min	*	*	*	
40s – 5 min	*	*	*	
40s – 10 min	*	*	*	*
40s – 20 min	*	*	*	*
1 min – 5 min	*	*	*	
1 min – 10 min	*	*	*	
1 min – 20 min	*	*	*	
5 min – 10 min		*	*	
5 min – 20 min	*	*		
10 min – 20 min		*		

(*) Indicates significant differences at the level $p < 0.05$.

Table 7-10: One-way ANOVA of polymerisation shrinkage strain of VLC materials when cured by **Full intensity**. The analysis was performed between the different materials.

Source	D.F.	Sum of Square	Mean Squares	F Ratio	F Prob.
Between groups	3	2.2178	0.7393	100.5790	0.0000
Within groups	8	0.0588	0.0073		
Total	11	2.2766			

Table 7-11: Comparison of means (Scheffé procedure) of shrinkage strain between the materials investigated.

Materials	**LF2**	**CHR**	**Z100**	**PER2**
LF2				
CHR	*			
Z100	*			
PER2	*	*	*	

(*) Indicates significant differences at the level $p < 0.05$.

7.4.3 Effect of temperature (37 versus 23 °C) on shrinkage

The mean values and standard deviation of polymerisation shrinkage-strain are summarised in Table 7-12. The data are plotted graphically in Figures 7-10 to 7-17.

For specimens measured at 23°C, Table 7-13 shows one-way ANOVA of the time dependence of polymerisation shrinkage and Table 7-14 shows the means comparison between ageing times by using the Scheffé procedure at $p < 0.05$.

For all materials investigated at 23°C (Fig 7-16), there were significant differences between shrinkage at 10 s and 40 s (end of light curing), and 40 s and 20 min. There were significant differences between 40 s and 1 min for **CHRF** and **SOL** only, and the difference was not significant for 40 s and 1 min for **CHR**, **P50**, **TETC** and **Z100**. The one-way ANOVA (Table 7-15) shows the statistical difference between the VLC resin composites. The comparisons between those materials are summarised in Table 7-16. **P50** has the lowest shrinkage (1.97 %) and **Z100** has the highest shrinkage (2.78%). There were significant differences between **Z100** and **P50**, **CHRF**, and **TETC**; between **TETC** and **P50** and **CHRF**; between **CHR** and **CHRF** and **P50** and between **SOL** and **P50**, **CHRF** and **TETC**.

For specimens measured at 37°C, Table 7-17 shows one-way ANOVA of the time dependence of polymerisation shrinkage and Table 7-18 shows the mean comparison between ageing time using the Scheffé procedure at $p < 0.05$.

At 37°C (Fig 7-17), there were significant differences between data for 10 s and 40 s, 40 s (end of cure) and 20 min for all investigated materials. On the other hand, there were significant differences between 40 s and 1 min for **P50** and **SOL**, and the difference was not significant for **CHR**, **CHRF**, **TETC** and **Z100**. The one-way ANOVA (Table 7-19) shows the statistical differences between the VLC resin composites. The comparison between those materials is summarised in Table 7-20. **P50** has the lowest shrinkage (2.45%) and **SOL** has the highest shrinkage (3.45%). There were significant differences between **SOL** and **P50**; **CHRF**, **TETC**, **Z100** and **CHR**; between **CHR** and **CHRF**, **P50** and **TETC**; between **Z100**

and **P50**, **CHRF** and **TETC**, between **TETC** and **P50**, and finally between **CHRF** and **P50**.

There were significant deference in shrinkage-strain due to increase in temperature from 23°C to 37°C ($p = 0.0000$, Table 7-21).

Table 7-11: Mean values (SD in parenthesis) of effect of increased **temperature** on polymerisation shrinkage strain (%) for the investigated resin composites.

Mat.	Temp.	10 s	20 s	30 s	40 s	1 min	5 min	10 min	20 min
CHR	23°C	1.13 (0.06)	1.68 (0.04)	1.92 (0.02)	2.05 (0.02)	2.20 (0.03)	2.40 (0.03)	2.48 (0.03)	2.56 (0.02)
	37°C	1.62 (0.08)	2.23 (0.04)	2.52 (0.07)	2.67 (0.09)	2.83 (0.11)	3.09 (0.10)	3.17 (0.10)	3.27 (0.09)
CHRF	23°C	0.44 (0.06)	0.97 (0.02)	1.24 (0.04)	1.41 (0.04)	1.58 (0.06)	1.86 (0.05)	1.94 (0.04)	2.01 (0.06)
	37°C	1.13 (0.02)	1.79 (0.05)	2.03 (0.04)	2.26 (0.07)	2.31 (0.04)	2.58 (0.06)	2.65 (0.08)	2.72 (0.06)
P50	23°C	0.30 (0.20)	0.76 (0.17)	1.12 (0.12)	1.37 (0.06)	1.54 (0.04)	1.79 (0.03)	1.88 (0.04)	1.97 (0.03)
	37°C	0.76 (0.02)	1.41 (0.01)	1.69 (0.02)	1.89 (0.03)	2.03 (0.02)	2.27 (0.04)	2.35 (0.04)	2.45 (0.04)
SOL	23°C	0.031 (0.03)	0.41 (0.03)	1.10 (0.04)	1.66 (0.02)	2.18 (0.03)	2.63 (0.07)	2.66 (0.03)	2.69 (0.03)
	37°C	0.03 (0.01)	0.53 (0.03)	1.45 (0.06)	2.13 (0.07)	2.75 (0.05)	3.22 (0.04)	3.35 (0.05)	3.45 (0.05)
TET	23°C	1.0 (0.07)	1.47 (0.04)	1.75 (0.06)	1.87 (0.05)	1.99 (0.06)	2.24 (0.06)	2.29 (0.04)	2.48 (0.05)
	37°C	1.48 (0.08)	2.05 (0.04)	2.27 (0.01)	2.39 (0.02)	2.50 (0.03)	2.71 (0.02)	2.76 (0.03)	2.78 (0.04)
Z100	23°C	1.32 (0.03)	1.94 (0.03)	2.16 (0.02)	2.31 (0.03)	2.42 (0.03)	2.59 (0.09)	2.64 (0.09)	2.68 (0.09)
	37°C	1.68 (0.14)	2.33 (0.03)	2.59 (0.02)	2.73 (0.01)	2.83 (0.02)	3.0 (0.03)	3.05 (0.03)	3.11 (0.04)

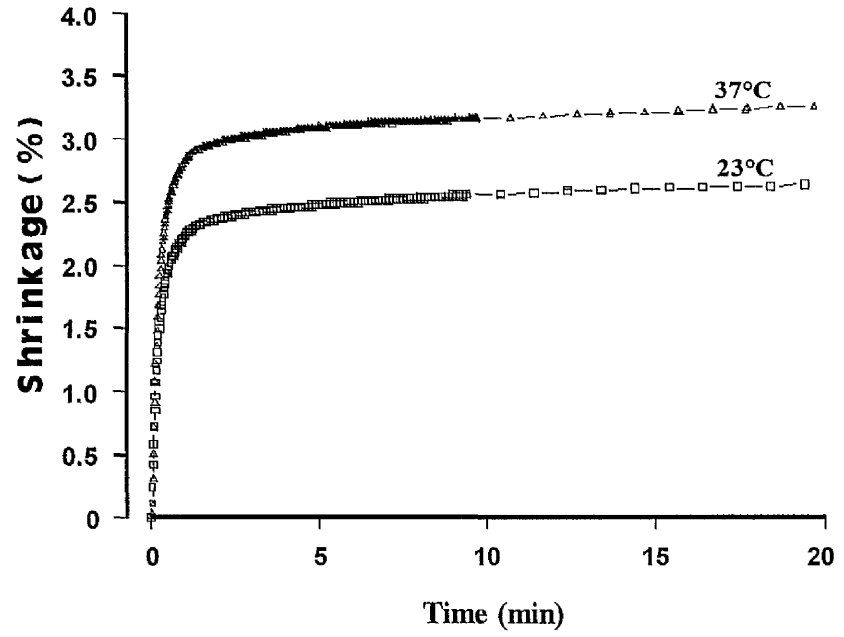

Fig 7-10: Polymerisation shrinkage-strain of **CHR**, at different temperatures.

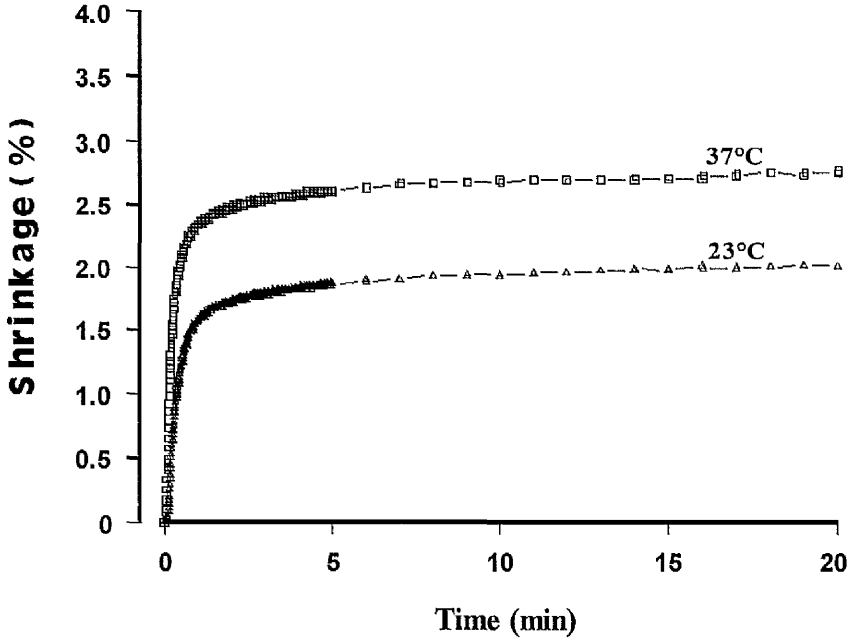

Fig 7-11: Polymerisation shrinkage-strain of **CHRF**, at different temperatures.

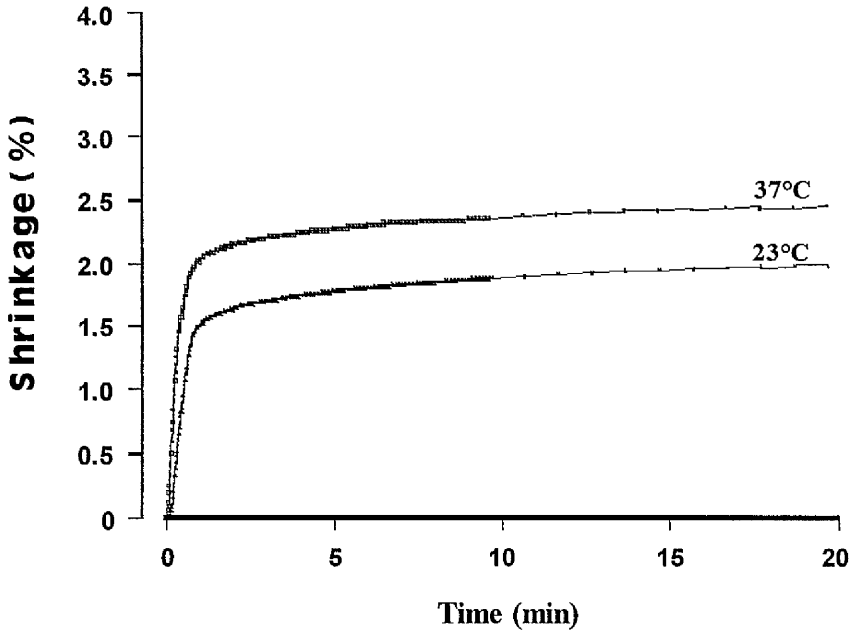

Fig 7-12: Polymerisation shrinkage-strain of **P50**, at different temperatures.

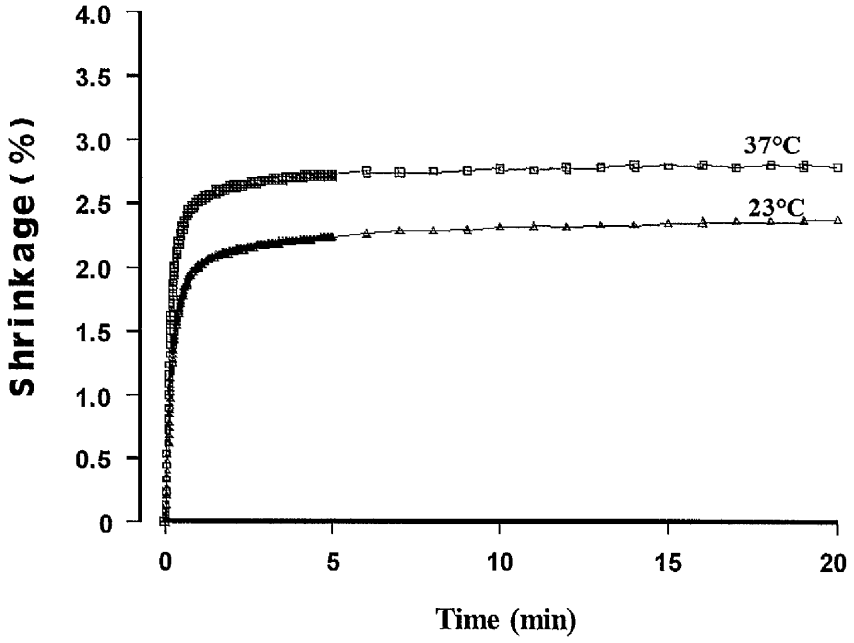

Fig 7-13: Polymerisation shrinkage-strain of **TETC**, at different temperatures.

(A)

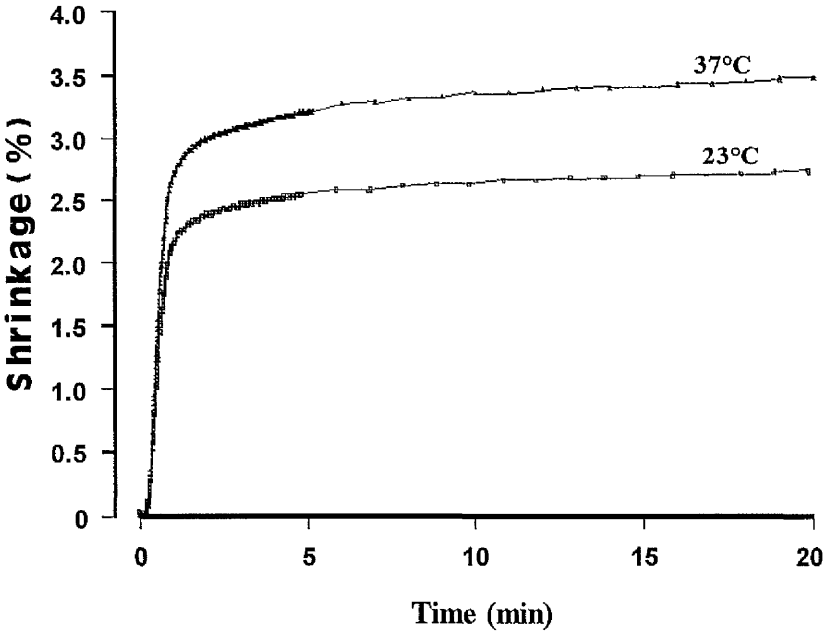

(B)

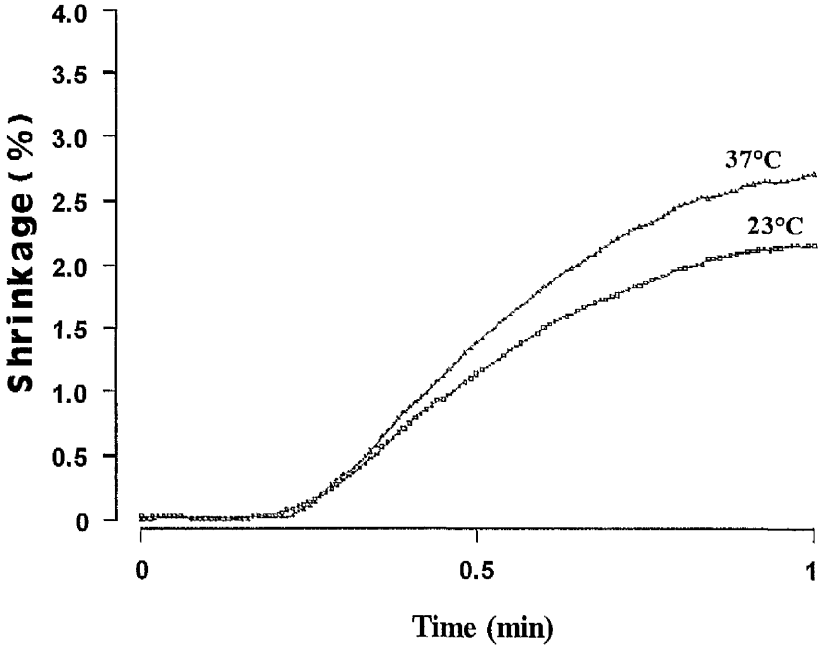

Fig 7-14: Polymerisation shrinkage-strain of **SOL**, at different temperatures. Full (A) and (B) expanded scales.

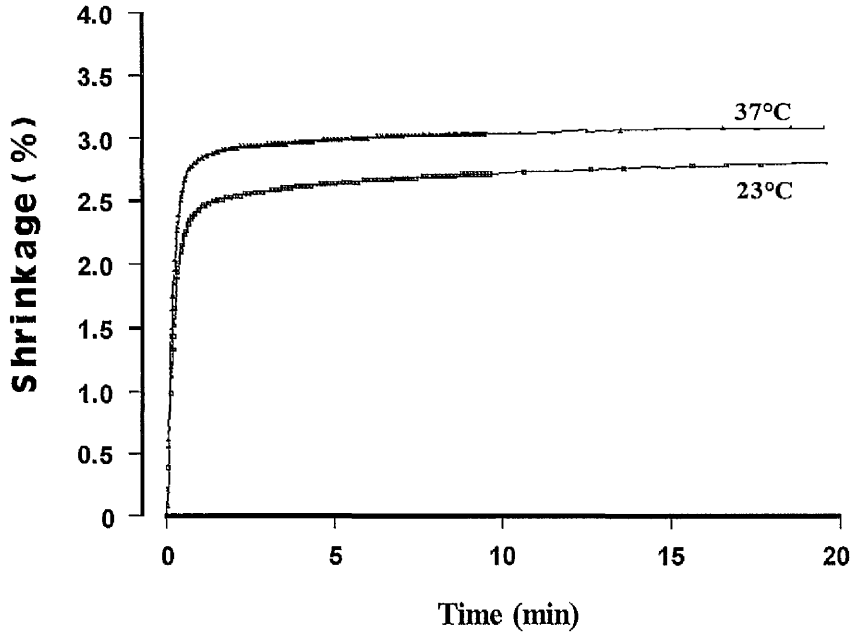

Fig 7-15: Polymerisation shrinkage-strain of **Z100**, at different temperatures.

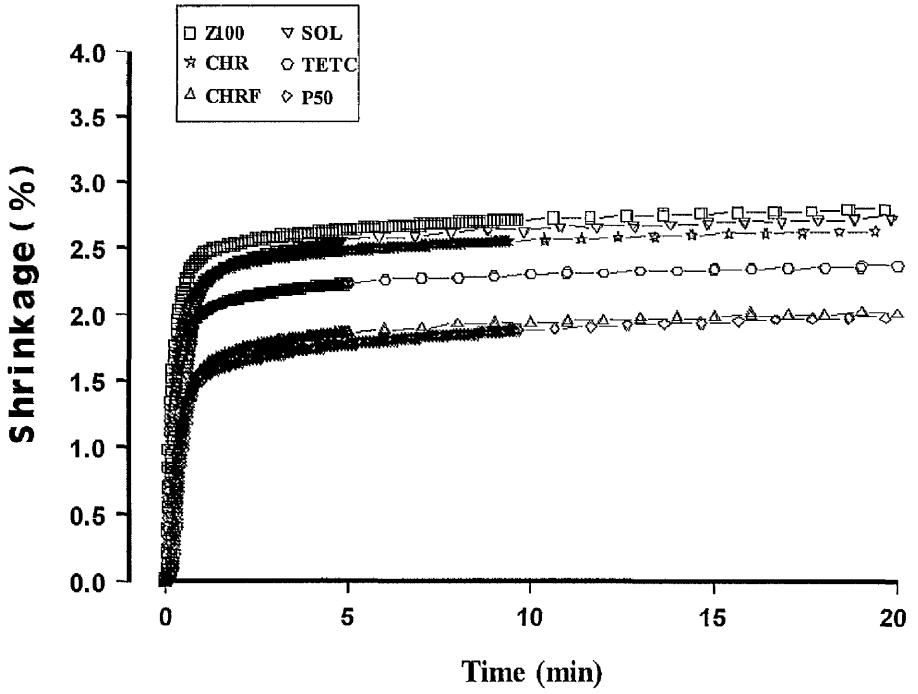

Fig 7-16: Polymerisation shrinkage-strain for six resin composite materials, at **23°C**.

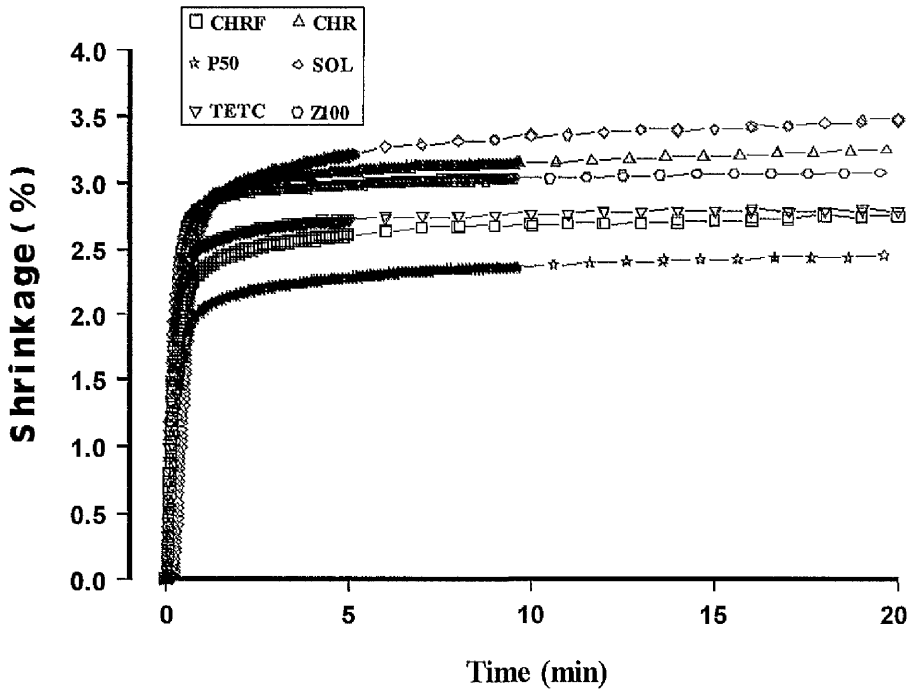

Fig 7-17: Polymerisation shrinkage-strain for six resin composite materials, at **37°C**.

Table 7-13: One-way ANOVA of polymerisation shrinkage-strain of VLC materials when cured at **23°C**. The analysis was performed at different times.

Material	D.F.	Sum of Square	Mean Squares	F Ratio	F Prob.
CHR	7	4.8942	0.6992	129.7765	0.0000
CHRF	7	6.1065	0.8724	403.4019	0.0000
P50	7	7.1684	1.0241	94.9673	0.0000
SOL	7	23.3760	3.3394	2607.3204	0.0000
TETC	7	4.9106	0.7015	259.8199	0.0000
Z100	7	4.8754	0.6965	658.1035	0.0000

Table 7-14: Comparison of means (Scheffé procedure) of shrinkage-strain at different times for investigated materials at **23°C**.

Time	CHR	CHRF	P50	SOL	TETC	Z100
10s – 20s	*	*	*	*	*	*
10s – 30s	*	*	*	*	*	*
10s – 40s	*	*	*	*	*	*
10s – 1 min	*	*	*	*	*	*
10s – 5 min	*	*	*	*	*	*
10s – 10 min	*	*	*	*	*	*
10s – 20 min	*	*	*	*	*	*
20s – 30s		*		*	*	*
20s – 40s	*	*	*	*	*	*
20s – 1 min	*	*	*	*	*	*
20s – 5 min	*	*	*	*	*	*
20s – 10 min	*	*	*	*	*	*
20s – 20 min	*	*	*	*	*	*
30s – 40s		*		*		*
30s – 1 min	*	*	*	*	*	*
30s – 5 min	*	*	*	*	*	*
30s – 10 min	*	*	*	*	*	*
30s – 20 min	*	*	*	*	*	*
40s – 1 min		*		*		
40s – 5 min	*	*	*	*	*	
40s – 10 min	*	*	*	*	*	*
40s – 20 min	*	*	*	*	*	*
1 min – 5 min		*		*	*	*
1 min – 10 min	*	*		*	*	*
1 min – 20 min	*	*	*	*	*	*
5 min – 10 min						
5 min – 20 min					*	*
10 min – 20 min					*	

(*) Indicates significant differences at the level $p < 0.05$.

Table 7-15: One-way ANOVA of polymerisation shrinkage-strain of VLC materials when measured at 23°C. The analysis was performed between the different materials.

Source	D.F.	Sum of Square	Mean Squares	F Ratio	F Prob.
Between groups	5	1.8903	0.3781	126.4907	0.0000
Within groups	12	0.0359	0.0030		
Total	17	1.9262			

Table 7-16: Comparison of means (Scheffé procedure) of shrinkage-strain between the materials investigated.

Materials	**P50**	**CHRF**	**TETC**	**CHR**	**SOL**	**Z100**
P50						
CHRF						
TETC	*	*				
CHR	*	*				
SOL	*	*	*			
Z100	*	*	*			

(*) Indicates significant differences at the level $p < 0.05$.

Table 7-17: One-way ANOVA of polymerisation shrinkage-strain of VLC materials when cured at **37°C**. The analysis was performed at different times.

Material	D.F.	Sum of Square	Mean Squares	F Ratio	F Prob.
CHR	7	6.3729	0.9104	120.8507	0.0000
CHRF	7	5.9314	0.8473	356.1529	0.0000
P50	7	6.6584	0.9512	1392.0105	0.0000
SOL	7	36.7244	5.2463	2264.6102	0.0000
TETC	7	4.0754	0.5822	429.9354	0.0000
Z100	7	4.7657	0.6808	235.0995	0.0000

Table 7-18: Comparison of means (Scheffé procedure) of shrinkage-strain at different times for the investigated materials at **37°C**.

Time	**CHR**	**CHRF**	**P50**	**SOL**	**TETC**	**Z100**
10s – 20s	*	*	*	*	*	*
10s – 30s	*	*	*	*	*	*
10s – 40s	*	*	*	*	*	*
10s – 1 min	*	*	*	*	*	*
10s – 5 min	*	*	*	*	*	*
10s – 10 min	*	*	*	*	*	*
10s – 20 min	*	*	*	*	*	*
20s – 30s		*	*	*	*	*
20s – 40s	*	*	*	*	*	*
20s – 1 min	*	*	*	*	*	*
20s – 5 min	*	*	*	*	*	*
20s – 10 min	*	*	*	*	*	*
20s – 20 min	*	*	*	*	*	*
30s – 40s			*	*		*
30s – 1 min	*	*	*	*	*	*
30s – 5 min	*	*	*	*	*	*
30s – 10 min	*	*	*	*	*	*
30s – 20 min	*	*	*	*	*	*
40s – 1 min			*	*		
40s – 5 min	*	*	*	*	*	*
40s – 10 min	*	*	*	*	*	*
40s – 20 min	*	*	*	*	*	*
1 min – 5 min		*	*	*	*	
1 min – 10 min	*	*	*	*	*	*
1 min – 20 min	*	*	*	*	*	*
5 min – 10 min						
5 min – 20 min			*	*		
10 min – 20 min			*			

(*) Indicates significant differences at the level $p < 0.05$.

Table 7-19: One-way ANOVA of polymerisation shrinkage-strain of VLC materials when measured at **37°C**. The analysis was performed between the different materials.

Source	D.F.	Sum of Square	Mean Squares	F Ratio	F Prob.
Between groups	5	2.1505	0.4301	142.8373	0.0000
Within groups	12	0.0361	0.0030		
Total	17	2.1866			

Table 7-20: Comparison of means (Scheffé procedure) of shrinkage-strain between the materials investigated.

Materials	**P50**	**CHRF**	**TETC**	**Z100**	**CHR**	**SOL**
P50						
CHRF	*					
TETC	*					
Z100	*	*	*			
CHR	*	*	*			
SOL	*	*	*	*	*	

(*) Indicates significant differences at the level $p < 0.05$.

Table 7-21: One-way ANOVA result of the effect of increased temperature from 23°C to 37°C on polymerisation shrinkage-strain of VLC materials investigated.

Source	D.F.	Sum of Square	Mean Squares	F Ratio	F Prob.
Between groups	1	19.6653	19.6653	38.5622	0.0000
Within groups	286	145.8496	0.5100		
Total	287	165.5150			

7.5 Discussion

The current types of resin-based restoratives and resin composites exhibit polymerisation shrinkage during the setting process due to the dimethacrylate monomer components. The phenomenon is due mainly to the rearrangement of molecules of the material into less space than was required for the liquid phase of a mobile monomer molecule.

For compensation of the contraction and relief of some of the contraction stress, the restorative material should flow in the direction of the cavity walls during early setting (Davidson and De Gee, 1984).

7.5.1 Effect of two different light cure units

The small variation of polymerisation shrinkage strain with the use of various light sources may be attributed to the small variation in the light intensity of the two light-curing units. The Elipar and XL3000 units have the wavelength (400-500 nm) in the blue region of the visible light spectrum produced, which can be absorbed by camphorquinone and with the presence of the amine accelerators, forms free radicals. This could explain the non significant difference in the polymerisation shrinkage results of **Z100** and **CHR**.

7.5.2 Soft-start versus full intensity effect on shrinkage

The results of this study showed that soft-start polymerisation does not significantly reduce the equilibrium polymerisation shrinkage for the investigated materials (**CHR, LF2, PER2** and **Z100**) but there is some delay in the initial setting of the resin composites with the first 10 s low intensity. This definitely reduces the initial "shrinkage impulse" and this should be beneficial clinically. The initial suppression of shrinkage process despite the quite effective initial network formation (DC ≈ 30 %).

Light-curing units with very high intensity are often recommended for producing good curing depths and physical properties of the resin composites. However, it is important consider the possible effect of high intensity lights on stress development (Mehl *et al.*, 1997).

Prepolymerisation at low intensity followed by a post-cure at full intensity may result in

composite restorations with improved marginal adaptation without loss in material quality (Uno and Asmussen, 1991).

At a certain light intensity the number of activated starter radicals is optimal to form cross-linked long-chain molecules. A higher concentration of radicals leads to an earlier reaction stop with short-chain molecules, whereas a very low concentration cannot start the polymerisation process. This actually depends on the concentration and the specific chemistry of the initiator system (Mehl *et al.*, 1997).

Further soft-start polymerisation was obtained from **SOL** even using full intensity light. The reduction or delay in the early shrinkage-strain of this material may be designated an 'intrinsic soft-start' phenomenon. **SOL** is based on multi-functional acrylate monomers. Acrylates, lacking the methyl group of the methacrylates, are less sterically hindered. Thereby, greater segmental mobility is feasible for growing free-radicals during the polymerisation process. This may permit enhanced flow during the early period of reaction. However, **SOL** has a further special structural feature, namely the development of porous filler (Watts and Al-Hindi, 1999). Heindl, (1999), suggested that the reason for the slower polymerisation strain may be due to shielding from 400-500 nm light of the photo-initiator molecules within the porous filler. This may require time for a diffusion process of monomer or radicals in and/or out of the filler interstices.

7.5.2.1 Time-dependence (kinetics)

Polymerisation shrinkage-strain is time-dependent and a methodology for measurement and analysis of the kinetics of this phenomenon has been described by Watts and Cash (1991a). Once initiated, the initial rigid polymerisation shrinkage of VLC resin composites usually proceeds rapidly, in a linear manner with time. However, the "soft-start" phenomenon obviously with low intensity results in a greatly reduced rate of reaction and hence rate of shrinkage.

For most materials, the longer-term shrinkage, was approximately represented by Kohlrausch-Williams-Watts [KWW] stretched exponential relaxation function (Williams and Watts, 1970; Shlesinger, 1984):

$$\Delta V/V_o = 1 - \exp - (t/\tau)^{\beta}$$

Where $0 < \beta \leq 1$, typical values for β being 0.3-0.6. This is particularly appropriate to the situation following formation of a glassy network. The glassy state is generated by photo-polymerisation and the KWW function characterise the time-dependence of segmental motion in the glassy state. This is the governing factor for the longer-term self-limiting processes of bulk polymerisation and free volume shrinkage. Typically this is the shrinkage occurring from 2 minutes post-irradiation, and for periods of several hours or even days thereafter.

7.5.3 Effect of temperature (37 versus 23 °C) on shrinkage

The higher temperature will accelerate and intensify the setting reaction, resulting in a higher shrinkage rate and ultimate shrinkage volume (Bausch, *et al.*, 1982; Penn 1986). The shrinkage-strain increase with temperature is due to the enhanced thermal mobility of the reacting network that leads to enhanced conversion of C=C bonds (Watts and Al-Hindi, 1999).

The amount of increased shrinkage (%) from 23°C to 37°C were 0.64, 0.71, 0.48, 0.76, 0.30, 0.33 % for the materials investigated, **CHR**, **CHRF**, **P50**, **SOL**, **TETC**, and **Z100** respectively. **SOL** has the highest shrinkage (%) in both temperatures and **P50** has the lowest results. **TETC** was the least affected by the temperature rises. The increase in shrinkage was 0.30 %, while **SOL** was the highest affected (0.76 %).

CHR and **CHRF** were from the same manufacturer (Kulzer). The shrinkage of **CHR** was higher than **CHRF**. On the other hand, **CHRF** was more affected by temperature rise than **CHR**. **SOL** also from the same manufacturer has the highest shrinkage (2.7 % at 23°C and 3.5 % at 37°C). **P50** was found to have lower shrinkage than **Z100** (both from 3M Dental Products). On the other hand **Z100** was less affected by temperature rise than **P50**.

Resin-composites placed in dental cavities incrementally will rise in temperature towards 37°C at a rate normally general by their thermal diffusivity. Typically this temperature rise can take about 1-2 minutes. Hence the materials may be irradiated clinically at temperatures

anywhere between 23 – 37 °C. If the resin composites were pre-refrigerated, the temperature could stay close to or even below 23 °C.

In fabrication of composite inlays by direct or indirect procedures, shrinkage may be occurring at temperatures in excess of 37 °C. The post-curing temperature causes an additional polymerisation and increases in strength and conversion of double bonds (Cook and Johnasson, 1987). Viadyanathan and Viadyanathan (1991) suggested that preheating resin-composites to 40°C - 60°C improved degree of conversion.

The results in this study showed that the polymerisation shrinkage-strain of the investigated resin composites increased with elevated temperature to 37°C. Our findings were in agreement with the results of El-Hejazi (1995) who studied 5 VLC resin composites with four different temperatures (23, 37, 45, and 60°C). The highest shrinkage was found with 60°C for all investigated materials.

7.6 Conclusions

- The polymerisation shrinkage-strain of the resin composites varies with the use of different light sources. So, **Z100** and **CHR** have slightly lower polymerisation shrinkage-strain with the XL3000 than with the more intense Elipar unit.

- Soft-start polymerisation did not result in any significantly different final equilibrium shrinkage-strain from those specimens which cured with full light intensity.

- There was a delay of initiation of appreciable shrinkage-strain of the resin composites for the first 10 s with soft-start polymerisation.

- In the absence of "soft-start" effects, polymerisation shrinkage-strain increases linearly for the first 1 min followed by a gradual increase to the final shrinkage.

- The polymerisation shrinkage-strain significantly increased with rise in ambient temperature from 23 to 37 °C.

Chapter 8

Polymerisation Shrinkage-Stress Measurement: Method Development and Evaluation of "Soft-Start" Light Irradiation Effects

8.1 Literature Review

Polymerisation shrinkage strain may generate shrinkage stresses during setting, Whenever there is also adhesion of light-cured and chemically cured resin composites to dentine (Davidson *et al.*, 1984). These stresses at the tooth-restoration interface tend to pull the resin away from the cavity walls (Rees and Jacobsen, 1992).

The polymerisation contraction strain has been shown in preceding chapters to be a time-dependent phenomenon and generally proceeds in two stages: pre-gelation and post-gelation (or rigid) contraction (Bausch, *et al.*, 1982). Plastic flow may occur during the earlier phase such that internal stresses within the material undergo stress-relaxation (Davidson and deGee, 1984).

Light-cured resin composites undergo an immediate and rapid polymerisation reaction that permits less resin flow than chemically cured resin composites, because they do not exist in a gel stage for very long (Carvalho *et al.*, 1996). However, at the gel point and beyond, the material develops stiffness reflected in the modulus of elasticity. As the material continues to polymerise, the contraction places stresses within the composite-tooth bond which in turn are distributed into the surrounding tooth structure. After gelation, flow is unable to compensate for contraction stresses (Davidson and deGee, 1984; Feilzer, *et al.*, 1987).

These inevitable stresses depend primarily on the material's composition such as type of resin matrix, proportion of filler, stiffness and flow of the composite, and rate of

polymerisation (Braem *et al.*, 1986). The magnitude of the polymerisation shrinkage stress is also influenced by the volume of the material to be polymerised and the geometry of the restoration (Ciucchi *et al.*, 1997).

The development of the elastic modulus is influenced by the light intensity, and this probably represents the most important factor controlling shrinkage stress (Unterbrink and Muessner 1995). Beginning polymerisation with a reduced light intensity allows for increased flow of the material and a concomitant relaxation of polymerisation contraction stress (Uno and Asmussen 1991). These authors also reported that no loss in bonding strength or diametral compressive strength was observed. Ernst *et al.*, (1997); and Algera *et al.*, (1998) concluded that using the two-step polymerisation mode (10 s low light intensity followed by 30 s high light intensity) seems to be able to significantly reduce the polymerisation stress in resin composites.

Alster *et al.*, (1997) found that the curing stress and the curing stress development rate decreased as the layer thickness of cylindrical resin composite samples increased.

The result of the stresses can lead to bond failure and gap formation between the tooth and restoration and may be accompanied by postoperative sensitivity due to cuspal movement toward the long axis of the tooth (Eick and Welch, 1986), deformation of the surrounding tooth structure (Donly *et al.*, 1987; Morin *et al.*, 1988; Sheth *et al.*, 1988); and micro-cracks in the cervical enamel (Bowen *et al.*, 1983, Bausch *et al.*, 1982).

Shrinkage stress may be counteracted by adhesion to tooth substance. Adhesion to enamel is sufficient to withstand these forces, but the shrinkage stress is dissipated by causing movement of the cusps (Jensen and Chan 1985; Pearson and Hegarty, 1989).

Several studies demonstrated that the cusps of molars and premolars are deflected inward after placement of class II resin composite restorative materials (Pearson and Hegarty 1987, 1989; Suliman *et al.*, 1993a & b, 1994; Meredith and Setchell 1997). Causton *et al.*, (1989) reported that the placement of bonded composite restorations in extracted

polymerisation (Braem *et al.*, 1986). The magnitude of the polymerisation shrinkage stress is also influenced by the volume of the material to be polymerised and the geometry of the restoration (Ciucchi *et al.*, 1997).

The development of the elastic modulus is influenced by the light intensity, and this probably representing the most important factor towards alteration of shrinkage stress (Unterbrink and Muessner 1995). Beginning polymerisation with a reduced light intensity allows for increased flow of the material and a concomitant relaxation of polymerisation contraction stress (Uno and Asmussen 1991). These authors also reported that no loss in bonding strength or diametral compressive strength was observed. Ernst *et al.*, (1997); and Algera *et al.*, (1998) concluded that using the two-step polymerisation mode (10 s low light intensity followed by 30 s high light intensity) seems to be able significantly reduce the polymerisation stress in resin composites.

Alster *et al.*, (1997) found that the curing stress and the curing stress development rate decreased as the layer thickness of cylindrical resin composite samples increased.

The result of the stresses can lead to bond failure and gap formation between the tooth and restoration and may be accompanied by postoperative sensitivity due to cuspal movement toward the long axis of the tooth (Eick and Welch, 1986), deformation of the surrounding tooth structure (Donly *et al.*, 1987; Morin *et al.*, 1988; Sheth *et al.*, 1988); and micro-cracks in the cervical enamel (Bowen *et al.*, 1983, Bausch *et al.*, 1982).

Shrinkage stress may be counteracted by adhesion to tooth substance. Adhesion to enamel is sufficient to withstand these forces, but the shrinkage stress is dissipated by causing movement of the cusps (Jensen and Chan 1985; Pearson and Hegarty, 1989).

Several studies demonstrated that the cusps of molars and premolars are deflected inward after placement of class II resin composite restorative materials (Pearson and Hegarty 1987, 1989; Suliman *et al.*, 1993a & b, 1994; Meredith and Setchell 1997). Causton *et al.*, (1989) reported that the placement of bonded composite restorations in extracted

teeth resulted in a decrease in the distance between cusps measured using a dial gauge. They concluded that this was as a result of the polymerisation shrinkage stress that had occurred. Pearson and Hegarty (1987 and 1989) measured the cusp displacement of molar teeth and concluded that both cusps were either moving towards each other, moving in the same direction or with little or no movement of one cusp. Suliman *et al.*, (1993a&b, 1994) studied cuspal movement following placement of composite restorations and concluded that a degree of recovery was attributed to hydration of the teeth and water sorption of resin composite material. Jensen and Chan (1985) measured the influence of polymerisation shrinkage on cusp strain by using strain gauges. They reported that the cusp strain was reduced by an incremental technique. Meredith and Setchell (1997) measured the cuspal strain and displacement with resin composites. They concluded that the *in vitro* restoration of posterior teeth with a bonded composite material generates polymerisation stresses which can be recorded as tensile strains and displacements on the tooth surface. They also found that the strains measured during composite placement were greater when the remaining cusp width was less.

Various ways to relieve stress, include the design of the restorations, application of liners (Kemp-Scholte and Davidson 1990; Davidson and Feilzer 1997). Slowing down the polymerisation reaction causes less damage at the interface of restoration and cavity (Uno and Asmussen 1991; Feilzer *et al.,* 1995a; Unterbrink and Muessner 1995). The use an incremental technique for resin composite insertion in the cavity (Lutz *et al.*, 1986; Carvalho *et al.*, 1996). Stress relaxation through composite hydration is evident (Feilzer *et al.*, 1990) but this may occurs over a long period of time (Davidson and deGee, 1984; Sakaguchi *et al.*, 1992).

Stress inside and around the restoration can be relieved rapidly by the deformation of the cavity walls around the restorative material (Morin *et al.*, 1984; Suliman, *et al.*, 1994). It can also be reduced by different failure mechanisms, cohesive inside the material or the tooth, or adhesive at the interface, thus leading to the formation of gap between the material and cavity wall (Fusayama, 1987; Ciucchi, *et al.*, 1997).

8.2 Objectives

The objectives of this part of the present work were

1. To analyse the response of a new measurement instrument, for determining stress-kinetics and to evaluate the overall utility of the technique.

2. To present representative data on polymerisation shrinkage stress of the restorative resin composite materials during setting.

3. To study the effect of "soft-start" irradiation on the stress generated from polymerisation shrinkage of the resin based dental materials.

4. To determine whether the initial cure by low intensity followed by full intensity ("soft-start") reduces the final shrinkage stress of the resin composite restorative materials.

8.3 Materials and Methods

The materials investigated in this study are listed in Table 8-1. The Elipar unit was used for polymerisation.

Table 8.1: The materials investigated

Material	Code	Batch No.	Type	Manufacturer
Compolute	**CLA**	002	Luting Resin composite	Espé Dental AG, Seefeld, Germany
Pertac II	**PER2**	643081003	Restorative composite	
Z100	**Z100**	3021	Restorative composite	3M Dental Product-USA
Charisma F	**CHRF**	28	Restorative Composite	Heraeus Kulzer, Wehrheim, Germany
Solitaire	**SOL**	23	Restorative Composite	
Definite	**DEF**	201	Ormocer Composite	Degussa, Germany

8.3.1 Instrument Design

The apparatus (Fig 8-1) consisted of the following components:

8.3.1.1 Stress Apparatus

A custom-made cantilever load-cell was attached rigidly to a standard stainless steel base block (10 cm length, 5 cm width, 5 cm height). Two bolts were used to tighten the load beam cell to obtain maximum fixation of the rig from one end. The other end of the beam was left free. The capacity of the load beam cell was 500 kg. The shrinkage effects generated during the setting of the specimen allowed a minute compliance of the load beam cell toward the specimen. The load beam cell generates a signal which was read directly by a strain gauge indicator (Model 3800, Measurement Group, Reyleigh, NC, USA), and then by the computer. Data acquisition software was used for recording the signals (Bioman, Manchester, UK).

A split stainless steel clamp was attached to the free end of the beam cell to hold a round metal rod. The two halves of the clamps were closed together using four bolts. On the middle of the upper part of the clamp was a holder of into which an LVDT displacement transducer was placed to measure the compliance of the load cell.

The samples were placed between two surfaces: a rounded metal rod surface (10 mm diameter and 20 mm length) and a glass plate surface. These two surfaces were sand blasted to ensure optimal bond strength and retention with the investigated materials. The glass plate (3 mm thick) was held tight by a steel clamp (7.6 cm length, 3.7 cm width, 3.6 cm height) and a hollow cylindrical bolt (1.8 cm inner diameter, and 2.2 cm outer diameter). Specimen dishes of $\approx$ 1 mm thickness were studied.

The hollow cylindrical bolt was used to allow the insertion of light curing tip to the surface of the glass plate to polymerise the sample. The clamp for the glass plate was attached to the base of the stress instrument using two bolts.

8.3.1.2 Linear Variable Displacement Transducer (LVDT)

An aligned LVDT displacement transducer (type GT 2000, RDP Electronics, Wolverhampton, UK) was positioned in contact with the glass plate. The LVDT was connected to the top of the metal rod clamp by a further small clamp.

The stress beam load cell deflects slightly as the shrinkage stress takes place during the setting of the material, this deflection was monitored over time by the LVDT transducer which has a sensitivity greater than 0.1 μm. The LVDT was connected to a signal conditioning unit (type E307-3, RDP Electronics, Wolverhampton, UK) and a microcomputer transient-recorder and data logging system.

8.3.2 Calibration of Shrinkage-Stress Apparatus

This calibration was used to derive a calibration coefficient for the signal from the stress beam load cell. To calibrate the load beam cell, the instrument was stood vertically by

clamping. The two clamps were tightened at the free end of the load cell beam and the opposite end of the instrument was freed of superfluous parts to allow insertion of a long iron bar with rounded end to hold a series of 5 kg weights (Fig 8-2).

The loads were applied at known intervals while the beam output was recorded on the Strain Gauge Indicator, and then the data recorded in the computer. The voltage/load calibration factor was then calculated by linear regression. The calibration coefficient was used to convert the voltage signals to load in Newton, then to convert the collected data for the investigated materials to stress (MPa), by dividing by the area of the specimen disk in mm^2.

8.3.3 Calibration of LVDT

The calibration method of LVDT was explained previously in chapter 6.

8.3.4 Statistical Analysis

The difference between the results of the materials cured by full light intensity and soft-start were performed by using the paired sample t-Test.

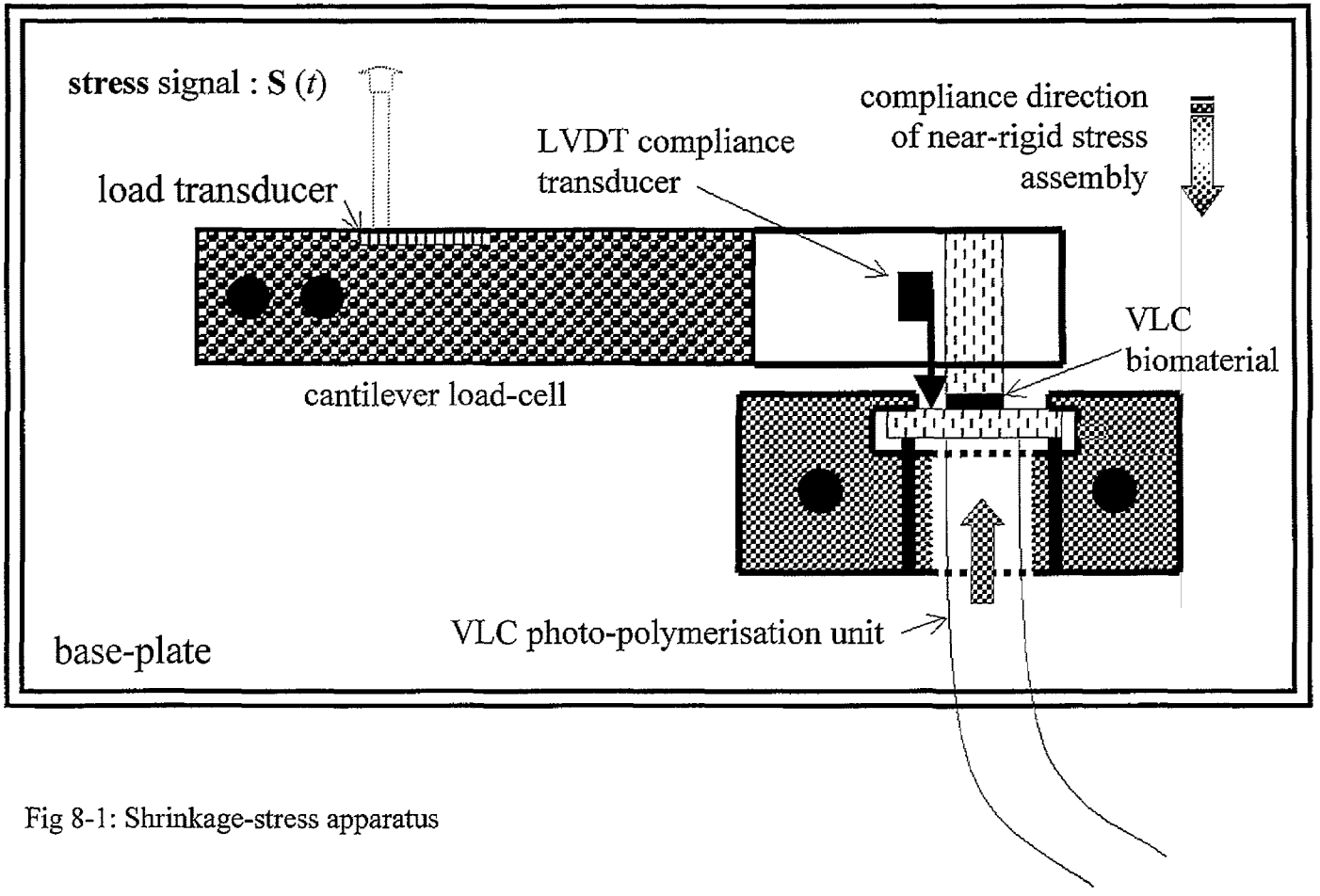

Fig 8-1: Shrinkage-stress apparatus

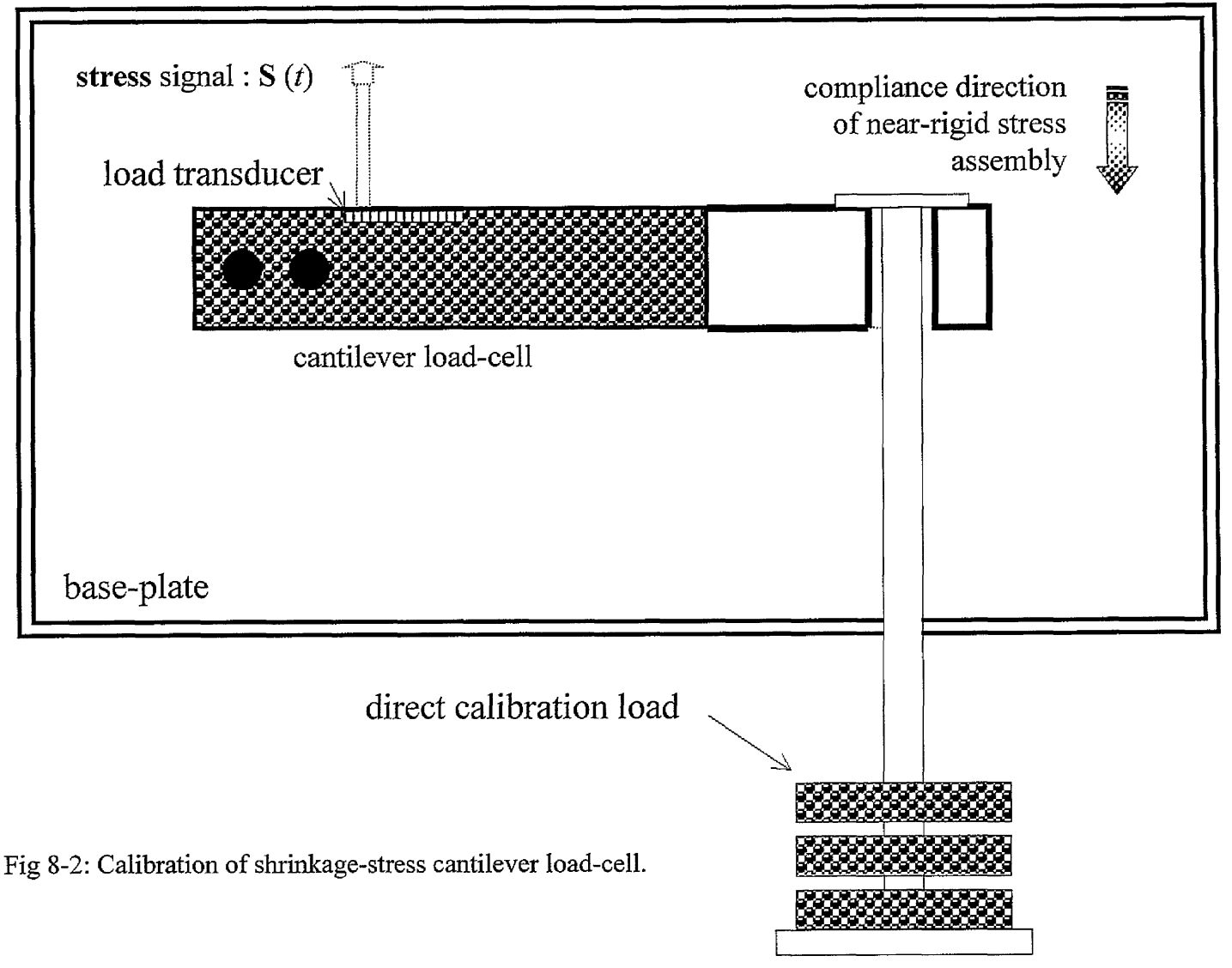

Fig 8-2: Calibration of shrinkage-stress cantilever load-cell.

8.4 Results

Polymerisation shrinkage stress was calculated from the given equation:

$$\textbf{Stress } (\sigma) = \mathbf{F/A}$$

where **F** is the force of the load cell during polymerisation process, and **A** is the cross sectional area of specimen. The area is given by

$$\textbf{Area of the specimen } (A) = \pi . \mathbf{r}^2$$

where **r** is the radius of the specimen.

8.4.1 Load and Stress Data Correction

In this assembly, the 'raw' stress data are decreased if the compliance of the system was large. Rather than correcting to zero compliance, the clinically relevant level of system (tooth) compliance was used as a standard.

The stress data were corrected using a Correction Factor (CF). CF was obtained from the compliance of the shrinkage stress rig measured with each measurement run. The compliance was obtained from the LVDT unit, which was used to monitor the movement of the shrinkage stress beam.

$$\text{Correction Factor (CF)} = \frac{\text{compliance value } (\Delta Z)}{\text{permitted compliance } (\Delta Z_p)}$$

The compliance values were obtained from the displacement of the LVDT, which measured the movement of the load cell beam of the shrinkage stress device, for each material. The *permitted* compliance was set as the basis of the magnitudes of cuspal compliances observed clinically for a comparable geometry. Therefore, the *permitted*

compliance (ΔZ_p) = 3 μm. The mean values of the compliance (ΔZ) of the beam load cell due to the shrinkage stress of the restorative materials and CF are demonstrated in Table 8.2 and the full details of data presented in Appendix VI in CD. Two examples of the compliance of the beam load cell with full intensity and soft-start polymerisation are plotted graphically in Figs 8-3 and 8-4. The mean of the five specimen data sets was chosen from each material tested.

Table 8-2: Mean values of the **Compliance** (ΔZ) of the load beam cell due to the shrinkage stress of the restorative materials and **Correction Factors (CF)**

Materials	Full intensity		Soft-start	
	ΔZ	CF	ΔZ	CF
CLA	11.34	3.78	11.07	3.69
PER2	18.86	6.29	19.57	6.52
Z100	13.68	4.56	11.91	3.97
CHRF	13.13	4.38	12.39	4.13
SOL	17.38	5.79	17.09	5.70
DEF	12.44	4.15	12.19	4.06

The averaged values and standard deviation of shrinkage-stress of each material were collected for time intervals, 5, 10, 20, 30, 40, 60, 300 and 480 seconds. The data before and after correction are presented in Tables 8-3 to 8-6. The full data are presented in Appendix VI in CD.

The measured shrinkage stresses, after correction, as a function of time dependence of the materials investigated are shown in Figures 8-5 to 8-16.

CLA material is luting cement, which had the lowest shrinkage-stress with both cure modes. **PER2** had the highest shrinkage-stress recorded at the maximum time for specimens cured by both full intensity and soft-start, 12.98 and 12.04 MPa respectively. **Z100** and **DEF** have rapid stress generation in the first 5 sec with specimens cured by full intensity light, but the maximum shrinkage-stress obtained was lower than for **PER2** and

SOL. In the first 5 sec, **CHRF** had more rapid stress generation than **SOL**, while the maximum shrinkage-stress at the final time was lower than **SOL**.

Full intensity light had a greater stress effect than soft-start polymerisation with **CLA**, **Z100** and **CHRF** materials. The differences in this effect were statistically significant ($p < 0.05$). On the other hand this effect was not statistically significant ($p > 0.05$) with **PER2**, **SOL** and **DEF** materials (Table 8.7).

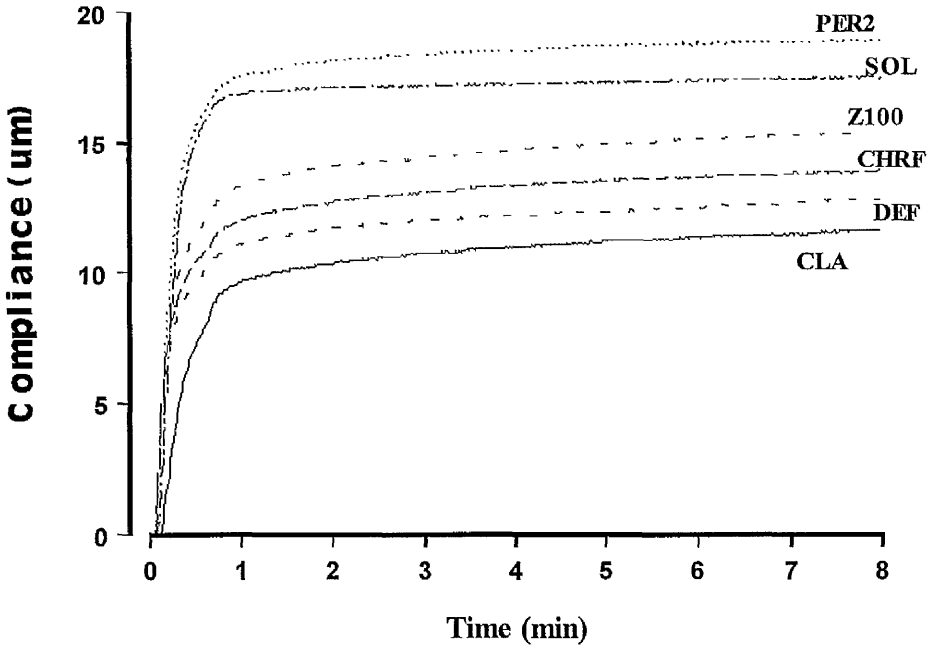

Fig 8-3: Compliance (μm) of cantilever load-cell with **full intensity**.

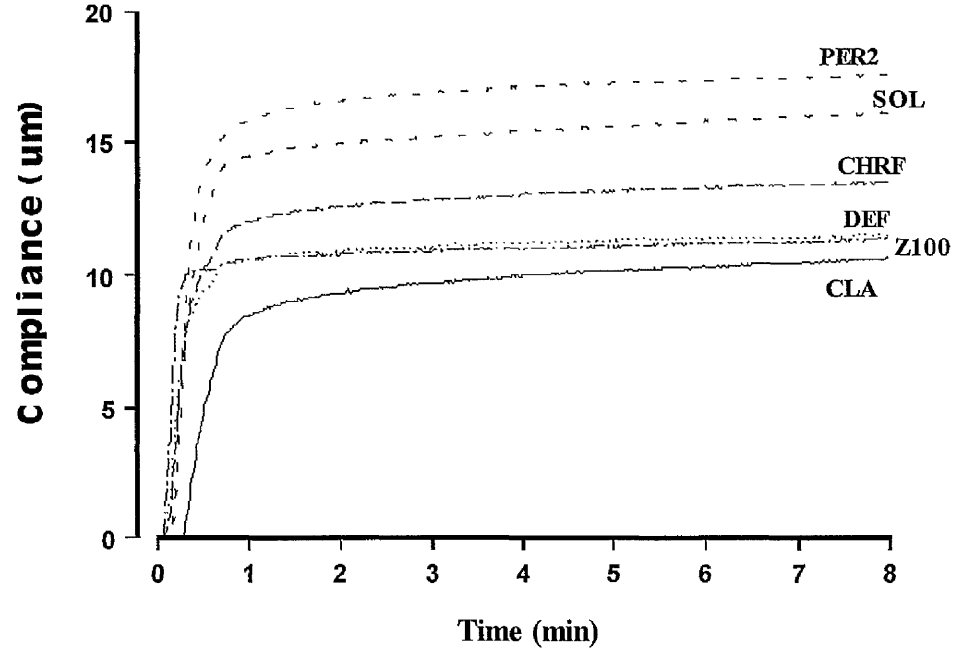

Fig 8-4: Compliance (μm) of cantilever load-cell with **"soft-start"** polymerisation.

(A)

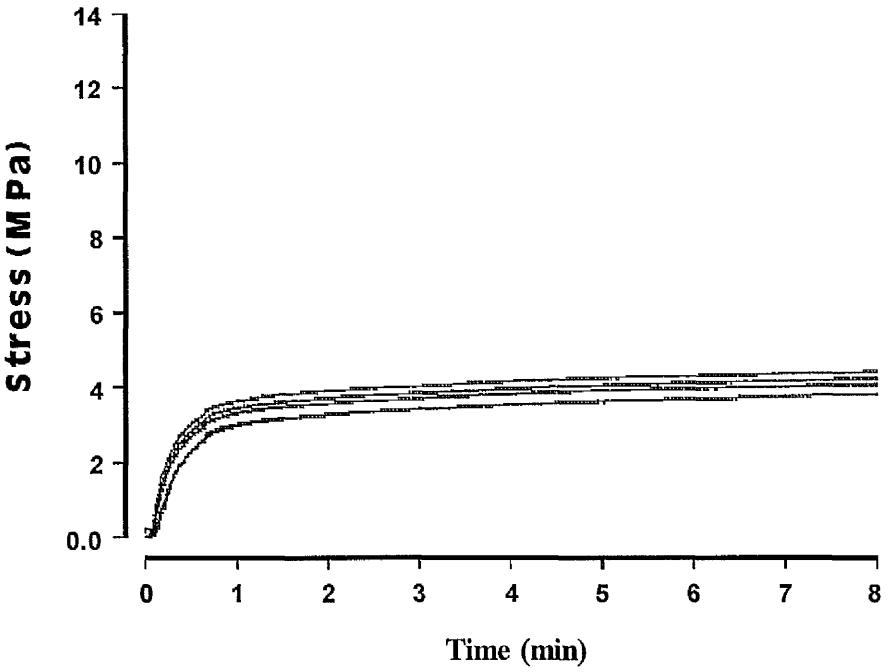

(B)

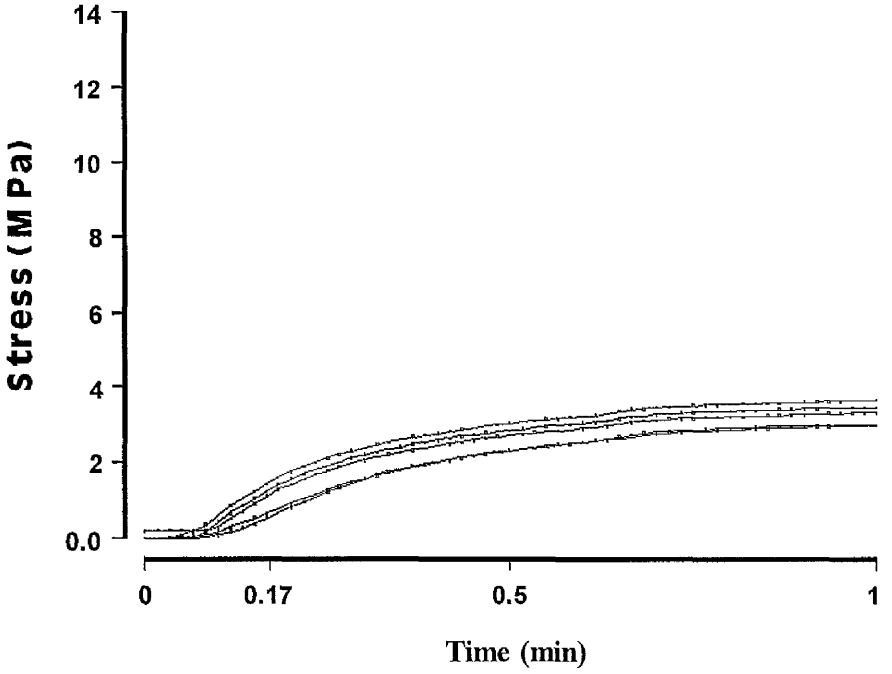

Fig 8-5: Shrinkage-stress of **CLA**, with **full intensity** polymerisation. (A) full scale and (B) expanded scale for 1 min.

(A)

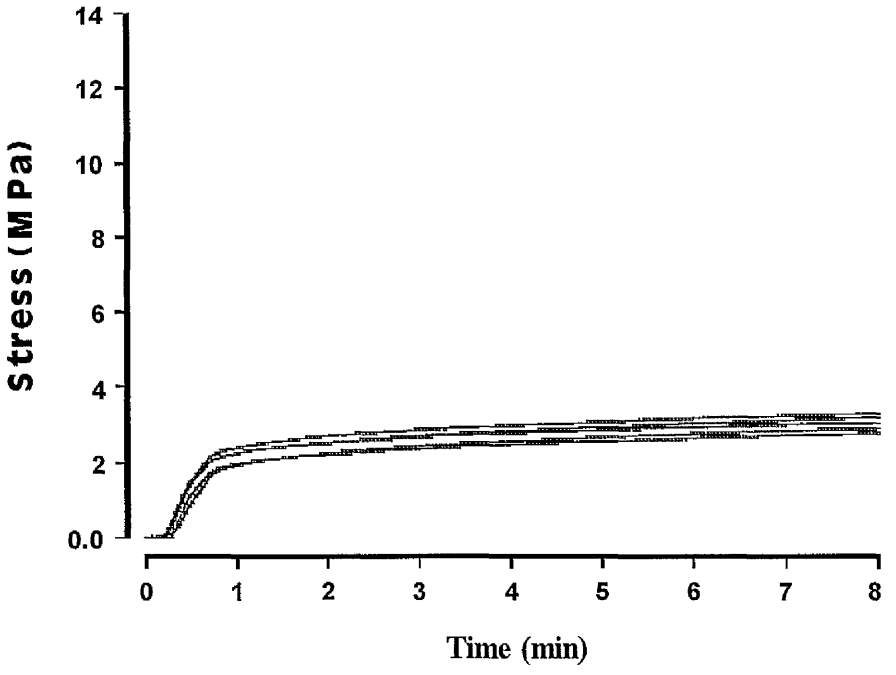

(B)

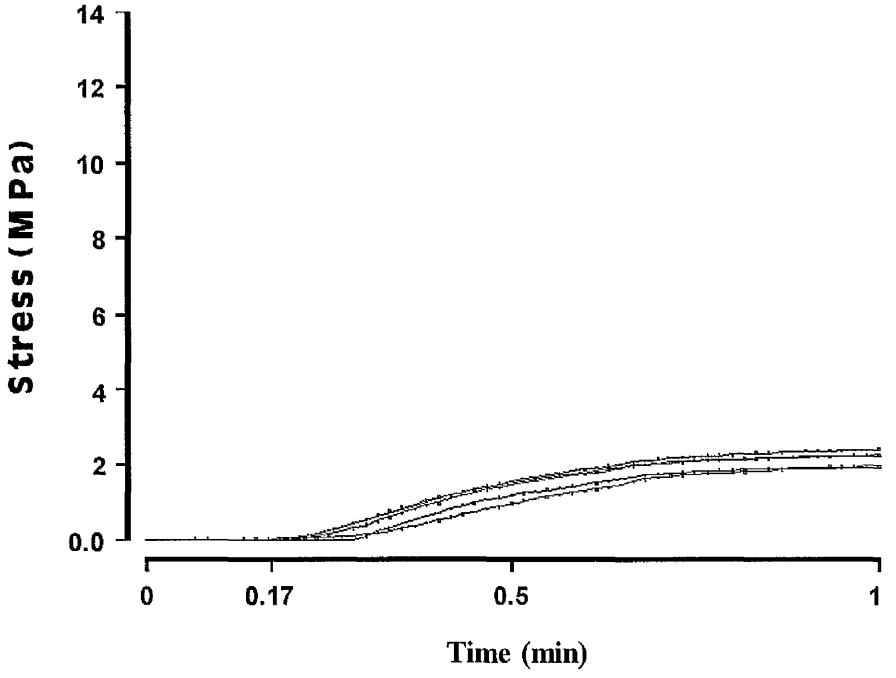

Fig 8-6: Shrinkage-stress of **CLA**, with **soft-start** polymerisation. (A) full scale and (B) expanded scale for 1 min.

(A)

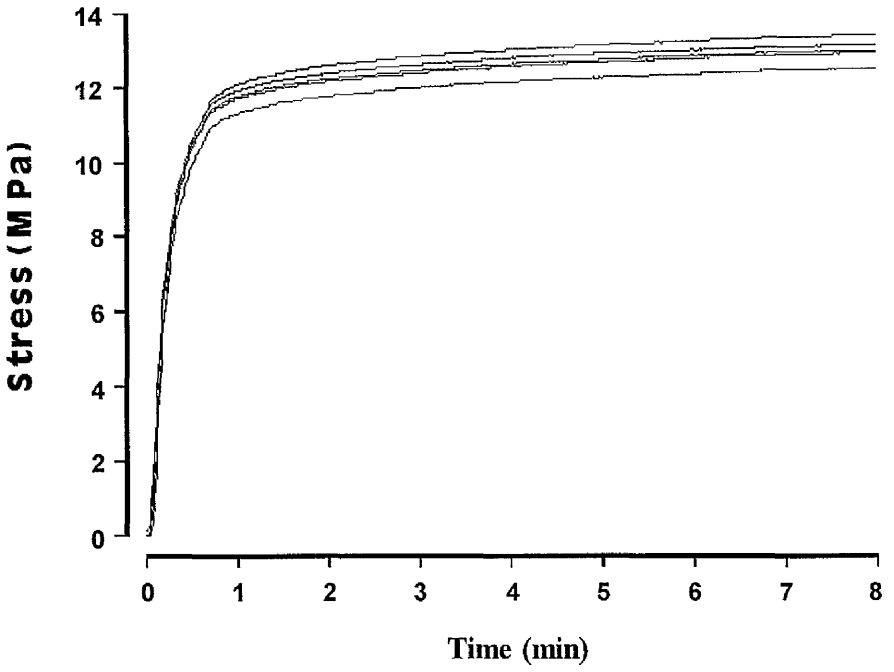

(B)

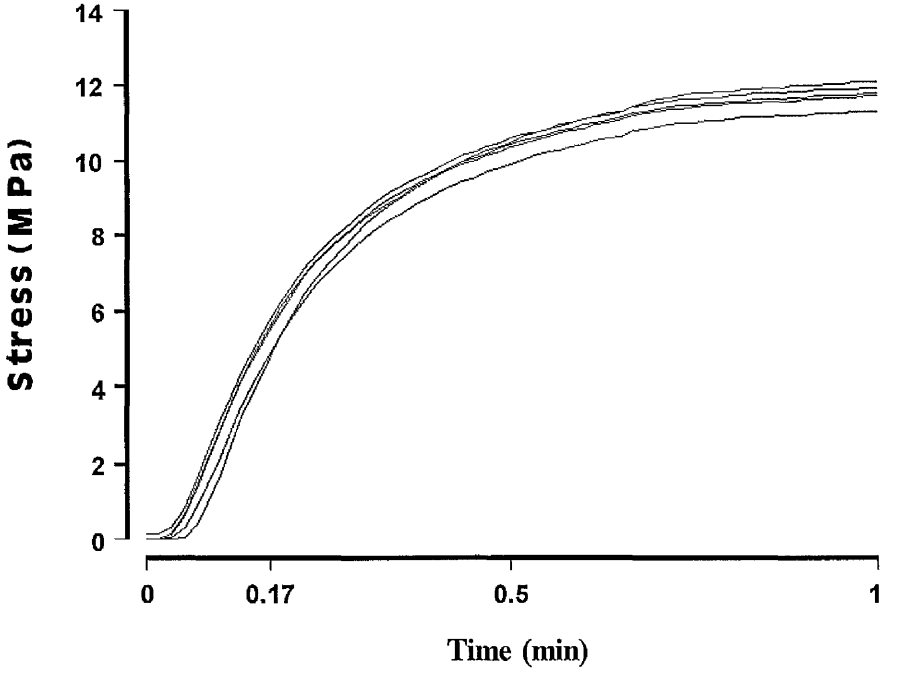

Fig 8-7: Shrinkage-stress of **PER2** with **full intensity** polymerisation. (A) full scale and (B) expanded scale for 1 min.

(A)

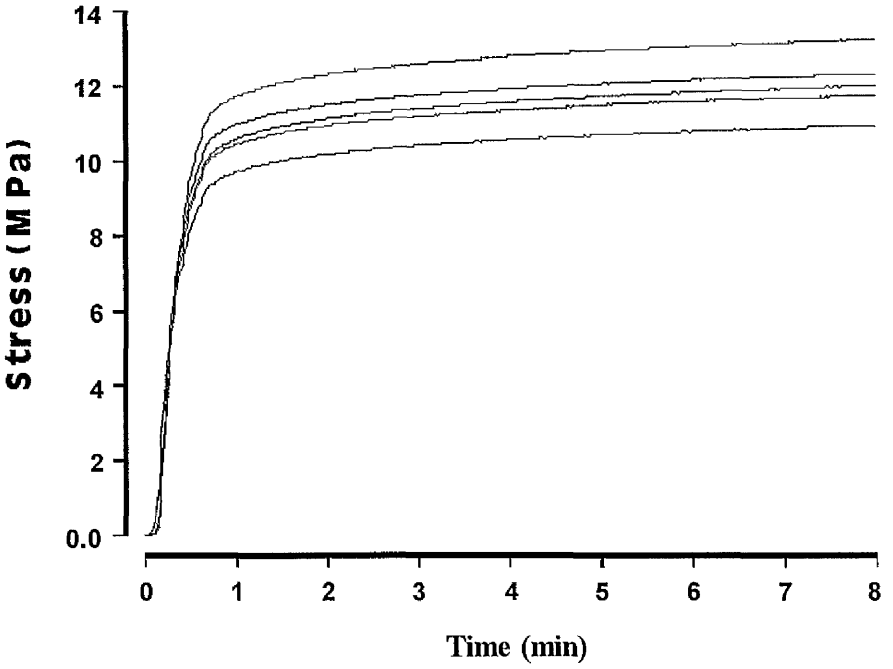

(B)

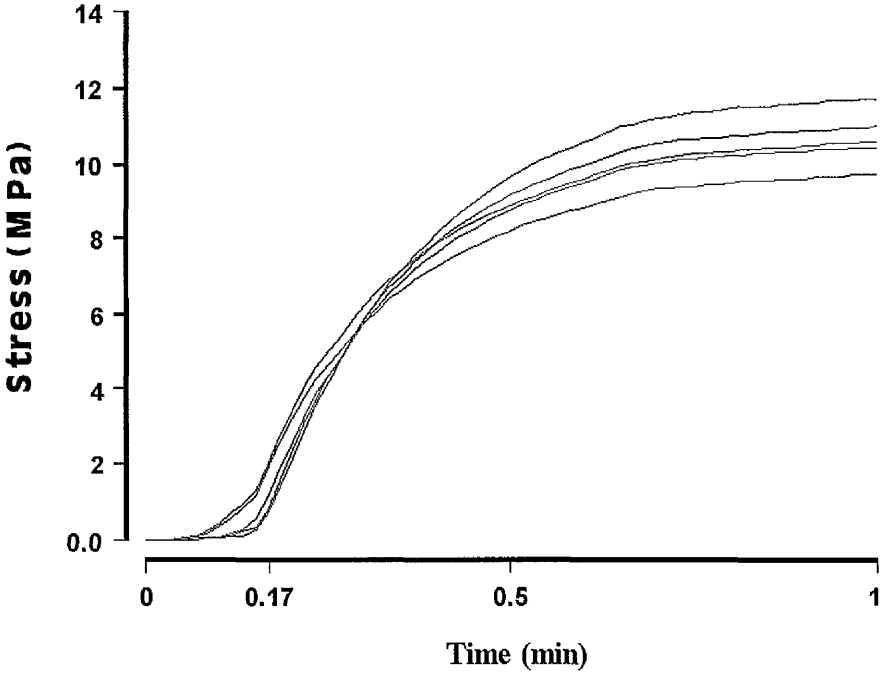

Fig 8-8: Shrinkage-stress of **PER2** with **soft-start** polymerisation. (A) full scale and (B) expanded scale for 1 min.

(A)

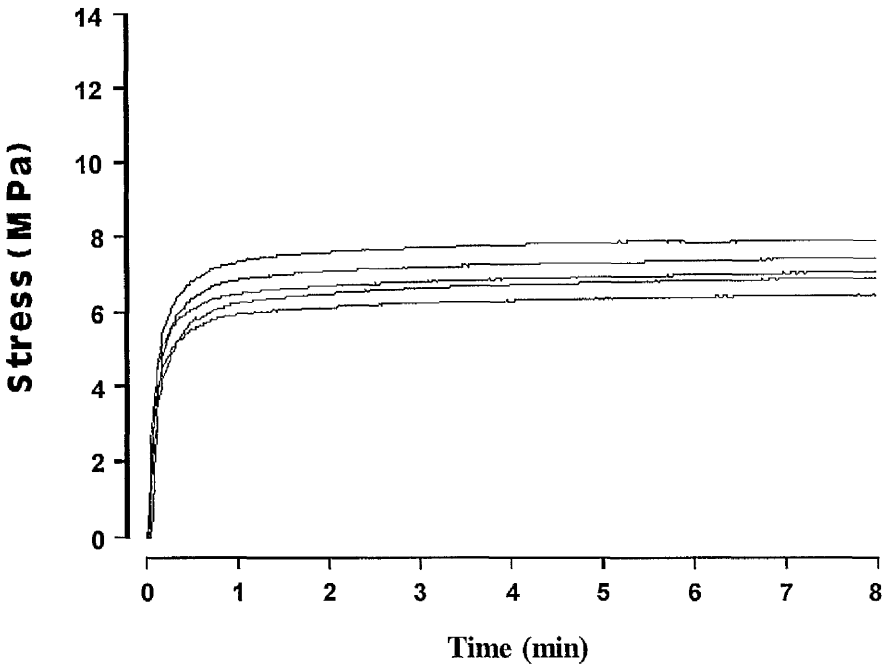

(B)

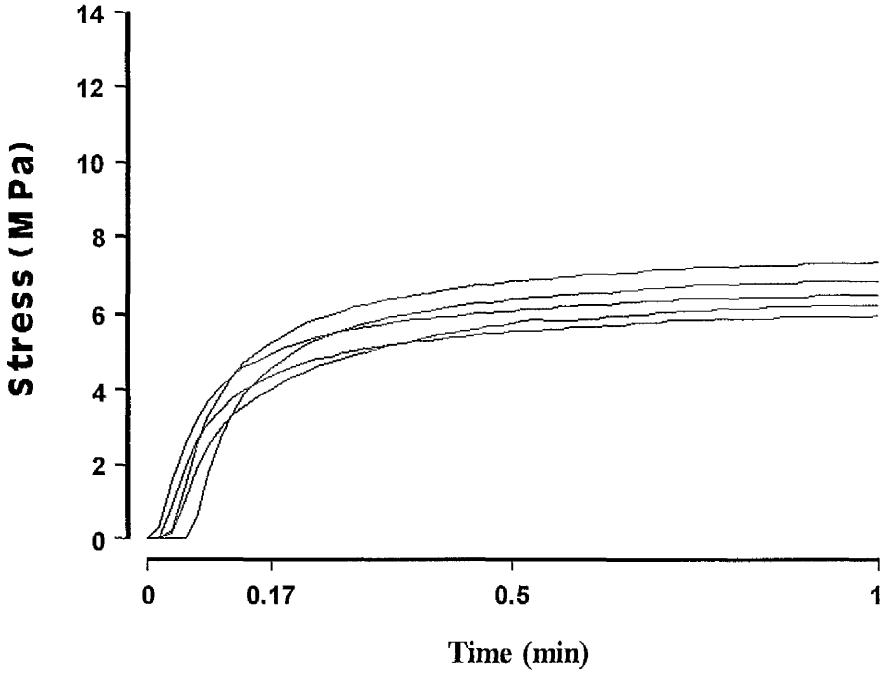

Fig 8-9: Shrinkage-stress of **Z100** with **full intensity** polymerisation. (A) full scale and (B) expanded scale for 1 min.

(A)

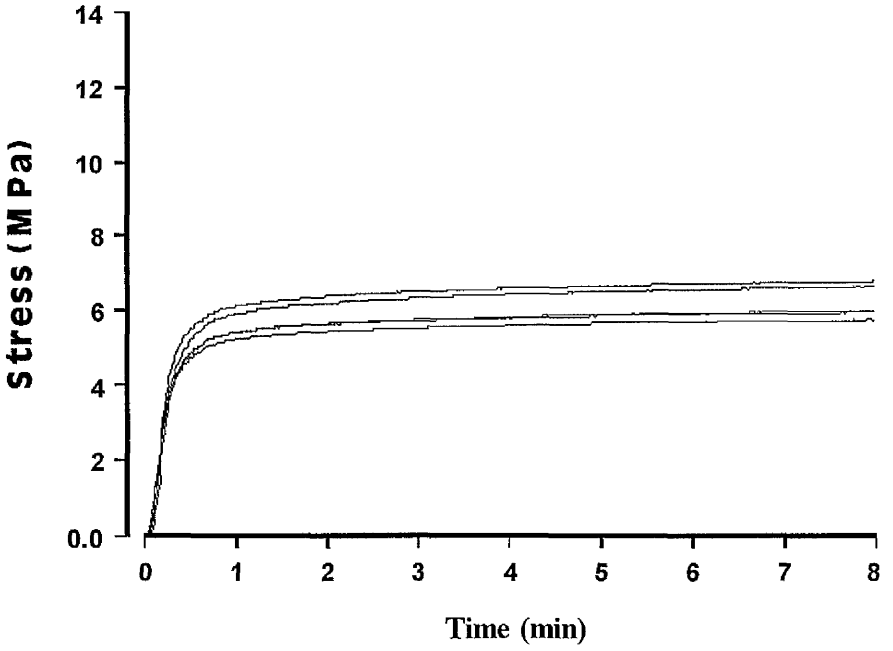

(B)

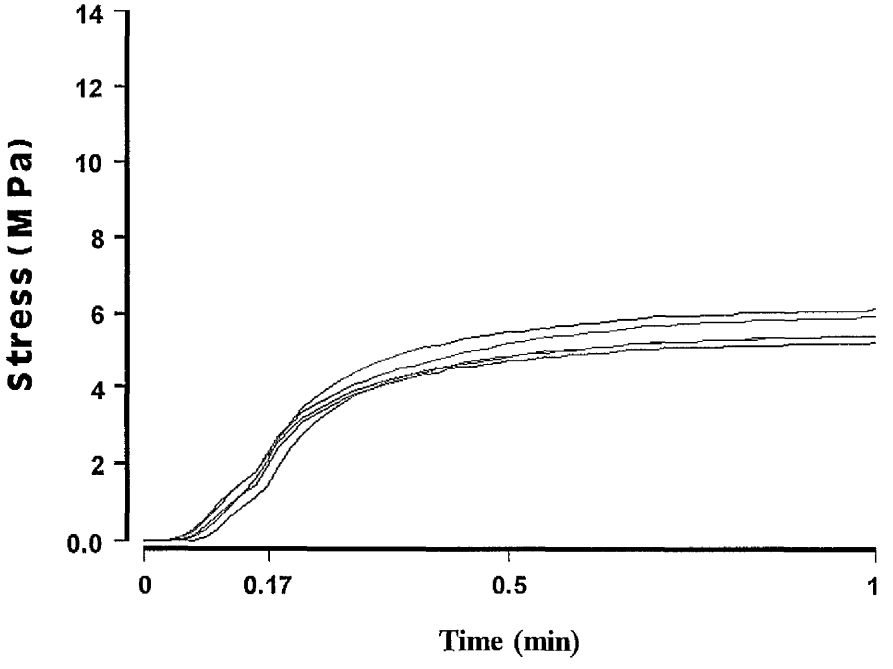

Fig 8-10: Shrinkage-stress of **Z100** with **soft-start** polymerisation. (A) full scale and (B) expanded scale for 1 min.

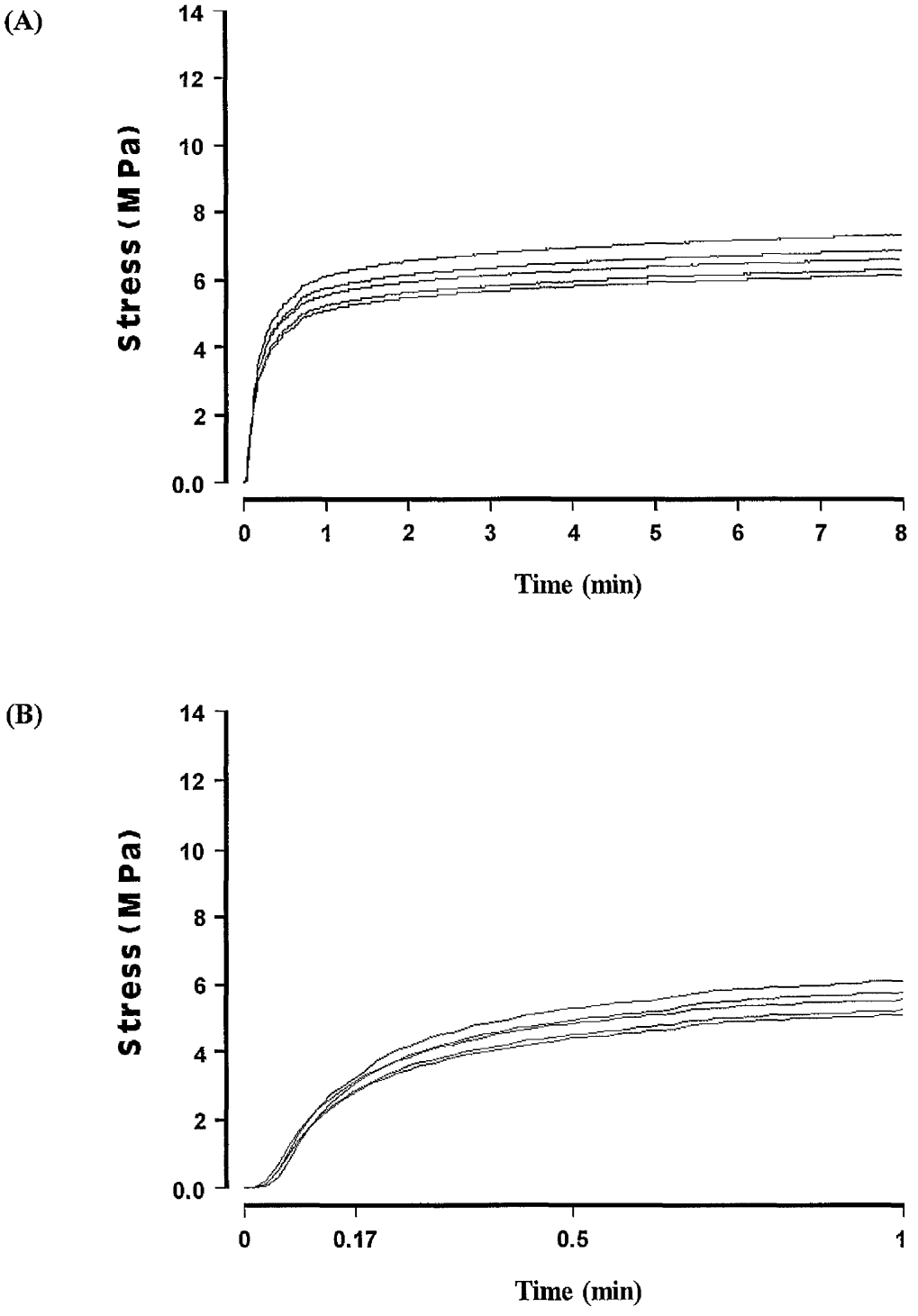

Fig 8-11: Shrinkage-stress of **CHRF**, with **full intensity** polymerisation. (A) full scale and (B) expanded scale for 1 min.

(A)

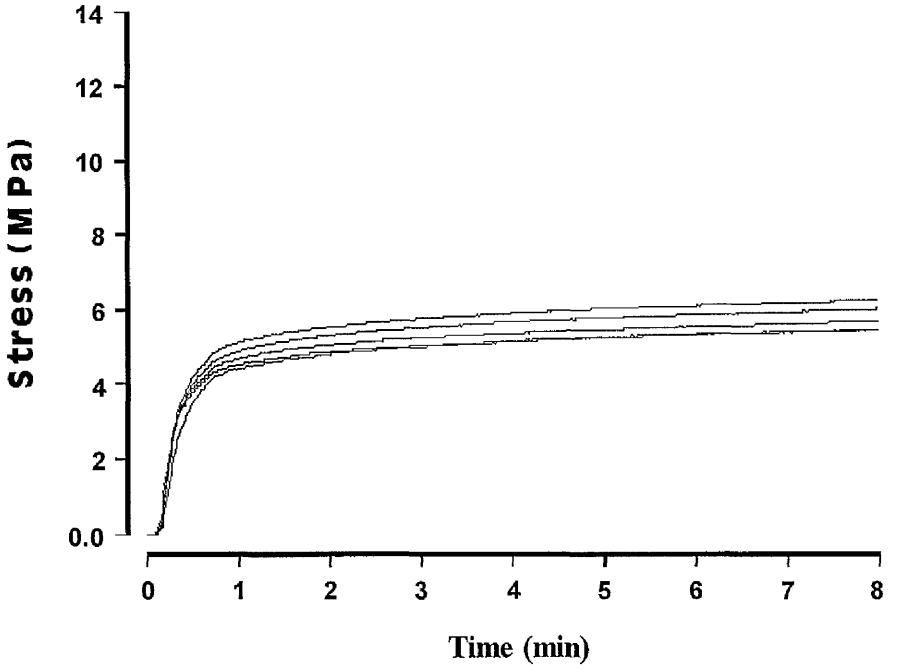

(B)

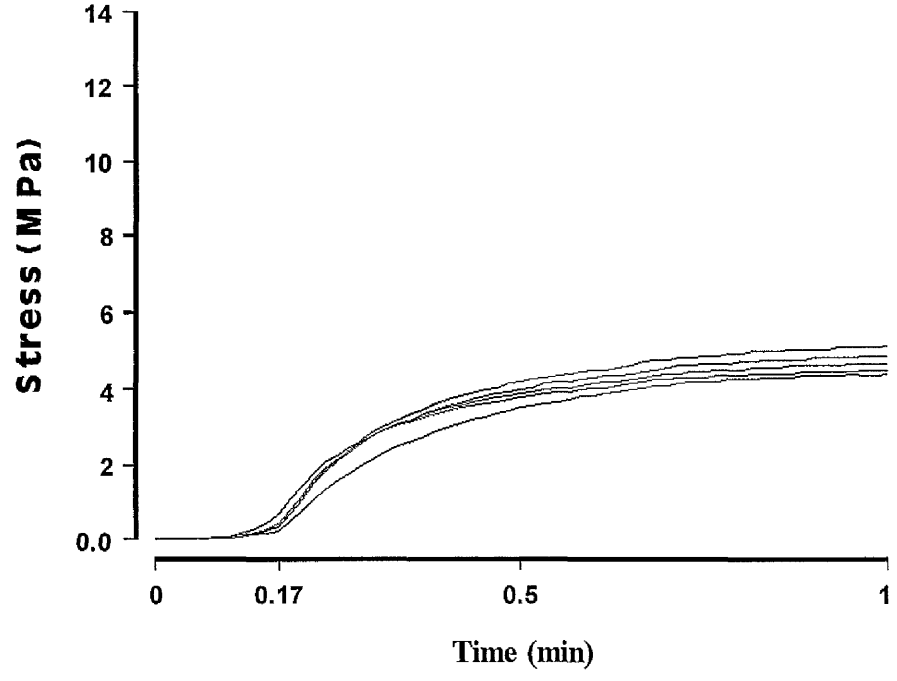

Fig 8-12: Shrinkage-stress of **CHRF**, with **soft-start** polymerisation. (A) full scale and (B) expanded scale for 1 min.

(A)

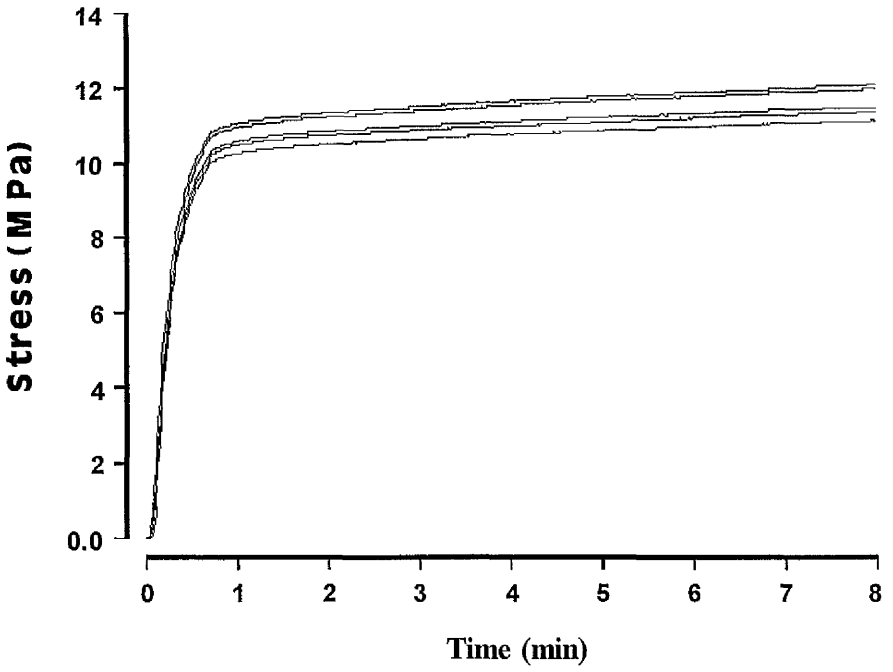

(B)

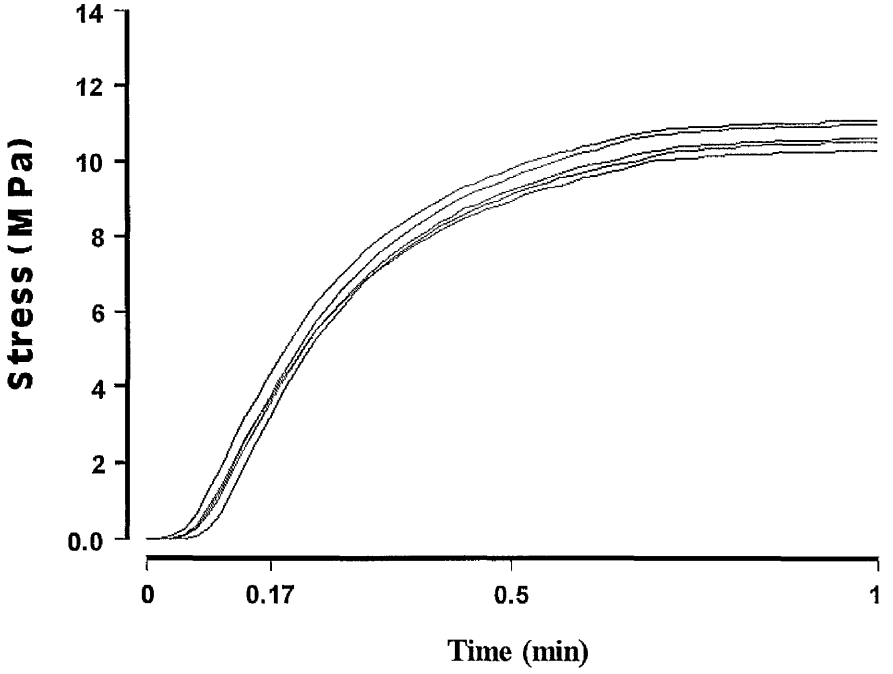

Fig 8-13: Shrinkage-stress of **SOL**, with **full intensity** polymerisation. (A) full scale and (B) expanded scale for 1 min.

(A)

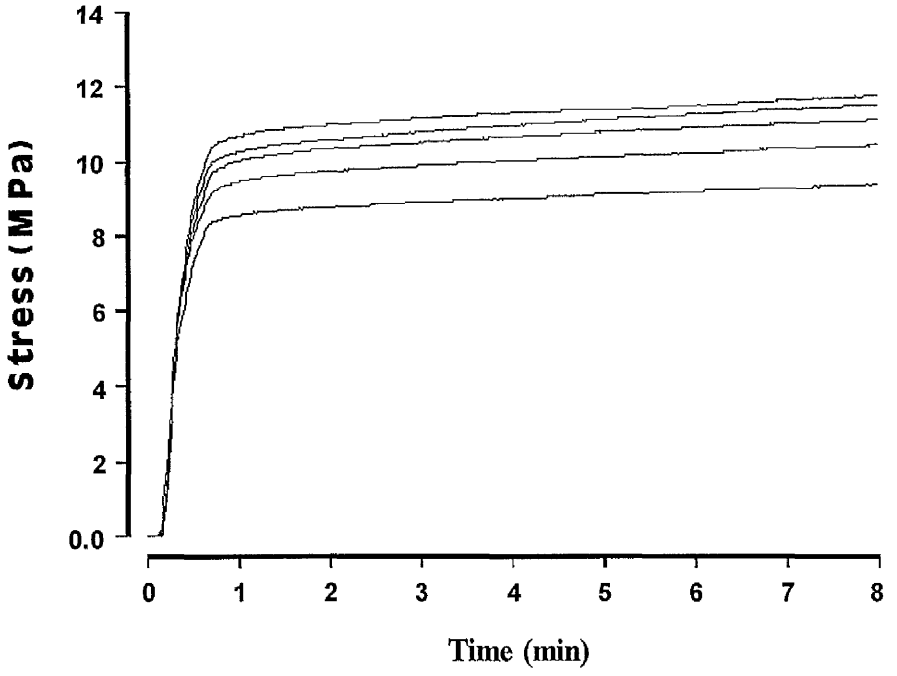

(B)

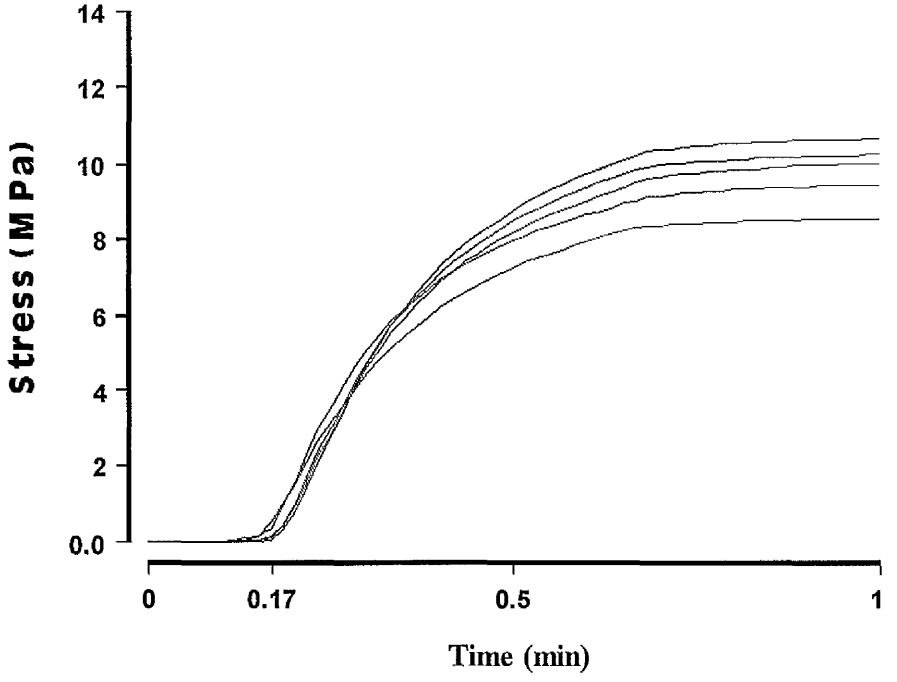

Fig 8-14: Shrinkage-stress of **SOL** with **soft-start** polymerisation. (A) full scale and (B) expanded scale for 1 min.

(A)

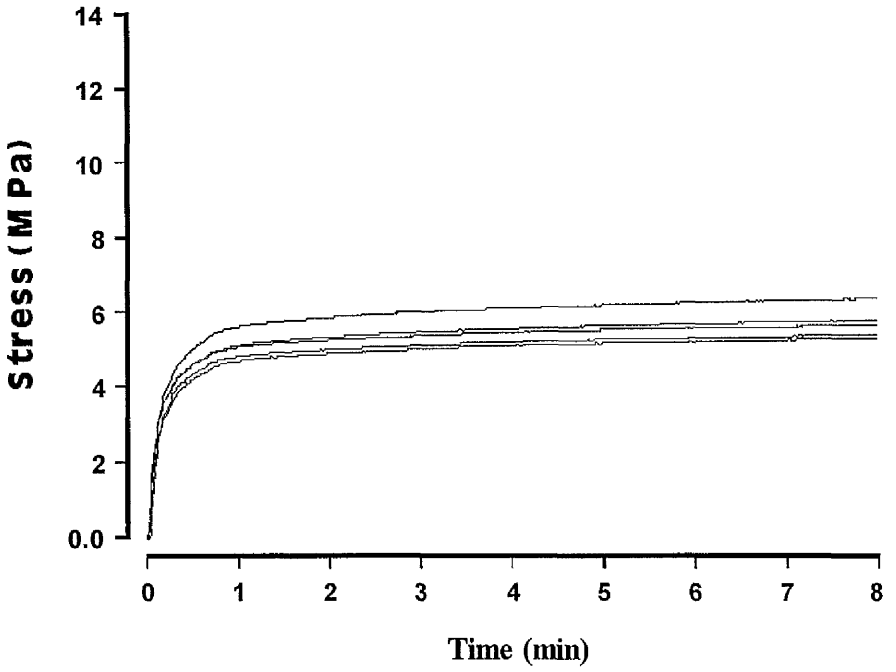

(B)

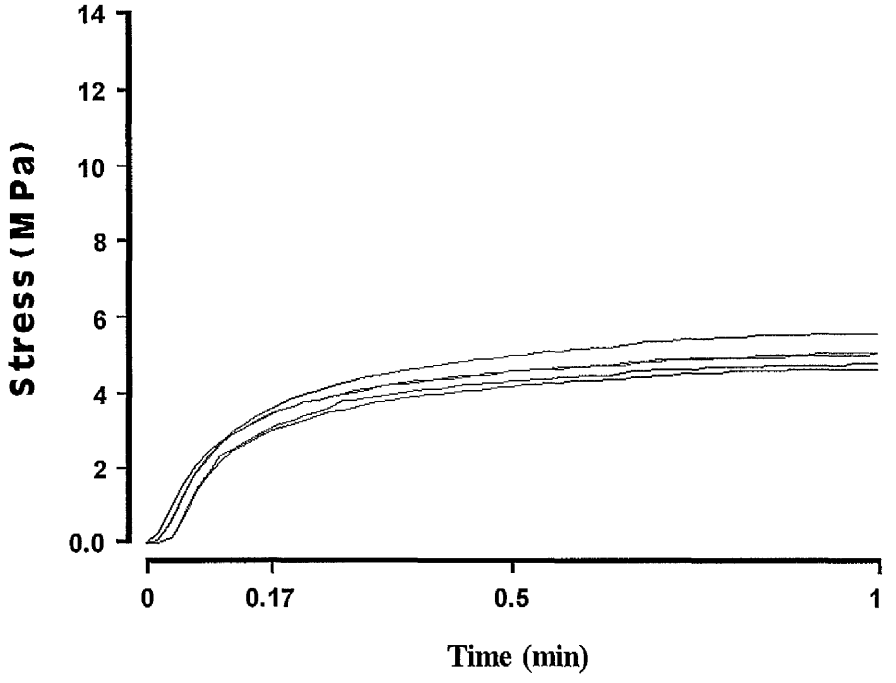

Fig 8-15: Shrinkage-stress of **DEF** with **full intensity** polymerisation. (A) full scale and (B) expanded scale for 1 min.

(A)

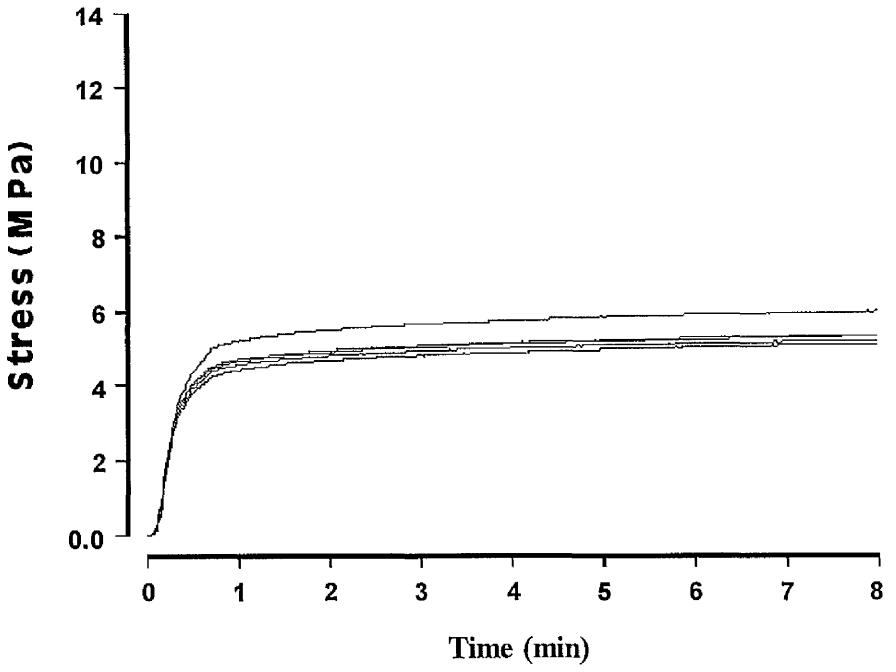

(B)

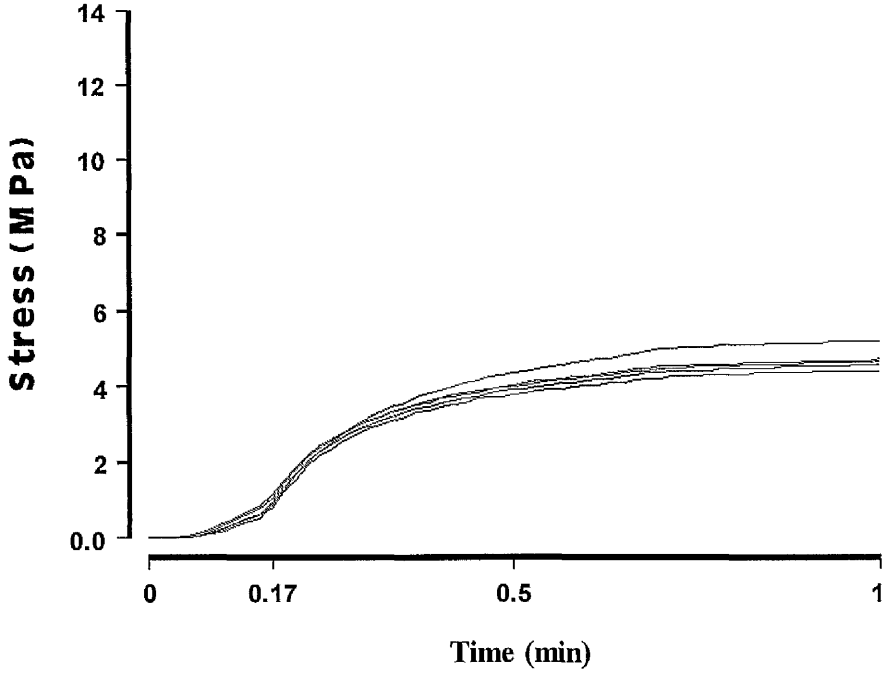

Fig 8-16: Shrinkage-stress of **DEF** with **soft-start** polymerisation. (A) full scale and (B) expanded scale for 1 min.

Table 8-3: Mean values and SD (in parentheses) of shrinkage-stress (MPa) **before correction.** The materials cured by **full intensity.**

Material	Time (sec)							
	5	**10**	**20**	**30**	**40**	**60**	**300**	**480**
CLA	0.05 (0.03)	0.26 (0.1)	0.56 (0.09)	0.69 (0.09)	0.79 (0.08)	0.87 (0.07)	1.03 (0.07)	1.08 (0.07)
PER2	0.28 (0.04)	0.83 (0.07)	1.40 (0.04)	1.64 (0.04)	1.78 (0.04)	1.87 (0.05)	2.02 (0.05)	2.06 (0.05)
Z100	0.63 (0.17)	1.01 (0.11)	1.24 (0.11)	1.34 (0.11)	1.39 (0.12)	1.44 (0.12)	1.55 (0.13)	1.57 (0.12)
CHRF	0.34 (0.04)	0.68 (0.04)	0.97 (0.07)	1.09 (0.08)	1.17 (0.08)	1.26 (0.09)	1.46 (0.10)	1.51 (0.11)
SOL	0.13 (0.06)	0.63 (0.07)	1.32 (0.06)	1.61 (0.06)	1.77 (0.06)	1.84 (0.06)	1.95 (0.06)	2.00 (0.07)
DEF	0.51 (0.07)	0.80 (0.06)	1.004 (0.07)	1.10 (0.08)	1.16 (0.08)	1.22 (0.08)	1.34 (0.1)	1.37 (0.1)

Table 8-4: Mean values and SD of shrinkage-stress (MPa) **after correction.** The materials cured by **full intensity.**

Material	Time (sec)							
	5	**10**	**20**	**30**	**40**	**60**	**300**	**480**
CLA	0.20 (0.13)	0.98 (0.38)	2.11 (0.36)	2.62 (0.32)	2.99 (0.30)	3.28 (0.27)	3.88 (0.26)	4.07 (0.26)
PER2	1.79 (0.54)	5.25 (0.43)	8.83 (0.25)	10.34 (0.25)	11.20 (0.26)	11.76 (0.29)	12.73 (0.32)	12.98 (0.33)
Z100	2.87 (0.77)	4.61 (0.5)	5.67 (0.5)	6.11 (0.52)	6.33 (0.53)	6.58 (0.55)	7.05 (0.57)	7.15 (0.54)
CHRF	1.47 (0.15)	3.0 (0.19)	4.25 (0.3)	4.78 (0.40)	5.14 (0.4)	5.53 (0.41)	6.39 (0.5)	6.62 (0.5)
SOL	0.76 (0.34)	3.77 (0.64)	7.62 (0.33)	9.31 (0.35)	10.26 (0.35)	10.67 (0.33)	11.31 (0.37)	11.59 (0.41)
DEF	2.13 (0.3)	3.30 (0.26)	4.17 (0.29)	4.56 (0.31)	4.81 (0.33)	5.05 (0.35)	5.55 (0.4)	5.69 (0.42)

Table 8-5: Mean values of shrinkage-stress (MPa) **before correction**. The materials cured by **soft-start**.

Material	Time (sec)							
	5	**10**	**20**	**30**	**40**	**60**	**300**	**480**
CLA	0.00 (0.0)	0.001 (.002)	0.14 (0.07)	0.36 (0.07)	0.50 (0.06)	0.58 (0.06)	0.77 (0.05)	0.82 (0.06)
PER2	0.07 (0.13)	0.20 (0.09)	1.02 (0.02)	1.37 (0.08)	1.55 (0.11)	1.64 (0.11)	1.81 (0.13)	1.85 (0.13)
Z100	0.10 (0.05)	0.49 (0.09)	1.09 (0.07)	1.26 (0.08)	1.35 (0.09)	1.41 (0.1)	1.53 (0.11)	1.57 (0.12)
CHRF	0.003 (.003)	0.10 (0.04)	0.73 (0.07)	0.94 (0.06)	1.05 (0.06)	1.14 (0.07)	1.34 (0.08)	1.39 (0.09)
SOL	0.00 (0.0)	0.04 (0.03)	0.98 (0.05)	1.43 (0.1)	1.65 (0.13)	1.72 (0.14)	1.84 (0.16)	1.90 (0.17)
DEF	0.04 (0.02)	0.23 (0.04)	0.81 (0.03)	0.99 (0.05)	1.09 (0.06)	1.16 (0.06)	1.29 (0.09)	1.33 (0.09)

Table 8-6: Mean values of shrinkage stress (MPa) **after correction**. The materials cured by **soft-start**.

Material	Time (sec)							
	5	**10**	**20**	**30**	**40**	**60**	**300**	**480**
CLA	0.00 (0.0)	0.004 (.006)	0.53 (0.24)	1.32 (0.26)	1.84 (0.22)	2.16 (0.21)	2.83 (0.20)	3.04 (0.2)
PER2	0.11 (0.1)	1.33 (0.6)	6.66 (0.15)	8.92 (0.52)	10.13 (0.7)	10.68 (0.7)	11.80 (0.86)	12.04 (0.86)
Z100	0.40 (0.21)	1.96 (0.34)	4.34 (0.28)	5.01 (0.32)	5.35 (0.35)	5.61 (0.39)	6.09 (0.43)	6.22 (0.46)
CHRF	0.005 (.004)	0.40 (0.2)	3.0 (0.27)	3.87 (0.25)	4.35 (0.25)	4.72 (0.29)	5.54 (0.33)	5.75 (0.36)
SOL	0.00 (0.0)	0.24 (0.2)	5.60 (0.28)	8.14 (0.59)	9.38 (0.76)	9.80 (0.8)	10.49 (0.9)	10.81 (0.95)
DEF	0.15 (0.06)	0.93 (0.14)	3.30 (0.14)	4.02 (0.2)	4.43 (0.26)	4.70 (0.3)	5.46 (0.41)	5.40 (0.35)

Table 8-7: Summary of statistical analysis of the difference in the final shrinkage-stress value between results of full intensity and soft-start irradiation.

Material	Sig.
Compolute	0.002
Pertac II	0.118
Z 100	0.016
Charisma F	0.036
Solitaire	0.095
Definite	0.352

8.5 Discussion

The new method provides reproducible measurement of time-dependence of the shrinkage-stress. The primary concern of the construction of this new device was to make it similar to the clinical situation of two tooth cusps. When the resin composite contracted during setting, the stress generated caused the slight movement (compliance) of the stress beam cell to move towards the glass plate. This movement was recorded by using the LVDT. This movement simulates the clinical situation of cusps movement during polymerisation of the restorative materials. Pearson and Hegarty (1987), measured the cusps movement of molar teeth and they recognised that polymerisation shrinkage is the main contributory factor to this movement.

In the laboratory setting, the curing stress measured becomes increasingly dependent on the compliance of the measuring apparatus and various measuring errors, as the thickness of the resin layer decreased (Alster *et al.*, 1997). The magnitude of the contraction stress is thus dependent on the compliance of the surrounding structures as well as the nature of the shrinking material, notably the visco-elastic properties (Davidson and Feilzer 1997)

The compliance of the load cell beam was towards the rigidly fixed glass plate. Hence, during the polymerisation shrinkage process, the material acts to pull the load cell beam in the same axial direction as the material contraction due to the stress.

The movement of the load cell beam in this study was varied with the measurements of different brands of resin-composites. This phenomenon has been noticed by Pearson and Hegarty (1987, 1989); Suliman *et al.*, (1993a & b, 1994); Meredith and Setchell (1997), who measured the deflection of the cusps. **PER2** was recorded the highest deflection. The higher deflection of this material may be attributed to high modulus.

The polymerisation shrinkage-stress of **Z100** was rapidly developed with full light intensity. The stress obtained at 5 sec was 2.87 MPa, which was the highest stress value

at this time. This may be attributed to the presence of a high concentration of the photo-activator in this material. The shrinkage-stress of this material at 8 min was 7.1 MPa. This result is in close with the finding of Kemp-Scholte and Davidson, (1990) who measured the shrinkage-stress of P-10. The highest shrinkage-stress was recorded with **PER2** and **SOL**. This result coincides with the finding of Alster *et al.*, (1997), who used different resin-composite and different specimen thickness.

The shrinkage-stress of **CLA**, resin composite dual-cured luting cement, was lower than that of the restorative light cured resin composites. This may be attributed to greater flow and a lower volume fraction of the filler in this material and cause a lower modulus. Theoretically, the greater the capacity to flow, the lower will be the contraction-stress, which can be decisive for the success of the bonding procedure (Carvalho *et al.*, 1996).

CHRF material was stiff, difficult to handle, and resisted compression pressure between the glass plate and metal rod surfaces. The shrinkage-stress of this material was lower than **SOL**, which is from the same manufacturer. Hence, the viscosity of the material may be playing an important part in the shrinkage-stress.

The full intensity has a greater stress effect than soft-start polymerisation with **CLA**, **Z100** and **CHRF** materials. The difference was statistically significant ($p < 0.05$). On the other hand, the difference was not statistically significant ($p > 0.05$) with **PER2**, **SOL** and **DEF** materials. The results of this study were in agreement with the finding of Ernst *et al.*, (1997) and Algera *et al.*, (1998) in some investigated materials (**CLA**, **Z100** and **CHRF**). But in the other materials (**PER2**, **SOL** and **DEF**) as mentioned above the differences were not significant. Uno and Asmussen (1991) concluded that prepolymerisation at low intensity followed by a post-cure at full intensity may be a viable means to produce fillings of resin composites with improved marginal adaptation.

DEF is an Organically Modified Ceramic-matrix (ORMOCER) material. They are a large family of (meth) acrylate substitued alkoxysilanes. Generically they are inorganic-organic copolymers. The alkoxysilyl groups allow the formation of an organic Si-O-Si network

by hydrolysis and polycondensation (sol-gel) process. The methacrylate groups are available for thermal, redox, UV or light-cure polymerisation. Thus solvent-free functionalised resins can be obtained after hydrolysis and condensation without, or in combination with, other sol-gel precursors to build up the inorganic polymer structure. Besides these principles of variation, fillers (77%wt) may also be added to modify the properties (Watts 1996). The shrinkage during setting of this material behaved similarly to the resin-composites. The shrinkage stress was slightly lower than the investigated light-cured resin composites and higher than **CLA** luting resin composites. The shrinkage- stress was rapidly increased when cured by full light intensity (2.1 MPa) and the maximum shrinkage-stress was 5.7 MPa.

8.6 Conclusions

- The newly developed instrument gave reproducible results of time dependence of shrinkage stress.

- The soft-start polymerisation of the Elipar Highlight significantly reduced the final shrinkage stress of some restorative materials (**CLA, Z100** and **CHRF**) and did not significantly reduce the final shrinkage stress of other materials (**PER2, SOL** and **DEF**).

- **PER2** has the highest shrinkage stress, cured by either soft-start or full intensity.

- Rapid shrinkage stress development at the first 5 sec was noted for **Z100** and **DEF**, but they have lower maximum stress than **PER2** and **SOL**.

- **DEF** was found to have lower shrinkage stress than light-cured resin composites and higher than **CLA** dual-cure luting cement.

Chapter 9
General Conclusions and Recommendations for Further Study

9.1 General Conclusions

The polymerisation efficiency of restorative resin composites is reflected in a number of properties. This work was focused on studying this area of polymerisation efficiency by evaluation of the degree of conversion; depth of cure; exotherm; surface hardness and polymerisation shrinkage. The study concentrated on the factors influencing polymerisation efficiency, namely the effect of the intensity of the light curing units and temperature.

The intensity of the light-curing units significantly influenced the polymerisation efficiency of the resin-composites. The efficiency of the light-curing units was measured directly by using the light intensity radiometer, which indicated that, the light intensity of the Elipar light-source (510 mW $\approx$ 750 mW.cm^{-2}) was significantly greater than that of the XL3000 light-source (217 mW $\approx$ 500 mW.cm^{-2}), and produced correspondingly greater temperature rises. The high temperature generated from the Elipar unit was considered a slight disadvantage of this light-curing unit, which may possibly damage the pulp. But the temperature generated from the XL3000 light source was reasonable and safer for use in clinical treatment.

The Elipar unit has the advantage of the presence of two types of cure-mode, the standard intensity and 2-step polymerisation ("soft-start"). The presence of high intensity light is of benefit when producing well-cured restorative materials and hence, high physical and mechanical properties.

The degree of conversion, depth of cure and surface hardness were studied for the evaluation of the efficiency of the resin-composites as well as efficiency of the Elipar Highlight unit in both its standard and 2-step modes.

It was useful network-conversion (polymerisation) attained by the application of the 10 s low-intensity phase of the "soft-start" mode. The polymerisation of the resin composites with "soft-start" was as great as with "full" irradiation by measuring the degree of conversion, depth of cure and polymerisation shrinkage, but it was beneficial in decreasing the polymerisation shrinkage-stress. "Soft-start" also reduces the exothermic reaction due to the delaying in the vigour of the setting reaction in the first 10 s.

The use of different light intensities indicated that the degree of conversion of the resin composites decreased with reducing light intensity. The increase of exposure time can compensate the reduction in intensity light, but does not give as high a degree of conversion as full intensity does. The first 10 sec low intensity of the Elipar unit does not cure the resin composites properly. This problem was also encountered with the measurement of the depth of cure and surface hardness. With increased exposure time of the low intensity to 40 sec the degree of conversion was improved, but not as effectively as those cured by either full intensity or "soft-start". Nevertheless, the low intensity irradiation did produce degree of conversion up to 30%.

The higher the degree of conversion the greater the improvement in the surface hardness and the increase in polymerisation shrinkage. From the results obtained in this study, **PER2** was found to have a higher degree of conversion and hence polymerisation shrinkage was higher than **Z100**, **CHRF**. But the surface hardness was slightly lower than **Z100**, which may be attributed to the difference in filler type in these two materials. The depth of cure was found lower in **PER2** than **Z100** and **CHRF**. This may be attributed to the filler transmission of these materials.

The evaluation of the low light intensity of the Elipar was found insufficient to fully polymerise the resin composite. It results in a low degree of conversion (30 %), minimal or nil surface hardness and low depth of cure. However, quite appreciable hardness was attained for upper surfaces with low intensity, confirming the definite network-creating potential of even low light-levels. It is beneficial to start the polymerisation with low intensity in order to increase the period of low elastic of modulus and hence decrease the initial shrinkage stress.

The hardness measurement and depth of cure intensity demonstrated the effect of the full light intensity on the polymerisation efficiency of the investigated resin composites in deep area. This light-curing unit can polymerise the resin composite materials to *circa* 5 mm.

Effects of "soft-start" and "full" intensity curing on polymerisation shrinkage-strain were investigated. During the first 10 s, the polymerisation shrinkage was minimal, with low-intensity light, compared to the rapid rise in shrinkage with full light-intensity. But the final equilibrium shrinkage-strain was not significantly different. It was concluded that light-programmed "soft-start" polymerisation was beneficial in reducing the rapidity of kinetic-profile of the shrinkage-strain event. When combined with the preceding studies on degree-of-cure, this shows that early network-growth can occur during this period of minimal early shrinkage. Some molecular flow or network re-arrangement must be possible. A novel discovery was that an acrylate-based composite material exhibited an *inherent* "soft-start" regime under full-irradiation conditions.

The measurements of polymerisation shrinkage-stress kinetics of resin-composites with a newly designed apparatus, based around a cantilever load cell were gave reproducible results of the polymerisation shrinkage-stress magnitudes. Materials were again cured with "full" intensity and "soft-start" modes. The "soft-start" mode significantly reduced the final shrinkage-stress of some materials, but not others. This was important finding showing that, although more difficult to conduct, stress measurements are a valuable adjunct to strain studies of shrinkage phenomena.

The slow flow of the resin composites during polymerisation would be the important factor in shrinkage stress relaxation. The use of full intensity from the beginning led to rapid shrinkage strain and stress with some resin composites (e.g. **Z100**), which may cause early failure of the bond interface between the tooth cavity and restorations. **Z100** and **DEF** were found to rapidly generate relatively high shrinkage-stress in the first 5 sec, but the maximum shrinkage stress was low. The shrinkage stress of **PER2** and **SOL** was generated gradually, but the maximum shrinkage stress was significantly higher in these two materials.

The post-cure temperature enhanced the polymerisation efficiency of the resin-composites. This was noticed in the evaluation of the surface hardness of the resin-composites. The surface hardness was improved with specimens groups were pre-conditioned at 37°C with both full and low intensity light of the Elipar unit. Shrinkage-strain increased with temperature because of greater network conversion.

9.2 Recommendations for Further Study

1. Study is recommended on evaluation of the polymerisation efficiency of the restorative materials *in situ* in human teeth. The adverse effects of the exothermic reaction and shrinkage stress during polymerisation are very important to consider for the pulp vitality and the success of the restorations. So, the study of the polymerisation shrinkage stress, exotherm reaction and temperature rises from light sources on human teeth would be valuable.

2. Measurement of the shrinkage stress by using adhesives between the resin composite specimen and the glass plate from one side and the metal rod from the other side.

3. Evaluation of the effect of different restorative thicknesses on the shrinkage stress with the newly constructed instrument.

4. A whole range of newly developed materials may be routinely characterised with respect to stress-kinetics, by the new instrument. Also new types of programmable light sources may evaluated similarly.

5. Correlation of strain-kinetics and stress-kinetics can load to data on the rate of modulus development.

References

Aboush, Y.E.Y, Elderton, R.J. (1990): Bonding of light-curing glass-ionomer to dental amalgam. *Dent Mater* **7:** 130-132.

Adamson, M., Lloyd, C.H. and Watts, D.C. (1988): The temperature rise beneath a light-cured cement lining during light curing. *J Dent,* **16:** 182-187.

Algera, T., Feilzer, A., DeGee, A. and Davidson, C. (1998): The influence of slow-start polymerisation on the shrinkage stress development. *J Dent Res,* **77(special issue B):** Abs No 429, 685.

Al-Hindi, A.M. (1995): Polymerisation efficiency of dual-cure resin composites for luting. In *Restorative department, Biomaterials Science.* The University of Manchester, Manchester. M. Sc. Thesis. pp. 1 -147.

Alster, D., Feilzer, AJ., DeGee, A. and Davidson, C.L (1997): Polymerisation contraction stress in thin resin composite layers as a function of layer thickness. *Dent Mater,* **13:** 146-150.

Antonucci, J.M., McKeinney J.E. and Stansbury J.W. (1988): Resin modified glass ionomer dental cement. US Patent 160856.

Antonucci, J.M., Stansbury, J. (1989): Polymer modified glass ionomer cements. *J Dent Res,* **68:** 251 Abs No. 555.

Asmussen, E. (1975): Composite restorative resins composition versus wall-to-wall polymerisation contraction. *Acta Odont Scand,* **33:** 337-344.

Asmussen, E. (1980): Quantitative analysis of peroxides in restorative resins. *Acta Odont Scand,* **38:** 269-272.

Asmussen, E. (1982a): Factors affecting the quantity of remaining double bonds in restorative resin polymers. *Scand J Dent Res,* **90:** 490-496.

Asmussen, E. (1982b): Restorative resin, hardness and strength *vs* quantity of remaining double bonds. *Sean J Dent Res,* **90:** 484-489.

Asmussen, E. and Peutzfeldt, A. (1990): Mechanical properties of heat treated restorative resins for use in the inlay/onlay technique. *J Dent Res,* **98:** 564-567.

Attin, T., Buchalla, W., Kielbassa, A.M. and Hellwig, E. (1995): Curing shrinkage and volumetric changes of resin-modified glass ionomer restorative materials. *Dent Mater,* **11:** 359-362.

Bagis, Y. and Reuggeberg, F. (1997): Effect of post-cure temperature and heat on monomer conversion of photo-activated dental resin composite. *Dent Mater,* **13(4):** 228-232.

Bandyopadhyay, S. (1982): A study of the volumetric shrinkage of some dental materials. *J Biomed Mater Res,* **16:** 135-144.

Baum, L., Phillips, R. and Lund, M.R. (1985): "Textbook of Operative Dentistry" 2nd Edn WB Saunders, Philadelphia,. *U S A,* **:** 204.

Bausch, J.R., deLange, C. and Davidson, C.L. (1981): The influence of temperature on some physical properties of dental composites. *J Oral Rehabil,* **18:** 309-317.

Bausch, J.R., deLange, C., Davidson, C.L., Peters, A. and DeGee, A.J. (1982): Clinical significance of polymerisation shrinkage of composite resin. *J Prosthet Dent,* **48:** 59-67.

Benham, P., Crawford, R. and Armstrong, C. (1998): Mechanics of engineering materials, Longman. Chapter 3, pp. 70-71.

Bowen, R.L. (1962): Dental filling material comprising vinyl silane treated fused

silica and a binder consisting of a reaction product of bisphenol and glycidyl acrylate. *U S Patent No,* 3066: 112.

Bowen, R.L., Nemoto, K. and Rapson, J.E. (1983): Adhesive bonding of various materials to hard tooth tissues: forces developing in composite materials during hardening. *J Am Dent Assoc,* **106:** 475-477.

Bower, D.I., and Maddams, W.F. (1989): Quantitive analysis. *In: The vibrational spectroscopy of polymers.* Cambridge University Press, Cambridge. Chapters 1 and 5, pp. 28-30 and 215-226.

Braden, M., Causton, E.E. and Clarke, R.L. (1976): Diffusion of water in composite filling materials. *J Dent Res,* **55:** 730-732.

Braem, M., Lambrechts, P., vanDoren, V. and Vanherle, G. (1986): The impact of composite structure on its elastic response. *J Dent Res,* **65:** 648-653.

Buonocore, M.G. and Davita, J. (1973): Restoration of fractured anterior teeth with ultraviolet light polymerised bonding materials: A new technique. *J Am Dent Assoc,* **86:** 1349.

Burgess, J.O., Barghi, N., Chan, D.C.N., Hummert, T.A. (1993): A comparative study of three glass-ionomer base materials. *Am J Dent,* **6:** 137-141.

Carvalho, R.M., Pereira, J.C., Yoshiyama, M. and Pashley, D.H. (1996): A review of polymerisation contraction: the influence of stress development versus stress relief. *Oper Dent,* **21:** 17-24.

Castelnuovo, J. and Tjan, A.H.L. (1997): Temperature rise in pulpal chamber during fabrication of provisional resinous crowns. *J Prosthet Dent,* **78:** 441-446.

Caughman, W., Caughman, G., Sheflett, R., Rueggeberg, F. and Schuster, G. (1991): Correlation of cytotoxicity, filler loading and curing time of dental composites. *Biomaterials,* **12:** 737-740.

Causton, B., Miller, B. and Sefton, J. (1989): The deformation of cusps by bonded posterior composite restorations: an *in vitro* study. *Br Dent J,* **159:** 397-400.

Chadwick, R.G., Woolford, M.J. (1993): A comparison of the shear bond strengths to a resin composites of two conventional and two resin-modified glass polyalkenoate (ionomer) cements. *J Dent,* **21:** 111-116.

Christensen, G.J. (1996): Restoration of paediatric posterior teeth. *J Am Dent Assoc,* **127:** 106-108.

Ciucchi, B., Bouillaguet, S., Delaloye, M. and Holz, J. (1997): Volume of the internal gap formed under composite restorations *in vitro*. *J Dent,* **25:** 305-312.

Compoton, A.M., Meyers, C.E., Hondrum, S.O., Lorton, L.E. (1992): Comparison of the shear bond strength of a light-cured glass ionomer and chemically cure glass ionomer for use as an orthodontic bonding agent. *Am J Ortho Dentofac Orthop,* **101:** 138-144.

Cook, W.D. (1980): Factors affecting the depth of cure of UV polymerised composites. *J Den Res,* **95:** 800-808.

Cook, W.D. and Johannson, M. (1987): The influence of post-curing on the fracture properties of photo-cured dimethacrylate based dental composite resin. *J Biomed Mater Res,* **21:** 979-989.

Cook, W.D. and Standish, P.M. (1983): Cure of resin based restorative materials: II. White light photo-polymerised resins. *Aust Den J,* **28:** 307-311.

Council on Dental Materials, Instrument and Equipment (1982): Status report on microfilled composite restorative resins. *J Am Dent Assoc,* **105(3):** 488-492.

Cox, C.F., Keal, C.L., Keal, H.J., Ostro, E. and Bregenholtz, G. (1987): Biocompatibility of surface-sealed dental materials against exposed pulps. *J*

Prosthet Dent, **57:** 1-8.

Craig, R.G. (1981): Chemistry, composition and properties of composite resins. *Dent Clin North Am,* **25:** 219-239.

Craig, R., O'Brien, W. and Powers, J. (1983): Dental Materials Properties and Manipulation, Mosby, St Louis, USA.

Craig, R.G (1997) Restorative Dental Materials. Tenth Ed., Mosby, St. Louis, USA, pp 30-38, 192-195 and 274-276.

Crisp, S., Lewis, B. and Wilson, A. (1976): Glass-ionomer cements; Chemistry of erosion. *J Dent Res,* **55:** 1032-1041.

Davidson, C.L. (1985): Conflicting interests with posterior teeth use of composite materilas. In: *Posterior composite resin, dental restorative materials* (Eds, Vanherle, G. and Smith, D.C.) Amsterdam, pp. 61-65.

Davidson, C.L. and de Gee, A.J. (1984): Relaxation of polymerisation contraction stresses by flow in dental composites. *J Dent Res,* **63:** 146-148.

Davidson, C.L., DeGee, A.J. and Feilzer, A.J (1984): The competition between the composite-dentin bond strength and the polymerisation contraction stress. *J Dent Res,* **63:** 1396-1399.

Davidson, C.L. and Feilzer, A.J. (1997): Review: Polymerisation shrinkage and polymerisation shrinkage stress in polymer-based restoratives. *J Dent,* **25:** 435-440.

Davidson, C.L., Duysters, P.P., DeLang, C. and Bausch, J.R. (1981): Structural changes in composite surface material after dry polishing. *J Oral Rehabil,* **8:** 431-439.

DeGee, A.J., Davidson, C.L. and Smith, A.A. (1981): A modified dilatometer for continuous recording of volumetric polymerisation shrinkage of composite restorative materials. *J Dent,* **9:** 36-42.

DeLange, C., Bauch, J.R. and Davidson, C.L. (1980): The curing pattern of photoinitiated dental composites. *J Oral Rehabil,* **7:** 369-377.

DeWald, J.P. and Ferracane, J.L. (1987): A comparison of four modes of evaluating depth of cure of light-activated composites. *J Dent Res,* **66:** 727-730.

Dionysopoulos, P. and Watts, D.C. (1989): Dynamic mechanical properties of an inlay composite. *J Dent,* **17:** 140-144.

Donly, K.J., Jensen, M.E., Reinhardt, J. and Walker J.D. (1987): Posterior composite polymerisation shrinkage in primary teeth: an *in vivo* comparison of three restorative techniques. *Pediat. Dent,* **9:** 22-25.

Dugan, W.T. and Hartleb, J.H. (1989): Influence of a glutaraldehyde disinfecting solution on curing light effectiveness. *Gen Dent,* **37:** 40-43.

Eick, D.J., Robinson, S.J., Byerley, T.J. and Chappelow, C.C. (1993): Adhesives and nonshrinking dental resins of the future. *Quintessence Int,* **24:** 632-640.

Eick, D.J. and Welch, F.H. (1986): Polymerisation shrinkage of posterior composite resin and its possible influence on postoperative sensitivity. *Quintessnece Int,* **17:** 103-111.

El-Hejazi, A.A. (1995): Structure and properties of light-cured dental restorative materials. Ph. D. Thesis from *Dental medicine and surgery.* The University of Manchester, Manchester, pp. 88-124.

Eliades, G.C., Vougiouklakis, G.J. and Caputo, A.A. (1987): Degree of double bond conversion in light-cured composites. *Dent Mater,* **3:** 19-25.

Ellingson, O.L., Landry, R.J. and Bostrom, R.G. (1986): An evaluation of optical radiation emissions from dental visible photo-polymerisation devices. *J Am Dent Assoc,* **112:** 67-70.

Ernst, C., Kurschner, R. and Willershausen, B. (1997): Stress reduction in composite resin by means of a two-step polymerisation unit- a photoelastic investigation. In: *IADR/CED*Madrid, Abs No. 292, pp. 97.

Fan, P. L., Wozniak, W. T., Reyes, W. D. and Stanford, J. W. (1987): Irradiance of visible light-curing units and voltage variation effects. *J Am Dent Assoc,* **115:** 442-445.

Fan, P., Edhal, A., Leung, R. and Standford, J. (1985): Alternative interpretations of water sorption values of composite resins. *J Dent Res,* **64:** 78-80.

Fano, V., Ortalli, I., Pizzi, S. and Bonanini, M. (1997): Polymerisation shrinkage of microfilled composites determined by laser beam scanning. *Biomaterials,* **18:** 467-470.

Feilzer, A.J., DeGee, A.J. and Davidson, C.L. (1987): Setting stress in composite resin in relation to configuration of the restoration. *J Dent Res,* **66:** 1636-1639.

Feilzer, A.J., DeGee, A.J. and Davidson, C.L. (1990): Relaxation of polymerisation contraction shear stress by hygroscopic expansion. *J Dent Res,* **69:** 36-39.

Feilzer, A.J., DeGee, A.J. and Davidson, C.L. (1989): Increased wall-to-wall curing contraction in thin bonded resin layers. *J Dent Res,* **68:** 48-50.

Feilzer, A.J., Dooren, L.H., DeGee, A.J. and Davidson, C.L. (1995a): Influence of light intensity on polymerisation shrinkage and integrity of restoration cavity interface. *Eur J Oral Sci,* **103:** 322-326.

Feilzer, A.J., Kakabowra, A.I., DeGee, A.J. and Davidson, C.L. (1995b): The influence of water sorption on the development of setting shrinkage stress in traditional and resin-modified glass ionomer cements. *Dent Mater,* **11:** 186-190.

Feilzer, A.J., DeGee, A.J., and Davidson, C.L. (1988): Curing contraction of composites and glass-ionomer cements. *J Prosthet Dent,* **59:** 297-300.

Ferracane, J.L. (1985): Correlation between hardness and degree of conversion during the setting reaction of unfilled dental restorative resins. *Dent Mater,* **1:** 11-14.

Ferracane, J.L. (1995): Current trends in dental composites. *Cri Rev Oral Biol Med,* **6(4):** 302-318.

Ferracane, J.L. and Greener, E.H. (1984): Fourier Transform infrared analysis of degree of polymerisation in unfilled resins-methods comparison. *J Dent Res,* **63:** 1093-1095.

Ferracane, J.L. and Greener, E. H. (1986): The effect of resin formulation on the degree of conversion and mechanical properties of dental restorative resins. *J Biomed Mater Res,* **20:** 121-133.

Ferracane, J., Mitchem, J., Condon, J. and Todd, R. (1997): Wear and marginal breakdown of composites with various degree of cure. *J Dent Res,* **76(8):** 1508-1516.

Fusayama, T. (1987): Factors and prevention of pulp irritation by adhesive composite resin restorations. *Quintessence Int,* **18:** 633-641.

Glenn, J. (1982): Biocompatibility of Dental Materials. Smith D C, Williams D F Eds, Vol. 3: 97-130.

Goodis, H.E., White, J.M., Andrews, J. and Watanabe, L.G. (1989): Measurement of temperature generated by visible light-cure lamps in an *in vitro* model. *Dent Mater,* **5:** 230-234.

Goodis, H.E., White, J.M., Marshall, S., Koshrovi, P., Watanabe, L.G. and Marshall, G.W. (1993): The effect of glass ionomer liners in lowering pulp

temperatures during composite placement, *in vitro*. *Dent Mater,* **9:** 146-150.

Grajower, R. and Guelmann, M. (1989): Dimensional changes during setting of a glass ionomer filling material. *Quintessence Int,* **20:** 505-511.

Greener, E.H., Greener, C.J. and Moser, J.B. (1984): The hardness of composite as a function of temperature. *J Oral Rehabil,* **11:** 335-340.

Hansen, E. (1983): After-polymerisation of visible light activated resins: surface hardness *vs* light source. *Scand J Dent Res,* **91:** 406-410.

Hansen, E.K. and Asmussen, E. (1993a): Correlation between depth of cure and surface hardness of a light-activated resin. *Scand J Dent Res,* **101:** 62-64.

Hansen, E. and Asmussen, E. (1993b): Reliability of three dental radiometers. *Scand J Dent Res,* **101:** 115-119.

Hansen, E.K. and Asmussen, E. (1993c): Correlation between depth of cure and temperature rise of a light-activated resin. *Scand J Dent Res,* **101:** 176-179.

Hansen, E. and Asmussen, E. (1997): Visible-light curing units: correlation between depth of cure and distance between exit window and resin surface. *Acta Odontol Scand,* **55:** 162-166.

Harrington, E. and Wilson, H. (1995): Determination of radiation energy emitted by light activation unit. *J Oral Rehabil,* **22:** 377-385.

Harrington, E. and Wilson, H.J. (1993): Depth of cure of radiation-activated materials- effect of mould material and cavity size. *J Dent,* **21:** 305-311.

Harrington, E., Wilson, H.J. and Shortall, A.C. (1996): Light-activated restorative materials: a method of determining effective radiation times. *J Oral Rehabil,* **23:** 210-218.

Hay, J.N. and Shortall, A.C. (1988): Polymerisation contraction and reaction kinetics of three chemically activated restorative resins. *J Dent,* **16:** 172-176.

Hegdahl, T. and Gjerdet, N. R. (1977): Contraction stresses of composite resin filling materials. *Acta Odont Scand,* **35:** 191-195.

Helvatjoglou-Antoniadi, M., Papadogianis, Y., Koliniotou-Kubia, E. and Kubias, S. (1991): Surface hardness of light-cured and self-cured composite resins. *J Prosthet Dent,* **65:** 215-220.

Heindl, D. (1999): Personal communication with Watts D.C.

Hirabayashi, S., Hood, J. and Hirasawa, T. (1993): The extent of polymerisation of class II light-cured composite resin restorations: effects of incremental placement technique, exposure time and heating of resin inlays. *Dent Mater J,* **12(2):** 159-170.

Hosoda, H., Yamada, T. and Inokoshi, S. (1990): SEM and elemental analysis of composite resins. *J Prosthet Dent,* **64:** 669-676.

Hussey, D., Biagioni, P. and Lamey, P. (1995): Thermographic measurement of temperature change during resin polymerisation *in vivo*. *J Dent,* **23(5):** 267-271.

Ikemi, T., and Nomoto, K. (1994): Effects of lining materials on the composite resins shrinkage stresses. *Dent Mater J.* **13(1):** 1-8.

Imazato, S., Tarumi, H., Kobayashi, K., Hiraguri, H., Oda, K. and Tsuchitani, Y. (1995): Relationship between the degree of conversion and internal discoloration of light-activated composites. *Dent Mater J,* **14(1):** 632-637.

Inoue, K. and Hayashi, I. (1982): Residual monomer (Bis-GMA) of composite resins. *J Oral Rehabil,* **9:** 493-497.

Inoue, K., Terachi, M. and Utsumi, S. (1988): A study of composite resin inlay. *J Dent Res,* **67:** 222.

Jafarzadeh Kashi, T. and Watts, D.C. (1998): Polymerisation shrinkage *versus* layer

thickness of a dentin bonding resin. *J Dent Res,* 77 **(special issue B):** Abs No. 1411: 808.

Jensen, M.E. and Chan, D.C.N. (1985): Polymerisation shrinkage and microleakage. *In: Posterior Composite resin dental materials,* Peter Szule Publishing, The Netherlands.

Jorgensen, K.D., Itoh, K., Munksgaard, E.C. and Asmussen, E. (1985): Composite wall-to-wall polymerisation contraction in dentin cavities treated with various bonding agents. *Scand J Dent Res,* **93:** 276-279.

Kanchanavasita, W., Pearson, G. L. and Anstice, H. M. (1996): Factors contributing the temperature rise during polymerisation of resin-modified glass-ionomer cements. *Biomaterials,* **17:** 2305-2312.

Kemp-Scholte C.M., and Davidson C.L. (1990): Complete marginal seal of class V resin composite restorations effected by increased flexibility. *J Dent Res,* **69(6):** 1240-1243.

Kildal KK and Ruyter IE (1994): How different curing methods affect the degree of conversion of resin-based inlay/onlay materials. *Acta Odontol Scand,* **52:** 315-322.

Lai, J. and Johnson, A. (1993): Measuring polymerisation shrinkage of photo-activated restorative materials by a water-filled dilatometer. *Dent Mater,* **9:** 139-143.

Lang, B., Jaarda, M. and Wang, R. (1992): Filler particle size and composite resin classification system. *J Oral Rehabil,* **19:** 569-584.

Ledwith, A. (1977): Photoinitiation of polymerisation. *Pure Appl Chem,* **149:** 431-441.

Lee, L., Orlowski, J.A. and Rogers, B.J. (1976): A comparison of ultraviolet curing and self curing polymers in preventive, restorative and orthodontic dentistry. *Int Dent J,* **26:** 134.

Leinfelder, K. (1989): Composite resins; Properties and clinical performance .In: O'Brian WJ, ed Dental material; properties and selection. Chicago, Quintessence Publ. 139-157.

Leinfelder, K. (1991): Using composite resin as a posterior restorative material. *J Am Dent Assoc,* **122:** 65-70.

Lekka, M.P., Papagiannoulis, L., Eliades, G.C. and Caputo, A.A. (1989): A comparative *in vitro* study of visible light-cured sealants. *J Oral Rehabil,* **16:** 287-299.

Leung, R.L., Fan, P.L. and Johnston, W. (1983): Post-irradiation polymerisation of visible-light activated composite resins. *J Dent Res,* **62:** 363-365.

Leung, R.L., Khan, R.L. and Fan, P.L. (1984): Comparison of depth of polymerisation evaluation methods for photoactivated composites. *J Dent Res,* **61:** 188.

Lloyd, C.H (1984): A differential thermal analysis (DTA) for the heats of reaction and temperature rises produced during the setting of tooth coloured and restorative materials. *J Oral Rehabil.* **11:** 111-121.

Lloyd, C.H, Joshi, A. and McGlynn, E. (1986): Temperature rise produced by light sources and composites during curing. *Dent Mater,* **2:** 170-174.

Loza-Herrero, M., Rueggeberg, F., Caughman, W., Schuster, G., Lefebvre, C. and Gardner, F. (1998): Effect of heating delay on conversion and strength of a post-cured resin composite. *J Dent Res,* **77(2):** 426-431.

Lutz, F. and Phillips, R. (1983): Classification and evaluation of composite resin systems. *J Prosthet Dent,* **50:** 480.

Lutz, F., Krejci, I. and Oldenburg, T.R. (1986): Elimination of polymerisation stresses at the margins of posterior composite resin restorations: a new restorative technique. *Quintessnece Int,* **17:** 777-784.

Lutz, F., Phillips, R.W., Roulet, J.F. and Setcos, J.C. (1984): *In vitro* and *in vitro* wear of potential posterior composites. *J Dent Res,* **63:** 914-920.

Marshall, G., Marshall, S. and Bayne, S. (1988): Restorative Dental Materials; scanning electron microscopy and x-ray microanalysis. Scanning Microscopy. **2:** 2007-2028.

Martin, F. (1998): A survey of the efficiency of visible light curing units. *J Dent,* **26(3):** 239-243.

Masutani, S., Setcos, J., Schnell, R. and Phillips, R. (1988): Temperature rise during polymerisation of visible light-activated resins. *Dent Mater,* **4:** 174-178.

Matsumoto, H., Gres, J.E., Marker, V.A., Okabe, T., Ferracane, J.L. and Harvey, G.A. (1986): Depth of cure of visible light-cured resin: clinical simulation. *J Prosthet Dent,* **55:** 574-578.

McAndrew, R., Lloyd, C.H. and Watts, D.C. (1987): The effect of a cement lining upon the temperature rise during the curing of composite by visible light. *J Dent,* **15:** 218-221.

McCabe, J.F. (1985): Cure performance of light-activated composites by differential thermal analysis (DTA). *Dent Mater,* **1:** 231-234.

McCabe, J.F (1992): Setting reactions of dental materials: methods for monitoring the rate of set. In *Setting mechanisms of dental materials* (Ed, DC, Watts.) Cameron House, Loch Lomond, Scotland, pp. 1-25.

McCabe, J.F (1990): Applied dental materials. 7th Ed., Blackwell Scientific Publication. Chapter 1 pp. 1-27, Chapter 12, pp. 78-80 and Chapter 23, pp. 145-156.

McCabe, J.F and Wilson, H. (1980): The use of differential scanning calorimetry for the evaluation of dental materials. *J Oral Rehabil,* **7:** 103-110.

McCabe, J.F. and Carrick, T.E. (1989): Output from visible-light activation units and depth of cure of light-activated composites. *J Dent Res,* **68:** 1534-1539.

McClean, J. (1984): Alternative to amalgam alloys. *Br Dent J,* **157:** 432-433.

McGinnis, V. (1975): Acrylate system for UV curing. Part I: Light source and photoinitiators. *J Radiat Curing,* **2:** 3-13.

Mehl, A., Hickel, R. and Kunzelmann, K. (1997): Physical properties and gap formation of light-cured composites with and without "soft-start polymerisation". *J Dent,* **25 (53):** 321-330.

Meredith, N. and Setchell, D. (1997): *In vitro* measurement of cuspal strain and displacement in composite restored teeth. *J Dent,* **25:** 331-337.

Morin, D., Delong, R. and Douglas, W. (1984): Cusp reinforcement by the acid-etch technique. *J Dent Res,* **63:** 1075-1078.

Morin, D., Douglas, W., Cross, M. and al, e. (1988): biophysical stress analysis of restored teeth: experimental strain measurements. *Dent Mater,* **4:** 41-48.

Moseley, H., Strang, R. and Stephen, K. W. (1986): An assessment of visible-light polymerising sources. *J Oral Rehabil,* **13:** 215-224.

Munksgaard, E.C. Hansen E.K., and Kato H. (1987): Wall-to-wall polymerization contraction of composite resins versus filler content. *Scand J Dent* **95**: 526.

Newmann, S.M., Murray, G.A. and Yatesb, J.L. (1983): Visible lights and visible light activated composite resins. *J Prosthet Dent,* **14:** 45-51.

Nomoto, R. and Hirasawa, T. (1992): Residual monomer and pendant methacryloyl group in light-cured composite resins. *Dent Mater J,* **11(2):** 177-188.

Lutz, F., Krejci, I. and Oldenburg, T.R. (1986): Elimination of polymerisation stresses at the margins of posterior composite resin restorations: a new restorative technique. *Quintessnece Int,* **17:** 777-784.

Lutz, F., Phillips, R.W., Roulet, J.F. and Setcos, J.C. (1984): *In vitro* and *in vitro* wear of potential posterior composites. *J Dent Res,* **63:** 914-920.

Marshall, G., Marshall, S. and Bayne, S. (1988): Restorative Dental Materials; scanning electron microscopy and x-ray microanalysis. Scanning Microscopy. **2:** 2007-2028.

Martin, F. (1998): A survey of the efficiency of visible light curing units. *J Dent,* **26(3):** 239-243.

Masutani, S., Setcos, J., Schnell, R. and Phillips, R. (1988): Temperature rise during polymerisation of visible light-activated resins. *Dent Mater,* **4:** 174-178.

Matsumoto, H., Gres, J.E., Marker, V.A., Okabe, T., Ferracane, J.L. and Harvey, G.A. (1986): Depth of cure of visible light-cured resin: clinical simulation. *J Prosthet Dent,* **55:** 574-578.

McAndrew, R., Lloyd, C.H. and Watts, D.C. (1987): The effect of a cement lining upon the temperature rise during the curing of composite by visible light. *J Dent,* **15:** 218-221.

McCabe, J.F. (1985): Cure performance of light-activated composites by differential thermal analysis (DTA). *Dent Mater,* **1:** 231-234.

McCabe, J.F (1992): Setting reactions of dental materials: methods for monitoring the rate of set. In *Setting mechanisms of dental materials* (Ed, DC, Watts.) Cameron House, Loch Lomond, Scotland, pp. 1-25.

McCabe, J.F (1990): Applied dental materials. 7th Ed., Blackwell Scientific Publication. Chapter 1 pp. 1-27, Chapter 12, pp. 78-80 and Chapter 23, pp. 145-156.

McCabe, J.F and Wilson, H. (1980): The use of differential scanning calorimetry for the evaluation of dental materials. *J Oral Rehabil,* **7:** 103-110.

McCabe, J.F. and Carrick, T.E. (1989): Output from visible-light activation units and depth of cure of light-activated composites. *J Dent Res,* **68:** 1534-1539.

McClean, J. (1984): Alternative to amalgam alloys. *Br Dent J,* **157:** 432-433.

McGinnis, V. (1975): Acrylate system for UV curing. Part I: Light source and photoinitiators. *J Radiat Curing,* **2:** 3-13.

Mehl, A., Hickel, R. and Kunzelmann, K. (1997): Physical properties and gap formation of light-cured composites with and without "soft-start polymerisation". *J Dent,* **25 (53):** 321-330.

Meredith, N. and Setchell, D. (1997): *In vitro* measurement of cuspal strain and displacement in composite restored teeth. *J Dent,* **25:** 331-337.

Morin, D., Delong, R. and Douglas, W. (1984): Cusp reinforcement by the acid-etch technique. *J Dent Res,* **63:** 1075-1078.

Morin, D., Douglas, W., Cross, M. and al, e. (1988): biophysical stress analysis of restored teeth: experimental strain measurements. *Dent Mater,* **4:** 41-48.

Moseley, H., Strang, R. and Stephen, K. W. (1986): An assessment of visible-light polymerising sources. *J Oral Rehabil,* **13:** 215-224.

Munksgaard, E.C. and Irie, M. (1987): Dentin-polymer bond established by gluma and tested by thermal stress. *J Dent Res,* **95:** 185-190.

Newmann, S.M., Murray, G.A. and Yatesb, J.L. (1983): Visible lights and visible light activated composite resins. *J Prosthet Dent,* **14:** 45-51.

Nomoto, R. and Hirasawa, T. (1992): Residual monomer and pendant methacryloyl group in light-cured composite resins. *Dent Mater J,* **11(2):** 177-188.

Øysaed, H. and Ruyter, I.E. (1986): Water sorption and filler characteristics of composites for use in posterior teeth. *J Dent Res,* **65:** 1315-1318.

Park, S. (1996): Comparison of degree of conversion for light-cured and additionally heat-cured composites. *J Prosthet Dent,* **76:** 613-618.

Pearson, G.J. and Hegarty, S.M. (1987): Cusp movement in molar teeth using dentine adhesives and composite filling material. *Biomaterials,* **8:** 473-476.

Pearson, G.J. and Hegarty, S.M. (1989): Cusp movement of molar teeth with composite filling material in conventional and modified MOD cavities. *Br. Dent. J,* **166:** 162.

Penn, R.W. (1986): A recording dilatometer for measuring polymerisation shrinkage. *Dent Mater,* **2:** 78-79.

Peutzfeldt, A. (1994): Correlation between recordings obtained with a light intensity tester and degree of conversion of a light-curing resin. *Scand J Dent Res,* **102:** 73-75.

Phillips, R.W., (1991): Chemistry of the synthetic resins. *In: Skinner's Science of Dental Materials*. W.B. Saunders Company, Harcourt Brace Jovanovich, Inc. 9th Ed, Chapter 10. Pp. 157-176.

Pilo R.and Cardash H.S. (1992): Post-irradiation polymerisation of different anterior and posterior visible light-activated resin composites. *Dent Mater*, **8:** 299.

Pires, J.A., Cvitko, E., Denehy, G.E. and Swift, E.J. (1993): Effect of curing tip distance on light intensity and composite resin microhardness. *Quintessnce Int,* **24:** 517-521.

Prosser, H., Powis, D. and Wilson, A. (1986): Glass-ionomer cements of improved flexural strength. *J Dent Res,* **65:** 146-148.

Quian , X.J., and Huth, S. (1998): Correlation of three-body wear to mechanical properties of compomers. *J Dent Res,* **77:** 292 Abs No. 482.

Rees, J.S. and Jacobsen, P.H. (1989): The polymerisation shrinkage of composite resins. *Dent Mater.* **5:** 41-44.

Rees, J.S. and Jacobsen, P.H. (1992): Stresses generated by luting resins during cementation of composite and ceramic inlays. *J Oral Rehabil,* **19:** 115-122.

Retief, D.H. (1994): Do adhesives prevent microleakage? *J Dent Int.* **44(1):** 19-26.

Roulet I.E., Øysaed H. (1987): Composites for use in posterior teeth. Composition and conversion. *J Biomed Mater Res.* **21:** 11-23.

Rueggeberg, F. (1993): Precision of hand-held dental radiometers. *Quintessence Int,* **24:** 391-396.

Rueggeberg, F.A. and Caughman, W.F. (1993): The influence of light exposure on polymerisation of dual-cure resin cements. *Oper Dent,* **18:** 48-55.

Rueggeberg, F.A. and Craig, R.G. (1988): Correlation of parameters used to estimate monomer conversion in a light-cured composite. *J Dent Res,* **67:** 932-937.

Rueggeberg, F.A., Caughman, W.F. and Curtis, J.W. (1994): Effect of light intensity and exposure duration on cure of resin composite. *Oper Dent,* **19:** 26-32.

Rueggeberg, F.A., Caughman, W.F., Curtis, J.W. and Davis, H. (1993): Factors affecting cure at depths within light-activated resin composites. *Am J Dent,* **6 (2):** 90-95.

Rueggeberg, F.A., Hashinger, D.T. and Fairhurst, C.W. (1990): Calibration of FTIR conversion analysis of contemporary dental composites. *Dent Mater,* **6:** 241-249.

Rueggeberg, F. and Jordan, D. (1993): Effect of Light tip distance on polymerisation of resin composite. *Int J Prosthodontic,* **6:** 364-370.

Ruyter, I.E. and Gyorosi (1976): An infra-red spectroscopic study of sealants. *Scand J Dent Res,* **84:** 396-400.

Ruyter, I. (1985) *Monomer systems and polymerization In: posterior composite resin dental restorative materials,* Peter Szulc Publishing Co., Netherlands.

Ruyter, I.E. and Øysaed, H. (1987): Composites for use in posterior teeth: composition and conversion. *J Biomed Mater Res,* **21:** 11-23.

Ruyter, I.E. and Øysaed, H. (1988): *Critical reviews in biocombatibility,* DF Williams, Ed 4(3), pp 247-279.

Ruyter, I.E. and Øysaed, H. (1982): Conversion in different depths of ultraviolet and visible light activated composite materials. *Acta Odontol Scand,* **40:** 179-192.

Ruyter, I.E. and Sjøvik, I. (1981): Composition of dental resin and composite materials. *Acta Odont Scand,* **39:** 133-146.

Ruyter, I.E. and Svendsen, S. (1978): Remaining methacrylate groups in composite restorative materials. *Acta Odontol Scand,* **36:** 75-82.

Sakaguchi, R.L., Peters, M. C.R., Nelson, S.R., Douglas, W.H. and Poort, H.W. (1992): effects of polymerisation contraction in composite restorations. *J. Dent,* **20:** 178-182.

Sakaguchi, R.L., Saski, C.T., Bunczak, M.A. and Douglas, W.H. (1991): Strain gauge method for measuring polymerisation contraction of composite restoratives. *J Dent,* **19:** 312-316.

Sheth, J.J., Fuller, J.L. and Jensen, M.E. (1988): Cuspal deformation and fracture resistance of teeth with dentine adhesives and composites. *J Prosthet Dent,* **60:** 560-596.

Shlesinger, M.F. (1984): Williamas-Watts dielectric relaxation: a fractal time stochastic process. *J Stat Phys.* **36:** 639-648.

Shortall, A.C. and Harrington, E. (1996): Guidelines for the selection, use, and maintenance of visible light activation units. *Br Dent J,* **180:** 383-387.

Shortall, A. C., Harrington, E. and Wilson, H. J. (1995a): Light curing unit effectiveness assessed by dental radiometers. *J Dent,* **23:** 227-232.

Shortall, A., Wilson, H. and Harrington, E. (1995b): Depth of cure of radiation-activated composite restoratives-influence of shade and opacity. *J Oral Rehabil,* **22:** 337-342.

Sidhu, S.K., Sherrif, M., and Watson, T.F. (1996): In vivo surface wear of resin-modified glass ionomer restorative materials. *J Dent Res,* **75:** Abs No. 40

Sidhu, S.K., and Watson, T.F. (1995): Resin-modified glass ionomer materials, Part I: Properties. *Dent Update,* 429-432.

Skeeters, T., Timmons, J. and Mitchell, R. (1983): Curing depth of visible light-cured composite resin. *J Dent Res,* **62.**

Smail, S., Patterson, C., McLundie, A. and Strang, R. (1988): In vitro temperature rise during visible-light curing of a lining material and a posterior composite. *J Oral Rehabil,* **15:** 361366.

Smith, D.C. (1985): *In: posterior composite resin dental restorative materials.* Vanherle G, Smith DC Eds. Peter Szulc Publishing Co., Netherlands, P 50-52.

Smith, D.C. (1968): A new dental cement. *Br Dent J,* **125:** 380-384.

Smith, D.C. and Schoonover, I.C. (1953): Direct filling resins: dimensional changes resulting from polymerisation shrinkage and water sorption. *J Am Dent Assoc,* **46:** 540-544.

Söderholm, K.-J. (1983): Leaking of fillers in dental composites. *J Dent Res,* **62:**

126-130.

Soltsez, U., Bath, P. and Klaiber, B. (1986): Dimensional behaviour of dental composites due to polymerisation shrinkage and water sorption. *In: "Biological and biomechanical performance of biomaterials".* Christel P., Meunier A., Lee AJC Eds. Elsevier Science, Amasterdam, Netherlands. pp 123-128.

Stansbury, J.W (1990): Cyclopolymerisable monomer for use in dental resin composites. *J Dent Res,* **69:** 844-848.

Stewart, G., Bachman, B. and Hatton, J. (1991): Temperature rise due to finishing of direct restorative materials. *Am J Dent,* **4:** 23-28.

Strang, R., Macdonald, I., O'Hagan, S., Murry, J. and Stephen, K. (1987): Variation in performance of curing light units by determination of composite resin setting time. *Br Dent J,* **162:** 63-65.

Suliman, A., Boyer, D. and Lakes, R. (1993a): Cusp movement in premolars resulting from composite polymerisation shrinkage. *Dent Mater,* **9:** 6-10.

Suliman, A., Boyer, D. and Lakes, R. (1993b): Interferometric measurements of cusp deformation of teeth restored with composites. *J Dent Res,* **72:** 1532-1536.

Suliman, A., Boyer, D. and Lakes, R. (1994): Polymerisation shrinkage of composite resins: comparison with tooth deformation. *J Prosthet Dent,* **71:** 7-12.

Swarts, M.L, Moore, B., Phillips, R.W. and Rhodes, B. (1982): Direct restorative resins. A comparative study. *J Prosthet Dent,* **47:** 163-170.

Swarts, M.L., Philips, R.W. and Rhodes, B. (1983): Visible light-activated resins-depth of cure. *J Am Dent Assoc,* **106:** 634-637.

Taira, M., Urabe, H., Hirose, T., Wakasa, K. and Yamaki, M. (1988): Analysis of photo-initiators in visible-light-cured dental composite resins. *J Dent Res,* **67:** 24-28.

Takamizu, M., K, M.B., Setcos, J.C. and Philips, R.W. (1988): Efficiency of visible-light generators with changes in voltage. *Oper Dent,* **13:** 173-180.

Tanoue, N., Matsumura, H. and Atsuta, M. (1998a): Curing depth of four composite veneering materials polymerized with different laboratory photo-curing units. *J Oral Rehabil,* **25:** 348-352.

Tanoue, N., Matsumura, H. and Atsuta, M. (1998b): Curing depth of composite veneering material polymerized with seven different laboratory photo-curing units. *J Oral Rehabil,* **25:** 199-203.

Tanoue, N., Matsumura, H. and Atsuta, M. (1998c): Properties of four composite veneering materials polymerized with different laboratory photo-curing units. *J Oral Rehabil,* **25:** 358-364.

Timoshenko, S. (1980) *Strength of materials,* Van Nostrand Reinhold Company. Part I. 3rd Ed., chapter 1, pp. 1-4; chapter IV, pp. 96; chapter V pp. 137 and 141.

Tirtha, R., Fan, P. L., Dennison, J. B. and Powers, J. M. (1982): *In vitro* Depth of cure of photo- activated composites. *J Dent Res,* **61:** 1184-1187.

Uno, S. and Asmssen, E. (1991): Marginal adaptation of a restorative resin polymerized at reduced rate. *Scand J Dent Res,* **99:** 440-444.

Unterbrink, G.L. and Muessner, R. (1995): Influence of light intensity on two restorative systems. *J Dent,* **23:** 183-189.

Venhoven, B.A.M., DeGee, A.J. and Davidson, C.L. (1993): Polymerisation contraction and conversion of light-curing BisGMA-based methacrylate

resins. *Biometrials,* **14:** 871-875.

Versluis, A. (1994): Origin and development of internal stresses during polymerisation of composite resins. Ph. D. Thesis, University of Greenwich, London, pp. 78-101.

Viadyanathan, J., Viadyanathan, T.K. (1991): Role of temperature and resin composite on degree of cure. *J Dent Res.* **70:** 295

Walls, A.W.G., McCabe, J.F. and Murray, J. (1988): The polymerisation contraction of visible-light activated composite resins. *J Dent,* **16:** 177-181.

Watts, D.C. (1992): Kinetic mechanisms of visible-light-cured resins and resin-composites. In: *Setting mechanisms of dental materials* (Ed, Watts, D.C.) Cameron House, Loch Lomond, Scotland, pp. 43-97.

Watts, D.C. (1990): Composite inlay system. Material properties and design. *J Dent,* **18:** 67-70.

Watts, D.C. (1996): The structural scope of biomaterials as amalgam alternatives. *In: Academy of dental materials, Proceedings of conference on Clinically appropriate alternatives to amalgam: Biophysical factors in restorative decision-making.* **9:** 51-67.

Watts, D.C. (1999): Personal communication.

Watts, D.C. and Al-Hindi, A.M. (1999): Intrinsic 'soft-start' polymerisation shrinkage-kinetics in an acrylate-based resin-composite. *Dent Mater,* **15:** 39-45.

Watts, D.C. and Cash, A.J. (1991a): Determination of polymerisation shrinkage kinetics in visible-light-cured materials: methods development. *Dent Mater,* **7:** 281-287.

Watts, D.C. and Cash, A.J. (1991b): Kinetic measurements of photo-polymerisation contraction in resins and composites. *Means. Sci. Technol.* **2:** 788-794.

Watts, D.C. and Cash, A.J. (1994): Analysis of optical transmission by 400-500 nm visible light into aesthetic dental biomaterials. *J Dent,* **22:** 112-117.

Watts, D.C., Haywood, C.M., and Smith, R. (1983): Thermal diffusion through composite restorative materials. *Br Dent J,* **154:** 101-103.

Watts, D.C., and McNaughton, V. (1986): Degradation of posterior composites in acidic and alkaline media. *J Dent Res,* **65(special issue):** 797, No. 645.

Watts, D.C., Amer, O. and Combe, E.C. (1984): Characteristics of visible-light-activated composite systems. *Br Dent J,* **156:** 209-215.

Watts, D.C., Amer, O. and Combe, E.C. (1987): Surface hardness development in light-cured composites. *Dent Mater.* **3:** 265-269.

Watts, D.C., McNaughton, V. and Grant, A.A. (1986): The development of surface hardness in visible light-cured posterior composites. *J Dent,* **14:** 169-174.

Wendt, S.L. (1987a): The effect of heat used as a secondary cure upon the physical properties of three composite resins. I. Diametral tensile strength, compressive strength, and marginal dimensional stability. *Quintessence Int,* **18:** 265-271.

Wendt, S.L. (1987b): The effect of heat used as a secondary cure upon the physical properties of three composite resins. II. Wear, hardness, and colour stability. *Quintessence Int,* **18:** 351-356.

Wendt, S.L. (1989): Time as a factor in the heat curing of composite resins. *Quintessence Int,* **20:** 259-263.

Williams G., and Watts D.C., (1970): Non-symmetrical dielectric behaviour arising from a simple empirical decay function. *Trans Farad Soc.* **66:** 80-85.

Wilson, A. and Kent, B. (1972): A new translucent cement for dentistry, the glass

ionomer cement. *Br Dent J,* **132:** 133-135.

Wilson, A. and McLean, J. (1988): *"Glass-ionomer Cement"*, , Chicago USA.

Wilson, A. and Prosser, J. (1984): A survey of inorganic and polyelectrolyte cements. *Br Dent J,* **157:** 449-454.

Wilson, A., Crisp, S. and Abel, G. (1977): Characterisation of glass-ionomer cements, 4; Effect of molecular weight on physical properties. *J Dent,* **5:** 117-120.

Wilson, H.J. (1978): Properties of radiation-cured restorative resins. In: *proceedings of the international symposium on fotofil dental restorative* Franklin scientific projects, London, pp. 11-16.

Yearn, J. A. (1985): Factors affecting cure of visible light activated composites. *Int Dent J,* **35:** 218-225.

Young, K. C., Hussey, M., Gillespie, F. C. and Stephen, K. W. (1977): The performance of ultraviolet lights used to polymerize fissure sealants. *J Oral Rehabil,* **4:** 181-191.

Yoshida, K. and Greener, E.H. (1994): Effect of photoinitiator on degree of conversion of unfilled light-cured resin. *J Dent,* **22:** 296-299.